PhD-FSTC-2017-41
The Faculty of Sciences, Technology and Communication

École doctoral IAEM Lorraine
Département Contrôle Identification Diagnostic (CID), CRAN

DISSERTATION

Defence held on 07/07/2017 in Luxembourg
to obtain the degree of

DOCTEUR DE L'UNIVERSITÉ DU LUXEMBOURG
EN SCIENCES DE L'INGÉNIEUR

AND

DOCTEUR DE L'UNIVERSITÉ DE LORRAINE
EN AUTOMATIQUE, TRAITEMENT DU SIGNAL ET DES IMAGES, GÉNIE INFORMATIQUE

by

Khadidja CHAIB DRAA

Observation and Control of Anaerobic Digestion Processes for Improved Biogas Production
Observation et Commande des Procédés de Digestion Anaérobie pour l'Amélioration de la Production de Biogaz

Dissertation defence committee

Dr-Ing Holger VOOS, dissertation supervisor
Professor, Université du Luxembourg

Dr-Ing Mohamed DAROUACH, dissertation supervisor
Professor, Université de Lorraine

Dr-Ing Joachim HANSEN, Chairman
Associate Professor, Université du Luxembourg

Dr. Marouane ALMA, dissertation examiner
Associate Professor, Université de Lorraine

Dr-Ing. Driss BOUTAT, dissertation reviewer
Professor, INSA Centre Val de Loire

Dr-Ing Ping ZHANG, dissertation reviewer
Professor, Technical University of Kaiserslautern

Declaration of Authorship

I, Khadidja CHAIB DRAA, declare that this thesis titled, 'Observation and Control of Anaerobic Digestion Processes for Improved Biogas Production' and the work presented in it are my own. I confirm that:

- This work was done wholly or mainly while in candidature for a research degree at this University.
- Where any part of this thesis has previously been submitted for a degree or any other qualification at this University or any other institution, this has been clearly stated.
- Where I have consulted the published work of others, this is always clearly attributed.
- Where I have quoted from the work of others, the source is always given. With the exception of such quotations, this thesis is entirely my own work.
- I have acknowledged all main sources of help.
- Where the thesis is based on work done by myself jointly with others, I have made clear exactly what was done by others and what I have contributed myself.

Signed: ____

Date: ____

"The thesis is dedicated to my family, especially, my lovely grandfather Dadi"

To my family.

Acknowledgements

First, I would like to thank my supervisors: Prof. Holger VOOS, Prof. Mohamed DAROUACH, Dr. Marouane ALMA, and Prof. Joachim HANSEN. I am grateful for their continuous support, guidance and kindness throughout the years of my PhD.

I would also like to thank Prof. Driss BOUTAT (INSA Centre Val de Loire) and Prof. Ping ZHANG (Technical University of Kaiserslautern, Institute of Automatic Control) for being members of my defense committee. I am thankful for their thorough review and fruitful remarks.

My special thanks go to Dr. Ali ZEMOUCHE for being a source of inspiration. I am very grateful for his persistent scientific and personal support. Similarly, I would like to thank Dr. Souad BEZZAOUCHA, Dr. Sebastian HIEN and all my colleagues in both universities, Université du Luxembourg and Université de Lorraine, the team members of the SnT Automation & Robotic Research Group, and the team members of the CRAN-Control Identification Diagnostic (CID) group. Their constructive discussions have helped in the successful completion of my PhD. I am thankful to them for providing such a comfortable working atmosphere. I would also like to express my deep gratitude to my friends for their encouragement and support.

Finally, I am so grateful to my family for their unstoppable support. I am so grateful to them for surrounding me with the utmost love and for everything they have done for me.

Contents

List of Figures

List of Tables

Abbreviations

$(\star)$	Blocks induced by symmetry
A^T	Transposed matrix of A
$\mathbb{I}_r$	Identity matrix of dimension r
$S,\ S > 0\ (S < 0)$	Square matrix positive definite (negative definite)
$\mathbb{R}^n_+$	for the positive orthant of dimension n
block-diag	Block diagonal matrix
iff	if and only if
$\mathbb{R}$	Set of real numbers
$\mathbb{R}^*$	Set of non-zero real numbers
$\mathbb{R}^n$	Euclidean space of dimension n
$\mathbb{R}^{m\times p}$	Set of real matrices of dimension $m \times p$
$\mathcal{B}_r$	Ball of $\mathbb{R}^n$ of radius $r > 0$
$Co(x,y)$	Convex set defined by $Co(x,y) := \Big\{\lambda x + (1-\lambda)y, 0 \leq \lambda \leq 1\Big\}$
$\triangleq$	Defined as
EKF	Extended Kalman Filter
LMI	Linear Matrix Inequality
LTI	Linéaire à Temps Invariant
LPV	Linear Parameter Varying
DMVT	Differential Mean Value Theorem
ADM1	Anaerobic Digestion Model N° 1
AM2	Acidogenesis Methanogenesis, 2 steps model
LCFA	Long Chain Fatty Acids
COD	Chemical Oxygen Demand
liq	Liquid
dec	Decay

hyd	Hydrolysis
dis	Disintegration
T	Temperature
$\rho_{T,i}$	Liquid/gas Transfer rate of component i
Cat^+	Cations
An^-	Anions
ρ_j	Kinetic rate of process j
S_i	Concentration of substrate i
su	Monosaccharides
aa	Amino acids
fa	Long chain fatty acids
va	Valerate
bu	Butyrate
pro	Propionate
ac	Acetate
h_2	Hydrogen gas
ch_4	Methane gas
ic	Inorganic carbon
IN	Inorganic Nitrogen
IC	Inorganic Carbon
S_I	Soluble Inerts
X_c	Composites
X_{ch}	Carbohydrates
X_{pr}	Proteins
X_{li}	Lipids
X_{su}	Sugar degraders
X_{aa}	Amino acids degraders
X_{fa}	LCFA degraders
X_{c4}	Valerate and Butyrates
X_{pro}	Propionate degraders
X_{ac}	Acetate degraders
X_{h_2}	Hydrogen degraders
X_I	Particulate Inert

Chapter 1

General Introduction

In the last few decades, planet temperature has risen unusually fast, about 2°C per decade in the past 30 years [5], [6]. A group of more than thousand scientists concluded, in the Fifth Assessment Report of the Intergovernmental Panel on Climate Change (IPCC) [7], that human activities have driven the temperature up. A process known as global warming or climate change. Eventually, since the beginning of the Industrial Revolution when humans started burning fossil fuels and polluting the air, green house gasses have risen sharply in the atmosphere and intensifying the greenhouse effect. Evidence for global warming includes extreme effects such considerable sea level rise [8], fresh water polluting, decreased snow cover, rainfall events and ocean acidification. Moreover, according to the NASA studies the extent of Arctic sea ice has declined about 10% in the last 30 years. Future climate change will differ from a region to another, some climate models predict harmful effects on ecosystems, biodiversity and the livelihoods of people worldwide [9].

Against this background, a worldwide challenge against the global warming has been engaged in Paris. On 30^{th} November 2015, 190 states have participated in the historical Conference of the parties (COP21) to limit global warming to 2°C by 2100. The participating states have formulated some action plans to reduce their emissions of greenhouse gases. Moreover, a progressive introduction of carbon price has been proposed to oblige industrials to reduce their gas emissions, modify their behaviour while investing and introduce green energies in the developing economies.

Within this context, the European Commission has also adopted a climate-energy package which was revised in 2014 to set the new goals for 2030 listed bellow

- 40% reduction in greenhouse gas emissions compared to 1990 levels,
- At least a 27% share of renewable energy in the mix energy,
- At least 27% energy savings compared to the usual scenario.

These targets aim to help the European Union (EU) toward a low-carbon economy and achieve a more competitive, secure and sustainable energy system and to meet its long-term 2050 greenhouse gas reduction target.

The term Renewable Energy (RE) refers to a power that comes from resources which are naturally replenished on a human time-scale. Advantages of the REs are numerous. Firstly, they increase energy independence and security energy supplies by providing local means of production, and secondly, they have a positive impact on the planet because they are replacing fossil fuels, and thus, limiting the greenhouse gas emissions.

Within this context, biomass is regarded as one of the most dominant future renewable energy sources [1] that needs to be used carefully and thoughtfully.

Biomass is all biologically-produced material based in carbon, hydrogen and oxygen. It includes a wide variety of materials, wood, forestry residues, straw, manure, sugar-cane, stover, green agricultural wastes, rice husk, . . . , sewage sludge, animal wastes and food processing wastes. Thus, unlike the wind and solar energies, a continuous availability of biomass energy can always be guaranteed.

In 1997, Gosh [10] estimated that recovery of organic waste and industrial effluents could reduce 20% of global warming. Indeed, there exists many smart ways to make use of biomass. It can either be used directly via combustion to produce heat, or indirectly after converting it into various forms of biofuel as depicted in Figure 1.1.

Among the possible conversion processes for biomass, Anaerobic Digestion (AD) has been evaluated as one of the most energy-efficient and environmentally beneficial technology for bioenergy production [11], [12], [13]. The reason why it is emerging spectacularly all over the word and attracting the interest of many researchers that we are among them.

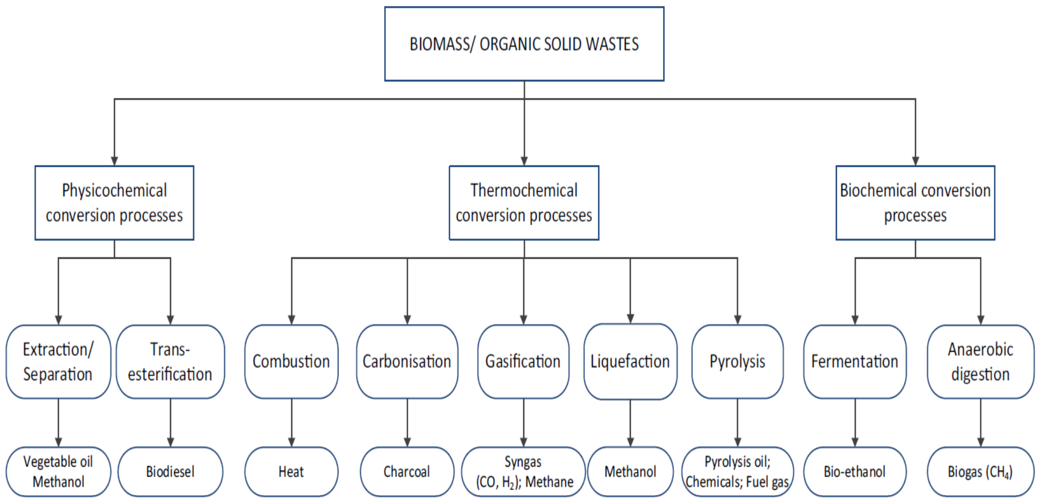

FIGURE 1.1: Biomass and waste conversion technologies (extracted from [1]).

Actually, AD is a promising process for waste recovery, environment protection and power grid stabilisation. It is an important process to produce a valuable energy which is named biogas, and a residue from the production that we call digestate. A schematic overview of the main products of AD process and their optional use is presented in Figure 1.2.

The biogas is a mixture of gaseous, generally composed of $45-65\%$ methane, $36-41\%$ carbon dioxide, up to 17% nitrogen, $< 1\%$ oxygen, $32-169$ ppm hydrogen sulphide, and traces of other gases [14] in [15], which can be used in many domains and replace the use of fossil fuel. Indeed, the biogas is classified as a renewable energy, which can be either cleaned and upgraded to natural gas standards or used in gas engines to produce electricity and heat energies, and thus, displace the polluting fossil fuel. Moreover, even if the produced biogas is not used to produce any other type of energy and is simply released into the air, the amount of unburned hydrocarbon emissions decreases when the biogas is rich in methane [16]. Besides, by storing biogas we prevent potent greenhouse gases from entering the atmosphere.

The digestate is the material that remains after the AD of biodegradable waste holds. It is never a loss since it can be used as a sol conditioner, or to produce a nutrient for plants to aide them for growth and inhibit them from diseases.

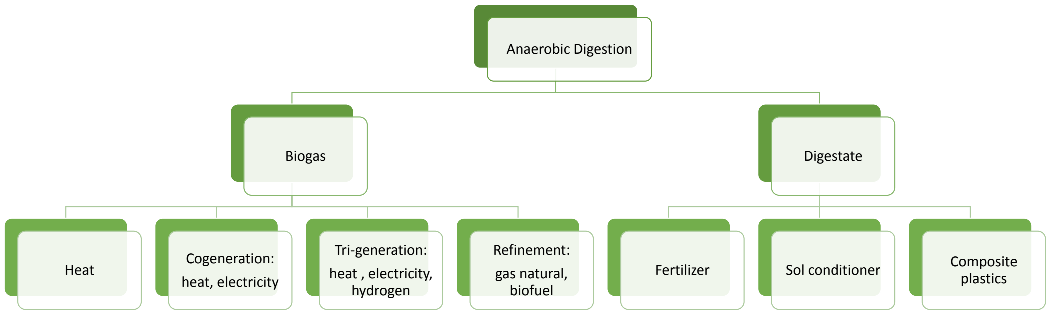

FIGURE 1.2: Main products of anaerobic digestion and their optional use.

At laboratory or industrial scales, the AD process occurs inside an anaerobic digester where degradation of organic material holds by a consortium of anaerobic bacteria. The number, behaviour and interaction of the included bacteria have been extensively questioned in the literature. The interest of these questions is first to understand the process and then optimize it and make it worldwide adopted.

One way to improve the AD efficiency and performances is the design and scale up of appropriate reactors [17], [18], [19], [20], [1]. Indeed, the reactor configuration and environmental conditions (retention time, temperature, feedstock . . . stirring) influence the dynamics and composition of the different groups of bacteria reponsible for the organic materials degradation [13], [1]. Actually, the AD process is a multi-step process, as it will be clarified further in the manuscript, and the subsequent steps of the process are directly related to the solids retention time (SRT) in the digester [1] and to the manner the micro-organisms are retained inside it [19]. Moreover, the microorganisms themselves and the biochemical reaction rates are influenced by the available temperature in the digester. Naturally, at different levels of temperature, different species of bacteria may be encountered. Consistently, in mesophilic digestion (30 to 38°C), the species of methanogens in the reactor are different from those found in the thermophilic digestion (49 to 57°C). Therefore, according to the user objectives, initial investment and the nature and texture of the biodegradable waste (high/ low solids, pumpable (wet)/ stackable (dry) substrate), several technologies can be granted. We quote here below some commonly cited reactors in the literature, and for more details about the used technologies (thermophilic, mesophilic . . .) for AD applications and their performances we orient the reader to [18], [19], [21], [1].

- Batch Reactor: the principle is simple, first the digester is filled with the biodegradable materials, left until all the substrate has been degraded and then the digester is emptied and a new cycle can begin again. The digestion time depends on the temperature and the substrate type.

  This technique has the advantage of being simple and robust, when the objective is the production of biomass, the initial biomass is chosen small. The dead-time necessary for initiation of the reaction after emptying and filling the tank, is the disadvantage of this type of reactors.

- Semi-Continuous Fermenter (Fed/ Sequencing Batch Reactors): the process is cyclic, the digester is filled gradually according to the progress of the reaction in order to avoid organic overload and ensure optimal growth conditions. At the end of the digestion phase, decantation allows to separate the liquid phase and suspended biomass, a portion of the supernatant (about 10%) is removed during the emptying stage [22].

  SBR reactors try to maintain a relatively high biomass concentration in the digester. This method is useful when the influent has an inhibitory nature.

- Continuous Bio-Reactor: the tank is fed at a constant rate and the digestat is evacuated by a mechanical action. This technology is ideal for large sized plants. Depending on the contact between the substrate and biomass or even where the later is landed, the feeding mode and where the different anaerobic digestion phases hold, the continuous bio-reactor fall into four general categories.

  * Free Cells Digesters: these are the simplest reactors where the biomass is suspended in the reactor, among these fermenters we find:
    - Continuous Stirred Tank Reactor (CSTR): herein a continuous mixing ensures the medium homogeneity, which promotes the contact between biomass and substrate. The mixing in the digester can be done mechanically by a system of blades, or by recirculating the contents of the digester. The biogas

can be reinjected at the bottom of the reactor to avoid accumulation of particulate matter which in the long term may reduce the useful volume and consequently the process performance reduces [22].

The drawback of CSTR reactors is the equality of biomass residence time (BRT) and the hydraulic retention time (HRT) and thus the feeding rate is limited in order to allow bacteria to grow [22]. Consequently, contact digesters have been implemented as a solution for this drawback.

– Contact Digesters: in order to increase the inflow and outflow rates, the amount of biomass in the digester is increased by decoupling the HRT of the BRT. This can be done by putting at the output of the digester a system to separate biomass from effluent and recirculating the concentrated biomass [22]. The recovery of the particulate material may also be done using a decanter or a membrane [23].

∗ Biofilm and Granules Digesters: a biofilm is a group of microorganisms sticking to eachother to forme granules [14]. The microorganisms grow either on mobile or fixed support, this allow high flow rates with no risk of leaching biomass. These digesters are more robust in face of hydraulic shocks. Varieties of this type of digesters are [22]:

– Fixed Bed Reactors: the reactor is filled with inert supports of varied nature (glass, plastic, ...) that can be in various forms (strips, grid, ...) on which biomass can settle and develop. The substrate is degraded while passing through the filter made by the support and the bacteria colonising it.

These digesters require less mixing and are particularly robust for organic overloads. However the risk of clogging the support by particulate materials is quite important. Thus, applying down-flow and biogas recirculation is frequently used to facilitate removal of excess biomass free (not bound to the support).

– UASB reactors: the process, the most common is the UASB reactor (Upflow Anaerobic Sludge Blanket), where the upward flow balance the tendency of the aggregates to settle, and provides the suspension of biomass. A system for separating liquid/ gas/ solid, situated on the top of the digester helps to retain the biomass in the reactor. Recycling is used to stir and homogenise the medium. The expanded bed reactors sludge EGSB (Expanded Granular

Sludge Bed) are UASB digesters where the upward flow is significantly higher which increases the sludge bed height [22].

* Mobile Support Reactors: they are reactors with mobile support are from the latest generation of fixed biomass digesters (high retention rate of biomass allows large feeding rates). They combine the advantages of attached biomass digesters and free cells digesters (low risk of clogging and good homogeneity of the medium).
  The digester is filled with small-sized inert supports where biomass can grow. The high surface/ volume report allows high flows and avoids clogging. If the bed is expanded by less than 20% then it is "expanded bed" and when the bed expansion exceeds 30% it becomes "fluidized bed". Mobility of carriers is increased in the fluidized beds which limits clogging and ensures efficient mixing.
* Two-Stage Reactors: the technology of two-stage digesters consists on operating the two limiting steps (acidogenesis and methanogenesis[1]) in two separate reactors in order to allow different operating conditions (different dilution rates) and thus avoid reactor acidification and allow optimal methane production [19]. The choice of a larger reactor for methanogenesis than acidogenesis reactor permits a lower dilution rate which is more favourable for methanogenic bacteria growth.

Remark 1. [22] Whatever the chosen reactor type, the designer has to consider a key parameter in biogas plants which is the dilution rate (D)

$$D = \frac{\text{The feed rate of the bioreactor (Q)}}{\text{volume of the digester (v)}} \left(\frac{1}{\text{day}}\right)$$

which also represents the inverse of HRT that should be sufficient to allow the different bacterial species to grow.

Depending on the used technology (reactor type), it will be related to SRT, such that the residence time of solids in the reactor is greater than the largest doubling time of bacterial populations

$$\text{SRT}_{min} \geq \frac{\ln(2)}{\mu_{max}}$$

where μ is the bacterial growth rate. Failure of this constraint causes decrease of biomass in the reactor, we speak then about leaching. Therefore, to avoid wash out of bacteria the dilution rate (D) is constrained.

[1]The AD steps will be emplaned later in the manuscript.

Another way to optimize and enhance the AD processes, for biogas production, can be achieved via validated mathematical models reflecting the bacteria kinetics and the complex transport phenomena occurring in the process [13], [1].

Indeed, modelling of the AD process has been extensively investigated in the literature. Often, the resulted models are specific to a couple of criteria such the designer objectives, waste nature and its composition, the used technology, collected data and its quality, the possible experiments and changes in the operating conditions. We schematize the commonly influencing parameters for AD modelling in Figure 1.3.

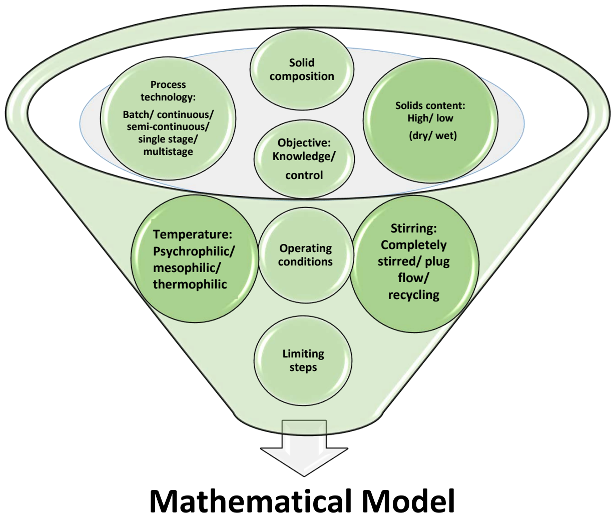

FIGURE 1.3: General parameters influencing the AD modelling.

Tentatively, we split the AD models into two categories, those designed for process knowledge and those dedicated to the process monitoring and control. Usually, the laters consider only the rate liming steps of the process and are relatively simple compared to the ones designed for process knowledge, which are complete, however, complex and difficult to exploit for control [24].

In the present work, we do not aim to represent the chemical reactions occurring in the AD process and their evolution with time, since this is largely available in the literature. However, we target to give a brief historical review on AD modelling and expansion of the process steps in line with development of the different bacteria species. Nevertheless, we give first the definition of some steps (hydrolysis, acidogenesis, acetogenesis, methanogenesis) that will be recalled in the short review.

- Hydrolysis: it is the step where polymers (macromolecule) are hydrolysed to monomers (simple organic matter), the speed of degradation depends on the substrate itself (by order from faster to slower: glucide, proteins and lipids, and cellulose).
- Acidogenesis: herein, monomers are degraded to Volatile Fatty Acids (VFA[2]) and alcohol.
- Acetogenesis: performed by acitogenic bacteria which transform the VFA into acetic acid ($CH_3 - COOH$), hydrogen (H_2) and dioxide carbon (CO_2). We would like to say that the responsible bacteria for this step produce H_2 and is at the same time inhibited by an excess of its concentration in the digester, that's why they live fixed to the methanogenic bacteria which consume the H_2.
- Methanogenesis: here, methanogenic bacteria reduce the specific substrate into methane.

The first attempts for AD modelling led to models describing only the limiting steps. In 1968, Andrews [25] modelled the methanogenic fermentation by only the final step methanogenesis. Then in 1973, Graef and Andrews included the acidogenesis step in their macroscopic description of fermentation [22]. Later on, other researchers, Hill and Barth (1977, [26]), Boone and Bryant (1980, [27]), Eastman and Ferguson (1981, [28]) added an initial hydrolysis step to their description, and obtained a three-step process. The acitogenesis step was initially highlighted by Stadtman and Barker (1951, [29]) and introduced later to the process description by many researchers [22]. Over time, inhibitions due to the competition of bacteria for the different substrates uptake was taken into account [30] and led to the expansion of the process steps which made its modelling very complex. Moreover, differences in the digested waste composition and in the modelling objectives increased the number of model-based application which can not be widely adopted (the reader is referred to [31] for more details about those models).

[2]The VFA are mainly composed of propionate, butyrate and valerate.

In addition to that, it has been agreed in the literature that during a wide range of operating conditions, the limiting steps are not always the same!

Besides, a key parameter in the AD description is the kinetic modelling of the substrate uptake, biomass growth and product formation, that we may find more than fifty proposed models in the literature (Monod, Blackman, Tessier, Haldane . . . Moser, Konak) [32]. In the sequel, a group of experts in the AD processes (IWA Task Group for Mathematical Modelling of Anaerobic Digestion Processes, 2002) has been in charge to develop a standard model for the AD process and make it worldwide adopted. The elected model names ADM1 (for Anaerobic Digestion Model N°1).

In order to make the ADM1 a standard platform for AD simulation, it has been decided to generalize the composition of waste. Therefore, it is measured by an unified unit "Chemical Oxygen Demand (COD)" and the process is supposed to occur in a Continuous-flow Stirred Tank Reactor (CSTR),[3] since this type of reactor is the most used in practice. Moreover, to make the model widely applicable, all the main relevant biochemical processes occurring in the AD process has been included, see Figure 1.4:

- Disintegration of composites,
- Hydrolysis of particulate such as carbohydrates, proteins, and lipids,
- Six substrate degradation processes together with their six specific biomass growth and decay processes.

The novelty of the ADM1 in comparison with other previously developed AD models (Vavilin [33], Angelidaki [34], Siegrist [35], Batstone [36], and the references therein), is the inclusion of the disintegration step. Cellular solubilisation steps are divided into disintegration and hydrolysis which are extracellular biological and non biological processes. In these steps, the complex organic matter is solubilised to carbohydrates, proteins and lipids (polymers), organic composite and inert. The dead biomass is recycled in the organic composite matter and undergoes again the disintegration step. Then, the model has 4 biological steps and 7 bacterial species. The mission and interest of each bacteria and step included in the ADM1 are explained in details in [2].

[3]The ADM1 is described for a CSTR but can also be used for batch and semi-batch mixed reactors.

The physico-chemical process for stripping the gaseous compounds, hydrogen, methane and carbon dioxide, is included to represent the production of biogas. It is defined as non biological process and two types are treated in the ADM1 (liquid-liquid processes (i.e. ion association/dissociation): they are so fast that they are considered as equilibrium processes and are presented by algebraic equations, 10 pairs are estimated to be important, and liquid-gas processes: may be considered as a fast or medium transfer). The pH calculation is based upon six additional physicochemical processes, describing

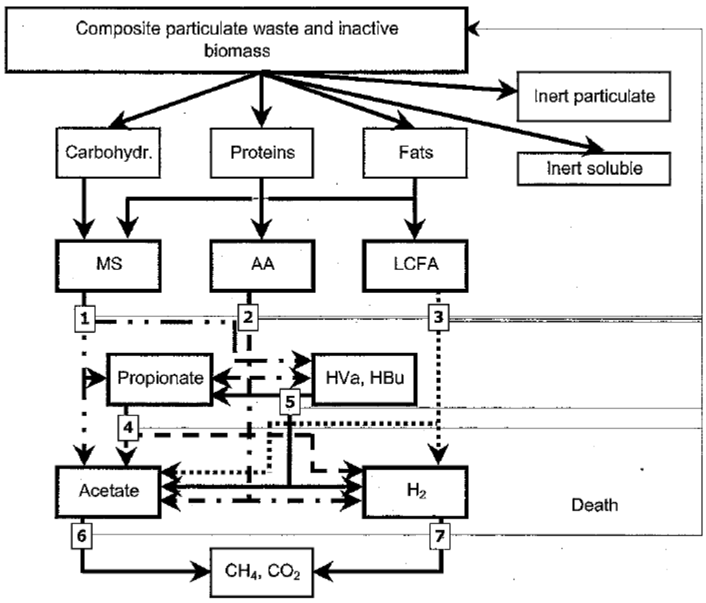

FIGURE 1.4: Anaerobic digestion model as implemented in the ADM1, including biochemical processes: (1) acidogenesis from sugars; (2) acidogenesis from amino acids; (3) acetogenesis from Long Chain Fatty Acids (LCFA); (4) acetogenesis from propionate; (5) acetogenesis from butyrate and valerate; (6) aceticlastic methanogenesis; (7) hydrogenotrophic methanogenesis (extracted from [2]).

the acid/base equilibria of: CO_2/HCO_3, NH_4^+/NH_3, acetic acid/acetate, propionic acid/propionate, butyric acid/butyrate and valeric acid/valerate:

$$\Sigma S_{C^+} + \Sigma S_{A^-} = 0$$

where ΣS_{C^+} is the sum of cation concentrations and ΣS_{A^-} represents the sum of anion concentrations. Changes in cation and anion concentrations are introduced to address the influence of positively and negatively charged ions present in the system on the pH. They may be described by algebraic equations or modeled by differential equations. Based on this feature, the state vector of the ADM1 can, respectively, have 26 or 32 state variables.

The cellular kinetics are described by three expressions, growth, uptake, and decay. All the extracellular steps are assumed to be first order. Moreover, growth is implicit in the uptake and are modeled by Monod-type kinetics. All included equations in the ADM1 are reported in Appendix A.

Since the ADM1 was developed to be a general framework for AD process modelling, its parameters were collected from different applications and the designers left some choices for the users to adapt, and make the model suitable for their specific applications. An example of adaptation of the ADM1 to anaerobic digestion of sludge at wastewater treatment plant can be found in [37]. Of course many modifications, adaptation and variations of the ADM1, for other specific applications, have been done later [38], [39], [40], [41] and the references therein.

However, the ADM1 and its variations are complex models suitable for process simulation, but not appropriate for process control and software sensors design [23], [24]. Indeed, the models complexity leads to the need of plenty input parameters which usually are difficult to obtain, and in addition to that, handling 32 differential equations and identifying all process parameters can prove arduous [38], [24]. Moreover, according to the digested substrate composition, only few parameters influence the model outputs, and many reactions occur rapidly and do not affect the overall process dynamics [13].

Therfore, to overcome the model complexity issue, a synthetic mass balance model has been developed in the AMOCO project (Advanced MOnitoring and COntrol System for anaerobic processes) called AM2 (Acidogenesis Methanogenesis, 2 steps model) [4]. This model is suited for control and design of software sensors for the AD process. The AM2 model is a two step model like those designed in [42], [43], [24], and the references therein, which are all suited for the process control and monitoring. However, the AM2 model has the advantage of being compared to the ADM1, which is considrred as the reference for AD modelling, in [22] and has shwon satisfactory results. The intefarce between the AM2 and the ADM1 is provided in Appendix B. Besides, the AM2 has been designed for both CSTR and fixed bed digester, and its parameters have been identified by using experimental results covering a wide range of operating conditions [4]. This particularly oriented our interest to the AM2 model that will be investigated in Chapter 2.

In addition to the required knowledge of the system, a good management and control of a system require a good information about the internal state of that system. Particularly, in biological processes, things seem to work fairly well and reasobably until some failures or faults occur [44]. This may be due to the specific behaviour of the system itself or to the presence of disturbances which can highly affect the process [45]. Thus, an obvious need for an efficient control and monitoring of such systems arises.

When we look at the current status in monitoring of AD processes, it seems that it should be possible to follow the evolution of almost all process variables (gas flow and gas components, carbon dioxide, bicarbonate, . . . , chemical indicators, alkalinity, metabolic activity, VFA, pH, microbial communities, biomass/suspended solids). A summury and review of the different sensoring can be found in [46], [15], [47], [48], [49]. However, the majority of sensors intended to measure the process key variables require, often, complex equipment and careful maintenance, or need difficult sample preparation which prevent their wide application [49]. Moreover, the plant costs climb quickly when some specific sensors are selected, and thus, they are not desirable from industrial standpoint [50]. Therefore, it is crucial to find a methodology which allows the monitoring of AD applications while being cost-effective and easily adopted by industrials.

One remedy for this issue is the development of accurate and efficient software sensors (also called observers). These observers are auxiliary dynamical systems that mirror the internal state of the system. Actually, when we have a mathematical model of the process, it is possible, under some conditions, to design an observer which provides information about the unmeasurable state variables of the system by using its model and its input and output signals (measurable variables of the system).

Usually, the observer design depends on many factors, such the model reliability, the available measurements and their quality, and the inputs certainties. In the case of linear systems, the observer design problematic has been extensively studied, vigorous and confirmed methodologies do exist [51], [52], [53], [54], [55]. Whereas, for the nonlinear case there is no generalized methodology and it is still an open area for research. Indeed, the available results are suitable for specific nonlinear structures [56]. This is probably due to the restrictive conditions to be satisfied [57] and the difficulties involved in dealing with the nonlinear systems [58]. Among the complex nonlinear systems for which the observer design is still an open area, we find the AD processes which exhibit some very specific behaviours and are intrinsically unstable systems [44], [59]. Therefore, considerable attention has been paid towards the development of observers for AD processes.

Regardless to the neural network observers [60], [61], we may split the designed observers for AD processes, and relying on the availability of a mathematical model, into two classes. Observers designed based on full knowledge of the model, and others based on its partial knowledge. Among the formers, we find the asymptotic observer [32] which considers the kinetic functions as unknown functions and does a systematic linear change of variables whose dynamics do not depend on that kinetic functions. Since the asymptotic observer is widely referred, we briefly show how it works for a second order system, but it can be easily extended for higher orders.

Let the system be described by

$$\begin{aligned} \dot{x}_1 &= u(x_{1in} - x_1) - k\mu(x)x_2 \\ \dot{x}_2 &= (\mu(x) - u)x_2 \end{aligned} \tag{1.1}$$

where x_1 represents the concentration of the substrate to be digested by the bacteria x_2, u and x_{1in} are the system inputs. The state vector $x = [x_1, x_2]^T \in \mathbb{R}^2$, and the scalar function $\mu(x)$ is the unknown kinetic function. Let us suppose that x_1 is measurable and the objective is to estimate x_2. Thus, we introduce the following variable [32]

$$z = x_1 + kx_2 \tag{1.2}$$

whose dynamic is

$$\dot{z} = u(x_{1in} - z) \tag{1.3}$$

for which the asymptotic observer is given by

$$\dot{\hat{z}} = u(x_{1in} - \hat{z}) \tag{1.4}$$

where z is the estimate of $\hat{z}$. Once $\hat{z}$ is obtained, x_2 can be easily deduced by using equation (1.2) and measurement of x_1:

$$x_2 = \frac{1}{k}(z - x_1)$$

The observation error is defined as $e = z - \hat{z}$, whose dynamic follows from equations (1.3) and (1.4)

$$\dot{e} = -ue \tag{1.5}$$

For a positive control ($u > 0$), it can be seen clearly from equation (1.5) that the estimation error converges asymptotically to zero. However, when $u = 0$, the convergence of the error to zero is not any more guaranteed and any initial estimation error persists throughout the estimation procedure. In addition to the dependence of the rate of convergence on the operating conditions (u), the asymptotic observer requires enough measurable state variables [32], and provides poor estimates when the inputs or the parameters are uncertain [23]. Therefore, a more appropriate solution has been proposed in [62], [63] when the time-varying bounds enclosing the uncertainties are known. Indeed, the solution in this case is the use of interval observer which is composed usually of two asymptotic observers, one to estimate the state upper bound $x^+(t)$ and a second one to estimate the lower bound $x^-(t)$, and then the actual state will be enclosed in the envelope drown by $x^-(t)$ and $x^+(t)$ provided that at the initial time $x^-(t_0) \leq x(t_0) \leq x^+(t_0)$. Unfortunately, it happens sometimes to obtain a large envelope of the state and thus the estimation becomes useless! Therefore, Bernard and his co-workers [64] have proposed to launch a bundle of interval observers with different initial conditions and then select the best (smallest) envelope. The advantage of the bundle observers is the improvement of the asymptotic bounds and the ability to partially tune the rate of convergence due to the use of additional measurements which are nonlinear functions of the state variables. However, the interval observers are applied only when the dynamic of the estimation error is cooperative[4]. Actually, the cooperativity property of a dynamic system is what guaranties that when $x^-(t_0) \leq x^+(t_0)$ then $\forall t \geq 0$, $x^-(t, x^-(t_0)) \leq x^+(t, x^+(t_0))$. Therefore, the interval observers can be applied only for a specific class of systems. In addition to that, it is not easy to exploit the estimate intervals for control.

Another kind of observers, among others, can be designed when the system is partially known. It is the observer based estimator [32], [65], [66], [43], wich is based on the use of the estimated (considered to be measured) state variables to estimate the unknown kinetic functions or the model parameters. The key idea of this observer is to consider that the dynamics of the unknown parameters to be slow [23]. Its advantage is that in some cases the rate of convergence can be tuned. However, this requires the calibration

[4]All elements of the Jacobian matrix of the system are positive.

of many tuning parameters and the available data have to be sufficiently rich to design the observer.

If a reliable model is available, one can design different types of observers depending again on the application objectives and the available data. Among many designed observers in the literature, we may cite firstly the extended Kalman filter (based on a linear approximation of the nonlinear process model) which has been extensively applied to the AD applications, [67], [32], [68], [69], [70], [71] and the references in [72], with success and has even covered the situations where measurements of the process outputs arrive at different sampling rates [73]. However, in some cases the Kalman filter may not possess globall asymptotically stable error dynamics [74], and even if it does than, it is difficult to prove the global convergence analytically [75]. Moreover, it has been prooved in [59] that due to the highly nonlinear structure of the AD model and the number of input variables, it becomes impossible to apply the extended Kalman filter when one wants to estimate the biomass concentration (the system is not uniformly observable for any input), which is a key state variable to estimate since it reflects the system health and stability [50].

The high gain observer has also been, in the last decade, the object of growing interest in the AD applications due to its fast convergence. We may mention the paper of Gauthier and his co-authors [76], where the high gain observer has been applied successfully to a second order AD model. To design the observer, the transformed canonical form is performed, it is defined through Lie derivatives of the output which is a function of the state variables. The convergence of the estimates to the model state variables is fast enough, however the estimation is very sensitive to noise and the high gain observer design for high order models may be complex. Indeed, it happens that the resulting canonical form, for systems having dimensions greater than two, is not strictly linear and thus involves exogenous inputs and a finite number of their derivatives [57], and moreover such transformation is not always possible to perform [56]. In order to reduce the sensitivity of estimates to noise, Lombardi and his co-autors [59] have proposed an nonlinear observer for the on-line estimation of biomass and substrate concentrations in presence of noise, where a certain diffeomorphism is applied to the model in order to divide it into two partitions, a first system which is exponentially stable and a second one which admits an observer. Then the high gain observer proposed in [76] is applied to the second subsystem, where the observer gain is a compromise between the observer robustness and the convergence fastness.

In regard to observers applying the same transformation performed in [76], we may cite the nonlinear observer designed in [44] for a forth order AD model. Due to the cascade structure of the considered model and the decoupling of its subsystems, two cascade high gain observers have been synthesized in order to detect and isolate some sensor faults. The results have shown that it is possible to only detect and isolate a set of sensor errors and specific faults.

For the same class of systems considered in [76], a cascad observer has been proposed in [77] and [78] for a time delayed output. The proposed observer is composed of $(m+1)$ subsystems, the first one is a high gain observer which provides the delayed state and the rest m subsystems are what the authors called "predictors", where the state of the $m^{\mathbf{th}}$ predictor is an estimate of the system actual state (m is the number of predictors chosen such that stability conditions are satisfied). Although some satisfactory simulation results, the assumed assumptions and the canonical transformation appear to be the bottleneck.

Actually, the question of uncertainties, delayed measurements and disturbances must arise in such applications, because they can hold for different reasons, such the response time of sensors which depends on the relaxation of components and also their location in the digester [50], hydraulic or thermodynamic disturbances, intoxications to heavy metals and to antibiotics, . . . , overload of the system, whether the model has been thoroughly identiffied and validated! failure in measurement devices and effect of parasite signals. Therefore, Kravarisa and his co-authors [45] have designed a nonlinear observer to estimate the process state variables together with the process or sensor disturbances. The gain of the proposed observer depends on the system state variables. It is calculated from the solution of a system of singular first-order partial differential equations (PDEs). The nonlinear observer has shown suitable results, but unfortunately, its response can become easily unstable due to the initial conditions and the truncation orders of the power-series solution algorithm for the PDEs. Moreover, performances of the designed observer depend on its eigenvalues and their magnitude. Last but not least, the exponential stability of the system equilibrium point is required to design the proposed observer.

A new kind of nonlinear observers has been synthetized in [79] which is based on the rewriting of the AD model by including dynamics of the methane flow rate (which is the system output) to estimate the volatiles fatty acids in presence of model uncertainties. The proposed observer is based on the modified structure of the model, it is composed of a linear and a sigmoid injection of the error which enable the rejection of the model uncertainties. However, the methodology for the parameters tuning is still to be revised.

Another type of observers has also been established in [80], [81], [82], and applied to a class on chemical reactors in [82], [83]. They are called invariant observers and are based on Lie group symmetries. In these observers, the invariance refers to the invariance under a group action that it and some invariant functions and vector fields are required to design the observer. The advantage of these observers is their fast convergence as it has been shown in [84]. However, unfortunately, theirs design is not systematic, and for high order systems it may prove difficult to compute the observer parameters. Therefore, in the sequel, we will extend the invariant observer to higher system orders but under a somewhat different form.

Moreover, we will propose in Chapter 3 a new and simple methodology to design nonlinear generalised Luenberger observers for AD models. The methodology is based on the use of the Differential Mean Value Theorem (DMVT), which allows the transformation of the nonlinear error to a Linear Parameter Variant (LPV) system. Then, using the LPV techniques, the stability conditions may be obtained in the form of Linear Matrix Inequalities (LMIs). Besides, we will enhance the feasibility of LMI conditions by using a new and suitable reformulation of the Young's inequality.

In addition to the modelling and observer design for AD processes, which are still active areas of research, the AD control, in biogas plants, is gaining an increased importance in both academic and industrial communities. The main reasons for this fact are the significant growth of bioenergy markets, and the beginning of new era where biogas plants are regarded as a novel financial investment device by individuals as well as institutional investors [85], [86]. Moreover, due to the ambitious climate-energy package of the European Commission, many EU countries have defined quality standards for biogas injection into the natural gas grid [12]. In addition to that, the produced biogas must be rich in methane to fulfil requirements of the different gas appliances, and the effluent must fulfil the environmental standards.

In recent years, improvement of bioreactor performances and application of automatic control to the bioprocesses have shown that their functioning can be optimized, and an efficient biological pollutant removal can be achieved [87]. However, controlling the AD processes is delicate, because they exhibit some very specific behaviours and are intrinsically unstable systems [44], [59]. Moreover, when dealing with the AD processes several factors are to be handled [88]. Among these factors, we may mention the highly nonlinear behaviour of the system, load disturbances, system uncertainties, constraints on manipulated and state variables and the limited online measurements information [89]. Moreover, the AD process involves living organisms which are very sensitive to the operating conditions and may be washed out or inhibited due to an accidental toxic feeding, leading, in the worst case, to a definite stop of the digester [90]. In the sequel, control of the AD processes has aroused much interest amongst the researchers in automatic control.

Naturally, the control design varies with the application objectives. Usually, in biogas plants, the controller is designed to satisfy one specific criteria. Either economical (maximizing methane production) or ecological (minimizing COD concentration of the effluent) or stability (VFA, VFA/TA[5], propionate or dissolved hydrogen) criteria [91]. Moreover, the controller type depends on many factors. Such the controllability of the process, accuracy of the monitoring, knowledge of the system and availability and complexity of the considered model.

At the outset, controllers designed for the AD applications were of type on/off controllers [92], [93], [94]. They were designed to control the pH of the digester in order to prevent its acidification. Indeed, following an organic overload of the digester, acids may accumulate and consequently the digester pH drops. In the sequel, functioning of the survival micro-organisms gets disturbed and their growth may be inhibited. Later, Proportional Integral Derivative (PID) controls including, P, PI, and PID, have been found suitable for stabilizing the process. We may cite the control of bicarbonate alkalinity in [42] and the control of pH and dissolved H_2 concentration in [95], [96]. These controls have been widely used, developed, and extended for other objectives in the literature. For example, we mention the adaptive PI control proposed in [97] to regulate the bicarbonate concentration of the AD process. The adaptive PID and the cascade PI controls designed in [98] and [99], respectively, to control the methane flow rate. The

[5]TA for Total Alkalinity

cascade PID control proposed in [100] to satisfy multiple objectives (methane and VFA concentration control). The PID controls have also been used conjointely with extremum seeking control [101] and supervisory expert systems [102]. Despite the widespread use of the PID controls and their easy implementation in industry, they are not very suitable for varying feed conditions [103], [104] and are not robust face to multiple challenges. Besides, optimal tuning of the PID gains may prove to be complex.

An other type of control designed for the AD processes, based on the availability of a mathematical model, is the linearizing control, [32], [105]. The principle, herein, is to synthesize a control law so that the evolution of closed loop system turns to be linear. To illustrate how this controller works, we apply it to the system (1.1) to stabilize the substrate concentration x_1 around a desired reference x_1^*. To do so, we compute the control law so that substrate dynamic becomes

$$\dot{x}_1 = \lambda\ (x_1^* - x_1) \tag{1.6}$$

where the parameter $\lambda > 0$ represents the convergence rate of the substrate x_1 to its desired reference x_1^*. The control action, in this case, can be either x_{1in} or u. Depending on the selected action and by assuming that all variables are available, whether the control x_{1in} or u are computed by using equations (1.1) and (1.6):

$$\begin{aligned} x_{1in} &= \frac{\lambda\ (x_1^* - x_1) + u x_1 + k\mu(x) x_2}{u} \\ u &= \frac{\lambda\ (x_1^* - x_1) - k\mu(x) x_2}{x_{1in} - x_1} \end{aligned} \tag{1.7}$$

Although the linearizing control is a global approach, it relies of full knowledge of the system parameters. Therefore, Mailleret et his coauthors [106] have proposed an adaptive version of it and prove the global asymptotic stability of the closed-loop system. A variant of the linearizing control has been proposed in [107], where the convergence rate of the controlled variable to its desired reference does not depend on the parameter λ, for example

$$\dot{x}_1 = u\ (x_1^* - x_1) \tag{1.8}$$

and thus, the control action can be either x_{1in} or u obtained by using the equations (1.1) and (1.8):

$$\begin{aligned} x_{1in} &= \frac{ux_1^* + k\mu(x)x_2}{u} \\ u &= \frac{k\mu(x)x_2}{x_{1in} - x_1^*} \end{aligned} \tag{1.9}$$

If we compare the control laws given by equations (1.7) and (1.9), we quickly realize that the number of required measurements decreases (no need of x_1 measurement). However, the convergence rate depends on the operating conditions (u) which makes it, generally, slow [106].

To overcome model errors or in the absence of some model parameters, adaptive linearizing control has also been extenvely used in the literature [108], [109], [110], [111]. Besides, when intervals of the model uncertainties are known a priori, robust linearizing control based on interval observers have been proposed in [112], [113] and [114]. Although, these controllers are global, there performances decrease as the size of the uncertainties interval increases. Moreover, they do not explicitly consider the non-negativity constraints on the manipulated variables [106].

In order to take into account positivity and boundedness constraints of the manipulated control input (dilution rate), Antonelli and his coauthors [115], [116] have proposed a nonlinear output feedback PI control law to stabilize the temperature of a certain class of chemical reactors. Likewise, for the same class of systems and same objective, Viel and his coauthors [117] have designed state feedback controllers that were able to globally stabilize the temperature at an arbitrary set point in spite of uncertainties on the kinetics. The same authors have proven that inclusion of robust state observer to estimate the missing parameters for the control does not impair the nominal stabilization properties of the controllers. But the study was only for lower bounds constraints on the input.

Further, input to output linearising control based on the use of geometrical tools [118] has been proposed in [88]. We insist to say that this control, is different from the linearizing control discussed earlier ([32], [107], ...). Indeed, the approach, herein, is of the same philosophy as the approach used to design the high gain observer. Where, under some conditions, the differential geometry allows to transform the nonlinear model into a partially or totally linear one, by means of a nonlinear state transformation. When only partial information of the state variables is available, the input to output linearising control has been completed by the use of different types of state observers, ranging from high gain observer [119] to Extended Luenberger Observer (ELO) [120]. Moreover, to deal with the saturation constraints on the control input, antiwindup schemes have been, repeatedly, introduced in the closed loop system [119], [121], [89], [122], [123], [120]. Finally, to prove the practical stability of the system, the authors used the tools stated in [124]. Suitable regulation results have been obtain by using the input to output linearizing control. However, the control relies on an exact inversion of the AD model, and thus the magnitude on the control action can be high under some disturbances with certain frequency components. This means that we can not set a satisfactory tradeoff between robust regulation and low magnitude control action [125].

Expert systems (rule based systems) have also been applied to the AD processes with success [126], [127], [101], [128]. But, the stability of the closed loop can not be proved. Similarly, relying on proper data, good results have been obtained by using neural network controls [129], [130]. However, these controls can not be applied to a full scale plant, because a huge data is needed to train the neural network, and very often, it is not possible to obtain data covering all the range of operating conditions [91]. Other advanced controllers have been designed for the AD processes, we refer the reader to the excellent review [131].

Recently, Model Predictive Control (MPC) has been proposed to adapt the biogas production according to a fluctuating timetable of energy demand [132]. In other words, the set point (reference) of the system output (in this case biogas flow) varies with respect to the requested energy from the power grid. Thus, the control input (feeding rate) is computed by the MPC so that the system output follows the reference scenario. This controller has been validated by Full-scale experiments and has shown promising results. However, the analytic stability of the closed loop system can not be performed. Therefore, using the same idea, we will propose in Chapter 4, a control scheme to track a reference trajectory. As well as the timetable in [132], the reference trajectory will be planed according to the user objectives. In order to account for the partial measurements of the state variables, we will include the nonlinear observer that will be designed in Chapter 3 in the controller design. The stability of the closed loop system will be performed by using the Barbalat's lemma [133], [134] and the tools used in Chapter 3, DMVT, LPV and LMIs techniques.

1.1 Aim and Objectives

The main objectives of the present thesis are

- Design of modelling framework which promotes the integration of biogas plants in virtual power plants.
- Development of state observers (software sensors) for the AD models.
- Synthesis of adequate control strategies to stabilize the AD reactor and enhance the biogas production.

1.2 Main Contributions of the Thesis

In order to promote the integration of biogas plants in the power grid, we have proposed a modelling framework where we introduce additional control inputs [90], [135]. These added inputs reflect the addition of stimulating substrates which contribute in the enhancement of both, biogas quantity and quality [22], [105], [66].

Moreover, due to the lack of monitoring that the AD applications at industry scale experience [116], the highly nonlinear dynamics of AD models [59], and the exposition of AD processes, in reality, to measurement and dynamic disturbances [45], we have designed robust nonlinear observers to monitor the evolution of the internal state of the digester [136], [137]. Actually, this is the main contribution of the thesis. We have developed, indeed, new methods to design nonlinear observers, for the AD models, providing non-restrictive synthesis conditions [138]. The idea is based on the use of the Differential Mean Value Theorem (DMTV) which allows the transformation of the nonlinear estimation error to a Linear Parameter Variant (LPV) system. Then, using the LPV techniques we have synthesised the stability conditions in the form of Linear Matrix Inequalities (LMIs). We stress out that the feasibility of the obtained LMI conditions was enhanced due to a use of a suitable reformulation of the Young's inequality. Moreover, we have generalized the designed observers to the case of nonlinear outputs which is, actually, the most encountered case in real plants. In addition to that, we have extended the designed observers to the discrete time, because in real applications the observers are usually driven by sampled data [139], [137].

Finally, using the designed nonlinear observers, we have proposed a control strategy to track a reference trajectory. Indeed, the biogas plant operator can plan for a desired evolution of biogas production, over a time period, to satisfy the power grid demand. This desired evolution is regarded as a reference trajectory for the system. Hence, we have proposed to implement a state feedback control to track the reference trajectory. To account for the lack of measurements, we have included an exponential nonlinear observer in the control design. Therefore, to compute the controller and the observer parameters, we have synthesized LMI conditions to ensure the stability of the closed loop system (composed from the system, controller and the observer). We would like to say that we have proposed two different methods to compute the controller and the observer parameters. In the first one, we propose to compute them separately. While, in the second one we compute the parameters simultaneously.

1.3 Outline of the Thesis

The present thesis is composed of four chapters organised as the following

- In chapter 1, we will present the elected model to work on. Then, we will perform a slight modification to the elected model in order to render it suitable for the control of biogas quantity and quality. After, doing the modification, we will analyse the positiveness and the boundedness of the model state variables.
- In Chapter 3, we will present the designed nonlinear observers in a general way for some specific class of nonlinear systems. Then, we will apply them to the AD model provided in Chapter 2.
- In Chapter 4, we will synthesize observer-based control strategy which allows the AD process to track a reference trajectory.

List of Publications

Refereed international conferences:

- K.Chaib Draa, H. Voos, M. Darouach, M. Alma (2015, March). A Formal Modeling Framework for Anaerobic Digestion Systems. IEEE UKSim-AMSS International Conference on Modelling and Simulation, UKSIM'15, Cambridge, UK.
- K.Chaib Draa, H. Voos, M. Alma, M. Darouach (2015, May). Adaptive Control of the Methane Flow Rate in Biogas Plants. IEEE International Conference on Control, Engineering and Information Technology, CEIT'15, Tlemcen, Algeria.
- K.Chaib Draa, H. Voos, M. Alma, M. Darouach (2015, September). Linearizing Control of Biogas Flow Rate and Quality. IEEE International Conference on Emerging Technologies and Factory Automation, ETFA'15, Luxembourg, Luxembourg.
- K.Chaib Draa, H. Voos, M. Alma, M. Darouach (2016, September). Invariant Observer Applied to Anaerobic Digestion Model. IEEE International Conference on Emerging Technologies and Factory Automation, ETFA'16, Berlin, Germany.
- K. Chaib Draa, H. Voos, M. Alma, A. Zemouche, M. Darouach (2017, May). LMI-Based Discrete-Time Nonlinear State Observer for an Anaerobic Digestion Model. IEEE International Conference on Systems and Control, ICSC'17, Batna, Algeria.
- K. Chaib Draa, H. Voos, M. Alma, A. Zemouche, M. Darouach (2017, July). LMI-Based $\mathcal{H}_\infty$ Nonlinear State Observer Design for Anaerobic Digestion Model. IEEE Mediterranean Conference on Control and Automation, Med'17, Valletta, Malta.
- K. Chaib Draa, H. Voos, M. Alma, A. Zemouche, M. Darouach (2017, July). LMI-Based Invariant Like Nonlinear State Observer for Anaerobic Digestion Model. IEEE Mediterranean Conference on Control and Automation, Med'17, Valletta, Malta.

- K. Chaib Draa, H. Voos, M. Alma, A. Zemouche, M. Darouach (2017, July). An LMI-Based $\mathcal{H}_\infty$ Discrete-Time Non Linear State Observer Design for an Anaerobic Digestion Model. World Congress of the International Federation of Automatic Control, IFAC'17, Toulouse, France.

National colloquiums and posters

- K.Chaib Draa, H. Voos, M. Alma, M. Darouach (2016, October). Invariant Observer Applied to Anaerobic Digestion Model. Annual PhD students conference IAEM Lorraine 2016, APIL'16, Nancy, France.
- K.Chaib Draa, H. Voos, M. Alma, M. Darouach (2017, April). Integration of Biogas Plants in the Power Grid. 4$^{\text{th}}$ International Symposium: Energy & City of the Future, EVF'17, Longwy, France.

Chapter 2

Anaerobic Digestion Modelling

2.1 Introduction

Anaerobic digestion (AD) is one of the most optimal ways to convert organic waste into useful energy, such as methane-rich biogas and fertilizer products [11], [12], [13]. However, it is a complex biochemical process where combinations of chemical and physico-chemical reactions occur in series and/ or in parallel, involving different survival species which are responsible for degradation of the organic matter (proteins, fats and carbohydrates) into biogas. Hence, due to the complexity of the process it may, unfortunately, exhibit some instability behaviour and fail in the production of an energetic biogas. The reason why research related to the modelling and knowledge of the process for understanding the behaviour of the microbial organisms and improving it has a long track in the literature. Indeed, the process modelling has been complicated as long as perception of the different bacteria species and substrates has been. Therefore, an important step in dealing with AD processes is to choose a certain description level of the process, that is usually guided by the application objectives.

In our research, as already mentioned at the beginning of the manuscript, we target to enhance the control of biogas production and more precisely the methane production while, of course, preserving the plant stability. Thus, among all the existing AD models in the literature, we have focussed our attention on those including the methanogenesis step.

A simple model as the one of Andrews [25] could be sufficient to predict production of methan, however it was not selected because it does not include production of VFA, which is often used as an indicator for the digester stability. Therefore, two-step models have been found to be more suited for our application. Among the suitable two-step models in the literature [32], [108], [42], [22], [24], the AM2 model [4] has been elected because it was validated with riche data information extracted from a real plant, and moreover it was compared to the AD benchmark model "ADM1" and has shown good prediction results.

Therefore, we will present in the next section the AM2 model. Then, we will perform a slight modification to the AM2 model in order to adapt it to some research objectives. Later, we will explain how its parameters should be identified. Further, we will investigate the positiveness and boundedness of the resulted model state variables and finally, we will conclude the chapter.

2.2 AM2 Model

The AM2 model is a synthetic mass balance model which has been developed in the AMOCO project [4]. This model is suited for control and design of software sensors for the AD process. The AM2 model is a two step model like those designed in [42], [43], [24], and the references therein, which are all suited for control and observer design. However, the AM2 model has the advantage of being compared with sucesss to the ADM1, which is considrred as the reference for AD modelling. The intefarce between the AM2 and the ADM1 is provided in Appendix B.

In the AM2 model, acidogenesis and methanogenesis are supposed to be the rate limiting steps:

1. Acidogenesis with reaction rate $r_1 = \mu_1 x_2$

$$k_1 x_1 \stackrel{r_1}{\rightarrow} x_2 + k_2 x_3 + k_4 co_2 \tag{2.1}$$

2. Methanogenesis with reaction rate $r_2 = \mu_2 x_4$

$$k_3 x_3 \stackrel{r_2}{\rightarrow} x_4 + k_5 co_2 + k_6 ch_4 \tag{2.2}$$

where in the first step (2.1), acidogenic bacteria (x_2) consume organic substrate (x_1) and produce VFA (mainly composed of acetate, propionate and butyrate) and co_2. In the second step (2.2), methanogenic bacteria (x_4) consume the produced VFA (x_3) for growth and produce co_2 and methane (ch_4).

Assuming that the reactor is perfectly stirred (biomass uniformly distributed in the reactor), the organic substrate (x_1) is available in dissolved form, the pH and temperature (T) range between 6 to 8 and 35° C to 38° C, respectively, and finally VFA (x_3) behave like pure acetate. Bernard and his co-authors [4], modelled the reactions (2.1) and (2.2) by (for writing transparency, dependence of variables in time (t) will be omitted except when it can lead to confusion)

$$\begin{aligned}
\dot{x}_1 &= u(S_{1in} - x_1) - k_1\mu_1(x_1)x_2 \\
\dot{x}_2 &= (\mu_1(x_1) - \alpha u)x_2 \\
\dot{x}_3 &= u(S_{2in} - x_3) + k_2\mu_1(x_1)x_2 - k_3\mu_2(x_3)x_4 \\
\dot{x}_4 &= (\mu_2(x_3) - \alpha u)x_4 \\
\dot{x}_5 &= u(C_{in} - x_5) + k_4\mu_1(x_1)x_2 + k_5\mu_2(x_3)x_4 - q_c(x) \\
\dot{x}_6 &= u(Z_{in} - x_6)
\end{aligned} \tag{2.3}$$

with, the growth rate functions $\mu_1(x_1)$ and $\mu_2(x_3)$ of type Monod and Haldane, respectively:

$$\begin{cases} \mu_1(x_1) = \overline{\mu}_1 \frac{x_1}{x_1 + k_{s1}} \\ \\ \mu_2(x_3) = \overline{\mu}_2 \frac{x_3}{x_3 + k_{s2} + \frac{x_3^2}{k_{i2}}} \end{cases} \tag{2.4}$$

where the state vector $x = [x_1, x_2, x_3, x_4, x_5, x_6]^T$ and the control input $u = \frac{q_{in}}{v}$ (day^{-1}), q_{in} is the feeding flow rate to the digester and v is the later volume (assumed to be constant). Moreover, S_{1in}, S_{2in}, C_{in} and Z_{in} are the input concentrations of the fed waste. In addition to the states $x_1 - x_4$ included in the chemical reactions (2.1) and (2.2), the states x_5 (inorganic carbon) and x_6 (digester alkalinity) have been added to give more information about the digester and thus help for its monitoring and control.

They are related by an on-line and easily done measurement (pH) as the following

$$\begin{cases} bic = x_6 - x_3 \\ \\ co_2 = x_5 - bic \\ \\ k_b = \frac{[H^+]bic}{co_2} \\ \\ pH = -\log_{10}(k_b \frac{co_2}{bic}) \end{cases} \tag{2.5}$$

where k_b is the acidity constant of bicarbonates (bic).

In equations (2.3), $q_c(x)$ represents the co_2 gas flow rate

$$\begin{cases} q_c(x) = k_{La}[x_5 + x_3 - x_6 - K_H P_C(x)] \\ \\ P_C(x) = \frac{\phi - \sqrt{\phi^2 - 4K_H P_T(x_5 + x_3 - x_6)}}{2K_H} \\ \\ \phi = x_5 + x_3 - x_6 + K_H P_T + \frac{k_6}{k_{La}\mu_2(x_3)x_4} \end{cases} \tag{2.6}$$

The methane (ch_4) is supposed to be very lightly soluble, and is instantly found in the gas phase, its flow rate is given by

$$q_m(x) = k_6 \mu_2(x_3) x_4 \tag{2.7}$$

Finally biogas flow rate is assumed to be the sum of co_2 and ch_4 flow rates

$$q_g(x) = q_m(x) + q_c(x) \tag{2.8}$$

All used parameters in the previous equations are defined in Table 2.1, and for a detailed mathematical analysis of the model, the reader is referred to [23].

Both flow rate and quality of biogas are important. An energetic biogas is a biogas which is rich in methane, and thus it is important to control percentage of methane in the produced biogas. In the AM2 model, it is assumed that biogas is only composed of co_2 and ch_4, and thus from the content of biogas in co_2 we can deduce its content in ch_4 and vice versa. From equations (2.3), (2.6), (2.7) and (2.8), we deduce the content of

TABLE 2.1: Parameters of the AM2 Model.

Acronyms	Definition	Units
α	Proportion of dilution rate for bacteria	mmol/l
k_1	Yield for substrate (x_1) degradation	$g/(g$ of $x_2)$
k_2	Yield for VFA (x_3) production	mmol/(g of x_2)
k_3	Yield for VFA consumption	mmol/(g of x_4)
k_4	Yield for co_2 production	mmol/g
k_5	Yield for co_2 production	mmol/g
k_6	Yield for ch_4 production	mmol/g
$\overline{\mu}_1$	Maximum acidogenic bacteria (x_2) growth rate	1/day
$\overline{\mu}_2$	Maximum methanogenic bacteria (x_4) growth rate	1/day
k_{s_1}	Half saturation constant associated with x_1	g/l
k_{s2}	Half saturation constant associated with x_3	mmol/l
k_{i2}	Inhibition constant associated with x_3	mmol/l
k_b	Acidity constant of bicarbonate	mol/l
K_H	Henry s constant	mmol/($l.atm$)
k_{La}	Liquid/gas transfer constant	1/day
P_T	Total preasure	atm
T	Temperature	Kelvin

biogas in co_2, $\%co_2 = \frac{q_c(x)}{q_g(x)}$:

$$\%co_2 = \frac{k_{La}\left[x_5 + x_3 - x_6 - \frac{\phi - \sqrt{\phi^2 - 4K_H P_T(x_5+x_3-x_6)}}{2}\right]}{k_{La}\left[x_5 + x_3 - x_6 - \frac{\phi - \sqrt{\phi^2 - 4K_H P_T(x_5+x_3-x_6)}}{2}\right] + k_6\mu_2(x_3)x_4} \tag{2.9}$$

When the objective is to optimize operation of biogas plants in order to integrate them in Virtual Power Plants (VPPs), both quantity (2.8) and quality (2.9) of the produced biogas become key parameters to control. Therefore, we propose in the next section a formal modelling framework, where we slightly modify the AM2 model in order to adapt it to some research objectives.

2.3 Formal Modelling Framework

In the last few decades, AD process control has attracted much attention in academic research. Generally, we find in the literature many papers dealing with the control of biogas quantity, where repeatedly the dilution rate (waste flow rate divided by the digester volume) is the controlled variable [108], [32], [140], [126], [87], [101], [22]. However, the dilution rate can range only in a small interval for stability and plant infrastructure (waste storage capacity) issues. In addition to that, some biogas plants are constrained, by internal rules, to treat a certain quantity of waste per day. Therefore, an alternative solution to control biogas flow rate by addition of stimulating acetate to the feeding influent was proposed in [105]. Nevertheless, accumulation of accids may break down the pH in the digester and causses its failure, especially when the digester buffering capacity is low. Hence, usually addition of acetate is accompanied by an increase of the fed waste pH (increase until $pH = 8.5$ [66]). This may be done by addition of bicarbonates to the fed waste. However, often the way the pH is increased is not optimal since it does not take into account the dynamics of inorganic carbon and alkalinity inside the reactor.

Regarding, the biogas quality, it is influenced by the buffering capacity of the digester. Indeed, after addition of carbonate salts or strong bases to the digester, the co_2 is removed from the gas phase. Actually, it has been shown in [22], [42], [141] that an increase of bicarbonate alkalinity in the digester leads to an increase of pH, this promotes the dissolution of the gaseous co_2 in order to elaborate equilibrium with the dissolved co_2 and thus enhance the biogas quality.

Combining the two ideas, from the literature, of adding stimulating acids to control the biogas quantity and simulating bases to enhance the biogas quality, we slightly modify the AM2 model to include the addition of stimulating substrates. Indeed, we propose in the following to add more degree of freedom in control of AD process while respecting the storage constraints and preserving the digester safety as depicted in Figure 2.1. Moreover, we insist to specify that addition of the stimulating substrates (acetate $C_2H_3O_2^-$) and basses (sodium hydroxide $NaOH$) is included directly in the model in order to account for its effect in all process state variables, and optimize it. Hereafter, we give the mass balance equations required for modelling

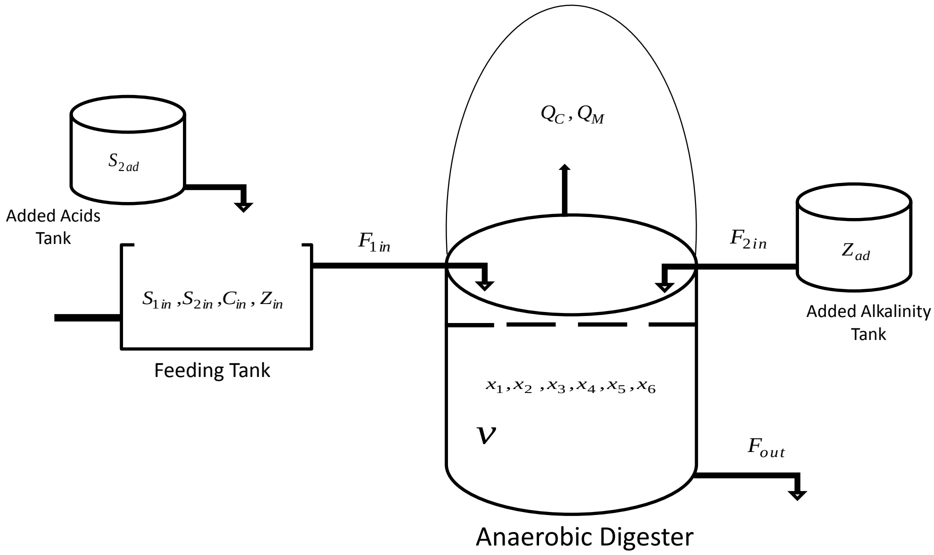

Figure 2.1: Scheme of a Proposed strategy for Controlling the Anaerobic Digestion Process.

$$
\begin{aligned}
\frac{dv}{dt} &= F_{1in} + F_{2in} - F_{out} \\
\frac{dx_1 v}{dt} &= -k_1\mu_1(x_1)x_2 v + F_{1in}S_{1in} - F_{out}x_1 \\
\frac{dx_2 v}{dt} &= (\mu_1(x_1)v - \alpha F_{out})x_2 \\
\frac{dx_3 v}{dt} &= k_2\mu_1(x_1)x_2 v - k_3\mu_2(x_3)x_4 v + F_{1in}(S_{2in} + S_{2ad}) - F_{out}x_3 \\
\frac{dx_4 v}{dt} &= (\mu_2(x_3)v - \alpha F_{out})x_4 \\
\frac{dx_5 v}{dt} &= k_4\mu_1(x_1)x_2 v + k_5\mu_2(x_3)x_4 v + F_{1in}C_{in} - F_{out}x_5 - q_c(x)v \\
\frac{dx_6 v}{dt} &= F_{1in}Z_{in} + F_{2in}Z_{ad} - F_{out}x_6
\end{aligned}
\tag{2.10}
$$

where the state vector $x = [x_1, x_2, x_3, x_4, x_5, x_6]^T$.

We have

$$\frac{dxv}{dt} = x\frac{dv}{dt} + v\frac{dx}{dt}$$

and let us define $u_1 = \frac{F_{1in}}{v}$, $u_2 = \frac{F_{2in}}{v}$ and $u_{out} = \frac{F_{out}}{v}$. Thus, when the digester volume is kept constant ($F_{out} = F_{1in} + F_{2in}$), we obtain the following model

$$\begin{aligned}
\dot{x}_1 &= -k_1\mu_1(x_1)x_2 + u_1 S_{1in} - u_{out}x_1 \\
\dot{x}_2 &= (\mu_1(x_1) - \alpha u_{out})x_2 \\
\dot{x}_3 &= k_2\mu_1(x_1)x_2 - k_3\mu_2(x_3)x_4 + u_1(S_{2in} + S_{2ad}) - u_{out}x_3 \\
\dot{x}_4 &= (\mu_2(x_3) - \alpha u_{out})x_4 \\
\dot{x}_5 &= k_4\mu_1(x_1)x_2 + k_5\mu_2(x_3)x_4 + u_1 C_{in} - u_{out}x_5 - q_c(x) \\
\dot{x}_6 &= u_1 Z_{in} + u_2 Z_{ad} - u_{out}x_6
\end{aligned} \tag{2.11}$$

with $\mu_1(x_1)$, $\mu_2(x_3)$, q_m and q_c the same as defined in (2.4), (2.7) and (2.6), respectively. Moreover, all used parameters are the same as those defined in Table 2.1 for the AM2 models.

2.4 About the Parameters Identification

Complexity and particularity of AD models give arise to certain considerations when dealing with their parameters identification. Indeed, investigations on parameters identifiability have reported that the AD models are not practically identifiable [142], [105], [32], [143], in other words a very good fit between the model and measurements can be obtained with different values of parameters. Besides, the identifiability problem is difficult to solve due to the number of parameters to be identified, and moreover real experimental data is often corrupted by unknown noise characteristics [144]. Therefore, identification becomes meaningful only when uniqueness of the obtained parameters can be proved. Thus, facing the structural identifiability issue, Bernard and his coauthers [4] have proposed a systematic step-by-step identification procedure. Actually, taking advantage from the cascade structure of the model, the parameters were classified in different groups in order to identify them as independently as possible from each another. Indeed, the structural identifiability was possible to prove due to the use of steady state equations. We would like to say that even tough parameters identification was performed at the steady state, this did not prevent the model to reproduce properly the transitory behaviour [4], [22], [23], [145].

The same identification procedure reported in [4] can be applied to the system (2.11), where the first group of parameters to be identified is the kinetic parameters (k_{s1}, k_{s2}, k_{i2}, $\overline{\mu}_1$, $\overline{\mu}_2$) while the second group concerns the yield coefficients (k_i, $i = 1 \dots 6$). We will illustrate by an example of estimating the kinetic parameters how this methodology is applied.

Usually, biological processes exhibit multiple equilibrium states, if we do not consider the washout of bacteria steady state ($x_2 = 0$ and/or $x_4 = 0$), then the steady states of the system (2.11) are given by the following equations

$$
\begin{cases}
\mu_1(x_1) = \alpha u_{out} & (2.12a) \\
\mu_2(x_3) = \alpha u_{out} & (2.12b) \\
x_1^* = k_{s1} \dfrac{\alpha u_{out}}{\overline{\mu}_1 - \alpha u_{out}} & (2.12c) \\
x_2^* = \dfrac{1}{\alpha k_1} \left(\dfrac{u_1}{u_{out}} S_{1in} - x_1^* \right) & (2.12d) \\
x_3^{*2} + \left(k_{i2} - \dfrac{\overline{\mu}_2 k_{i2}}{\alpha u_{out}} \right) x_3^* + k_{s2} k_{i2} = 0 & (2.12e) \\
x_4^* = \dfrac{1}{k_3} \left(\dfrac{u_1}{\alpha u_{out}} S_{2in} - \dfrac{x_3^*}{\alpha} + k_2 x_2^* \right) & (2.12f) \\
x_5^* = \alpha k_4 x_2^* + \alpha k_5 x_4^* + \dfrac{u_1}{u_{out}} C_{in} - q_c(x^*) & (2.12g) \\
x_6^* = \dfrac{u_1 Z_{in} + u_2 Z_{ad}}{u_{out}} & (2.12h) \\
q_m = \alpha k_6 u_{out} x_4^* & (2.12i)
\end{cases}
$$

where the solutions of equation (2.12e) are

$$
\begin{cases}
x_3^{*1} = \frac{1}{2} \frac{(\overline{\mu}_2 - \alpha u_{out}) k_{i2} - \sqrt{\left((\overline{\mu}_2 - \alpha u_{out})^2 k_{i2} - 4 k_{s2} \alpha^2 u_{out}^2 \right)^2 k_{i2}}}{\alpha u_{out}} \\
\\
x_3^{*2} = \frac{1}{2} \frac{(\overline{\mu}_2 - \alpha u_{out}) k_{i2} + \sqrt{\left((\overline{\mu}_2 - \alpha u_{out})^2 k_{i2} - 4 k_{s2} \alpha^2 u_{out}^2 \right)^2 k_{i2}}}{\alpha u_{out}}
\end{cases}
\tag{2.13}
$$

where only the smaller solution is physically meaningful.

Suppose that some state variables are available for measurement and that the experimental conditions cover a wide range of expected operating situations. Let us denote the mean value at steady state of x_1, x_3 by $\overline{x}_1$, $\overline{x}_3$, respectively. Thus, from equations (2.4), (2.12a) and (2.12b) we have

$$\frac{1}{u_{out}} = \frac{\alpha}{\overline{\mu}_1} + k_{s1}\frac{\alpha}{\overline{\mu}_1}\frac{1}{\overline{x}_1} \tag{2.14}$$

equation (2.14) contains an operational parameter u_{out} and the measurements $\overline{x}_1$ wich are both known, thus using linear regression we identify $\frac{\alpha}{\overline{\mu}_1}$ and k_{s1}. However, unfortunately the parameters α and $\overline{\mu}_1$ cannot be distinguished by using equation (2.14), thus the parameter $\overline{\mu}_1$ will be fixed from the literature [4].

Similarly from the same equations (2.4), (2.12a) and (2.12b), we obtain the following relationship

$$\frac{1}{u_{out}} = \frac{\alpha}{\overline{\mu}_2} + k_{s2}\frac{\alpha}{\overline{\mu}_2}\frac{1}{\overline{x}_3} + \frac{1}{k_{i2}}\frac{\alpha}{\overline{\mu}_2}\overline{x}_3 \tag{2.15}$$

which by using linear regression and the estimated value of α from the previous step, gives the parameters k_{i2}, k_{s2} and $\overline{\mu}_2$.

Following the same philosophy, all model parameters can be identified when the required measurements are available. For more details related to this issue, we refer the reader to [4], [22], [23], [145]. In what follows, we will use the parameter values provided in [4] because we do not hold measurements for the proposed framework. However, in order to obtain convenient results we will take u_2 much more smaller than u_1, and moreover the term $S_{2in} + S_{2ad}$ can be viewed as a controllable input $\tilde{S}_{2in}$ in the model (2.3).

2.5 Model Analysis

In this section, while analysing the model (2.11), we will consider that all model parameters $(k_i, k_{La}, ..\ k_6)$ are known and constant, and moreover, we suppose that the following assumptions hold[1]

A1. All the input concentrations $(S_{1in}, S_{2in}, C_{in}, Z_{in})$ have a maximum noted $\overline{X}_{in}$, such that $S_{1in} \leq \overline{S}_{1in}$, $S_{2in} \leq \overline{S}_{2in}$, $C_{in} \leq \overline{C}_{in}$, and $Z_{in} \leq \overline{Z}_{in}$.

[1] We point out that the undertaken assumptions are logical and commonly assumed in biological processes.

A2. The added input concentrations S_{2ad}, Z_{ad} are bounded: $(0,0) \leq (S_{2ad}, Z_{ad}) \leq (\overline{S}_{2ad}, \overline{Z}_{ad})$

A3. The control variables u_1 and u_2 are positive and thus:
$\forall T > 0$, $\forall t \geq 0$, $\int_t^{t+T} u_{out}(\tau)\, \mathrm{d}\tau \geq 0$

A4. The vector of initial conditions belongs to the positive orthant: $x(0) \in R_+^6$ and moreover $x_1(0) \leq \overline{S}_{1in}$

2.5.1 Positiveness of state variables

The state vector x in equations (2.11) represents, physically, chemical concentrations which have to be positive. Thus, we have to prove mathematically the positiveness of $x(t)$. For this end we recall the following definition and theorem:

Definition 1. Positive System
A dynamic system $\dot{x}(t) = f(x(t), u(t))$ is a positive system if, for any admissible input $u(t)$ the state vector $x(t)$ is confined to the positive orthant when the initial state is positive:

$$x(t_0) \in \mathbb{R}_+^n \text{ and } u(t) \in \mathcal{U} \Rightarrow x(t) \in \mathbb{R}_+^n \quad \forall t \geq t_0$$

Theorem 1. *[146] A dynamic system $\dot{x} = f(x, u)$ is a positive system if $f(x, u)$ is a differentiable function and if*

$$x \in \mathbb{R}_+^n \text{ and } x_i = 0 \Rightarrow \dot{x}_i \geq 0 \forall i$$

Using equations (2.11), (2.4) and (2.5), and taking into account the earlier mentioned assumptions, we can easily verify that Theorem 1 is satisfied. Therefore, $x(t) \in \mathbb{R}_+^6$.

After the positiveness of the state vector has been checked, we deal now with the boundedness of each state variable.

2.5.2 Boundedness of variable x_1

From equations (2.11), we have

$$\dot{x_1} = -k_1\mu_1(x_1)x_2 + u_1 S_{1in} - u_{out} x_1$$

Being given $k_1\mu_1(x_1)x_2 \geq 0$, we get

$$\dot{x_1} \leq u_1 S_{1in} - u_{out}x_1 \tag{2.16}$$

Let us add $u_2 S_{1in} \geq 0$ to right hand side of the inequality, we obtain

$$\dot{x_1} + u_{out}x_1 \leq u_{out}S_{1in} \tag{2.17}$$

Multiplying both sides of the inequality by $e^{\int_0^t u_{out}(\tau)\,\mathrm{d}\tau}$:

$$\dot{x_1}e^{\int_0^t u_{out}(\tau)\,\mathrm{d}\tau} + x_1 u_{out}e^{\int_0^t u_{out}(\tau)\,\mathrm{d}\tau} \leq S_{1in}u_{out}e^{\int_0^t u_{out}(\tau)\,\mathrm{d}\tau} \tag{2.18}$$

Based on the undertaken assumptions, we can also write

$$\dot{x_1}e^{\int_0^t u_{out}(\tau)\,\mathrm{d}\tau} + x_1 u_{out}e^{\int_0^t u_{out}(\tau)\,\mathrm{d}\tau} \leq \overline{S}_{1in}u_{out}e^{\int_0^t u_{out}(\tau)\,\mathrm{d}\tau} \tag{2.19}$$

Now, we integrate the inequality from 0 to t:

$$\int_0^t \left(\dot{x_1}(tt)e^{\int_0^{tt} u_{out}(\tau)\,\mathrm{d}\tau} + x_1(tt)u_{out}(tt)e^{\int_0^{tt} u_{out}(\tau)\,\mathrm{d}\tau}\right)\mathrm{d}tt \leq \overline{S}_{1in}\int_0^t \left(u_{out}(tt)e^{\int_0^{tt} u_{out}(\tau)\,\mathrm{d}\tau}\right)\mathrm{d}tt \tag{2.20}$$

we directly obtain

$$x_1(t)e^{\int_0^t u_{out}(\tau)\,\mathrm{d}\tau} - x_1(0) \leq \overline{S}_{1in}[e^{\int_0^t u_{out}(\tau)\,\mathrm{d}\tau} - 1] \tag{2.21}$$

Multiplying both sides by $e^{-\int_0^t u_{out}(\tau)\,\mathrm{d}\tau}$:

$$x_1(t) \leq x_1(0)e^{-\int_0^t u_{out}(\tau)\,\mathrm{d}\tau} + \overline{S}_{1in}[1 - e^{-\int_0^t u_{out}(\tau)\,\mathrm{d}\tau}] \tag{2.22}$$

We can also write

$$x_1(t) \leq (x_1(0) - \overline{S}_{1in})e^{-\int_0^t u_{out}(\tau)\,\mathrm{d}\tau} + \overline{S}_{1in}$$

Hence two cases are possible, if $u_{out}(\tau) = 0$:

$$x_1(t) \leq x_1(0) \tag{2.23}$$

otherwise $0 \leq e^{-\int_0^t u_{out}(\tau)\,\mathrm{d}\tau} < 1$ and thus

$$x_1(t) \leq \overline{S}_{1in} \tag{2.24}$$

because $x_1(0) - \overline{S}_{1in} \leq 0$ from assumption **A3**. Since $x_1(0) \leq \overline{S}_{1in}$ we retain equation (2.24) as the upper bound of $x_1(t)$.

2.5.3 Boundedness of variable x_2

First of all, let us define

$$\xi_1 = x_1 + k_1 x_2 \tag{2.25}$$

whose dynamic is given by

$$\dot{\xi}_1 = u_1 S_{1in} - u_{out} x_1 - \alpha k_1 u_{out} x_2 \tag{2.26}$$

We know that $0 < \alpha \leq 1$ and $S_{1in} \leq \overline{S}_{1in}$, thus

$$\dot{\xi}_1 \leq u_1 \overline{S}_{1in} - \alpha u_{out} x_1 - \alpha k_1 u_{out} x_2 \tag{2.27}$$

$$\dot{\xi}_1 \leq u_1 \overline{S}_{1in} - \alpha u_{out} \xi_1$$

Adding $u_2 \overline{S}_{1in} \geq 0$ to right hand side of the equality, we obtain

$$\dot{\xi}_1 \leq \alpha u_{out} \Big(\frac{\overline{S}_{1in}}{\alpha} - \xi_1 \Big)$$

$$\dot{\xi}_1 + \alpha u_{out} \xi_1 \leq \alpha u_{out} \Big(\frac{\overline{S}_{1in}}{\alpha} \Big) \tag{2.28}$$

Multiplying both sides of the inequality by $e^{\int_0^t \alpha u_{out}(\tau)\,\mathrm{d}\tau}$ and then integrating them from 0 to t (as previously done for the state x_1), we obtain

$$\xi_1(t) e^{\int_0^t \alpha u_{out}(\tau)\,\mathrm{d}\tau} - \xi_1(0) \leq \frac{\overline{S}_{1in}}{\alpha} [e^{\int_0^t \alpha u_{out}(\tau)\,\mathrm{d}\tau} - 1] \tag{2.29}$$

Multiplying both sides by $e^{-\int_0^t \alpha u_{out}(\tau)\,\mathrm{d}\tau}$:

$$\xi_1(t) \leq \Big(\xi_1(0) - \frac{\overline{S}_{1in}}{\alpha}\Big) e^{-\int_0^t \alpha u_{out}(\tau)\,\mathrm{d}\tau} + \frac{\overline{S}_{1in}}{\alpha} \tag{2.30}$$

Since $0 \leq e^{-\int_0^t \alpha u_{out}(\tau)\,\mathrm{d}\tau} \leq 1$, we have

$$\xi_1(t) \leq \max\Big(\xi_1(0), \frac{\overline{S}_{1in}}{\alpha}\Big) \tag{2.31}$$

Now, replacing ξ_1 by its equation (2.25), we get

$$x_1(t) + k_1 x_2(t) \leq \max\Big(x_1(0) + k_1 x_2(0), \frac{\overline{S}_{1in}}{\alpha}\Big) \tag{2.32}$$

Since $x_1(t) \geq 0$ and $x_1(0) \leq \overline{S}_{1in}$ it follows that

$$x_2(t) \leq \max\Big(\frac{\overline{S}_{1in}}{k_1} + x_2(0), \frac{\overline{S}_{1in}}{\alpha k_1}\Big) \tag{2.33}$$

2.5.4 Boundedness of variable x_3

We define a variable ξ_2 by the following equation

$$\xi_2 = x_3 - k_2 x_2 \tag{2.34}$$

whose dynamic is given by

$$\dot{\xi}_2 = -k_3 \mu_2(x_3) x_4 + u_1(S_{2in} + S_{2ad}) - u_{out} x_3 + \alpha k_2 u_{out} x_2 \tag{2.35}$$

Being given $k_3 \mu_2(x_3) x_4 \geq 0$ and $0 \leq \alpha \leq 1$, and $(S_{2in} + S_{2ad}) \leq (\overline{S}_{2in} + \overline{S}_{2ad})$, we can write

$$\dot{\xi}_2 \leq u_1(\overline{S}_{2in} + \overline{S}_{2ad}) - \alpha u_{out} x_3 + \alpha k_2 u_{out} x_2 \tag{2.36}$$

Adding $u_2(\overline{S}_{2in} + \overline{S}_{2ad}) \geq 0$ to the right hand side, we obtain

$$\dot{\xi}_2 \leq \alpha u_{out}\Big(\frac{\overline{S}_{2in} + \overline{S}_{2ad}}{\alpha} - \xi_2\Big)$$

$$\dot{\xi}_2 + \alpha u_{out}\xi_2 \leq \alpha u_{out}\Big(\frac{\overline{S}_{2in} + \overline{S}_{2ad}}{\alpha}\Big) \tag{2.37}$$

Following the same procedure as before (for the previous states), we can easily find

$$\xi_2(t) \leq \max\Big(\xi_2(0), \frac{\overline{S}_{2in} + \overline{S}_{2ad}}{\alpha}\Big) \tag{2.38}$$

Now, we replace ξ_2 by its equation (2.34), we obtain

$$x_3(t) \leq \max\Big(x_3(0) - k_2x_2(0), \frac{\overline{S}_{2in} + \overline{S}_{2ad}}{\alpha}\Big) + k_2x_2(t) \tag{2.39}$$

Using equation (2.33), it holds that

$$x_3(t) \leq \max\Big(x_3(0) - k_2x_2(0), \frac{\overline{S}_{2in} + \overline{S}_{2ad}}{\alpha}\Big) + \max\Big(\frac{k_2\overline{S}_{1in}}{k_1} + k_2x_2(0), \frac{k_2\overline{S}_{1in}}{\alpha k_1}\Big) \tag{2.40}$$

2.5.5 Boundedness of variable x_4

Let us define the variable ξ_3:

$$\xi_3 = k_3x_4 + x_3 - k_2x_2 \tag{2.41}$$

its dynamic is given by

$$\dot{\xi}_3 = -k_3\alpha u_{out}x_4 + u_1(S_{2in} + S_{2ad}) - u_{out}x_3 + k_2\alpha u_{out}x_2 \tag{2.42}$$

Adding $u_2(\overline{S}_{2in} + \overline{S}_{2ad}) \geq 0$ to the right hand side and being given $0 \leq \alpha \leq 1$, we obtain

$$\dot{\xi}_3 \leq \alpha u_{out}\Big(\frac{\overline{S}_{2in} + \overline{S}_{2ad}}{\alpha} - \xi_3\Big)$$

$$\dot{\xi}_3 + \alpha u_{out}\xi_3 \leq \alpha u_{out}\Big(\frac{\overline{S}_{2in} + \overline{S}_{2ad}}{\alpha}\Big) \tag{2.43}$$

As before, following the same procedure we obtain

$$\xi_3(t) \leq \max\Big(\xi_3(0), \frac{\overline{S}_{2in} + \overline{S}_{2ad}}{\alpha}\Big) \tag{2.44}$$

Replacing ξ_3 by its equation (2.41):

$$k_3x_4(t) + x_3(t) - k_2x_2(t) \leq \max\Big(k_3x_4(0) + x_3(0) - k_2x_2(0), \frac{\overline{S}_{2in} + \overline{S}_{2ad}}{\alpha}\Big) \tag{2.45}$$

since $x_3(t) \geq 0$, we have

$$x_4(t) \leq \max\Big(x_4(0) + \frac{x_3(0) - k_2x_2(0)}{k_3}, \frac{\overline{S}_{2in} + \overline{S}_{2ad}}{\alpha k_3}\Big) + \frac{k_2}{k_3}x_2(t) \tag{2.46}$$

Using equation (2.33), the following holds

$$\begin{aligned} x_4(t) \quad \leq \quad & \max\Big(x_4(0) + \frac{x_3(0) - k_2x_2(0)}{k_3}, \frac{\overline{S}_{2in} + \overline{S}_{2ad}}{\alpha k_3}\Big) \\ & + \max\Big(\frac{k_2\overline{S}_{1in}}{k_1k_3} + \frac{k_2}{k_3}x_2(0), \frac{k_2\overline{S}_{1in}}{\alpha k_1k_3}\Big) \end{aligned} \tag{2.47}$$

2.5.6 Boundedness of variable x_5

Let us define the variable ξ_4:

$$\xi_4 = x_5 - k_5x_4 - k_4x_2 \tag{2.48}$$

which has the following dynamic

$$\dot{\xi}_4 = u_1C_{in} - u_{out}x_5 - q_c(x) + k_5\alpha u_{out}x_4 + k_4\alpha u_{out}x_2 \tag{2.49}$$

Adding $u_2\overline{C}_{in} \geq 0$ to the right hand side, we obtain

$$\dot{\xi}_4 \leq u_{out}\overline{C}_{in} - u_{out}x_5 - q_c(x) + k_5\alpha u_{out}x_4 + k_4\alpha u_{out}x_2 \tag{2.50}$$

Being given $q_c(x) \geq 0$ and $0 \leq \alpha \leq 1$:

$$\dot{\xi}_4 \leq \alpha u_{out}\Big(\frac{\overline{C}_{in}}{\alpha} - \xi_4\Big)$$

$$\dot{\xi}_4 + \alpha u_{out}\xi_4 \leq \alpha u_{out}\Big(\frac{\overline{C}_{in}}{\alpha}\Big) \tag{2.51}$$

and thus,

$$\xi_4(t) \leq \max\left(\xi_4(0), \frac{\overline{C}_{in}}{\alpha}\right) \tag{2.52}$$

Using equations (2.33), (2.47) and (2.48), we obtain

$$\begin{aligned} x_5(t) \quad \leq \quad & \max\left(x_5(0) - k_5 x_4(0) - k_4 x_2(0), \frac{\overline{C}_{in}}{\alpha}\right) \\ & + \max\left(k_5 x_4(0) + \frac{k_5(x_3(0) - k_2 x_2(0))}{k_3}, \frac{k_5(\overline{S}_{2in} + \overline{S}_{2ad})}{\alpha k_3}\right) \\ & + \max\left(\frac{k_5 k_2 \overline{S}_{1in}}{k_1 k_3} + \frac{k_2 k_5}{k_3} x_2(0), \frac{k_2 k_5 \overline{S}_{1in}}{\alpha k_1 k_3}\right) \\ & + \max\left(\frac{k_4 \overline{S}_{1in}}{k_1} + k_4 x_2(0), \frac{k_4 \overline{S}_{1in}}{\alpha k_1}\right) \end{aligned} \tag{2.53}$$

2.5.7 Boundedness of variable x_6

We have

$$\dot{x}_6 = u_1 Z_{in} + u_2 Z_{ad} - u_{out} x_6$$

Let us add $u_2 \overline{Z}_{in} + u_1 \overline{Z}_{ad} \geq 0$ to the right hand side, we get

$$\dot{x}_6 \leq u_{out}(\overline{Z}_{in} + \overline{Z}_{ad} - x_6)$$

$$\dot{x}_6 + u_{out} x_6 \leq u_{out}(\overline{Z}_{in} + \overline{Z}_{ad}) \tag{2.54}$$

and thus,

$$x_6(t) \leq \max\left(x_6(0), \overline{Z}_{in} + \overline{Z}_{ad}\right) \tag{2.55}$$

Remark 2. For more clarity in writing regarding each of the equations (2.33, 2.38, 2.40, 2.44, 2.47, 2.52, 2.53) and (2.55), one can simply sum up the bounds of the function max, as for example instead of equation (2.55), one can obtain

$$x_6(t) \leq x_6(0) + \overline{Z}_{in} + \overline{Z}_{ad} \tag{2.56}$$

however, the bounds on each state variable will be larger than what could be found using the proper given equations.

2.6 Simulation Results

Having described and analysed the model in the previous sections, we now proceed to evaluate, by numerical simulation, the effect of the added control inputs on the biogas production. In this section, our intention is not to control the system but to demonstrate what is achievable when stimulating substrates are added to the digester. Therefore, we will compare two case of studies. Firstly, we only increase the acids concentration of the fed waste. Then, we add the alkalinity to the digester as depicted in Figure 2.1. We point out that to run the numerical simulation, we will use the same values of the model parameter as given in [4], reported in Table 2.2.

TABLE 2.2: Model Parameters [4].

Acronyms	Definition	Units	Value
k_1	Yield for substrate (x_1) degradation	$g/(g$ of $x_2)$	42.1
k_2	Yield for VFA (x_3) production	mmol$/(g$ of $x_2)$	116.5
k_3	Yield for VFA consumption	mmol$/(g$ of $x_4)$	268
k_4	Yield for co_2 production	mmol$/g$	50.6
k_5	Yield for co_2 production	mmol$/g$	343.6
k_6	Yield for ch_4 production	mmol$/g$	453
$\overline{\mu}_1$	Maximum acidogenic bacteria (x_2) growth rate	1/day	1.25
$\overline{\mu}_2$	Maximum methanogenic bacteria (x_4) growth rate	1/day	0.74
k_{s_1}	Half saturation constant associated with x_1	g/l	7.1
k_{s2}	Half saturation constant associated with x_3	mmol$/l$	9.28
k_{i2}	Inhibition constant associated with x_3	mmol$/l$	256
k_b	Acidity constant of bicarbonate	mol$/l$	6.5 10^{-7}
K_H	Henry's constant	mmol$/(l.atm)$	27
P_T	Total preasure	atm	1.013
k_{La}	Liquid/gas transfer constant	1/day	19.8

We run the simulation over a range of operating conditions as depicted in Figures 2.2-2.6 and $x(0) = [1.3, 0.5, 6, 0.7, 60.95, 55]^T$. After a period of time (after 32 days), we increase the concentration of the fed waste acids by adding S_{2ad} to S_{2in} as shown in Figure 2.7. We compare, in Figures 2.9-2.18, the response of the system (red dotted line) with the response of the AM2 model (blue dashed line) to the same operating conditions (u_1, S_{1in}, S_{2in}, C_{in} and Z_{in}). As expected the addition of S_{2ad} to the system has no effect on the states x_1 and x_2 (Figures 2.9-2.10) because the system has a cascade structure and S_{2ad} has no effect on the dynamics of the first two states. However, the effect of S_{2ad} on the states x_3 and x_4 is very clear in Figures 2.11-2.12. Indeed, a proper increase of the input acids concentration leads to an increase of the acids concentration in the digester and consequently growth of the methanogenic bacteria which is responsible to convert the acids into methane and co_2. This bacteria growth (increase of the concentration x_4) is naturally followed by an increase of the methane gas flow rate (see Figure 2.15) and consequently increase of the biogas flow rate (see Figure 2.17). Nevertheless, the increase of biogas production depicted in Figure 2.17 is not due to only the increase of methane gas flow rate but also due the increase of co_2 gas flow rate as depicted in Figure 2.16. This is actually due to the pH decrease in the digester which affects the equilibrium between the dissolved and the gaseous co_2 and consequently affects the biogas quality which has been marginally deteriorated as depicted in Figure 2.18. For this simulation, we notice only a slight affect on x_5 and no affect on x_6 as plotted in Figures 2.13 and 2.14. However, the effect could be more visible if the digester pH was more affected.

In the second case of study, we couple the previous study with the addition of alkalinity to the digester. Thus, for the same operating and initial conditions of the previous simulation, the increase of acids input concentration (Figure 2.7) is followed by addition of a stimulating alkalinity $Z_{ad} = 500$ (mmol/l) with dilution rate u_2 depicted in Figure 2.8. In order to better visualise the effect of alkalinity addition along with acids increase on the biogas quantity and quality, we plot the results (green dash dotted line) in Figures 2.9-2.18, where the results of the previous study have been reported. As it can be seen from the first six former figures, all the model state variables have been affected which is normal and expected since the modelling is a mass balance model and the dilution rate u_2 affects all the model dynamics. From the same figures, it can be noticed as well that the substrates concentrations are more than those of the previous simulation and the bacteria species concentrations are less, which is explained by the decreased time of degradation ($u_{out} = u_1 + u_2$) and the increased input concentrations (S_{2ad} and Z_{ad}). Moreover, increase of the alkalinity concentration x_6 is followed by an increase of the digester pH which promotes the dissolution of the gaseous co_2 and therefore increase of the inorganic carbon concentration (see Figures 2.13). Regarding the biogas production, it is increased compared to the AM2 model (blue dashed line) and decreased compared to the previous case of study (see in Figure 2.13). However, we do not consider this decrease in the biogas quantity as a loss in our application. Because, this is a consequence of a just slight decrease in the methane gas (burnable gas) production and a more important decrease in the co_2 gas (non-burnable gas) production as shown in Figures 2.15 and 2.16. For example, in Figure 2.15, when we compare the two case of studies (red dotted line and green dash dotted line) between 32 and 40 days, we see that the biogas production is decreased about 10.6 mmol/l per day which results from a decrease of about only 0.8 mmol/l per day of methane gas production and about 9.8 mmol/l per day of co_2 gas production as depicted in Figures 2.15 and 2.16, respectively. Consequently, the biogas quality is enhanced as it can be seen in Figure 2.18 and thus it is more energetic. Indeed, we can see clearly from the former figure, between 32 and 40 days that the biogas quality passes from 34% to 30% countenance of co_2, which is a considerable enhancement of the biogas quality.

The difference between the two case of studies may seem sometimes slight, yet it has essential consequences for the control of biogas quantity and quality and thus the introduction of biogas plants in the virtual power plant.

2.7 Conclusion

In this chapter, we have presented the reference model for the reduced AD modelling, the AM2 model. Then, we have performed a slight modification to the AM2 model by adding new control inputs. These added control inputs reflect the addition of stimulating substrates, acids and alkalinity. This was motivated by the aim to promote integration of biogas plants in the power grid. Or in other words, to add more degrees of freedom in the control of biogas production. We have also explained, in this chapter, how to identify the model parameters. Finally, we have proved the positiveness and boundedness of the model state variables which will play a crucial role in the observer design and control synthesis, as it will be seen further in the manuscript.

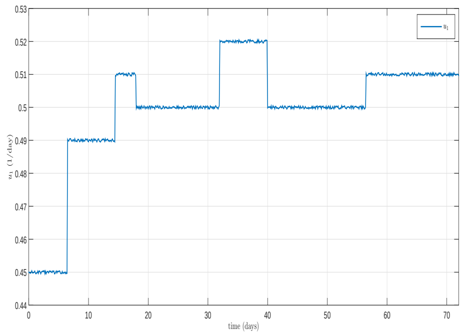

FIGURE 2.2: Control input u_1 (1/day).

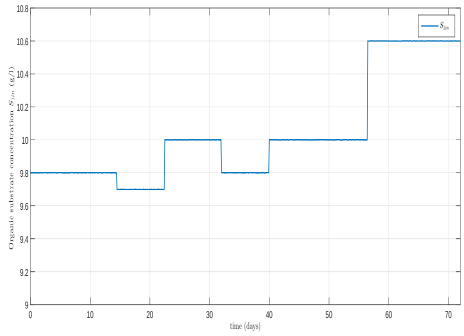

FIGURE 2.3: Input organic substrate concentration S_{1in} (g/l).

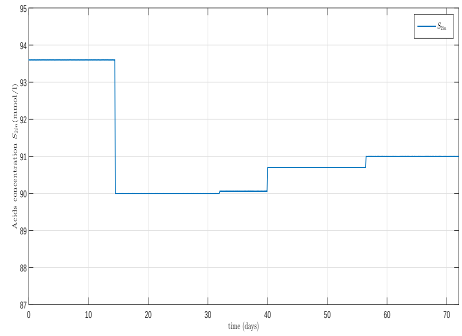

FIGURE 2.4: Input acids concentration S_{2in}(mmol/l).

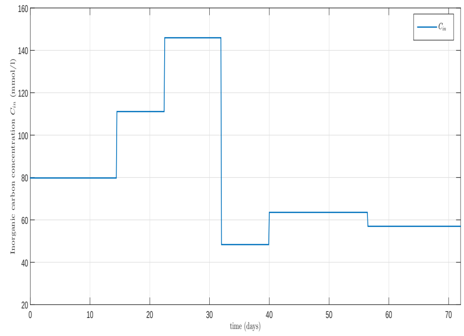

FIGURE 2.5: Input inorganic carbon concentration C_{in} (mmol/l).

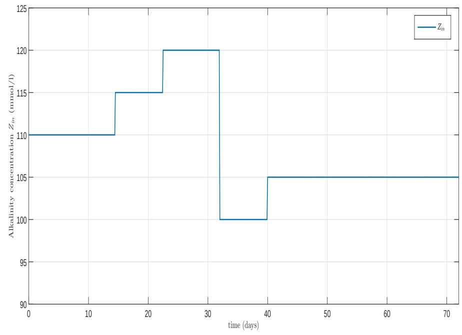

FIGURE 2.6: Input alkalinity concentration Z_{in} (mmol/l).

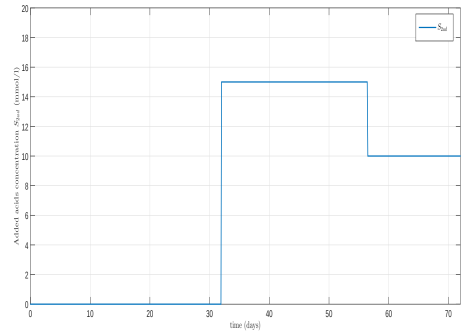

FIGURE 2.7: Added acids concentration S_{2ad} (mmol/l).

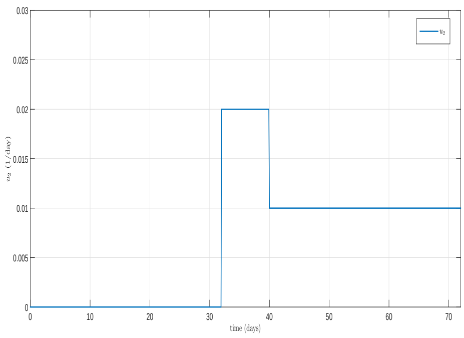

FIGURE 2.8: Control input u_2 (1/day).

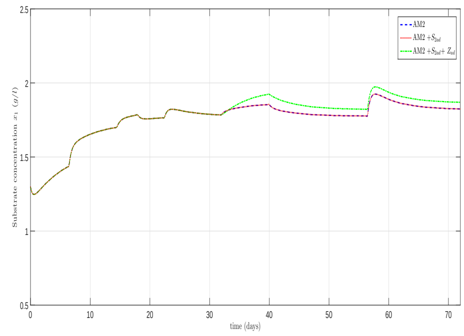

FIGURE 2.9: Organic substrate concentration x_1 (g/l).

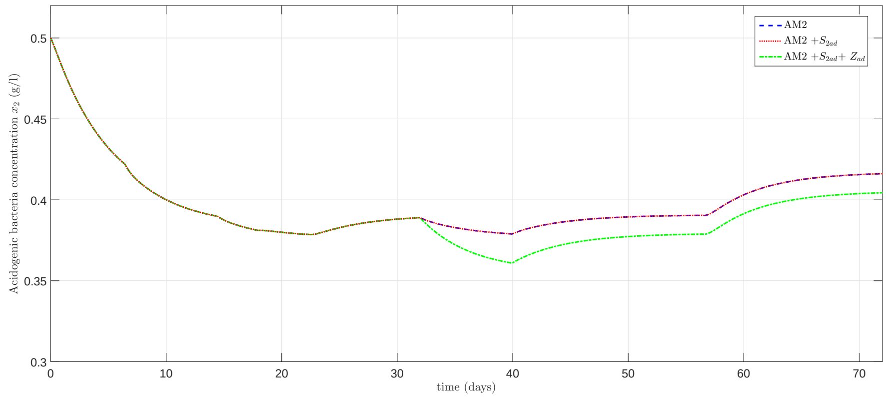

FIGURE 2.10: Acidogenic bacteria concentration (g/l).

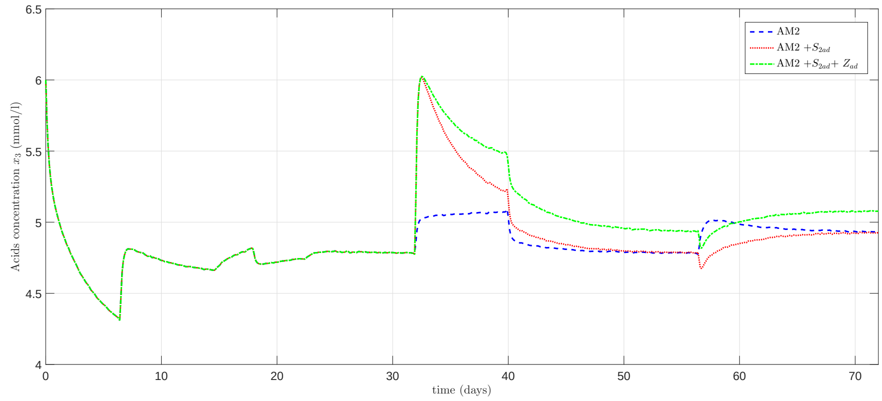

FIGURE 2.11: Acetate concentration (mmol/l).

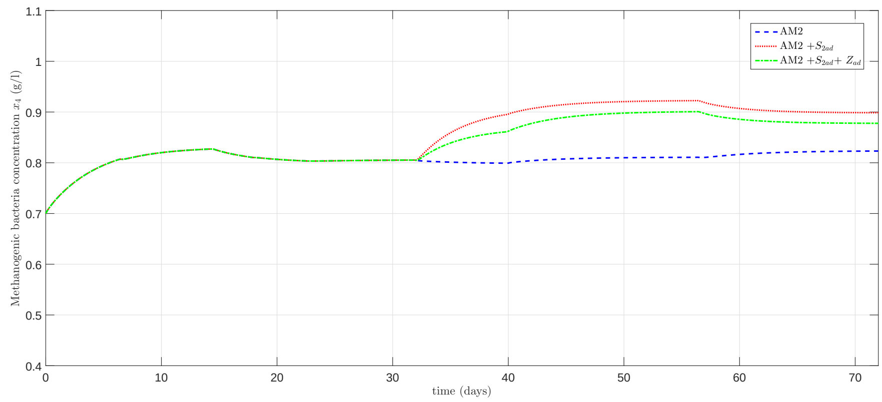

FIGURE 2.12: Mathenogenic bacteria concentration (g/l).

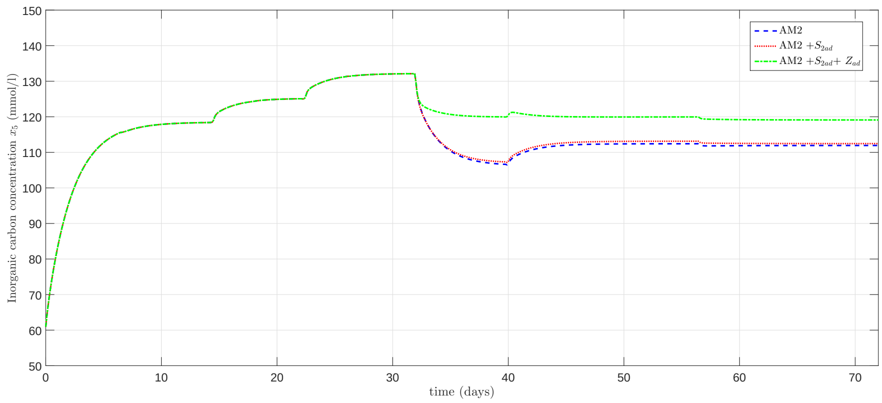

FIGURE 2.13: Inorganic carbon concentration (mmol/l).

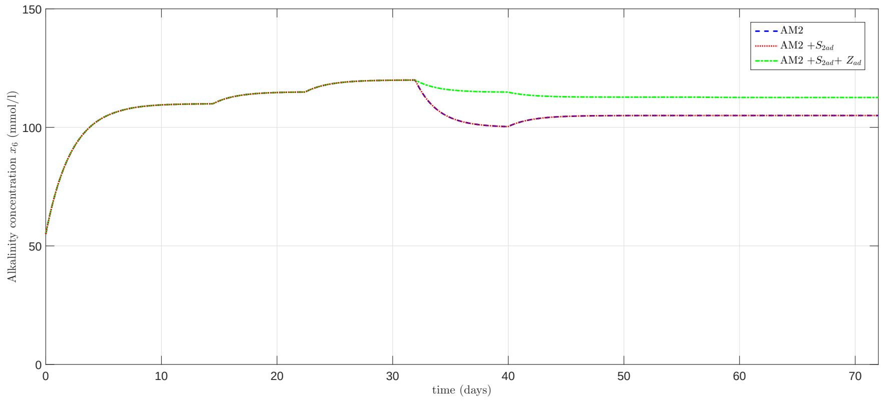

FIGURE 2.14: Alkalinity concentration (mmol/l).

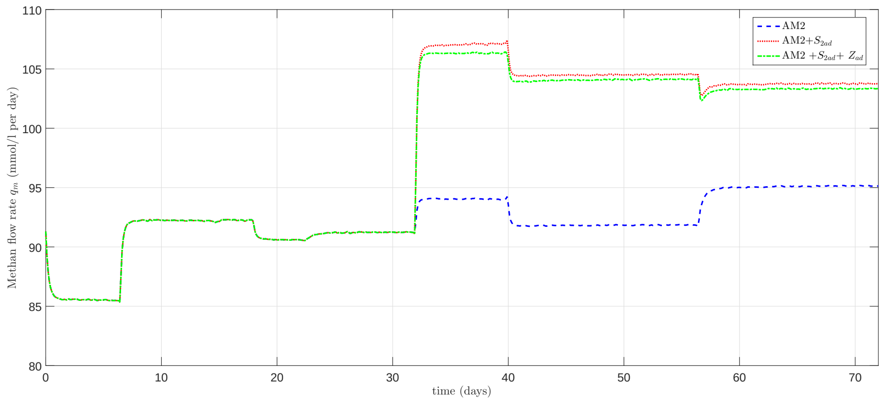

FIGURE 2.15: Methane flow rate q_m (mmol/l per day).

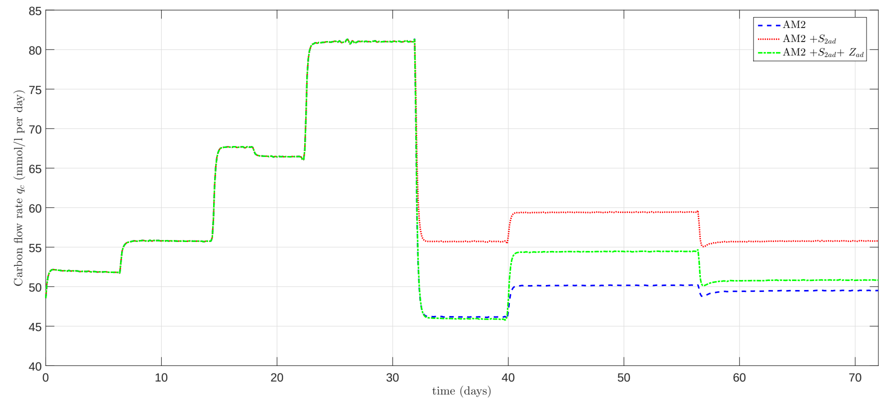

FIGURE 2.16: Carbon flow rate q_c (mmol/l per day).

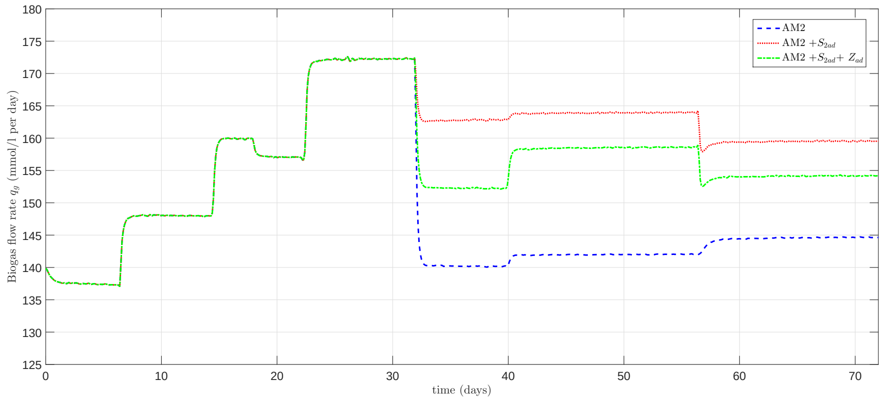

FIGURE 2.17: Biogas flow rate q_g (mmol/l per day).

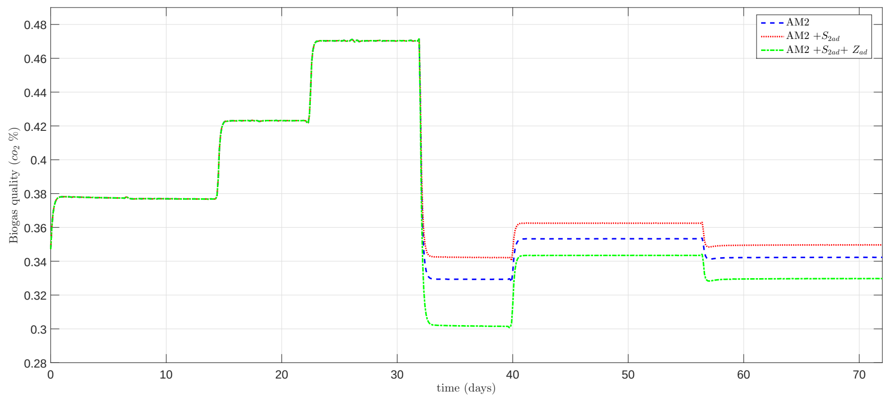

FIGURE 2.18: Biogas quality (co_2 %).

Chapter 3

State Estimation

3.1 Introduction

Observer is a an auxiliary system (O) that its input is the input and output signals of a system (S) and its output is the state estimate of the system (S) as depicted in Figure 3.1.

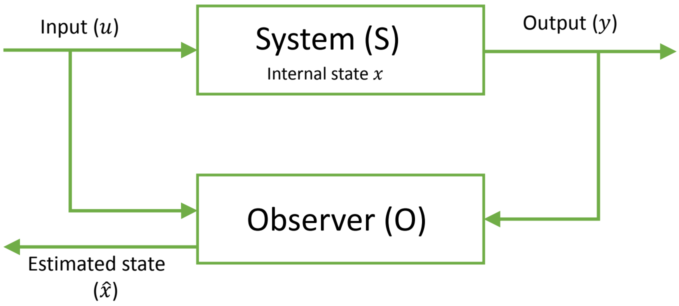

FIGURE 3.1: State observer principle.

In the last decades, observer design for the AD process has been the object of growing interest. Among many others, we may mention the asymptotic observer [32] which relies on a systematic linear change of variable (for a certain class of systems) that allows estimation of the state variables without requiring knowledge of the kinetic functions which are usually complex and uncertain. However, its convergence depends on the control input and it is sensitive to model uncertainties [23]. Therefore, it has been extended to the interval observer [62], [63] which is more appropriate when the time-varying bounds enclosing the uncertainties are known. Often, the interval observer is composed of two asymptotic observers, one to estimate the state upper bound $x^+(t)$ and a second one to estimate the lower bound $x^-(t)$. Then the system state will be enclosed in the envelope drown by $x^-(t)$ and $x^+(t)$ provided that at the initial time $x^-(t_0) \leq x(t_0) \leq x^+(t_0)$. Unfortunately, sometimes the obtained envelope is large. Therefore, it has been proposed in [64] proposed to launch a bundle of interval observers with different initial conditions and then select the smallest envelope where the actual state should be. The interval observers designed [64] have a partially tunable rate of convergence due to the use of some system outputs that are nonlinear functions of the state variables. However, the interval observers can be applied only to cooperative systems.

The extended Kalman filter, has been applied to the AD applications repeatedly, [73], [67], [32], [68], [69], [70], [71] and the references in [72], with success. However, it does not, always, possess a globall asymptotically stable error dynamics [74], and even if it does than it is difficult to prove the global convergence analytically [75]. Besides, it has been prooved in [59] that due to the nonlinear structure of the AD model and the number of input variables, it becomes impossible to apply the extended Kalman filter when one wants to estimate the biomass concentration (the system is not uniformly observable for any input), which is a key state variable to estimate, since it reflects the system health and stability [50].

We may also mention the high gain observer which has been applied successfully to a second order AD model [76], then enhanced in [59] and extended to forth order Ad model in [44]. For the same class of systems considered in [76], other nonlinear observers have been designed in [77], [78]. To design these observers and the high gain observer, the transformed canonical form is required and this is not always possible to perform [56].

Consequently, we will propose in the current chapter to design simple nonlinear observers that do not require the transformation of the model, and rely only on the nature of the involved nonlinearities in it (Lipschitz property of the nonlinear functions included in the model). Moreover, the design methodology is not restricted to a predefined order of the model, on contrary it is general and can be applied to a wide class of systems. Indeed, the design methodology will be based on the use of the DMVT which allows the transformation of the nonlinear dynamics of the estimation error to an LPV system. Then, by using the LPV techniques, we will synthesize the stability conditions in the form of LMIs. In addition to that, we will enhance the feasibility of the obtained LMIs by using a judicious reformulation of the Young's inequality.

Moreover, due to the exposition of AD processes, at real plants, to measurement and dynamic disturbances [45], we will extend the methodology to overcome the dynamics and measurement disturbances. This will be realized by the design of $\mathcal{H}_\infty$ nonlinear observers.

Furthermore, we will provide the discrete form of the nonlinear observers because in real plants the observers are, usually, driven by sampled data [147]. Last but not least, since we target to facilitate the introduction of biogas plants in VPPs, and the fact that at industry scale the most performed measurement are nonlinear functions of the state variables, then we will expand the deign methodology to the case of nonlinear outputs.

We want to say as well, that although the Kalman filtrating [59], all the nonlinear observers that we will design allow the estimation of the key process variables, bacteria concentrations, which reflect the health of the AD reactor [50].

The rest of the chapter is organized as the following. First, we will remember some notions related to the observability of nonlinear systems. Then, we will recall some definitions, theorems and notations that are required for understanding the methodology and allowing the extension of the results to a general class of systems. In order to not overload the chapter, we will review some elementary mathematical complement and notions related to the stability of the continuous and discrete dynamical systems (Lyapunov Stability) in Appendices C and D, respectively. After setting the required preliminaries and notation, we will present a general class of systems to which the considered AD model (2.11) belongs. Indeed, this step allows us to render the design methodology general and usable for other applications belonging to the same class of systems that we will present. Further, we will design an LMI-based invariant like observer and the apply it to the studied AD model. Later, to obtain an observer more global than the invariant like observer, we will design an LMI-based nonlinear observer of the same form as the generalized Arcak's observer [148]. Then, with the aim to render the obtained observer robust to disturbances affecting the model dynamics and measurements, we will enhance the synthesis by including the $\mathcal{H}_\infty$ criterion in observer design. Later, we will discretize both of the LMI-based nonlinear observer and the LMI-based $\mathcal{H}_\infty$ nonlinear observer. Obviously, we will perform numerical simulations, where we apply and compare the resulted nonlinear observers. Before concluding the chapter, we will devote a section to some discussions and an eventual extension of the design methodology to the case of nonlinear systems nonlinear outputs. This case being promising, it will definitely applied to the studied AD model. Finally, we will conclude the chapter with some remarks.

3.2 Observability of a dynamical system

Before designing an observer for a dynamical system, it has to be checked if the later is observable or not. In other words, if it is possible to reconstruct the state variables from the available input and output signals of the system or not.

A continuous time-invariant linear state-space model

$$\begin{cases} \dot{x} = Ax + Bu \\ y = Cx + Du \end{cases} \tag{3.1}$$

where $x \in X \subset R^n$ is the state vector, $u \in U \subset R^m$ the input and $y \in Y \subset R^p$ is the measured output, A the state matrix, B the input matrix, C the output matrix, and D the feed-forward matrix, all of appropriate dimensions, is observable if and only if the observability Kalman Criterium is satisfied [149]

$$\text{rank} \begin{bmatrix} C \\ CA \\ .\,. \\ CA^{n-1} \end{bmatrix} = n \tag{3.2}$$

However, for the nonlinear systems (3.3)

$$\begin{cases} \dot{x} = f(x, u) \\ y = h(x, u) \end{cases} \tag{3.3}$$

where, $f : \mathbb{R}^n \times \mathbb{R}^m \to \mathbb{R}^n$ and $h : \mathbb{R}^n \times \mathbb{R}^m \to \mathbb{R}^p$, the observability depends on the input signal and the initial conditions too.

Definition 2. Indistinguishability [150], [56]

A paire $(x_0, x_0') \in \mathbb{R}^n \times \mathbb{R}^n$ is indistinguishable for a system (3.3) if

$$\forall u \in U, \quad \forall t \geq 0, \quad h(\chi_u(t, x_0)) = h(\chi_u(t, x_0')).$$

where, $\chi_u(t, x_{t0})$ denotes the solution of the state equation (3.3) under the application of input u on $[t_0, t]$ and satisfying $\chi_u(t_0, x_{t0}) = x_{t0}$, while u will be omitted for uncontrolled cases [56].

A state x is indistinguishable from x_0 if the pair (x, x_0) is indistinguishable. From this, observability can be defined.

Definition 3. Observability [150], [56], [151]

The system (3.3) is observable at x_0 if x_0 is distinguishable from all $x \in \mathbb{R}^n$. Moreover, the system (3.3) is observable if $\forall x_0 \in \mathbb{R}^n$, the system (3.3) is observable at x_0.

In practice, these concepts are relatively difficult to verify and often the following criteria is used for the local observabilty.

Criterion 1. Rank Criterion

The nonlinear system (3.3) is observable if

$$\text{rank}\left(dh, dL_f h, \ldots, dL_f^{n-1} h\right)^T = n$$

where $L_f h$ is the Lie derivative of h along f:

$$L_f h = \sum_{i=1}^{n} f_i(x) \frac{\partial h}{\partial x_i}$$

and the expression $dL_f^k h$ given by

$$dL_f^k h = \begin{bmatrix} \frac{\partial L_f^k h}{\partial x_1} & \frac{\partial L_f^k h}{\partial x_2} & \ldots & \frac{\partial L_f^k h}{\partial x_n} \end{bmatrix}.$$

3.3 Notations and Preliminaries

In this section, we introduce some notations and preliminaries that will be useful to guarantee the asymptotic convergence of the estimation error to zero. Moreover, we will adopt a general notation in order to extend the observers, that will be presented in the subsequent sections, to a general class of systems

- the set $Co(x, y) = \{\lambda x + (1 - \lambda)y, 0 \leq \lambda \leq 1\}$ is the convex hull of $\{x, y\}$,
- $e_s(i) = \big(\underbrace{0, ..., 0, \overbrace{1}^{i \text{ th}}, 0, ..., 0}_{s \text{ components}}\big)^T \in \mathbb{R}^s, s \geq 1$ is a vector of the canonical basis of $\mathbb{R}^s$.

Definition 4 (*Lipschitz condition*)**.** Let $f(t, x)$ be piecewise continuous in t and satisfy the Lipschitz condition

$$\|f(t, x) - f(t, \hat{x})\| \leq \gamma_f \|x - \hat{x}\|, \quad \forall\ x, \hat{x} \in \mathbb{R}^n \text{ et } \forall\ u \in \mathbb{R}^m \tag{3.4}$$

then, the function $f(t, x)$ is said to be Lipschitz in x, and the positive constant γ_f is called a Lipschitz constant.The words locally Lipschitz and globally Lipschitz are used to indicate the domain over which the Lipschitz condition holds [152].

Theorem 2 (*Mean value theorem [153]*)**.** *Let $\varphi : \mathbb{R}^{\mathrm{n}} \to \mathbb{R}^q$. Let $x, y \in \mathbb{R}^{\mathrm{n}}$. We assume that φ is differentiable on $Co(x, y)$. Then, there are constant vectors $z_1, ..., z_q \in Co(x, y), z_i \neq x, z_i \neq y$ for $i = 1, ..., q$ such that :*

$$\varphi(x) - \varphi(y) = \left(\sum_{i,j=1}^{q,n} e_q(i) e_n^T(j) \frac{\partial \varphi_i}{\partial x_j}(z_i)\right)(x - y). \tag{3.5}$$

Lemma 1 (*a variant of Lipschitz reformulation*)**.** *Let $\varphi : \mathbb{R}^{\mathrm{n}} \to \mathbb{R}^q$ a differentiable function on $\mathbb{R}^n$. Then, the following items are equivalent:*

- *φ is a globally γ_φ-Lipschitz function,*
- *there exist finite and positive scalar constants a_{ij}, b_{ij} so that for all $x, y \in \mathbb{R}^n$ there exist $z_i \in Co(x, y), z_i \neq x, z_i \neq y$ and functions ψ_{ij}: $\mathbb{R}^{\mathrm{n}} \to \mathbb{R}$ satisfying the following:*

$$\varphi(x) - \varphi(y) = \sum_{i,j=1}^{q,n} \psi_{ij}(z_i) \mathcal{H}_{ij} \Big(x - y\Big) \tag{3.6}$$

$$a_{ij} \leq \psi_{ij}\Big(z_i\Big) \leq b_{ij}, \tag{3.7}$$

where

$$\psi_{ij}(z_i) = \frac{\partial \varphi_i}{\partial x_j}(z_i), \;\; \mathcal{H}_{ij} = e_q(i) e_n^T(j).$$

Notice that this lemma is obvious from the mean value theorem, but it is important to introduce it at this stage, under this formulation, in the aim to simplify the presentation of the proposed observers design method. Indeed, for our technique, we will exploit (3.6)-(3.7) instead of a direct use of Lipschitz property.

Lemma 2 (*[154]*)**.** *Let X and Y be two given matrices of appropriate dimensions. Then, for any symmetric positive definite matrix S of appropriate dimension, the following inequality holds:*

$$X^TY + Y^TX \leq \frac{1}{2}\Big[X + SY\Big]^T S^{-1}\Big[X + SY\Big]. \tag{3.8}$$

This lemma will be very useful for the main contributions of our work. It allows providing less restrictive LMI conditions compared to the classical LMI techniques for the considered class of systems.

3.4 Observer Design

In this part a couple of observers will be designed for continuous and discrete time, disturbed and undisturbed systems. Hence, to not overload the manuscript we will give the results in a general way. This means that we rewrite the studied AD model (2.11) in the following general form

$$\begin{cases} \dot{x} = A(\rho)x + B\gamma(x) + g(u,t) & \text{(3.9a)} \\ y = Cx & \text{(3.9b)} \end{cases}$$

where $x \in \mathbb{R}^n$ is the state vector, $y \in \mathbb{R}^p$ is the output measurement, $u \in \mathbb{R}^q$ is an input vector and $\rho \in \mathbb{R}^s$ is an $\mathcal{L}_\infty$ bounded and known parameter. The affine matrix $A(\rho)$ is expressed under the form

$$A(\rho) = A_0 + \sum_{j=1}^{s} \rho_j A_j \tag{3.10}$$

with $\rho_{j,\min} \leq \rho_j \leq \rho_{j,\max}$, which means that the parameter ρ belongs to a bounded convex set for which the set of 2^s vertices can be defined by

$$\mathbb{V}_\rho = \Big\{\varrho \in \mathbb{R}^s : \varrho_j \in \{\rho_{j,\min}, \rho_{j,\max}\}\Big\}. \tag{3.11}$$

The matrices $A_i \in \mathbb{R}^{n\times n}$, $B \in \mathbb{R}^{n\times m}$ and $C \in \mathbb{R}^{p\times n}$ are constant. The nonlinear function $\gamma: \ \mathbb{R}^n \longrightarrow \ \mathbb{R}^m$ is assumed to be globally Lipschitz, and it is obvious that $B\gamma(.)$ can always be written under the detailed form

$$B\gamma(x) = \sum_{i=1}^{m} B_i \gamma_i(\overbrace{H_i x}^{\vartheta_i}) \tag{3.12}$$

where $H_i \in \mathbb{R}^{n_i \times n}$ and B_i is the i^{th} column of the matrix B.

Remark 3. We can show that the assumptions on the global Lipschitz property of $\gamma_i(.)$ when applied to the considred AD model (2.11) are preserved. Indeed, due to the boundedness of the state variables of the model, as shown in Section 2.5, the state is confined in a compact set $\mathfrak{C}$, where we can construct a saturated version of each $\gamma_i(.)$, which is globally Lipschitz on $\mathfrak{C}$. For more details on this issue, we refer the reader to [155], [156] to see how we construct saturated versions of $\gamma(.)$.

3.4.1 LMI-Based Invariant Like State Observer

As already mentioned, the structure of the nonlinear invariant like observer that we will design is inspired from the invariant observer proposed in [82] and [83] for a chemostat model, where the invariance refers to the invariance under a group action. In the following, we will summarize some notions about this concept but for more comprehension the reader is referred to [84], [82] and for more details to [80].
Let consider the system (3.3) and let G be a Lie group of transformations which acts on X by φ_g: $X \to X \quad \forall g \in G$, φ_g is a diffeomorphism (at least of class C^1) on X with $(\varphi_g)^{-1} = \varphi_{g^{-1}}$ and $\varphi_{g_1} \circ \varphi_{g_2} = \varphi_{g_1 . g_2}$. Moreover, let us denote the action of the group G on U by $(\psi_g)_{g\in G}$ and on Y by $(\rho_g)_{g\in G}$.

Definition 3.1. G is a symmetry group of (3.3) if for every solution $(x(t), u(t))$ of (3.3) and $\forall g \in G, (\varphi_g(x(t)), \psi_g(u(t)))$ is also a solution.

Therefore, the system (3.3) is said to be invariant under G if and only if $\forall g, x$ and u:

$$f(\varphi_g(x), \psi_g(u) = D_{\varphi_g}(x) f(x, u)$$

where D_{φ_g} is the Jacobian matrix of $\varphi_g(x)$.
After finding the group of transformation, one can write the following pre-observer for

the system (3.3):

$$\dot{\hat{x}} = F(\hat{x}, u, \hat{y}) \tag{3.13}$$

if and only if $\forall x$ and u:

$$F(x, u, h(x, u)) = f(x, u) \tag{3.14}$$

Moreover, the pre-observer (3.13) is said to be invariant if and only if $\forall g, \hat{x}$ and $\hat{y}$:

$$F(\varphi_g(\hat{x}), \psi_g(u), \rho_g(\hat{y})) = D_{\varphi_g}(\hat{x}(t) F(\hat{x}, u, \hat{y}) \tag{3.15}$$

To design an invariant observer, we need invariant functions and invariant vector fields:

- A function defined on $X \subset R^n$ is invariant if and only if:
  $J(\varphi_g(x)) = J(x)$, $\forall g$ and x.
- A vector field ω is invariant with respect to the action of φ_g on X if and only if:
  $\omega(\varphi_g(x)) = D_{\varphi_g}(x)\omega(x)$, $\forall g$ and x.

Finally, it has been proven in [82] that the general form of an invariant pre-observer for the system (3.3) is given by

$$\dot{\hat{x}} = f(\hat{x}) + \sigma_i J_i(\hat{x}, y)\omega_i(\hat{x}) \tag{3.16}$$

with J_i being an invariant function satisfying $J_i(\hat{x}, h(\hat{x}, u)) = 0$ and ω_i an invariant vector field. Moreover if (3.16) converges to (3.3) then it is called invariant observer.

It has been found in [83] and [84] that for a fourth order AD model (composed of the first fourth equations of the model (2.11)), the invariant functions are the logarithm functions and the vector fields for each of the differential equation $\dot{\hat{x}}_i$ is the state x_i for $i = 1 \dots 4$. Thus, using the same invariant logarithm functions, we will design in our turn an invariant like nonlinear observer. It will be composed of a copy of the system and a logarithmic correction term as the following

$$\dot{\hat{x}} \quad = \quad A(\rho)\hat{x} + \sum_{i=1}^{m} B_i\gamma_i(\hat{\vartheta}_i) + g(u,t) + L(\rho)\Big[ln\Big(\frac{y_1}{e_p^T(1)C\hat{x}}\Big), \dots, ln\Big(\frac{y_p}{e_p^T(p)C\hat{x}}\Big)\Big]^T \tag{3.17}$$

with

$$\hat{\vartheta}_i = H_i\hat{x}, \quad \text{and,} \quad \mathrm{L}(\rho) = \mathrm{L}_0 + \sum_{\mathrm{j}=1}^{\mathrm{s}} \rho_{\mathrm{j}}\mathrm{L}_{\mathrm{j}}. \tag{3.18}$$

where $\hat{x}$ is the estimate of x, and the matrices $L_i \in \mathbb{R}^{n\times p}$ are the observer gains. They will be determined so that the estimation error $e = x - \hat{x}$ decreases asymptotically towards zero. Its dynamic is obtained by using equations (3.9a), (3.12) and (3.17)

$$\dot{e} \quad = \quad A(\rho)e + \sum_{i=1}^{m} B_i(\gamma_i(\vartheta_i) - \gamma_i(\hat{\vartheta}_i)) - L(\rho)\Big[ln\Big(\frac{y_1}{e_p^T(1)C\hat{x}}\Big), \ldots, ln\Big(\frac{y_p}{e_p^T(p)C\hat{x}}\Big)\Big]^T \tag{3.19}$$

For a clearer presentation and in order to refine the synthesized conditions under which the estimation error (3.19) converges asymptotically to zero, we will proceed step by step at this stage.

First, since $\gamma(.)$ is assumed to be globally Lipschitz, then from Lemma 1 there exist $r_i \in Co(\vartheta_i, \hat{\vartheta}_i)$, functions $\phi_{ij} \ : \ \mathbb{R}^{n_i} \longrightarrow \ \mathbb{R}$ and constants a_{ij}, b_{ij}, such that

$$B(\gamma(x) - \gamma(\hat{x})) = \sum_{i,j=1}^{m,n_i} \phi_{ij}(r_i)\mathcal{H}_{ij}\left(\vartheta_i - \hat{\vartheta}_i\right) \tag{3.20}$$

and

$$a_{ij} \leq \phi_{ij}(r_i) \leq b_{ij}, \tag{3.21}$$

where

$$\phi_{ij}(r_i) = \frac{\partial \gamma_i}{\partial \vartheta_i^j}(r_i), \;\; \mathcal{H}_{ij} = B_i e_{n_i}^T(j). \tag{3.22}$$

For shortness, we set $\phi_{ij} \triangleq \phi_{ij}(r_i)$. Without loss of generality, we assume that $a_{ij} = 0$ for all $i = 1, \ldots, m$ and $j = 1, \ldots, n_i$, and moreover, since $\vartheta_i - \hat{\vartheta}_i = H_i e$, then we have

$$B(\gamma(x) - \gamma(\hat{x})) = \sum_{i,j=1}^{m,n_i} \phi_{ij}\mathcal{H}_{ij}H_i e \tag{3.23}$$

Second, we can always write

$$ln\Big(\frac{y_i}{e_p^T(i)C\hat{x}}\Big) = \underbrace{ln(e_p^T(i)Cx) - ln(e_p^T(i)C\hat{x})}_{\Upsilon_i(x)-\Upsilon_i(\hat{x})} \tag{3.24}$$

thus, from Lemma 1 and in some specific invariant space (where the functions $\Upsilon_i(x)$ are defined), there exist $z_i \in Co(\min(x_i, \hat{x}_i), \max(x_i, \hat{x}_i))$, functions $\psi_{ij} \ : \ \mathbb{R}^n \longrightarrow \ \mathbb{R}$ and constants $\min(\psi_{ij}), \max(\psi_{ij})$, such that

$$\Upsilon(x) - \Upsilon(\hat{x}) = \sum_{i,j=1}^{p,n} \psi_{ij}(z_i) M_{ij} e \tag{3.25}$$

with $\Upsilon(x) = [\Upsilon_i(x), \ldots, \Upsilon_p(x)]^T$ and

$$\min(\psi_{ij}) \leq \psi_{ij}(z_i) \leq \max(\psi_{ij}), \tag{3.26}$$

where

$$\psi_{ij}(z_i) = \frac{\partial \Upsilon_i}{\partial x_j}(z_i), \;\; M_{ij} = e_p(i) e_n^T(j). \tag{3.27}$$

For shortness, we set $\psi_{ij} \triangleq \psi_{ij}(z_i)$.

Now, using equations (3.19), (3.23) and (3.25), we obtain

$$\dot{e} = \left(A(\rho) + \sum_{i,j=1}^{m,n_i} \phi_{ij} \mathcal{H}_{ij} H_i - L(\rho) \sum_{i,j=1}^{p,n} \psi_{ij} M_{ij} \right) e \tag{3.28}$$

Since we know a priori that $\min(\psi_{ij}) \neq 0$ in equation (3.26), we propose to write

$$0 \leq \psi_{ij} - \min(\psi_{ij}) \leq \underbrace{\max(\psi_{ij}) - \min(\psi_{ij})}_{\bar{b}_{ij}} \tag{3.29}$$

and then, add and subtract $\min(\psi_{ij})$ from the term ψ_{ij} in equation (3.28) as the following

$$\dot{e} \;\; = \;\; \left(A(\rho) + \sum_{i,j=1}^{m,n_i} \phi_{ij} \mathcal{H}_{ij} H_i - L(\rho) \sum_{i,j=1}^{p,n} (\psi_{ij} + \min(\psi_{ij}) - \min(\psi_{ij})) M_{ij} \right) e \tag{3.30}$$

hence, we obtain

$$\begin{aligned} \dot{e} \;\; = \;\; & \Bigg(\underbrace{A(\rho) - L(\rho) \sum_{i,j=1}^{p,n} \min(\psi_{ij}) M_{ij}}_{\overline{C}} + \\ & \sum_{i,j=1}^{m,n_i} \phi_{ij} \mathcal{H}_{ij} H_i - L(\rho) \sum_{i,j=1}^{p,n} \underbrace{(\psi_{ij} - \min(\psi_{ij}))}_{\varphi_{ij}} M_{ij} \Bigg) e \end{aligned} \tag{3.31}$$

where

$$0 \leq \varphi_{ij} \leq \bar{b}_{ij} \tag{3.32}$$

The objective, now, consists in finding the observer parameters so that the estimation error dynamics (3.31) be asymptotically stable. Hence, as usual for this class of systems concerned by the LMI techniques, we use a quadratic Lyapunov function to analyse the stability. That is, we use

$$V = e^T P e, \quad P = P^T > 0 \tag{3.33}$$

whose derivative $\dot{V}(e)$ along the trajectories (3.31) is given by

$$\begin{aligned}\dot{V} = e^T \Bigg[\Bigg(A(\rho) - L(\rho)\overline{C} + \sum_{i,j=1}^{m,n_i} \phi_{ij}\mathcal{H}_{ij}H_i - L(\rho)\sum_{i,j=1}^{p,n} \varphi_{ij}M_{ij} \Bigg)^T \mathbb{P} \\ + \mathbb{P}\Bigg(A(\rho) - L(\rho)\overline{C} + \sum_{i,j=1}^{m,n_i} \phi_{ij}\mathcal{H}_{ij}H_i - L(\rho)\sum_{i,j=1}^{p,n} \varphi_{ij}M_{ij} \Bigg) \Bigg] e\end{aligned} \tag{3.34}$$

that we rewrite as the following

$$\begin{aligned}\dot{V} \;\;=\;\; & e^T \Big(\underbrace{A^T(\rho)\mathbb{P} - \overline{C}^T L^T(\rho)\mathbb{P} + \mathbb{P}A(\rho) - \mathbb{P}L(\rho)\overline{C}}_{\Psi} \Big) e + e^T \sum_{i,j=1}^{m,n_i} \phi_{ij} \Big(\underbrace{\mathbb{P}\mathcal{H}_{ij}}_{\mathbb{X}_{ij}^T} \underbrace{H_i}_{\mathbb{Y}_i} + H_i^T \mathcal{H}_{ij}^T \mathbb{P} \Big) e \\ & + e^T \sum_{i,j=1}^{p,n} \varphi_{ij} \Big(\underbrace{\mathbb{P}L(\rho)}_{\overline{\mathbb{X}}_{ij}^T} \underbrace{(-M_{ij})}_{\overline{\mathbb{Y}}_{ij}} + (-M_{ij})^T L^T(\rho)\mathbb{P} \Big) e\end{aligned} \tag{3.35}$$

Now, by applying Lemma 2 we obtain

$$\mathbb{X}_{ij}^T\mathbb{Y}_i + \mathbb{Y}_i^T\mathbb{X}_{ij} \leq \frac{1}{2}\Big(\mathbb{X}_{ij} + \mathbb{S}_{ij}\mathbb{Y}_i\Big)^T \mathbb{S}_{ij}^{-1} \overbrace{\Big(\mathbb{X}_{ij} + \mathbb{S}_{ij}\mathbb{Y}_i\Big)}^{\Pi_{ij}} \tag{3.36}$$

and

$$\overline{\mathbb{X}}_{ij}^T\overline{\mathbb{Y}}_{ij} + \overline{\mathbb{Y}}_{ij}^T\overline{\mathbb{X}}_{ij} \leq \frac{1}{2}\Big(\overline{\mathbb{X}}_{ij} + \overline{\mathbb{S}}_{ij}\overline{\mathbb{Y}}_{ij}\Big)^T \overline{\mathbb{S}}_{ij}^{-1} \overbrace{\Big(\overline{\mathbb{X}}_{ij} + \overline{\mathbb{S}}_{ij}\overline{\mathbb{Y}}_{ij}\Big)}^{\overline{\Pi}_{ij}} \tag{3.37}$$

for any symmetric positive definite matrices $\mathbb{S}_{ij}$ and $\overline{\mathbb{S}}_{ij}$. Moreover, from (3.21) and (3.32) and the fact that $a_{ij} = 0$, inequality $\dot{V} < 0$ holds if

$$\Psi - \sum_{i,j=1}^{m,n_i} \Big(\Pi_{ij}^T \Big(-\frac{2}{b_{ij}}\mathbb{S}_{ij} \Big)^{-1} \Pi_{ij} \Big) - \sum_{i,j=1}^{p,n} \Big(\overline{\Pi}_{ij}^T \Big(-\frac{2}{\bar{b}_{ij}}\overline{\mathbb{S}}_{ij} \Big)^{-1} \overline{\Pi}_{ij} \Big) < 0 \tag{3.38}$$

consequently, by Schur lemma, inequality (3.38) is equivalent to

$$\begin{bmatrix} \Psi & \begin{bmatrix} \Pi_1^T & \dots & \Pi_m^T \end{bmatrix} & \begin{bmatrix} \overline{\Pi}_1^T & \dots & \overline{\Pi}_p^T \end{bmatrix} \\ & & \\ (\star) & -\Lambda\mathbb{S} & 0 \\ (\star) & (\star) & -\overline{\Lambda}\,\overline{\mathbb{S}} \end{bmatrix} < 0 \tag{3.39}$$

where

$$\Pi_i = \left[\Pi_{i1}^T \dots \Pi_{in_i}^T\right]^T, \quad \Pi_{ij} = \mathcal{H}_{ij}^T\mathbb{P} + \mathbb{S}_{ij}\mathcal{H}_i \tag{3.40}$$

$$\overline{\Pi}_i = \left[\overline{\Pi}_{i1}^T \dots \overline{\Pi}_{in}^T\right]^T, \quad \overline{\Pi}_{ij} = L^T(\rho)\mathbb{P} + \overline{\mathbb{S}}_{ij}(-M_{ij}) \tag{3.41}$$

and

$$\mathbb{S} = \text{block-diag}(\mathbb{S}_1, \dots, \mathbb{S}_m), \quad \mathbb{S}_i = \text{block-diag}(\mathbb{S}_{i1}, \dots, \mathbb{S}_{in_i}) \tag{3.42}$$

$$\Lambda = \text{block-diag}(\Lambda_1, ..., \Lambda_m), \quad \Lambda_i = \text{block-diag}\left(\Lambda_{i1}, \dots, \Lambda_{in_i}\right) \tag{3.43}$$

with

$$\Lambda_{ij} = \frac{2}{b_{ij}}\mathbb{I}_{n_i}, \tag{3.44}$$

and

$$\overline{\mathbb{S}} = \text{block-diag}(\overline{\mathbb{S}}_1, \dots, \overline{\mathbb{S}}_p), \quad \overline{\mathbb{S}}_i = \text{block-diag}(\overline{\mathbb{S}}_{i1}, \dots, \overline{\mathbb{S}}_{in}) \tag{3.45}$$

$$\overline{\Lambda} = \text{block-diag}(\overline{\Lambda}_1, ..., \overline{\Lambda}_p), \quad \overline{\Lambda}_i = \text{block-diag}\left(\overline{\Lambda}_{i1}, \dots, \overline{\Lambda}_{in}\right) \tag{3.46}$$

with

$$\overline{\Lambda}_{ij} = \frac{2}{\overline{b}_{ij}}\mathbb{I}_p \tag{3.47}$$

Finally, we use the change of variables $\mathcal{R}_i = L_i^T\mathbb{P}$ to solve the LMI (3.39).

3.4.1.1 Application and Simulation Results

In order to apply the nonlinear invariant like observer (3.17) to the AD model (2.10) for estimating its key state variables (bacteria concentrations [50]) and inorganic carbon, we first write the model in the form (3.9a), (3.9b). This can be easily done by using the following parameters

$$\rho = u_{out}, \quad A_0 = 0, \quad A_1 = -\text{block-diag}(1, \alpha, 1, \alpha, 1, 1) \tag{3.48}$$

$$B = \begin{bmatrix} -k_1 & 1 & k_2 & 0 & k_4 & 0 \\ 0 & 0 & -k_3 & 1 & k_5 & 0 \end{bmatrix}^T, \quad \gamma(x) = \begin{bmatrix} \mu_1(x_1)x_2 \\ \mu_2(x_3)x_4 \end{bmatrix} \tag{3.49}$$

$$g(u,t) = \begin{bmatrix} u_1 S_{1in} & 0 & u_1(S_{2in} + S_{2ad}) & 0 & u_1 C_{in} - q_c & u_1 Z_{in} + u_2 Z_{ad} \end{bmatrix}^T \tag{3.50}$$

and for assuming available, on line, measurements of x_1, x_3 and x_6, we take

$$C = \begin{bmatrix} 1 & 0 & 0 & 0 & 0 & 0 \\ 0 & 0 & 1 & 0 & 0 & 0 \\ 0 & 0 & 0 & 0 & 0 & 1 \end{bmatrix} \tag{3.51}$$

Moreover, for the observer design we have

$$m = 2, \quad s = 1, \quad n_1 = 2, \quad \gamma_1(x) = \mu_1(x_1)x_2, \quad n_2 = 2, \quad \gamma_2(x) = \mu_2(x_3)x_4 \tag{3.52}$$

and

$$\begin{aligned} H_1 &= \begin{bmatrix} 1 & 0 & 0 & 0 & 0 & 0 \\ 0 & 1 & 0 & 0 & 0 & 0 \end{bmatrix}, \quad & H_2 &= \begin{bmatrix} 0 & 0 & 1 & 0 & 0 & 0 \\ 0 & 0 & 0 & 1 & 0 & 0 \end{bmatrix} \\ B_1 &= \begin{bmatrix} -k_1 & 1 & k_2 & 0 & k_4 & 0 \end{bmatrix}^T, \quad & B_2 &= \begin{bmatrix} 0 & 0 & -k_3 & 1 & k_5 & 0 \end{bmatrix}^T \end{aligned} \tag{3.53}$$

The matrices $M_{ij} \in \mathbb{R}^{p \times n}$ are with all elements null except the element $M_{ij}(i,j)$, for example:

$$M_{23} = \begin{bmatrix} 0 & 0 & 0 & 0 & 0 & 0 \\ 0 & 0 & 1 & 0 & 0 & 0 \\ 0 & 0 & 0 & 0 & 0 & 0 \end{bmatrix} \tag{3.54}$$

The simulation has been run for $\rho_{min} = 0.1$ day^{-1}, $\rho_{max} = 0.9$ day^{-1}, $S_{1in} = 16$ g/l, $S_{2in} = 170$ mmol/l, $C_{in} = 76.15$ mmol/l, $Z_{in} = 200$ mmol/l, $Z_{ad} = 700$ mmol/l, $S_{2ad} = 0$ mmol/l, and the parameter values given in Table 2.2. After solving the LMIs (3.39) by using LMI MATLAB Toolbox, the following observer gains have been obtained

$$L_0 = \begin{bmatrix} 23.4241 & -54.7172 & 0 \\ -0.6227 & 1.4478 & 0 \\ -55.5205 & 626.7350 & 0 \\ -0.0335 & -1.8752 & 0 \\ -40.0327 & -543.4513 & 0 \\ 0 & 0 & 0.0118 \end{bmatrix}, \quad L_1 = \begin{bmatrix} 12.2058 & 6.0284 & 0 \\ -0.3258 & -0.1598 & 0 \\ -29.0052 & -13.8996 & 0 \\ -0.0198 & -0.0075 & 0 \\ -21.3754 & -10.9675 & 0 \\ 0 & 0 & -0.0166 \end{bmatrix}$$

Moreover, the system and the observer were initialized by $x(0) = [2, 0.5, 12, 0.7, 53.48, 55]^T$ and $\hat{x}(0) = [2, 1, 12, 0.4, 28.5, 55]^T$, respectively. The simulation results are depicted in Figures 3.2-3.7. It is quite clear from the later figures that the estimated state variables by the proposed nonlinear invariant like observer converge asymptotically to the simulated system states. Indeed, although the large initial estimation error, the designed observer is showing satisfactory behaviour where the estimations error is decreasing asymptotically to zero as presented in Figures 3.8-3.10. However, it has to be pointed out that the observer is applicable only locally, where the functions $\Upsilon_i(.)$ in (3.24) are well defined. In addition to that, if at the initial time the term $e_p^T(i)C\hat{x}$ approaches zero then, unfortunately, the observer may diverge. This motivates the search for a more globally applicable observer that will be designed in the next sections.

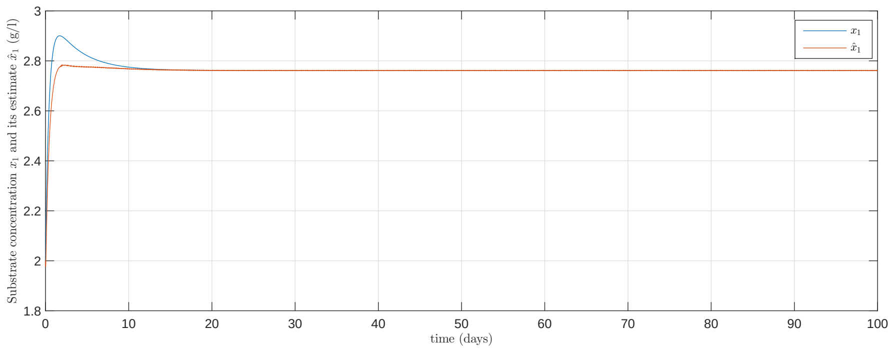

FIGURE 3.2: Substrate concentration x_1 and its estimate $\hat{x}_1$ (g/l).

3.4.2 Continuous Time LMI-Based Nonlinear State Observer

In order to design a global nonlinear state observer for the AD model (3.9a), (3.9b), we design, in this section, a nonlinear state observer of the same form as the generalized

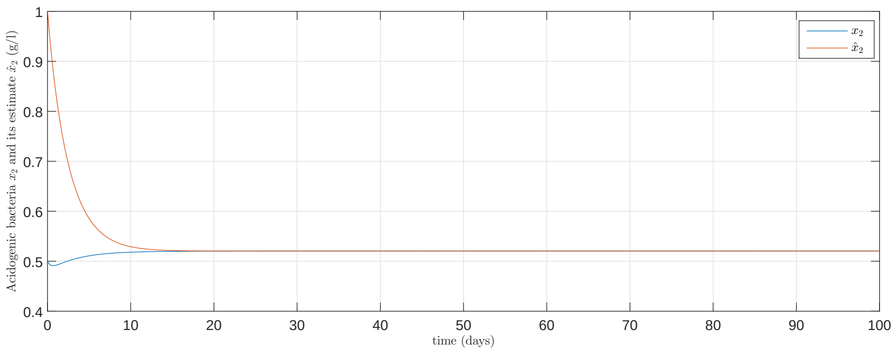

FIGURE 3.3: Acidogenic bacteria x_2 and its estimate $\hat{x}_2$ (g/l).

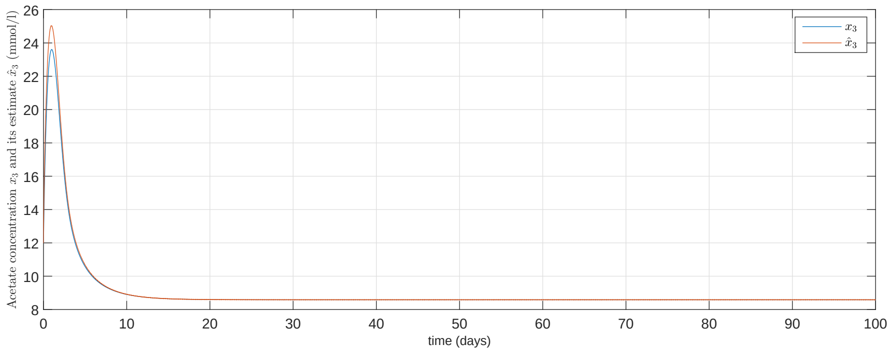

FIGURE 3.4: Acetate concentration x_3 and its estimate $\hat{x}_3$ (mmol/l).

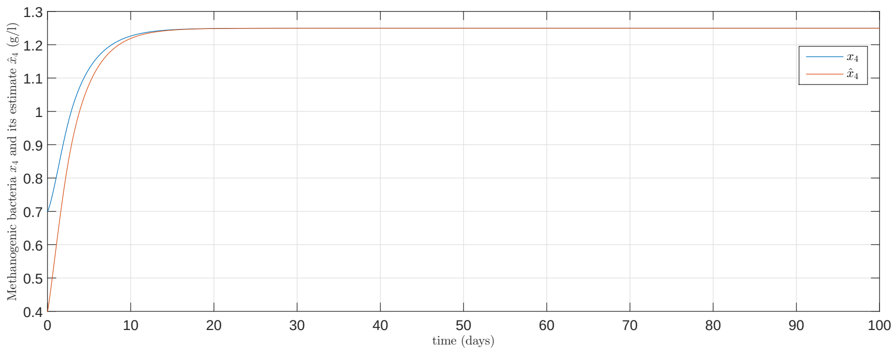

FIGURE 3.5: Mathenogenic bacteria x_4 and its estimate $\hat{x}_4$ (g/l).

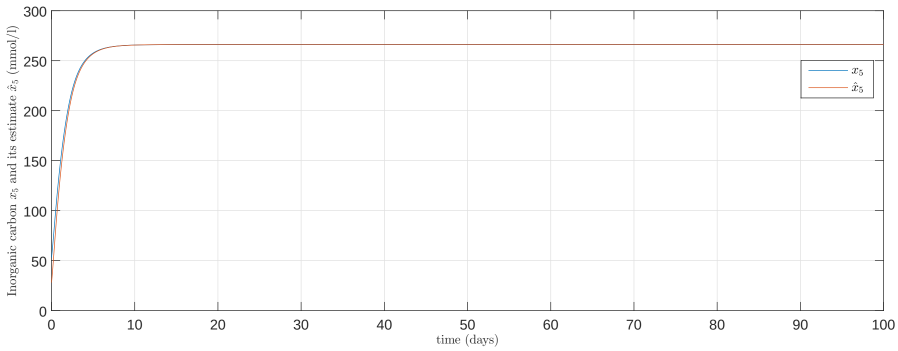

FIGURE 3.6: Inorganic carbon x_5 and its estimate $\hat{x}_5$ (mmol/l).

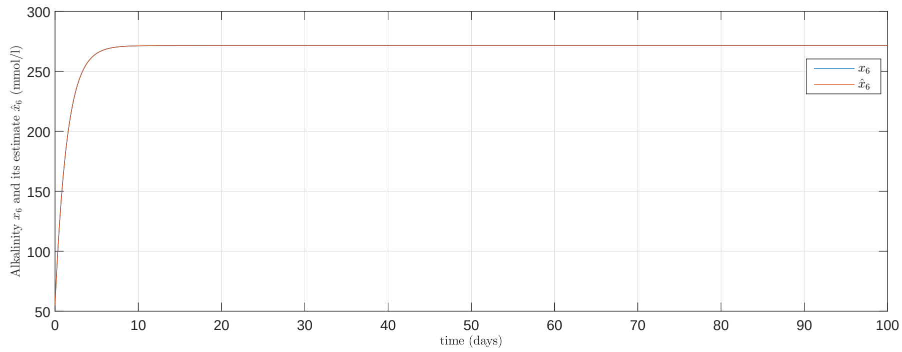

FIGURE 3.7: Alkalinity concentration x_6 and its estimate $\hat{x}_6$ (mmol/l).

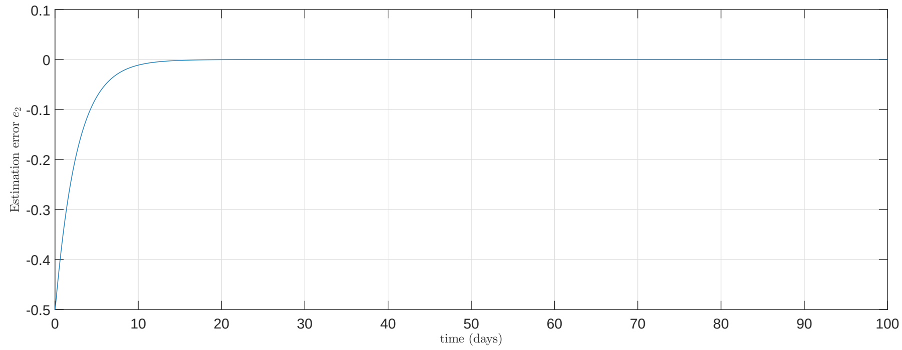

FIGURE 3.8: Estimation error $e_2 = x_2 - \hat{x}_2$.

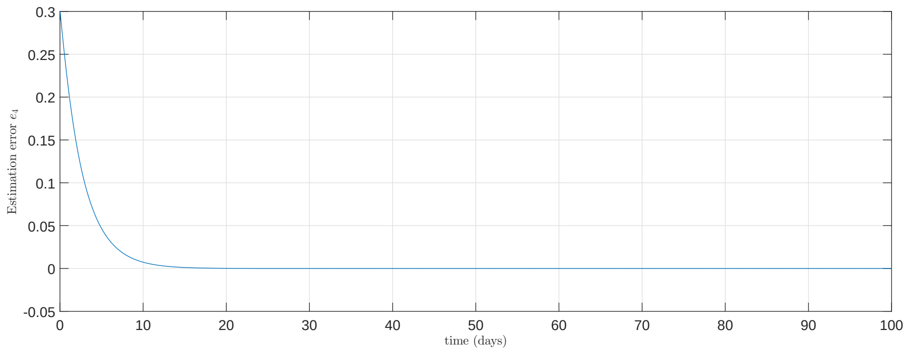

FIGURE 3.9: Estimation error $e_4 = x_4 - \hat{x}_4$.

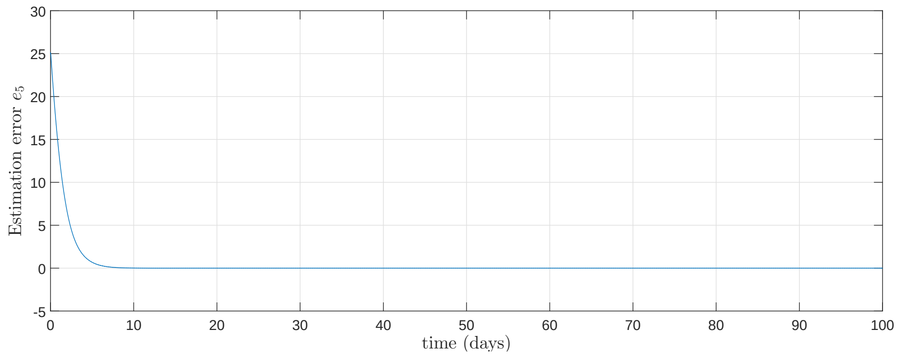

FIGURE 3.10: Estimation error $e_5 = x_5 - \hat{x}_5$.

Arcak's observer [148]. Its structure reads

$$\dot{\hat{x}} = A(\rho)\hat{x} + \sum_{i=1}^{m} B_i\gamma_i(\hat{\vartheta}_i) + g(u,t) + L(\rho)(y - C\hat{x}) \tag{3.55}$$

with

$$\hat{\vartheta}_i = H_i\hat{x} + K_i(\rho)(y - C\hat{x}) \tag{3.56}$$

where $\hat{x}$ is the estimate of x, and

$$K_i(\rho) = K_i^0 + \sum_{j=1}^{s} \rho_j K_i^j \;, \qquad L(\rho) = L_0 + \sum_{j=1}^{s} \rho_j L_j \tag{3.57}$$

The objective is to find the observer gains $L_i \in \mathbb{R}^{n\times p}$ and $K_i^j \in \mathbb{R}^{n_i\times p}$ so that the estimation error

$$e = x - \hat{x} \tag{3.58}$$

converges asymptotically to zero.

Using Lemmea 1, equations (3.12) and (3.56), we can easily obtain

$$\sum_{i=1}^{m} B_i(\gamma_i(\vartheta_i) - \gamma_i(\hat{\vartheta}_i)) = \sum_{i,j=1}^{m,n_i} \phi_{ij}(r_i)\mathcal{H}_{ij}\left(H_i - K_i(\rho)C\right)e \tag{3.59}$$

and

$$a_{ij} \leq \phi_{ij}(r_i) \leq b_{ij}, \tag{3.60}$$

where

$$\vartheta_i \leq r_i \leq \hat{\vartheta}_i, \qquad \phi_{ij}(r_i) = \frac{\partial\gamma_i}{\partial\vartheta_i^j}(r_i),\; \mathcal{H}_{ij} = B_i e_{n_i}^T(j). \tag{3.61}$$

For shortness, we set $\phi_{ij} \triangleq \phi_{ij}(r_i)$. Without loss of generality, we assume that $a_{ij} = 0$ for all $i = 1,\ldots,m$ and $j = 1,\ldots,n_i$. For more details about this, we refer the reader to [157].

Using equations (3.9a), (3.9b), (3.55) and (3.59) we obtain the following dynamic equation of the estimation error (3.158)

$$\dot{e} = \left(A(\rho) - L(\rho)C + \sum_{i,j=1}^{m,n_i} \phi_{ij}\mathcal{H}_{ij}\left(H_i - K_i(\rho)C\right)\right)e \tag{3.62}$$

Now, we summarize in Theorem 3 the LMI conditions under which the estimation error (3.62) decreases asymptotically toward zero.

Theorem 3. *If there exist symmetric positive definite matrices* $\mathbb{P} \in \mathbb{R}^{n\times n}$, $\mathcal{S}_i \in \mathbb{R}^{n_i\times n_i}$ *and matrices* $\mathcal{R}_j \in \mathbb{R}^{p\times n}$, $\mathcal{Y}_i^j \in \mathbb{R}^{p\times n_i}$, $i = 1,\dots m$, $j = 0,\dots\ s$, *of appropriate dimensions so that the following LMI conditions are feasible*

$$\begin{bmatrix} \mathbb{A}\Big(\mathbb{P},\mathcal{R}_j,\rho\Big) & \begin{bmatrix}\Sigma_1^T & \dots & \Sigma_m^T\end{bmatrix} \\ & \\ (\star) & -\Lambda\mathbb{S} \end{bmatrix} < 0,\ \forall\rho\in\mathbb{V}_\rho \tag{3.63}$$

where

$$\mathbb{A}\Big(\mathbb{P},\mathcal{R}_j,\rho\Big) = A_0^T\mathbb{P} + \mathbb{P}A_0 - C^T\mathcal{R}_0 - \mathcal{R}_0^T C + \sum_{j=1}^{s}\rho_j\Big(A_j^T\mathbb{P} + \mathbb{P}A_j - C^T\mathcal{R}_j - \mathcal{R}_j^T C\Big) \tag{3.64}$$

$$\Sigma_i = \Big[\Sigma_{i1}^T \dots \Sigma_{in_i}^T\Big]^T,\quad \Sigma_{ij}^T = \mathbb{P}\mathcal{H}_{ij} + H_i^T\mathcal{S}_i - C^T\left(\mathcal{Y}_i^0 + \sum_{l=1}^{s}\rho_l\mathcal{Y}_i^l\right) \tag{3.65}$$

$$\Lambda = \textit{block-diag}\Big(\Lambda_1,...,\Lambda_m\Big),\quad \Lambda_i = \textit{block-diag}\left(\Lambda_{i1},\dots,\Lambda_{in_i}\right),\quad \Lambda_{ij} = \frac{2}{b_{ij}}\mathbb{I}_{n_i} \tag{3.66}$$

$$\mathbb{S} = \textit{block-diag}\Big(\mathbb{S}_1,\dots,\mathbb{S}_m\Big),\quad \mathbb{S}_i = \textit{block-diag}\Big(\underbrace{\mathcal{S}_i,\dots,\mathcal{S}_i}_{ni\ \text{times}}\Big) \tag{3.67}$$

then, the estimation error converges asymptotically towards zero. Consequently, the observer parameters L_j *and* K_i^j *are to be computed as follows*

$$L_j = \mathbb{P}^{-1}\mathcal{R}_j^T,\quad K_i^j = \mathcal{S}_i^{-1}(\mathcal{Y}_i^j)^T,\qquad i = 1,\dots m,\quad j = 0,\dots\ s. \tag{3.68}$$

Proof. Usually, for this class of systems (3.62) concerned by LMI techniques, we use a quadratic Lyapunov function to analyse their stability. That is, we use

$$V = e^T Pe,\quad P = P^T > 0 \tag{3.69}$$

where its derivative $\dot{V}(e)$ along the trajectories (3.62) is given by

$$\dot{V}(e) = e^T\left[\left(\mathbb{A}_L(\rho) + \sum_{i,j=1}^{m,n_i}\phi_{ij}\mathcal{H}_{ij}\mathbb{H}_{K_i}\right)^T\mathbb{P} + \mathbb{P}\left(\mathbb{A}_L(\rho) + \sum_{i,j=1}^{m,n_i}\phi_{ij}\mathcal{H}_{ij}\mathbb{H}_{K_i}\right)\right]e \tag{3.70}$$

with

$$\mathbb{A}_L = A(\rho) - L(\rho)C, \qquad \mathbb{H}_{K_i} = H_i - K_i(\rho)C \tag{3.71}$$

The derivative of Lyapunov function (3.70) is negative if

$$\mathbb{A}_L^T(\rho)P + P\mathbb{A}_L(\rho) + \sum_{i,j=1}^{m,n_i} \phi_{ij} \left(\underbrace{\mathbb{P}\mathcal{H}_{ij}}_{\mathbb{X}_{ij}^T} \underbrace{\mathbb{H}_{K_i}}_{\mathbb{Y}_i} + \mathbb{Y}_i^T \mathbb{X}_{ij} \right) < 0 \tag{3.72}$$

From Lemma 2, we know that for all symmetric positive definite matrices $\mathbb{S}_{ij}$, we have

$$\mathbb{X}_{ij}^T \mathbb{Y}_i + \mathbb{Y}_i^T \mathbb{X}_{ij} \leq \frac{1}{2}\Big[\mathbb{X}_{ij} + \mathbb{S}_{ij}\mathbb{Y}_i\Big]^T \mathbb{S}_{ij}^{-1} \underbrace{\Big[\mathbb{X}_{ij} + \mathbb{S}_{ij}\mathbb{Y}_i\Big]}_{\Sigma_{ij}} \tag{3.73}$$

Since the matrix $\mathbb{Y}_i$ does not depend on the index j and depends on the same $K_i(\rho_k)$, then to obtain an LMI, we need to put

$$\mathbb{S}_{ij} = \mathcal{S}_i, \qquad \forall (i,j) \tag{3.74}$$

Consequently, from (3.60) and the fact that without loss of generality $a_{ij} = 0$, inequality (3.73) is satisfied if

$$\mathbb{A}_L^T(\rho)P + P\mathbb{A}_L(\rho) + \sum_{i,j=1}^{m,n_i} \left(\Sigma_{ij}^T \Big(-\frac{2}{b_{ij}} \mathcal{S}_i \Big)^{-1} \Sigma_{ij} \right) \leq 0. \tag{3.75}$$

Therefore, from Schur lemma, inequality (3.75) is equivalent to

$$\begin{bmatrix} \mathbb{A}_L^T(\rho)P + P\mathbb{A}_L(\rho) & \begin{bmatrix} \Sigma_1^T & \dots & \Sigma_m^T \end{bmatrix} \\ (\star) & -\Lambda\mathbb{S} \end{bmatrix} \leq 0 \tag{3.76}$$

Finally, with the change of variable $\mathcal{R}_j = L_j^T\mathbb{P}$ and $\mathcal{Y}_i^j = (K_i^j)^T\mathcal{S}_i$, and since (3.76) is affine in ρ, then the convexity principle [158] leads to (3.63). This ends the proof. □

3.4.3 Continuous Time LMI-Based $\mathcal{H}_\infty$ Nonlinear State Observer

In this section, we extend the designed observer in Section 3.4.2 to account for disturbances affecting the system dynamics and measurements, as the following

$$\begin{cases} \dot{x} = A(\rho)x + B\gamma(x) + g(u,t) + Ew \\ y = Cx + Dw \end{cases} \tag{3.77}$$

where the system parameters are as those defined for the system (3.9), and $w \in \mathbb{R}^z$ is the disturbance $\mathcal{L}_2$ bounded vector. The matrices $E \in \mathbb{R}^{n\times z}$ and $D \in \mathbb{R}^{p\times z}$ are constant.

Remark 4. Notice that the fact we use the same disturbances vector w in the dynamics and output measurements is not restrictive because the matrices E, D and the dimension of w are arbitrary. Indeed, if we assume that in the dynamics we have E_1w_1, and in the measurements equation, we have E_2w_2, then we can always write $E = [E_1 \quad 0]$, $D = [0 \quad E_2]$ and $w = \begin{bmatrix} w_1 \\ w_2 \end{bmatrix}$, which lead to the form (3.77).

To estimate the unmeasurable sate variables of (3.77), we use the same observer scheme (3.55). However, now, the objective is to find the observer gains $L_i \in \mathbb{R}^{n\times p}$ and $K_i^j \in \mathbb{R}^{n_i\times p}$ so that the estimation error (3.158) turns to be $\mathcal{H}_\infty$ asymptotically stable. This means, to find the observer gains so that the following $\mathcal{H}_\infty$ criterion [159] is satisfied

$$\|e\|_{\mathcal{L}_2} \leq \sqrt{\mu\|w\|^2_{\mathcal{L}_2} + \nu\|e_0\|^2} \tag{3.78}$$

where $\sqrt{\mu}$ is the disturbance attenuation level and $\nu > 0$ a parameter to be determined. In other words, $\sqrt{\mu}$ is the disturbance gain from w to e.

Using Lemmea 1, equations (3.12), (3.56) and (3.77) we obtain

$$\sum_{i=1}^{m} B_i(\gamma_i(\vartheta_i) - \gamma_i(\hat{\vartheta}_i)) = \sum_{i,j=1}^{m,n_i} \phi_{ij}(r_i)\mathcal{H}_{ij}\left[(H_i - K_i(\rho)C)\,e - K_i(\rho)Dw\right] \tag{3.79}$$

with $\phi_{ij}(r_i)$ and r_i as defined in (3.60) and (3.61), and for shortness, we set $\phi_{ij} \triangleq \phi_{ij}(r_i)$.

Now, using equation (3.55), (3.77) and (3.79), we obtain the following estimation error dynamics

$$\dot{e} = \left(\mathbb{A}_L(\rho) + \sum_{i,j=1}^{m,n_i} \phi_{ij} \mathcal{H}_{ij} \mathbb{H}_{K_i} \right) e + \left(\mathbb{E}_L(\rho) + \sum_{i,j=1}^{m,n_i} \phi_{ij} \mathcal{H}_{ij} \mathbb{D}_{K_i} \right) w \tag{3.80}$$

with

$$\mathbb{A}_L(\rho) = A(\rho) - L(\rho)C, \qquad \mathbb{E}_L(\rho) = E - L(\rho)D \tag{3.81}$$

$$\mathbb{H}_{K_i} = H_i - K_i(\rho)C, \qquad \mathbb{D}_{K_i} = -K_i(\rho)D \tag{3.82}$$

The $\mathcal{H}_\infty$ criterion (3.78) is satisfied if the following holds [159]:

$$\mathcal{W} \triangleq \dot{V}(e) + \|e\|^2 - \mu \|w\|^2 \leq 0 \tag{3.83}$$

where $\dot{V}(e)$ is the time derivative of the classical quadratic Lyapunov function $V(e) = e^T \mathbb{P} e$, $\mathbb{P} = \mathbb{P}^T > 0$, which is commonly used to analyse the $\mathcal{H}_\infty$ stability of the estimation error. Thus, by calculating $\mathcal{W}$ along the trajectories of (3.80), we obtain

$$\begin{aligned}
\mathcal{W} \;\; = \;\; & e^T \left[\mathbb{I}_n + \left(\mathbb{A}_L(\rho) + \sum_{i,j=1}^{m,n_i} \phi_{ij} \mathcal{H}_{ij} \mathbb{H}_{K_i} \right)^T \mathbb{P} + \mathbb{P} \left(\mathbb{A}_L(\rho) + \sum_{i,j=1}^{m,n_i} \phi_{ij} \mathcal{H}_{ij} \mathbb{H}_{K_i} \right) \right] e \\
& + w^T \left(\mathbb{E}_L(\rho) + \sum_{i,j=1}^{m,n_i} \phi_{ij} \mathcal{H}_{ij} \mathbb{D}_{K_i} \right)^T \mathbb{P} e + e^T \mathbb{P} \left(\mathbb{E}_L(\rho) + \sum_{i,j=1}^{m,n_i} \phi_{ij} \mathcal{H}_{ij} \mathbb{D}_{K_i} \right) w \\
& - \mu w^T w.
\end{aligned} \tag{3.84}$$

Hence, $\mathcal{W} < 0$ if the following holds

$$\overbrace{\begin{bmatrix} \mathbb{A}_L^T(\rho)\mathbb{P} + \mathbb{P}\mathbb{A}_L(\rho) + \mathbb{I}_n & \mathbb{P}\mathbb{E}_L(\rho) \\ \mathbb{E}_L^T(\rho)\mathbb{P} & -\mu \mathbb{I}_z \end{bmatrix}}^{\Psi} + \sum_{i,j=1}^{m,n_i} \phi_{ij} \left(\overbrace{\begin{bmatrix} \mathbb{P}\mathcal{H}_{ij} \\ 0 \end{bmatrix}}^{\mathbb{X}_{ij}^T} \overbrace{\begin{bmatrix} \mathbb{H}_{K_i} & \mathbb{D}_{K_i} \end{bmatrix}}^{\mathbb{Y}_i} + \mathbb{Y}_i^T \mathbb{X}_{ij} \right) \leq 0 \tag{3.85}$$

Many methods can be applied to solve the LMI (3.85), however the resulted conditions may be conservative. Thus, we will provide in Theorem 4 a suitable and enhanced LMI condition to cope with the conservatism issue.

Theorem 4. *If there exist symmetric positive definite matrices* $\mathbb{P} \in \mathbb{R}^{n\times n}$, $\mathcal{S}_i \in \mathbb{R}^{n_i \times n_i}$ *and matrices* $\mathcal{R}_j \in \mathbb{R}^{p\times n}$, $\mathcal{Y}_i^j \in \mathbb{R}^{p\times n_i}$, $i = 1, \dots m$, $j = 0, \dots\ s$, *of appropriate dimensions so that the following convex optimization problem is solvable*

$$\min(\mu) \quad \text{subject to (3.87)} \tag{3.86}$$

$$\begin{bmatrix} \overbrace{\begin{bmatrix} \mathbb{A}\Big(\mathbb{P}, \mathcal{R}_j, \rho\Big) & \mathbb{E}\Big(\mathbb{P}, \mathcal{R}_j, \rho\Big) \\ (\star) & -\mu I_z \end{bmatrix}}^{\Psi} & \begin{bmatrix} \Sigma_1^T & \dots & \Sigma_m^T \end{bmatrix} \\ (\star) & -\Lambda \mathbb{S} \end{bmatrix} \leq 0 \tag{3.87}$$

with

$$\begin{aligned} \mathbb{A}\Big(\mathbb{P}, \mathcal{R}_j, \rho\Big) &= A_0^T \mathbb{P} + \mathbb{P} A_0 - C^T \mathcal{R}_0 - \mathcal{R}_0^T C + \mathbb{I}_n + \sum_{j=1}^{s} \rho_j \Big(A_j^T \mathbb{P} + \mathbb{P} A_j - C^T \mathcal{R}_j - \mathcal{R}_j^T C \Big) \\ \mathbb{E}\Big(\mathbb{P}, \mathcal{R}_j, \rho\Big) &= \mathbb{P} E - \mathcal{R}_0^T D - \sum_{j=1}^{s} \rho_j \mathcal{R}_j^T D \end{aligned} \tag{3.88}$$

and

$$\Sigma_i = \Big[\Sigma_{i1}^T \dots\ \Sigma_{in_i}^T \Big]^T, \quad \Sigma_{ij}^T = \begin{bmatrix} \mathbb{P}\mathcal{H}_{ij} \\ 0 \end{bmatrix} + \begin{bmatrix} H_i^T \mathcal{S}_i - C^T \mathcal{Y}_i^0 - \sum_{l=1}^{s} \rho_j C^T \mathcal{Y}_i^l \\ -D^T \mathcal{Y}_i^0 - \sum_{l=1}^{s} \rho_j D^T \mathcal{Y}_i^l \end{bmatrix} \tag{3.89}$$

$$\Lambda = \textit{block-diag}\Big(\Lambda_1, ..., \Lambda_m\Big), \quad \Lambda_i = \textit{block-diag}\left(\Lambda_{i1}, \dots, \Lambda_{in_i}\right), \quad \Lambda_{ij} = \frac{2}{b_{ij}} \mathbb{I}_{n_i} \tag{3.90}$$

$$\mathbb{S} = \textit{block-diag}\Big(\mathbb{S}_1, \dots, \mathbb{S}_m\Big), \quad \mathbb{S}_i = \textit{block-diag}\Big(\underbrace{\mathcal{S}_i, \dots, \mathcal{S}_i}_{n_i \ \text{times}}\Big) \tag{3.91}$$

then, the $\mathcal{H}_\infty$ *criterion* (3.78) *is satisfied with* $\nu = \lambda_{\max}(\mathbb{P})$*. The observer gains* L_j *and* K_i^j *are to be computed by*

$$L_j = \mathbb{P}^{-1}\mathcal{R}_j^T, \quad K_i^j = \mathcal{S}_i^{-1}(\mathcal{Y}_i^j)^T, \qquad i = 1, \dots m, \quad j = 0, \dots \ s. \tag{3.92}$$

Proof. From Lemma 2, we deduce that for all symmetric positive definite matrices $\mathbb{S}_{ij}$ and scalars, we have

$$\mathbb{X}_{ij}^T\mathbb{Y}_i + \mathbb{Y}_i^T\mathbb{X}_{ij} \leq \frac{1}{2}\Big[\mathbb{X}_{ij} + \mathbb{S}_{ij}\mathbb{Y}_i\Big]^T\mathbb{S}_{ij}^{-1}\Big[\mathbb{X}_{ij} + \mathbb{S}_{ij}\mathbb{Y}_i\Big] \tag{3.93}$$

Regarding the form of the matrix $\mathbb{Y}_i$, the fact that it does not depend on the index j and depends on the same $K_i(\rho)$, then to obtain an LMI we take $\mathbb{S}_{ij} = \mathcal{S}_i \ , \ \ \forall(i,j)$.

Consequently, from (3.21) and the fact that without loss of generality $a_{ij} = 0$, inequality (3.85) is satisfied if

$$\Psi + \sum_{i,j=1}^{m,n_i}\left(\Sigma_{ij}^T\Big(-\frac{2}{b_{ij}}\mathcal{S}_i\Big)^{-1}\Sigma_{ij}\right) \leq 0. \tag{3.94}$$

Therefore, from Schur lemma, inequality (3.94) is equivalent to

$$\begin{bmatrix} \Psi & \begin{bmatrix}\Sigma_1 & \dots & \Sigma_m\end{bmatrix} \\ & \\ (\star) & -\Lambda\mathbb{S} \end{bmatrix} \leq 0 \tag{3.95}$$

Finally, with change of variables $\mathcal{R}_j = L_j^T\mathbb{P}$ and $\mathcal{Y}_i^j = (K_i^j)^T\mathcal{S}_i$, the inequality (3.95) becomes identical to (3.87). Hence, the $\mathcal{H}_\infty$ criterion (3.78) is satisfied with the minimum μ obtained by (3.86). This ends the proof. □

3.4.4 Discrete LMI-Based Nonlinear State Observer

Usually, in real applications, the observer operates in discrete time and is driven by discrete time measurements (sampled data) [147]. Consequently we will provide, in this section, the discrete version of the previously designed observers in Section 3.4.2 and

Section 3.4.3. Therefore, we will investigate the general class of discrete-time systems described by the following equations

$$\begin{cases} x_{k+1} = A(\rho_k)x_k + B\gamma(x_k) + g(u_k, k) \\ y_k = Cx_k \end{cases} \tag{3.96}$$

where $x_k \in \mathbb{R}^n$ is the state vector, $y_k \in \mathbb{R}^p$ is the output measurement, $u_k \in \mathbb{R}^q$ is an input vector and $\rho_k \in \mathbb{R}^s$ is an $\mathcal{L}_\infty$ bounded and known parameter. The affine matrix $A(\rho_k)$ is expressed under the form

$$A(\rho_k) = A_0 + \sum_{j=1}^{s} \rho_k^j A_j \tag{3.97}$$

with

$$\rho_{\min}^j \leq \rho_k^j \leq \rho_{\max}^j \tag{3.98}$$

which means that the parameter ρ_k belongs to a bounded convex set for which the set of 2^s vertices can be defined by

$$\mathbb{V}_\rho = \Big\{ \varrho \in \mathbb{R}^s : \varrho^j \in \{\rho_{\min}^j, \rho_{\max}^j\} \Big\}. \tag{3.99}$$

The matrices $A_i \in \mathbb{R}^{n\times n}$, $B \in \mathbb{R}^{n\times m}$, $C \in \mathbb{R}^{p\times n}$ are constant. The nonlinear function $\gamma : \mathbb{R}^n \longrightarrow \mathbb{R}^m$ is assumed to be globally Lipschitz. It is obvious that $B\gamma(.)$ can always be written under the detailed form

$$B\gamma(x_k) = \sum_{i=1}^{m} B_i \gamma_i(\overbrace{H_i x_k}^{\vartheta_i}) \tag{3.100}$$

where $H_i \in \mathbb{R}^{n_i\times n}$ and B_i is the i^{th} column of the matrix B.

In order to estimate the missing state variables of the discrete model (3.96), we propose the following discrete time nonlinear state observer

$$\hat{x}_{k+1} = A(\rho_k)\hat{x}_k + \sum_{i=1}^{m} B_i \gamma_i(\hat{\vartheta}_i) + g(y_k, u_k) + L(\rho_k)\Big(y_k - C\hat{x}_k\Big) \tag{3.101}$$

with

$$\hat{\vartheta}_i = H_i \hat{x}_k + K_i(\rho_k)\Big(y_k - C\hat{x}_k\Big) \tag{3.102}$$

where $\hat{x}_k$ is the estimate of x_k, and

$$L(\rho_k) = L_0 + \sum_{j=1}^{s} \rho_k^j L_j, \quad K_i(\rho_k) = K_i^0 + \sum_{j=1}^{s} \rho_k^j K_i^j \tag{3.103}$$

The aim consists in finding the observer parameters $L_i \in \mathbb{R}^{n \times p}$ and $K_i^j \in \mathbb{R}^{n_i \times p}$ so that the estimation error

$$e_k = x_k - \hat{x}_k \tag{3.104}$$

decreases asymptotically towards zero.

Since $\gamma(.)$ is assumed to be globally Lipschitz, then from Lemma 1 and equation (3.100), there exist $z_i \in Co(\vartheta_i, \hat{\vartheta}_i)$, functions $\phi_{ij} \; : \; \mathbb{R}^{n_i} \longrightarrow \mathbb{R}$, and constants a_{ij}, b_{ij}, such that

$$B(\gamma(x_k) - \gamma(\hat{x}_k)) = \sum_{i,j=1}^{m,n_i} \phi_{ij}(z_i)\mathcal{H}_{ij}\Big(\vartheta_i - \hat{\vartheta}_i\Big) \tag{3.105}$$

with

$$a_{ij} \leq \phi_{ij}(z_i) \leq b_{ij} \tag{3.106}$$

where

$$\phi_{ij}(z_i) = \frac{\partial \gamma_i}{\partial \vartheta_i^j}(z_i), \;\; \mathcal{H}_{ij} = B_i e_{n_i}(j) \tag{3.107}$$

For shortness, we set $\phi_{ij} \triangleq \phi_{ij}(z_i)$.

Using equations (3.100),(3.102) and (3.105) we obtain

$$B(\gamma(x_k) - \gamma(\hat{x}_k)) = \left[\sum_{i,j=1}^{m,n_i} \phi_{ij}\mathcal{H}_{ij}\Big(H_i - K_i(\rho_k)C\Big)\right] e_k \tag{3.108}$$

Hence, by using equation (3.96), (3.101) and (3.108) we obtain the following dynamic equation of the estimation error (3.104)

$$e_{k+1} = \left(A(\rho_k) - L(\rho_k)C + \sum_{i,j=1}^{m,n_i} \phi_{ij}\mathcal{H}_{ij}\left(H_i - K_i(\rho_k)C\right)\right) e_k \tag{3.109}$$

In the sequel, we will provide in Theorem 5 the LMI conditions for which the estimation error is asymptotically stable around zero.

Theorem 5. *If there exist symmetric positive definite matrices* $\mathbb{P} \in \mathbb{R}^{n\times n}$, $\mathcal{S}_i \in \mathbb{R}^{n_i\times n_i}$ *and matrices* $\mathcal{X}_j \in \mathbb{R}^{p\times n}$, $\mathcal{Y}_i^j \in \mathbb{R}^{p\times n_i}$, $i = 1,\dots,m$, $j = 0,\dots,s$, *of appropriate dimensions so that the following LMI conditions are feasible*

$$\begin{bmatrix} \mathbb{M}(\rho_k) & \begin{bmatrix}\Pi_1^T & \dots & \Pi_m^T\end{bmatrix} \\ \\ (\star) & -\Lambda\mathbb{S} \end{bmatrix} < 0, \ \forall \rho_k \in \mathbb{V}_\rho \tag{3.110}$$

with

$$\mathbb{M}(\rho_k) = \begin{bmatrix} -\mathbb{P} & \mathbb{M}_{12}(\rho_k) \\ \\ (\star) & -\mathbb{P} \end{bmatrix} \tag{3.111}$$

$$\mathbb{M}_{12}(\rho_k) = \left(A_0^T\mathbb{P} - C^T\mathcal{X}_0\right) + \sum_{l=1}^{s} \rho_k^l \left(A_l^T\mathbb{P} - C^T\mathcal{X}_l\right) \tag{3.112}$$

$$\Pi_i = \left[\Pi_{i1}^T \dots \Pi_{in_i}^T\right]^T, \ \ \Pi_{ij}^T = \begin{bmatrix} 0 \\ \mathbb{P}\mathcal{H}_{ij} \end{bmatrix} + \begin{bmatrix} \mathbb{H}\left(\mathcal{S}_i, \mathcal{Y}_i^l\right) \\ 0 \end{bmatrix} \tag{3.113}$$

$$\mathbb{H}\left(\mathcal{S}_i, \mathcal{Y}_i^l\right) = H_i^T\mathcal{S}_i - C^T\left(\mathcal{Y}_i^0 + \sum_{l=1}^{s}\rho_k^l\mathcal{Y}_i^l\right) \tag{3.114}$$

$$\Lambda = \textit{block-diag}\Big(\Lambda_1, ..., \Lambda_m\Big), \quad \Lambda_i = \textit{block-diag}\left(\Lambda_{i1}, \dots, \Lambda_{in_i}\right), \quad \Lambda_{ij} = \frac{2}{b_{ij}}\mathbb{I}_{n_i} \tag{3.115}$$

$$\mathbb{S} = \textit{block-diag}\Big(\mathbb{S}_1, \dots, \mathbb{S}_m\Big), \quad \mathbb{S}_i = \textit{block-diag}\Big(\underbrace{\mathcal{S}_i, \dots, \mathcal{S}_i}_{ni \ \text{times}}\Big) \tag{3.116}$$

then, the estimation error converges asymptotically towards zero. Consequently, the observer parameters L_j *and* K_i^j *are to be computed as follows*

$$L_j = \mathbb{P}^{-1}\mathcal{X}_j^T, \ \ K_i^j = \mathcal{S}_i^{-1}(\mathcal{Y}_i^j)^T, \quad i = 1,\dots m, \ \ j = 0,\dots \ s. \tag{3.117}$$

Proof. We use the following quadratic Lyapunov function to perform the stability analysis of the estimation error

$$V(e_k) = e_k^T\mathbb{P}e_k, \ \ \mathbb{P} = \mathbb{P}^T > 0 \tag{3.118}$$

By calculating $\Delta V = V(e_{k+1}) - V(e_k)$ along the trajectories of (3.109), we obtain

$$\Delta V = e_k^T \left[\left(\mathbb{A}_L(\rho_k) + \sum_{i,j=1}^{m,n_i} \phi_{ij} \mathcal{H}_{ij} \mathbb{H}_{K_i} \right)^T \mathbb{P} \times \left(\mathbb{A}_L(\rho_k) + \sum_{i,j=1}^{m,n_i} \phi_{ij} \mathcal{H}_{ij} \mathbb{H}_{K_i} \right) - \mathbb{P} \right] e \quad (3.119)$$

with

$$\mathbb{A}_L = A(\rho_k) - L(\rho_k)C, \qquad \mathbb{H}_{K_i} = H_i - K_i(\rho_k)C \quad (3.120)$$

Hence, $\Delta V < 0$ if the following inequality holds

$$\left(\mathbb{A}_L(\rho_k) + \sum_{i,j=1}^{m,n_i} \phi_{ij} \mathcal{H}_{ij} \mathbb{H}_{K_i} \right)^T \mathbb{P} \times \left(\mathbb{A}_L(\rho_k) + \sum_{i,j=1}^{m,n_i} \phi_{ij} \mathcal{H}_{ij} \mathbb{H}_{K_i} \right) - \mathbb{P} < 0. \quad (3.121)$$

Inequality (3.121) is equivalent, by Schur lemma, to

$$\begin{bmatrix} -\mathbb{P} & \left(\mathbb{A}_L(\rho_k) + \sum_{i,j=1}^{m,n_i} \phi_{ij} \mathcal{H}_{ij} \mathbb{H}_{K_i} \right)^T \mathbb{P} \\ (\star) & -\mathbb{P} \end{bmatrix} < 0 \quad (3.122)$$

On the other side, inequality (3.122) can be rewritten under the form

$$\overbrace{\begin{bmatrix} -\mathbb{P} & \mathbb{A}_L^T(\rho_k)\mathbb{P} \\ (\star) & -\mathbb{P} \end{bmatrix}}^{\mathbb{M}(\rho_k)} + \sum_{i,j=1}^{m,n_i} \phi_{ij} \left(\overbrace{\begin{bmatrix} 0 \\ \mathbb{P}\mathcal{H}_{ij} \end{bmatrix}}^{\mathbb{X}_{ij}^T} \overbrace{\begin{bmatrix} \mathbb{H}_{K_i} & 0 \end{bmatrix}}^{\mathbb{Y}_i} + \mathbb{Y}_i^T \mathbb{X}_{ij} \right) < 0. \quad (3.123)$$

Now, by applying Lemma 2 we have

$$\mathbb{X}_{ij}^T \mathbb{Y}_i + \mathbb{Y}_i^T \mathbb{X}_{ij} \leq \frac{1}{2} \left(\mathbb{X}_{ij} + \mathbb{S}_{ij} \mathbb{Y}_i \right)^T \mathbb{S}_{ij}^{-1} \overbrace{\left(\mathbb{X}_{ij} + \mathbb{S}_{ij} \mathbb{Y}_i \right)}^{\Pi_{ij}}$$

for any symmetric positive definite matrices $\mathbb{S}_{ij}$. Since the matrix block $\mathbb{Y}_i$ does not depend on the index j and depends on the same $K_i(\rho_k)$, then to obtain an LMI, we are constrained to put

$$\mathbb{S}_{ij} = \mathcal{S}_i, \ \forall(i,j)$$

with $\mathcal{S}_i \in \mathbb{R}^{n_i \times n_i}$.

Consequently, from (3.106) and the fact that $a_{ij} = 0$, inequality (3.123) holds if

$$\mathbb{M}(\rho_k) - \sum_{i,j=1}^{m,n_i} \left(\Pi_{ij}^T \Big(-\frac{2}{b_{ij}} \mathcal{S}_i \Big)^{-1} \Pi_{ij} \right) < 0. \tag{3.124}$$

Therefore, from Schur lemma, inequality (3.124) is equivalent to

$$\begin{bmatrix} \mathbb{M}(\rho_k) & \begin{bmatrix} \Pi_1^T & \dots & \Pi_m^T \end{bmatrix} \\ \\ (\star) & -\Lambda\mathbb{S} \end{bmatrix} < 0 \tag{3.125}$$

Finally, we use the change of variables $\mathcal{X}_i = L_i^T \mathbb{P}$ and $\mathcal{Y}_i^j = (K_i^j)^T \mathcal{S}_i$, and since (3.125) is affine in ρ_k, then the convexity principle [158] leads to (3.110). This ends the proof. □

3.4.5 Discrete LMI-Based $\mathcal{H}_\infty$ Nonlinear State Observer

In this section we will enhance the designed discrete time nonlinear observer in Section 3.4.4 to account for some disturbances affecting the system dynamics and corrupting the measurements. Therefore, we consider the following class of systems

$$\begin{cases} x_{k+1} = A(\rho_k) x_k + B\gamma(x_k) + g(u_k, k) + E w_k \\ y_k = C x_k + D w_k \end{cases} \tag{3.126}$$

where the model parameters are the same as those defined for the model (3.96), and $w_k \in \mathbb{R}^z$ is the disturbance $\mathcal{L}_2$ bounded vector. The matrices $E \in \mathbb{R}^{n \times z}$ and $D \in \mathbb{R}^{p \times z}$ are constant.

In order to reconstruct the missing state variables of the system (3.126), we use the same nonlinear observer structure (3.101). However, this time we target to find the observer gains $L_i \in \mathbb{R}^{n \times p}$ and $K_i^j \in \mathbb{R}^{n_i \times p}$ so that the estimation error $e_k = x_k - \hat{x}_k$ be $\mathcal{H}_\infty$ asymptotically stable. Or to put it in another way, we want to find the observer gains such that $\mathcal{H}_\infty$ criterion (3.78) is satisfied.

From Lemma 1 and using equations (3.100), (3.102), (3.106), (3.107), (3.126) and since

$$\vartheta_i - \hat{\vartheta}_i = \Big(H_i - K_i(\rho_k)C\Big)e_k - K_i(\rho_k)Dw_k \tag{3.127}$$

then, we have

$$B(\gamma(x_k) - \gamma(\hat{x}_k)) = \left[\sum_{i,j=1}^{m,n_i} \phi_{ij}\mathcal{H}_{ij}\Big(H_i - K_i(\rho_k)C\Big)\right] e_k - \left[\sum_{i,j=1}^{m,n_i} \phi_{ij}\mathcal{H}_{ij}K_i(\rho_k)D\right] w_k \tag{3.128}$$

Therefore, the difference equation of the estimation error can be obtained as

$$e_{k+1} = \left(\mathbb{A}_L(\rho_k) + \sum_{i,j=1}^{m,n_i} \phi_{ij}\mathcal{H}_{ij}\mathbb{H}_{K_i}\right) e_k + \left(\mathbb{E}_L(\rho_k) + \sum_{i,j=1}^{m,n_i} \phi_{ij}\mathcal{H}_{ij}\mathbb{D}_{K_i}\right) w_k \tag{3.129}$$

with

$$\mathbb{A}_L = A(\rho_k) - L(\rho_k)C, \qquad \mathbb{H}_{K_i} = H_i - K_i(\rho_k)C. \tag{3.130}$$

$$\mathbb{E}_L = E - L(\rho_k)D, \qquad \mathbb{D}_{K_i} = -K_i(\rho_k)D. \tag{3.131}$$

Usually, a quadratic Lyapunov function is used to analyse the $\mathcal{H}_\infty$ stability of the estimation error (3.129). That is to use

$$V(e_k) = e_k^T\mathbb{P}e_k, \quad \mathbb{P} = \mathbb{P}^T > 0 \tag{3.132}$$

Consequently the $\mathcal{H}_\infty$ criterion (3.78) is satisfied if the following holds

$$\mathcal{W} \triangleq \Delta V + \|e\|^2 - \mu\|w\|^2 \leq 0. \tag{3.133}$$

where $\Delta V = V(e_{k+1}) - V(e_k)$.

The main results related to the convergence analysis of the estimation error (3.129) are summarized in Theorem 6, which provides new enhanced LMI conditions.

Theorem 6. *If there exist symmetric positive definite matrices* $\mathbb{P} \in \mathbb{R}^{n\times n}$, $\mathcal{S}_i \in \mathbb{R}^{n_i\times n_i}$, *and matrices* $\mathcal{X}_j \in \mathbb{R}^{p\times n}$*,* $\mathcal{Y}_i^j \in \mathbb{R}^{p\times n_i}$*,* $i = 1, \ldots, m,\ j = 0, \ldots, s,$ *of appropriate dimensions so that the following convex optimization problem is solvable*

$$\min(\mu) \ \text{ subject to (3.135)} \tag{3.134}$$

$$\begin{bmatrix} \mathbb{M}(\varrho) & \begin{bmatrix} \Pi_1^T & \ldots & \Pi_m^T \end{bmatrix} \\ \\ (\star) & -\Lambda\mathbb{S} \end{bmatrix} < 0,\ \forall \varrho \in \mathbb{V}_\rho \tag{3.135}$$

with

$$\mathbb{M}(\varrho) = \begin{bmatrix} -\mathbb{P} + \mathbb{I}_n & 0 & \mathbb{M}_{13}(\varrho) \\ \\ 0 & -\mu\mathbb{I}_z & \mathbb{M}_{23}(\varrho) \\ \\ \mathbb{M}_{13}^\top(\varrho) & \mathbb{M}_{23}^\top(\varrho) & -\mathbb{P} \end{bmatrix} \tag{3.136}$$

$$\mathbb{M}_{13}(\varrho) = \left(A_0^T\mathbb{P} - C^T\mathcal{X}_0\right) + \sum_{l=1}^{s} \varrho^l \left(A_l^T\mathbb{P} - C^T\mathcal{X}_l\right) \tag{3.137}$$

$$\mathbb{M}_{23}(\varrho) = E^\top\mathbb{P} - D^\top \left(\mathcal{X}_0 + \sum_{l=1}^{s} \varrho^l \mathcal{X}_l\right) \tag{3.138}$$

$$\Pi_i = \left[\Pi_{i1}^T \ldots \Pi_{in_i}^T\right]^T, \quad \Pi_{ij}^T = \begin{bmatrix} \mathbb{H}\Big(\mathcal{S}_i, \mathcal{Y}_i^l\Big) \\ \mathbb{D}\Big(\mathcal{S}_i, \mathcal{Y}_i^l\Big) \\ \mathbb{P}\mathcal{H}_{ij} \end{bmatrix} \tag{3.139}$$

$$\mathbb{H}\Big(\mathcal{S}_i, \mathcal{Y}_i^l\Big) = H_i^T\mathcal{S}_i - C^T \left(\mathcal{Y}_i^0 + \sum_{l=1}^{s} \varrho^l \mathcal{Y}_i^l\right) \tag{3.140}$$

$$\mathbb{D}\Big(\mathcal{S}_i, \mathcal{Y}_i^l\Big) = -D^T \left(\mathcal{Y}_i^0 + \sum_{l=1}^{s} \varrho^l \mathcal{Y}_i^l\right) \tag{3.141}$$

$$\Lambda = \textit{block-diag}\Big(\Lambda_1, ..., \Lambda_m\Big), \quad \Lambda_i = \textit{block-diag}\left(\Lambda_{i1}, \ldots, \Lambda_{in_i}\right), \quad \Lambda_{ij} = \frac{2}{b_{ij}}\mathbb{I}_{n_i} \tag{3.142}$$

$$\mathbb{S} = \textit{block-diag}\Big(\mathbb{S}_1, \ldots, \mathbb{S}_m\Big), \quad \mathbb{S}_i = \textit{block-diag}\Big(\underbrace{\mathcal{S}_i, \ldots, \mathcal{S}_i}_{ni \text{ times}}\Big) \tag{3.143}$$

then, the estimation error satisfies the $\mathcal{H}_\infty$ criterion (3.78) with $\nu = \lambda_{\max}(\mathbb{P})$. Consequently, the observer parameters L_j and K_i^j are to be computed as follows:

$$L_j = \mathbb{P}^{-1}\mathcal{X}_j^T, \quad K_i^j = \mathcal{S}_i^{-1}(\mathcal{Y}_i^j)^T.$$

Proof. By calculating $\mathcal{W}$ (3.133) along the trajectories of (3.129), we obtain

$$\begin{aligned}
\mathcal{W} = e_k^T & \left[\left(\mathbb{A}_L(\rho_k) + \sum_{i,j=1}^{m,n_i} \phi_{ij}\mathcal{H}_{ij}\mathbb{H}_{K_i} \right)^T \mathbb{P} \times \left(\mathbb{A}_L(\rho_k) + \sum_{i,j=1}^{m,n_i} \phi_{ij}\mathcal{H}_{ij}\mathbb{H}_{K_i} \right) - \mathbb{P} + \mathbb{I}_n \right] e_k \\
& + w_k^T \left[\left(\mathbb{E}_L(\rho_k) + \sum_{i,j=1}^{m,n_i} \phi_{ij}\mathcal{H}_{ij}\mathbb{D}_{K_i} \right)^T \mathbb{P} \times \left(\mathbb{E}_L(\rho_k) + \sum_{i,j=1}^{m,n_i} \phi_{ij}\mathcal{H}_{ij}\mathbb{D}_{K_i} \right) - \mu\mathbb{I}_z \right] w_k \\
& + e_k^T \left[\left(\mathbb{A}_L(\rho_k) + \sum_{i,j=1}^{m,n_i} \left[\phi_{ij}\mathcal{H}_{ij}\mathbb{H}_{K_i} \right] \right)^T \mathbb{P} \times \left(\mathbb{E}_L(\rho_k) + \sum_{i,j=1}^{m,n_i} \phi_{ij}\mathcal{H}_{ij}\mathbb{D}_{K_i} \right) \right] w_k \\
& + w_k^T \left[\left(\mathbb{E}_L(\rho_k) + \sum_{i,j=1}^{m,n_i} \phi_{ij}\mathcal{H}_{ij}\mathbb{D}_{K_i} \right)^T \mathbb{P} \times \left(\mathbb{A}_L(\rho_k) + \sum_{i,j=1}^{m,n_i} \left[\phi_{ij}\mathcal{H}_{ij}\mathbb{H}_{K_i} \right] \right) \right] e_k
\end{aligned}$$

which is negative if the following matrix inequality holds

$$\begin{bmatrix} \Sigma_{11}^T\mathbb{P}\Sigma_{11} - \mathbb{P} + \mathbb{I}_n & \Sigma_{11}^T\mathbb{P}\Sigma_{22} \\ (\star) & \Sigma_{22}^T\mathbb{P}\Sigma_{22} - \mu\mathbb{I}_z \end{bmatrix} < 0 \tag{3.144}$$

where

$$\Sigma_{11} = \mathbb{A}_L(\rho_k) + \sum_{i,j=1}^{m,n_i} \phi_{ij}\mathcal{H}_{ij}\mathbb{H}_{K_i} \tag{3.145}$$

and

$$\Sigma_{22} = \mathbb{E}_L(\rho_k) + \sum_{i,j=1}^{m,n_i} \phi_{ij}\mathcal{H}_{ij}\mathbb{D}_{K_i} \tag{3.146}$$

Using the Schur lemma we deduce that $\mathcal{W} < 0$ if the subsequent matrix inequality holds:

$$\begin{bmatrix} \begin{bmatrix} -\mathbb{P} + \mathbb{I}_n & 0 \\ 0 & -\mu \mathbb{I}_z \end{bmatrix} & \begin{bmatrix} \left(\mathbb{A}_L(\rho_k) + \sum_{i,j=1}^{m,n_i} \left[\phi_{ij} \mathcal{H}_{ij} \mathbb{H}_{K_i} \right] \right)^T \mathbb{P} \\ \left(\mathbb{E}_L(\rho_k) + \sum_{i,j=1}^{m,n_i} \left[\phi_{ij} \mathcal{H}_{ij} \mathbb{D}_{K_i} \right] \right)^T \mathbb{P} \end{bmatrix} \\ (\star) & -\mathbb{P} \end{bmatrix} < 0 \tag{3.147}$$

which can be rewritten under the following form:

$$\overbrace{\begin{bmatrix} \begin{bmatrix} -\mathbb{P} + \mathbb{I}_n & 0 \\ 0 & -\mu \mathbb{I}_z \end{bmatrix} & \begin{bmatrix} \mathbb{A}_L^\top(\rho_k)\mathbb{P} \\ \mathbb{E}_L^\top(\rho_k)\mathbb{P} \end{bmatrix} \\ (\star) & -\mathbb{P} \end{bmatrix}}^{\Psi} + \sum_{i,j=1}^{m,n_i} \phi_{ij} \left(\overbrace{\begin{bmatrix} 0 \\ 0 \\ \mathbb{P}\mathcal{H}_{ij} \end{bmatrix}}^{\mathbb{X}_{ij}^T} \overbrace{\begin{bmatrix} \mathbb{H}_{K_i} & \mathbb{D}_{K_i} & 0 \end{bmatrix}}^{\mathbb{Y}_i} + \mathbb{Y}_i^T \mathbb{X}_{ij} \right) < 0 \tag{3.148}$$

Now, by applying Lemma 2 we have

$$\mathbb{X}_{ij}^T \mathbb{Y}_i + \mathbb{Y}_i^T \mathbb{X}_{ij} \leq \frac{1}{2} \Big(\mathbb{X}_{ij} + \mathbb{S}_{ij} \mathbb{Y}_i \Big)^T \mathbb{S}_{ij}^{-1} \overbrace{\Big(\mathbb{X}_{ij} + \mathbb{S}_{ij} \mathbb{Y}_i \Big)}^{\Pi_{ij}}$$

for any symmetric positive definite matrices $\mathbb{S}_{ij}$. Since the matrix block $\mathbb{Y}_i$ does not depend on the index j and depends on the same $K_i(\rho_k)$, then to obtain an LMI, we need to put

$$\mathbb{S}_{ij} = \mathcal{S}_i, \ \forall (i, j)$$

with $\mathcal{S}_i \in \mathbb{R}^{n_i \times n_i}$.

Consequently, from (3.60) and the fact that $a_{ij} = 0$, inequality (3.148) holds if

$$\Psi - \sum_{i,j=1}^{m,n_i} \left(\Pi_{ij}^T \Big(-\frac{2}{b_{ij}} \mathcal{S}_i \Big)^{-1} \Pi_{ij} \right) < 0. \tag{3.149}$$

Moreover, by Schur lemma, inequality (3.149) is equivalent to

$$\begin{bmatrix} \Psi & \begin{bmatrix} \Pi_1^T & \dots & \Pi_m^T \end{bmatrix} \\ & \\ (\star) & -\Lambda\mathbb{S} \end{bmatrix} < 0 \tag{3.150}$$

Finally, we use the change of variables $\mathcal{X}_i = L_i^T \mathbb{P}$ and $\mathcal{Y}_i^l = (K_i^l)^T \mathcal{S}_i$, and since (3.150) is affine in ρ_k, then the convexity principle [158] leads to (3.135). This ends the proof. □

3.4.6 Application and Simulation Results

The aim of this section is to apply and compare the designed nonlinear observers in Sections 3.4.2-3.4.5. In order to prevent recurrence, we will first compare the designed continuous nonlinear observers in presence of the same disturbances in dynamics and measurements. Then, we compare the designed discrete time nonlinear observers in presence different disturbances in dynamics and measurements.

3.4.6.1 Continuous Case

In order to apply the continuous nonlinear observers designed in Sections 3.4.2 and 3.4.3 (with and without including the $\mathcal{H}_\infty$ criterion), we first write the AD model (2.11) under the form (3.9a), (3.9b) and (3.77), respectively. To do so, we use the same parameters given by equations (3.48)-(3.51), and for simulation, we choose the matrices E and D to be equal to

$$E = [0.1, 0.2, 1, 0.1, 0.3, 0.2]^T, \quad D = [0.5, 0.4, 2]^T \tag{3.151}$$

Moreover, for the nonlinear observer (3.55)-(3.57) design, we use the same parameters given in equations (3.220), (3.53).

The simulation has been run for $\rho_{min} = 0.1$ day^{-1}, $\rho_{max} = 0.9$ day^{-1}, $S_{1in} = 16$ g/l, $S_{2in} = 170$ mmol/l, $C_{in} = 76.15$ mmol/l, $Z_{in} = 200$ mmol/l, $Z_{ad} = 700$ mmol/l,

$S_{2ad} = 0$ mmol/l, and the parameter values given in Table 2.2. After solving the LMI conditions (3.63) given by Theorem 3, which has been found to be feasible by using the LMI Toolbox of Matlab, we have obtained the following observer gains

$$L_0 = \begin{bmatrix} 70.4615 & -26.3655 & 0.0000 \\ -1.8869 & 0.6945 & -0.0000 \\ -27.5487 & 427.0033 & 0.0000 \\ -0.7332 & -1.5253 & -0.0000 \\ -298.0623 & -421.9481 & -0.0000 \\ -0.0000 & -0.0000 & 1.0002 \end{bmatrix}, \quad L_1 = \begin{bmatrix} 97.6669 & 21.8408 & 0.0000 \\ -2.6803 & -0.5943 & -0.0000 \\ 128.2053 & 80.4261 & -0.0000 \\ -1.7796 & -0.6275 & -0.0000 \\ -635.4521 & -208.7999 & -0.0000 \\ -0.0000 & -0.0000 & -0.8861 \end{bmatrix}$$

$$K_{10} = \begin{bmatrix} 0.8513 & 0.1385 & 0.0000 \\ -0.4132 & 0.3698 & -0.0000 \end{bmatrix}, \qquad K_{11} = \begin{bmatrix} 0.0029 & -0.0043 & -0.0000 \\ -0.0072 & 0.0090 & -0.0000 \end{bmatrix}$$

$$K_{20} = \begin{bmatrix} -0.0288 & 0.7702 & 0.0000 \\ -0.1227 & -0.9769 & -0.0000 \end{bmatrix}, \quad K_{21} = \begin{bmatrix} -0.0008 & -0.0057 & -0.0000 \\ 0.0009 & 0.0060 & -0.0000 \end{bmatrix}$$

Likewise, after solving the optimisation problem (3.86) given in Theorem 4, we have obtained the following $\mathcal{H}_\infty$ observer gains

$$L_0 = \begin{bmatrix} 67.2351 & -25.5664 & -11.6455 \\ -1.8176 & 0.6750 & 0.4194 \\ -76.9579 & 386.5060 & -57.5617 \\ -0.4787 & -1.3114 & 0.4320 \\ -220.7042 & -373.8534 & 130.0967 \\ -0.2057 & -0.0151 & 0.1545 \end{bmatrix}, \quad L_1 = \begin{bmatrix} 97.0686 & 33.0996 & -30.8871 \\ -2.7416 & -0.8949 & 0.8644 \\ 114.2877 & 49.4467 & -38.4613 \\ -1.7284 & -0.6196 & 0.5560 \\ -616.4464 & -222.5452 & 198.6207 \\ 0.2337 & 0.3001 & -0.1185 \end{bmatrix}$$

$$K_{10} = \begin{bmatrix} 0.7300 & 0.0768 & -0.1979 \\ -0.6614 & 0.4055 & 0.0843 \end{bmatrix}, \qquad K_{11} = \begin{bmatrix} 0.0002 & -0.0008 & 0.0001 \\ -0.0040 & 0.0036 & 0.0003 \end{bmatrix}$$

$$K_{20} = \begin{bmatrix} -0.1165 & 0.6410 & -0.0991 \\ -0.2875 & -1.1785 & 0.3076 \end{bmatrix}, \quad K_{21} = \begin{bmatrix} 0.0008 & -0.0000 & -0.0002 \\ -0.0018 & 0.0001 & 0.0004 \end{bmatrix}$$

and $\mu = 3.5845\ e^{-9}$.

Besides, for simulation, we have initialized the system and the observer by $x(0) = [2, 0.5, 12, 0.7, 53.5, 55]^T$ and $\hat{x}(0) = [2, 1.5, 12, 0.2, 40, 55]$, respectively. We have also injected in the system dynamics and measurements the disturbance depicted in Figure 3.11. After processing the simulation for 100 days, we have obtained the results

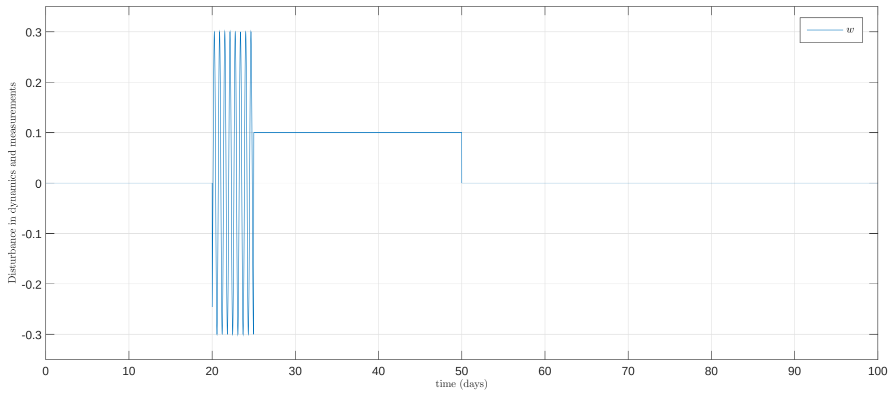

FIGURE 3.11: Disturbance in dynamics and measurements (w)

depicted in Figures 3.12-3.17 where we can see clearly that, although the large intial estimation error, both the continuous nonlinear observer designed in Sections 3.4.2 and the continuous $\mathcal{H}_\infty$ nonlinear observer designed in Section 3.4.3 behave similarly when no perturbation is affecting the system dynamics and measurements. However, once the system dynamics and measurements get disturbed, the performances of the observer which does not include the $\mathcal{H}_\infty$ criterion decrease and the $\mathcal{H}_\infty$ observer proves to be robust and rejects very well the perturbations. In order to give an idea on the level of attenuation of the disturbances by the designed $\mathcal{H}_\infty$ observer, we compare the estimation errors of the two observers in Figures 3.18-3.20. These figures give a quite good idea on the level of disturbance attenuation by the $\mathcal{H}_\infty$ observer. Thus, we conclude that the inclusion of the $\mathcal{H}_\infty$ criterion (3.78) in the observer design makes it robust to disturbances and render it more suitable for the AD systems which are often exposed to disturbances [45].

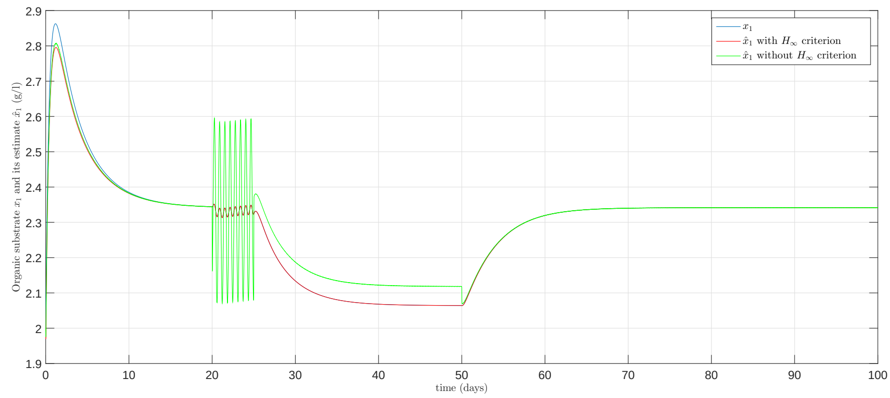

FIGURE 3.12: Substrate concentration x_1 and its estimate $\hat{x}_1$ (g/l).

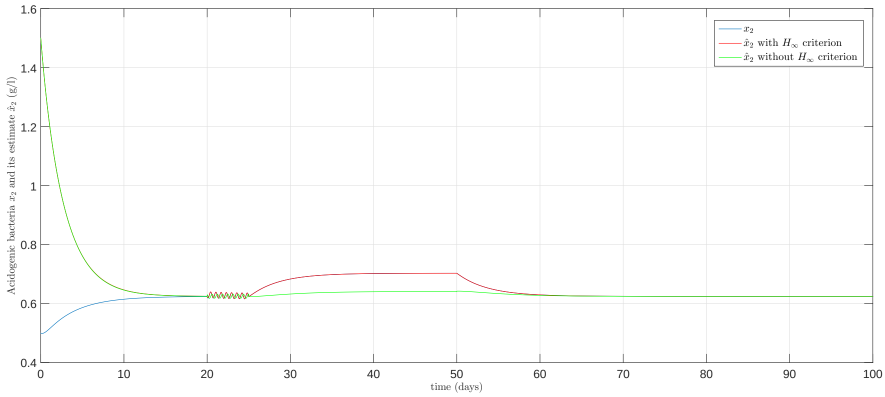

FIGURE 3.13: Acidogenic bacteria x_2 and its estimate $\hat{x}_2$ (g/l).

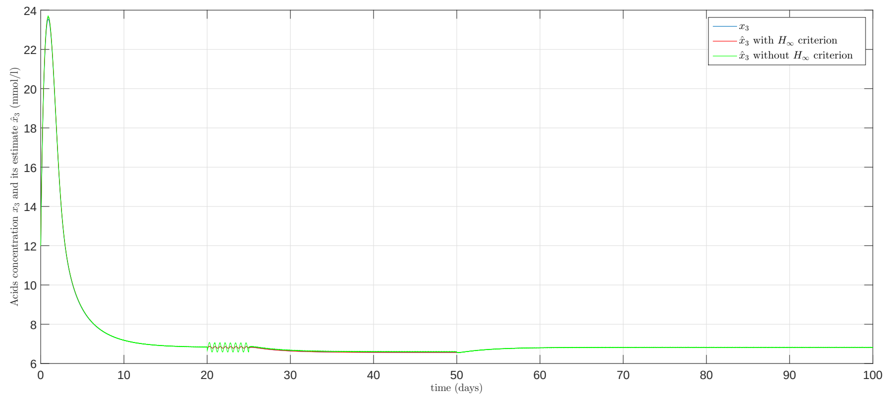

FIGURE 3.14: Acetate concentration x_3 and its estimate $\hat{x}_3$ (mmol/l).

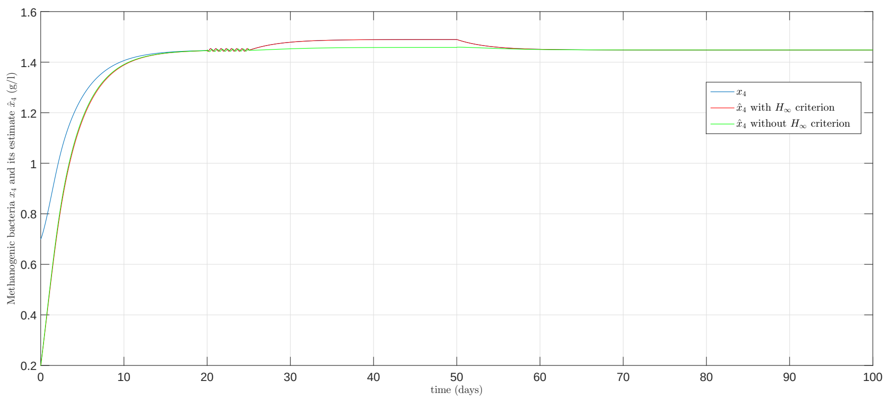

FIGURE 3.15: Mathenogenic bacteria x_4 and its estimate $\hat{x}_4$ (g/l).

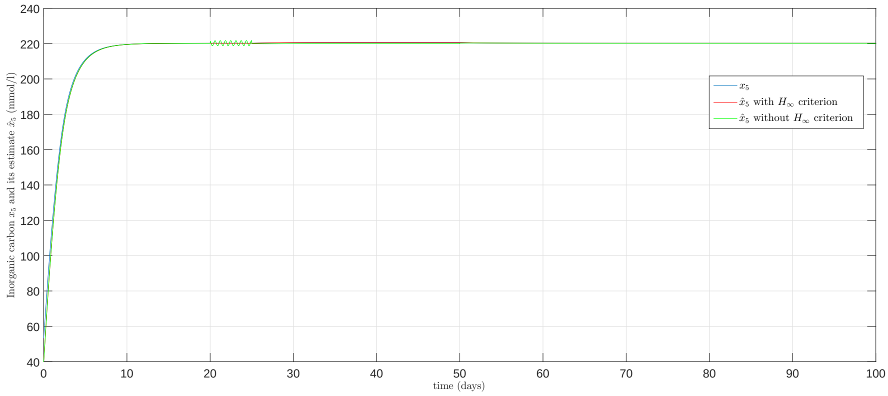

FIGURE 3.16: Inorganic carbon x_5 and its estimate $\hat{x}_5$ (mmol/l).

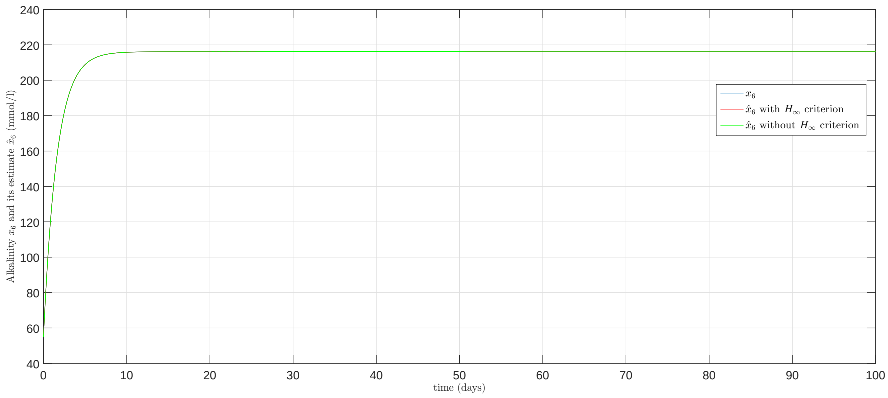

FIGURE 3.17: Alkalinity concentration x_6 and its estimate $\hat{x}_6$ (mmol/l).

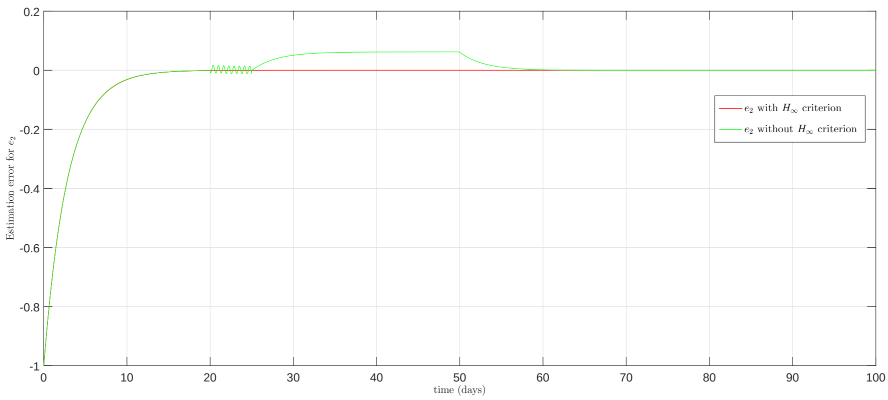

FIGURE 3.18: Estimation error $e_2 = x_2 - \hat{x}_2$.

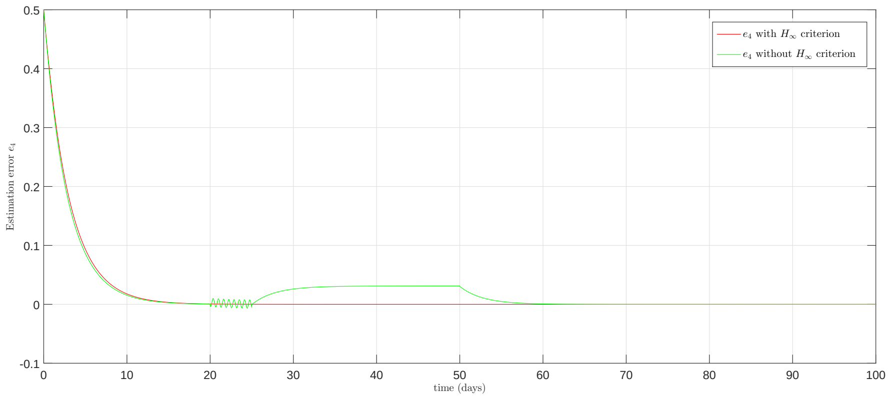

FIGURE 3.19: Estimation error $e_4 = x_4 - \hat{x}_4$.

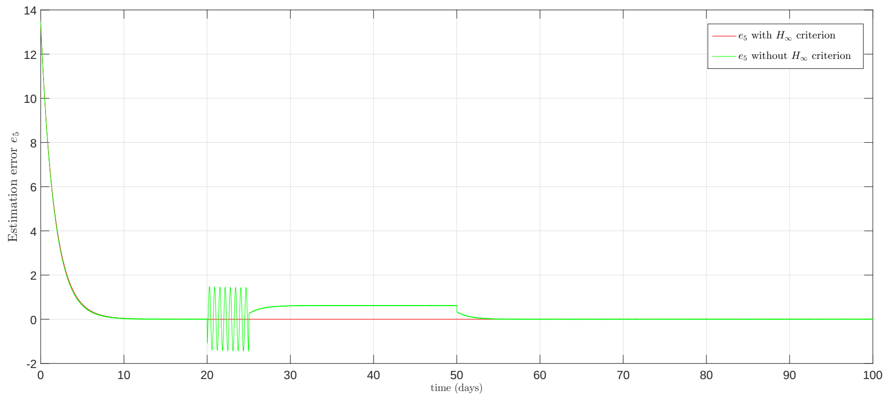

FIGURE 3.20: Estimation error $e_5 = x_5 - \hat{x}_5$.

3.4.6.2 Discrete Case

In this section, we target to apply the discrete time nonlinear observers, designed in Sections 3.4.4 and 3.4.5, to the AD model (2.11). Hence, before applying the considered discrete observers, we need first to write the model (2.11) under the discrete form (3.96) and (3.126).

Generally, for a given continuous-time nonlinear model, a closed form solution for an exact discretization is difficult to find explicitly, then we need to have approximate discrete-time models. In this section, we will present an Euler approximation which is important and easy to derive and it keeps the form of the original system. To obtain this approximation we assume that the control inputs are constant during the sampling intervals $[kT_s,\ (k+1)T_s]$, where T_s is the sampling period. Moreover, for simulation, we will take the same model outputs as in the previous Sections 3.4.6.1 and 3.4.1.1, that is to say the variables q_c, x_1, x_3 and x_6 are available for measurement. Thus, the system

(2.11) can be easily written in the form (3.96) using the following parameters

$$\rho_k = u_{out}(k), \quad A_0 = \mathbb{I}_6, \quad A_1 = -T_s \times \text{block-diag}(1, \alpha, 1, \alpha, 1, 1) \tag{3.152}$$

$$B = T_s \times \begin{bmatrix} -k_1 & 1 & k_2 & 0 & k_4 & 0 \\ 0 & 0 & -k_3 & 1 & k_5 & 0 \end{bmatrix}^T, \quad \gamma(x) = \begin{bmatrix} \mu_1(x_1)x_2 \\ \mu_2(x_3)x_4 \end{bmatrix} \tag{3.153}$$

$$g(u,t) = T_s \times \begin{bmatrix} u_1 S_{1in} & 0 & u_1(S_{2in} + S_{2ad}) & 0 & u_1 C_{in} - q_c & u_1 Z_{in} + u_2 Z_{ad} \end{bmatrix}^T \tag{3.154}$$

and

$$C = \begin{bmatrix} 1 & 0 & 0 & 0 & 0 & 0 \\ 0 & 0 & 1 & 0 & 0 & 0 \\ 0 & 0 & 0 & 0 & 0 & 1 \end{bmatrix}$$

Besides, as already mentioned, for an illustrative simulation we will suppose that the disturbances affecting the system dynamics are different from those affecting the measurements. Therefore, to obtain the model form (3.126), will need to put the matrices E and D as defined in Remark 4. This means to set

$$E = \begin{bmatrix} 0.01 & 0.02 & 0.1 & 0.01 & 0.03 & 0.02 \\ 0 & 0 & 0 & 0 & 0 & 0 \end{bmatrix}^T, \quad D = \begin{bmatrix} 0 & 0 & 0 \\ 0.1 & 0.5 & 1 \end{bmatrix}^T \tag{3.155}$$

Regarding the observer design, we have, $m = 2$, $s = 1$, $\gamma_1(x) = \mu_1(x_1)x_2$, $n_1 = 2$, $\gamma_2(x) = \mu_2(x_3)x_4$, $n_2 = 2$ and

$$H_1 = \begin{bmatrix} 1 & 0 & 0 & 0 & 0 & 0 \\ 0 & 1 & 0 & 0 & 0 & 0 \end{bmatrix}, \qquad H_2 = \begin{bmatrix} 0 & 0 & 1 & 0 & 0 & 0 \\ 0 & 0 & 0 & 1 & 0 & 0 \end{bmatrix}$$

$$B_1 = T_s \times \begin{bmatrix} -k_1 & 1 & k_2 & 0 & k_4 & 0 \end{bmatrix}^T, \quad B_2 = T_s \times \begin{bmatrix} 0 & 0 & -k_3 & 1 & k_5 & 0 \end{bmatrix}^T$$

The simulation has been run for the same operating condition as the continuous time case, and the sampling time has been set to $T_s = 0.001$ day, to emulate the sampling time that a sensor has experimentally [119].

By using the LMI MATLAB Toolbox, we have solved the LMI conditions (3.110) given in Theorem 5 and we have obtained the following observer gains

$$L_0 = \begin{bmatrix} 0.5415 & 0.0074 & 0.0000 \\ -0.0276 & -0.0003 & -0.0000 \\ -0.0027 & 0.4947 & 0.0000 \\ -0.0209 & -0.0072 & -0.0000 \\ -2.4631 & -0.6518 & -0.0000 \\ 0.0000 & 0.0000 & 0.4997 \end{bmatrix}, \quad L_1 = \begin{bmatrix} 0.8734 & 0.0119 & -0.0000 \\ -0.0444 & -0.0005 & 0.0000 \\ -0.0042 & 0.7979 & -0.0000 \\ -0.0337 & -0.0116 & 0.0000 \\ -3.9726 & -1.0514 & 0.0000 \\ -0.0000 & -0.0000 & 0.8059 \end{bmatrix}$$

$$K_{10} = \begin{bmatrix} 0.4985 & -0.0024 & 0.0000 \\ -0.0541 & 0.0504 & 0.0000 \end{bmatrix}, \quad K_{11} = \begin{bmatrix} 0.8040 & -0.0039 & -0.0000 \\ -0.0870 & 0.0809 & -0.0000 \end{bmatrix}$$

$$K_{20} = \begin{bmatrix} 0.0014 & 0.5012 & 0.0000 \\ -0.0944 & -0.0524 & 0.0000 \end{bmatrix}, \quad K_{21} = \begin{bmatrix} 0.0022 & 0.8084 & -0.0000 \\ -0.1524 & -0.0846 & -0.0000 \end{bmatrix}$$

Likewise, using the same LMI toolbox of Matlab, we have solved the optimization problem (3.134) given by Theorem 6, and it has been found that the gains of the $\mathcal{H}_\infty$ nonlinear state observer to be equal to

$$L_0 = \begin{bmatrix} 0.9848 & -0.0039 & -0.0657 \\ -0.1759 & -0.0393 & 0.3552 \\ -0.0768 & 0.9801 & -0.3338 \\ -0.0888 & -0.0240 & 0.1850 \\ -6.1235 & -1.6373 & 4.3213 \\ -0.1501 & -0.0388 & 0.3482 \end{bmatrix}, \quad L_1 = \begin{bmatrix} -0.0007 & 0.0001 & 0.0011 \\ 0.0004 & 0.0001 & 0.0009 \\ 0.0026 & -0.0003 & 0.0117 \\ 0.0002 & 0.0001 & 0.0004 \\ 0.0051 & 0.0013 & -0.0128 \\ 0.0005 & 0.0001 & 0.0007 \end{bmatrix}$$

$$K_{10} = \begin{bmatrix} 0.9856 & -0.0037 & -0.0620 \\ -0.1814 & -0.0407 & 0.3412 \end{bmatrix}, \quad K_{11} = \begin{bmatrix} -0.0009 & -0.0002 & -0.0016 \\ 0.0062 & 0.0016 & 0.0269 \end{bmatrix}$$

$$K_{20} = \begin{bmatrix} -0.0810 & 0.9791 & -0.3514 \\ -0.1070 & -0.0287 & 0.1085 \end{bmatrix}, \quad K_{21} = \begin{bmatrix} 0.0083 & 0.0022 & 0.0413 \\ 0.0247 & 0.0064 & 0.1091 \end{bmatrix}$$

with $\mu = 93.1623$.

Furthermore, for simulation, we have initialized the system and the observer by $x(0) = [2, 0.5, 12, 0.7, 53.5, 55]^T$ and $\hat{x}(0) = [2, 1.5, 12, 0.2, 40, 55]$, respectively (as the continuous case). Moreover, the simulated model dynamics have been disturbed by injecting a step signal disturbance to the system, and corrupting the measurements by a sinusoidal signal as depicted in Figure 3.21. Actually, theoretically, the disturbance signals could be of any shape, the most important is to check if the design assumptions are satisfied ($w \in \mathbb{R}^z$ is an $\mathcal{L}_2$ bounded vector) and if the state variables of the model remain positive or null under the effect of the injected disturbances (otherwise, the results become meaningful physically, since the state variables represent concentrations that can not be negative). The simulation results are depicted in Figures 3.22-3.27.

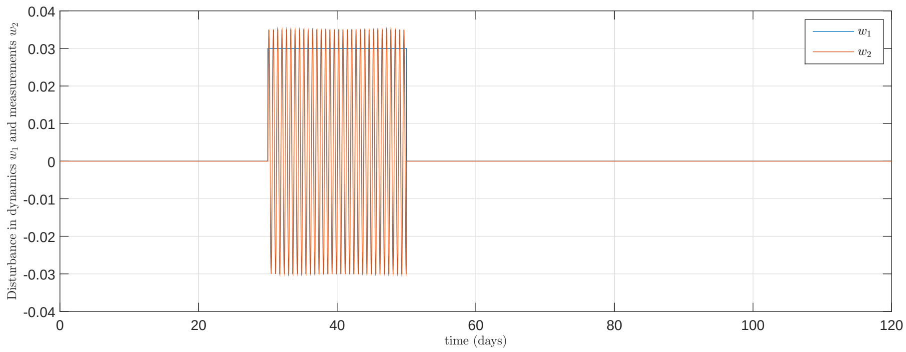

FIGURE 3.21: Disturbance in dynamics (w_1) and measurements (w_2)

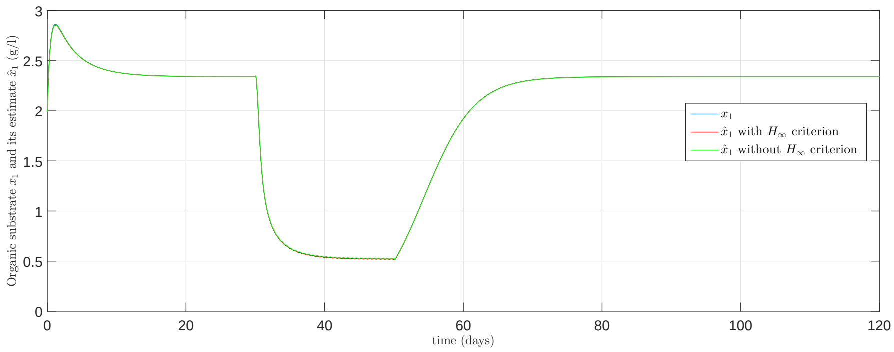

FIGURE 3.22: Substrate concentration x_1 and its estimate $\hat{x}_1$ (g/l).

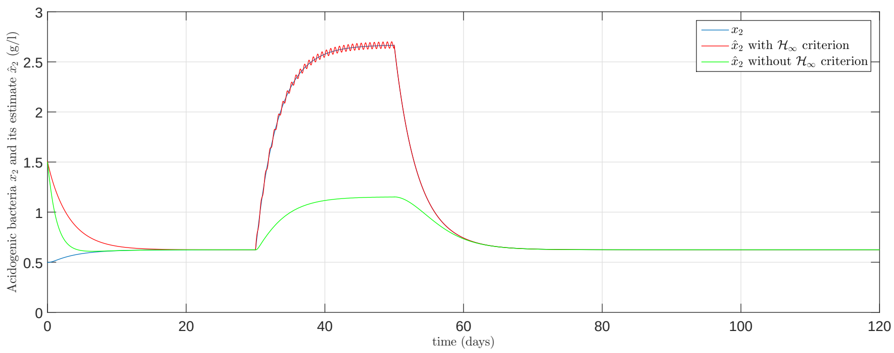

FIGURE 3.23: Acidogenic bacteria x_2 and its estimate $\hat{x}_2$ (g/l).

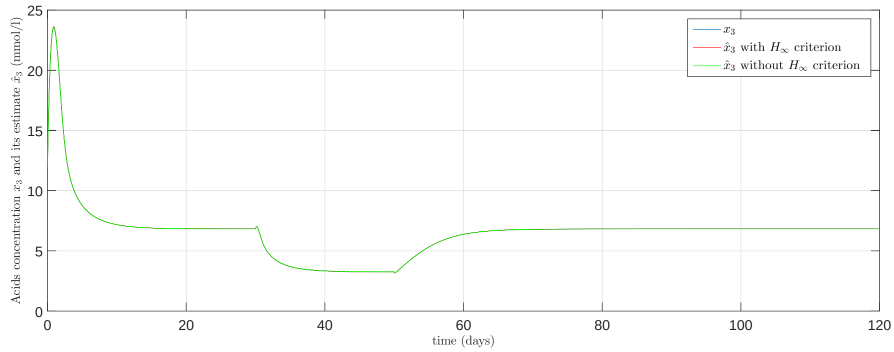

FIGURE 3.24: Acetate concentration x_3 and its estimate $\hat{x}_3$ (mmol/l).

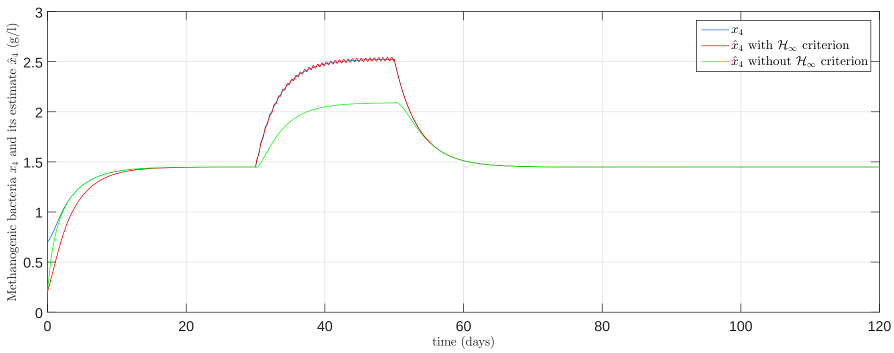

FIGURE 3.25: Mathenogenic bacteria x_4 and its estimate $\hat{x}_4$ (g/l).

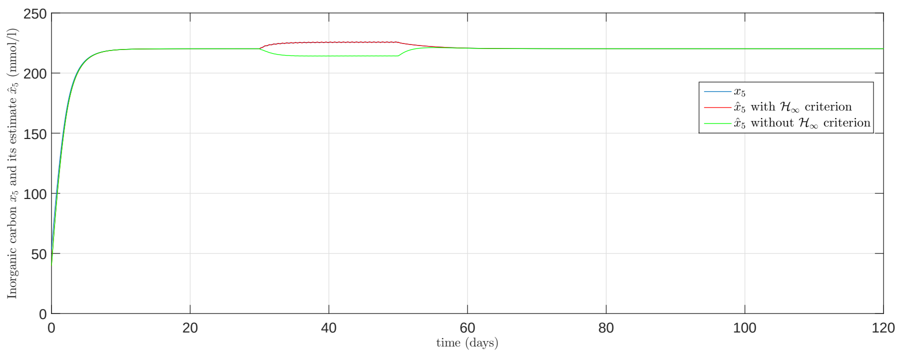

FIGURE 3.26: Inorganic carbon x_5 and its estimate $\hat{x}_5$ (mmol/l).

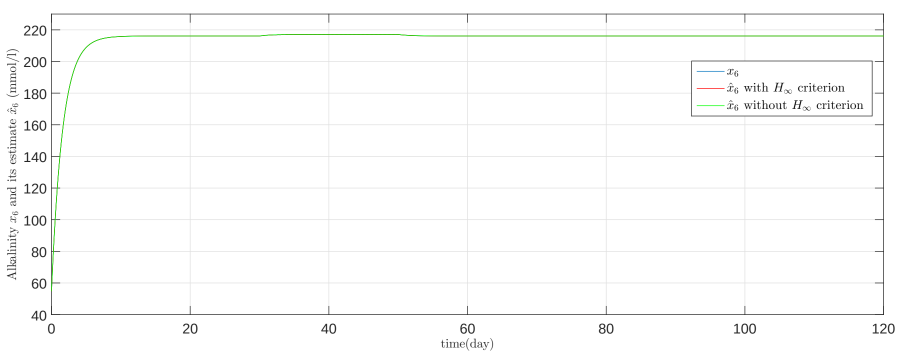

FIGURE 3.27: Alkalinity concentration x_6 and its estimate $\hat{x}_6$ (mmol/l).

From the simulation results, Figures 3.22-3.27, we can see that although the considerable range of mismatches between the initial values of the estimated and the simulated system concentrations, both nonlinear observers designed in Sections 3.4.4 and 3.4.5, including or not the $\mathcal{H}_\infty$ criterion, converge asymptotically to the model state variables. However, convergence of the nonlinear observers designed in Section 3.4.4 (without including the $\mathcal{H}_\infty$ criterion) to the model state variables is the fastest when no disturbance is affecting the system. But, once the system dynamics or measurements get disturbed, the observer performances decrease and the observer including the $\mathcal{H}_\infty$ criterion, designed in Section 3.4.3 turns to be the most robust, and naturally its convergence to the real simulated state becomes faster. In order to visualize this fact and give an idea on the level of disturbance effect attenuation that could be obtained when we include the $\mathcal{H}_\infty$ criterion in the observer design, we compare the estimation errors resulted from the two discrete time observers in Figures 3.28-3.30. As it can be seen from the later figures, although the effect of the injected disturbances in the system, the proposed $\mathcal{H}_\infty$ nonlinear observer shows satisfactory results and good performances. This illustrates how the inclusion of the $\mathcal{H}_\infty$ criterion in the observer design strength its robustness against the encountered disturbances.

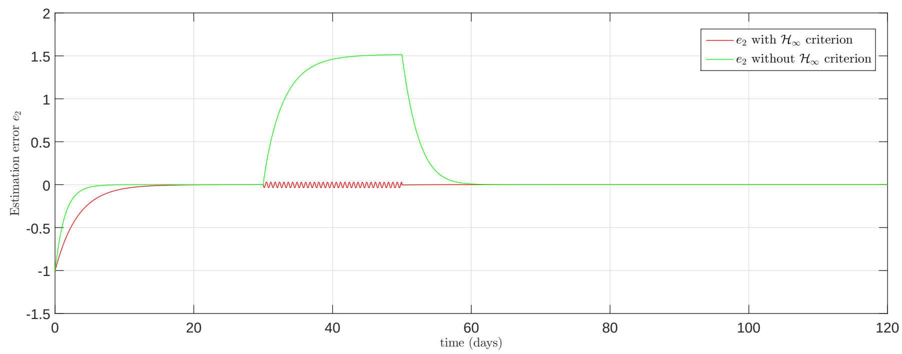

FIGURE 3.28: Estimation error $e_2 = x_2 - \hat{x}_2$.

3.4.7 Discussion and Extention to the Nonlinear Output Case

3.4.7.1 Discussion

In order to reconstruct the unmeasurable state variables of the AD model (2.11), we have designed in Section 3.4.1 an invariant like state observer which has been applied, by simulation, with success to the model. Then, due to some feasibility restrictions

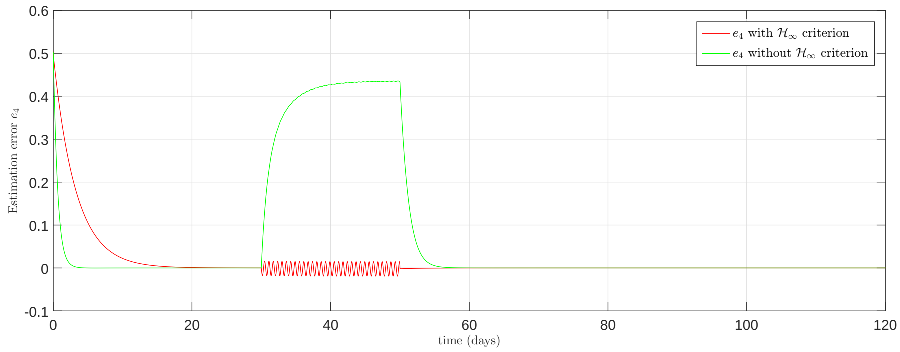

FIGURE 3.29: Estimation error $e_4 = x_4 - \hat{x}_4$.

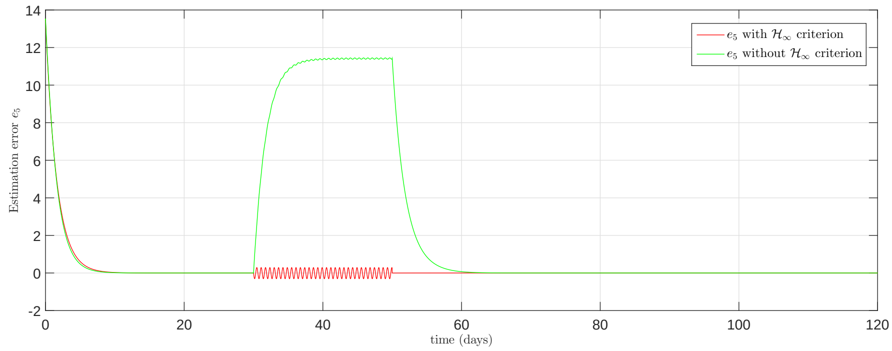

FIGURE 3.30: Estimation error $e_5 = x_5 - \hat{x}_5$.

(domain of definition of the logarithmic functions (3.24)), we have proposed in Section 3.4.2 to design a nonlinear state observer of the form of the generalized Arcak's observer [148]. The later contains two terms of correction, one in the dynamic equations as the conventional Luenberger observer, and a second term of correction inside the nonlinear part of the system. This addition of a second term of correction (through the gains $K_i^0, \dots, K_i^s$ in (3.57), in our study) promotes the observer design by adding more degrees of freedom in its synthesis. But, it has been found feasible and applicable also if you omit the second term of correction. In other word, it is possible to design a Luenberger like observer for the system (3.9). Hence, the observer structure becomes

$$\dot{\hat{x}} = A(\rho)\hat{x} + \sum_{i=1}^{m} B_i\gamma_i(\hat{\vartheta}_i) + g(u,t) + L(\rho)(y - C\hat{x}) \tag{3.156}$$

where $\hat{x}$ is the estimate of x, and

$$\hat{\vartheta}_i = H_i\hat{x}, \quad \text{and,} \quad \mathrm{L}(\rho) = \mathrm{L}_0 + \sum_{\mathrm{j}=1}^{\mathrm{s}} \rho_{\mathrm{j}}\mathrm{L}_{\mathrm{j}}. \tag{3.157}$$

The objective is to find the observer gains $L_i \in \mathbb{R}^{n\times p}$ so that the estimation error

$$e = x - \hat{x} \tag{3.158}$$

decreases asymptotically towards zero.

Since the design methodology is similar to the ones detailed for the nonlinear observers designed in Sections 3.4.2 and 3.4.3, we will simply summarize in Theorems 7 and 8 the LMI conditions under which the estimation error (3.158), obtained by the Luenberger like observer (3.156), is asymptotically stable and $\mathcal{H}_\infty$ asymptotically stable, respectively.

Theorem 7. *The estimation error obtained by applying the Luenberger like observer (3.156) to the system (3.9a), (3.9b) decreases asymptotically towards zero, if there exist symmetric positive definite matrices $\mathbb{P} \in \mathbb{R}^{n\times n}$, $\mathbb{S}_{ij} \in \mathbb{R}^{n_i\times n_i}$ for $j = 1,\dots,n_i$, $i = 1,\dots,m$, and matrices $\mathcal{R}_j \in \mathbb{R}^{p\times n}$, $j = 0,\dots,s$, so that the following LMI conditions are feasible*

$$\begin{bmatrix} \mathbb{A}\Big(\mathbb{P},\mathcal{R}_j,\rho\Big) & \overbrace{\begin{bmatrix}\Sigma_1 & \dots & \Sigma_m\end{bmatrix}}^{\Sigma} \\ (\star) & -\Lambda\mathbb{M} \end{bmatrix} \leq 0 \tag{3.159}$$

with

$$\mathbb{A}\Big(\mathbb{P},\mathcal{R}_j,\rho\Big) = A_0^T\mathbb{P} + \mathbb{P}A_0 - C^T\mathcal{R}_0 - \mathcal{R}_0^TC + \sum_{j=1}^{s}\rho_j\Big(A_j^T\mathbb{P} + \mathbb{P}A_j - C^T\mathcal{R}_j - \mathcal{R}_j^TC\Big) \tag{3.160}$$

and

$$\Sigma_i = \Big[\mathcal{N}_i^1\Big(\mathbb{P},\mathbb{S}_{i1}\Big)\dots\ \mathcal{N}_i^{n_i}\Big(\mathbb{P},\mathbb{S}_{in_i}\Big)\Big], \quad \mathcal{N}_i^j\Big(\mathbb{P},\mathbb{S}_{ij}\Big) = \mathbb{P}\mathcal{H}_{ij} + H_i^T\mathbb{S}_{ij} \tag{3.161}$$

$$\Lambda = \textit{block-diag}\Big(\Lambda_1,...,\Lambda_m\Big), \quad \Lambda_i = \textit{block-diag}\left(\Lambda_i^1,\dots,\Lambda_i^{n_i}\right), \quad \Lambda_i^j = \frac{2}{b_{ij}}\mathbb{I}_{n_i} \tag{3.162}$$

$$\mathbb{M} = \textit{block-diag}\Big(\mathbb{M}_1,\dots,\mathbb{M}_m\Big), \quad \mathbb{M}_i = \textit{block-diag}\Big(\mathbb{S}_{i1},\dots,\mathbb{S}_{in_i}\Big) \tag{3.163}$$

Finally, the observer gains are to be computed as

$$L_j = \mathbb{P}^{-1}\mathcal{R}_j^T \quad \text{for all} \quad \mathrm{j} = 0,\dots,\mathrm{s}. \tag{3.164}$$

Theorem 8. *The estimation error obtained by applying the Luenberger like observer* (3.156) *to the system* (3.77) *is* $\mathcal{H}_\infty$ *asymptotically stable, if there exist symmetric positive definite matrices* $\mathbb{P} \in \mathbb{R}^{n\times n}$, $\mathbb{S}_{ij} \in \mathbb{R}^{n_i\times n_i}$ *for* $j = 1, \ldots, n_i$, $i = 1, \ldots, m$, *and matrices* $\mathcal{R}_j \in \mathbb{R}^{p\times n}$, $j = 0, \ldots, s$ *so that the following convex optimization problem is solvable*

$$\min(\mu) \quad \text{subject to (3.166)} \tag{3.165}$$

$$\begin{bmatrix} \begin{bmatrix} \mathbb{A}\Big(\mathbb{P}, \mathcal{R}_j, \rho\Big) & \mathbb{E}\Big(\mathbb{P}, \mathcal{R}_j, \rho\Big) \\ (\star) & -\mu I_z \end{bmatrix} & \overbrace{\begin{bmatrix} \Sigma_1 & \ldots & \Sigma_m \end{bmatrix}}^{\Sigma} \\ (\star) & -\Lambda\mathbb{M} \end{bmatrix} \leq 0 \tag{3.166}$$

with

$$\begin{aligned} \mathbb{A}\Big(\mathbb{P}, \mathcal{R}_j, \rho\Big) &= A_0^T\mathbb{P} + \mathbb{P}A_0 - C^T\mathcal{R}_0 - \mathcal{R}_0^TC + \mathbb{I}_n + \sum_{j=1}^{s}\rho_j\Big(A_j^T\mathbb{P} + \mathbb{P}A_j - C^T\mathcal{R}_j - \mathcal{R}_j^TC\Big) \\ \mathbb{E}\Big(\mathbb{P}, \mathcal{R}_j, \rho\Big) &= \mathbb{P}E - \mathcal{R}_0^TD - \sum_{j=1}^{s}\rho_j\mathcal{R}_j^TD \end{aligned} \tag{3.167}$$

and

$$\Sigma_i = \Big[\mathcal{N}_i^1\Big(\mathbb{P}, \mathbb{S}_{i1}\Big) \ldots \mathcal{N}_i^{n_i}\Big(\mathbb{P}, \mathbb{S}_{in_i}\Big)\Big], \quad \mathcal{N}_i^j\Big(\mathbb{P}, \mathbb{S}_{ij}\Big) = \begin{bmatrix} \mathbb{P}\mathcal{H}_{ij} \\ 0 \end{bmatrix} + \begin{bmatrix} H_i^T \\ 0 \end{bmatrix}\mathbb{S}_{ij} \tag{3.168}$$

$$\Lambda = \textit{block-diag}\Big(\Lambda_1, ..., \Lambda_m\Big), \quad \Lambda_i = \textit{block-diag}\left(\Lambda_i^1, \ldots, \Lambda_i^{n_i}\right), \quad \Lambda_i^j = \frac{2}{b_{ij}}\mathbb{I}_{n_i} \tag{3.169}$$

$$\mathbb{M} = \textit{block-diag}\Big(\mathbb{M}_1, \ldots, \mathbb{M}_m\Big), \quad \mathbb{M}_i = \textit{block-diag}\Big(\mathbb{S}_{i1}, \ldots, \mathbb{S}_{in_i}\Big) \tag{3.170}$$

then, the $\mathcal{H}_\infty$ *criterion* (3.78) *is satisfied with* $\nu = \lambda_{\max}(\mathbb{P})$. *Hence, the observer gains are to be computed as*

$$L_j = \mathbb{P}^{-1}\mathcal{R}_j^T \quad \text{for all} \quad \mathrm{j} = 0, \ldots, \mathrm{s}. \tag{3.171}$$

In regard to the discrete time case, we can also design a discrete Luenberger like observer to the discrete system (3.96). The observer structure reads

$$\hat{x}_{k+1} = A(\rho_k)\hat{x}_k + \sum_{i=1}^{m} B_i\gamma_i(\hat{\vartheta}_i) + g(y_k, u_k) + L(\rho_k)\Big(y_k - C\hat{x}_k\Big) \tag{3.172}$$

with

$$\hat{\vartheta}_i = H_i\hat{x}_k \quad \text{and} \quad \mathrm{L}(\rho_\mathrm{k}) = \mathrm{L}_0 + \sum_{\mathrm{j}=1}^{\mathrm{s}} \rho_\mathrm{k}^\mathrm{j}\mathrm{L}_\mathrm{j} \tag{3.173}$$

where $\hat{x}_k$ is the estimate of x_k. The matrices $L_i \in \mathbb{R}^{n\times p}$ are the observer parameters to be determined so that the estimation error $e_k = x_k - \hat{x}_k$ converges asymptotically towards zero.

Following the same design methodology as in Section 3.4.4 and Section 3.4.5, we find the LMI conditions under which the estimations error obtained by applying the discrete Luenberger like observer (3.172) to the systems (3.96) and (3.126) is asymptotically stable and $\mathcal{H}_\infty$ asymptotically stable, respectively. We will summarize these conditions in Theorem 9 and Theorem 10, respectively.

Theorem 9. *If there exist symmetric positive definite matrices* $\mathbb{P} \in \mathbb{R}^{n\times n}$*,* $\mathbb{S}_{ij} \in \mathbb{R}^{n_i\times n_i}$ *and matrices* $\mathcal{X}_l \in \mathbb{R}^{p\times n}$*,* $i = 1,\dots,m$*,* $j = 1,\dots,n_i$*,* $l = 0,\dots,s$*, of appropriate dimensions so that the following LMI conditions are feasible*

$$\begin{bmatrix} \mathbb{M}(\rho_k) & \begin{bmatrix}\Sigma_1^T & \dots & \Sigma_m^T\end{bmatrix} \\ (\star) & -\Lambda\mathbb{S} \end{bmatrix} < 0, \ \forall \rho_k \in \mathbb{V}_{\rho_k} \tag{3.174}$$

with

$$\mathbb{M}(\rho_k) = \begin{bmatrix} -\mathbb{P} & \mathbb{M}_{12}(\rho_k) \\ (\star) & -\mathbb{P} \end{bmatrix} \tag{3.175}$$

$$\mathbb{M}_{12}(\rho_k) = \big(A_0^T\mathbb{P} - C^T\mathcal{X}_0\big) + \sum_{l=1}^{s} \rho_k^l\big(A_l^T\mathbb{P} - C^T\mathcal{X}_l\big) \tag{3.176}$$

$$\Sigma_i = \Big[\Sigma_{i1}^T \dots \Sigma_{in_i}^T\Big]^T, \qquad \Sigma_{ij}^T = \begin{bmatrix} 0 \\ \mathbb{P}\mathcal{H}_{ij} \end{bmatrix} + \begin{bmatrix} H_i^T\mathbb{S}_{ij} \\ 0 \end{bmatrix} \tag{3.177}$$

$$\begin{aligned}\Lambda &= \textit{block-diag}\Big(\Lambda_1, ..., \Lambda_m\Big), \quad \Lambda_i = \textit{block-diag}\left(\tfrac{2}{b_{i1}}\mathbb{I}_{n_i}, \ldots, \tfrac{2}{b_{in_i}}\mathbb{I}_{n_i}\right) \\ \mathbb{S} &= \textit{block-diag}\Big(\mathbb{S}_1, \ldots, \mathbb{S}_m\Big), \quad \mathbb{S}_i = \textit{block-diag}\Big(\mathbb{S}_{i1}, \ldots, \mathbb{S}_{in_i}\Big)\end{aligned} \tag{3.178}$$

then, the estimation error obtained by applying the discrete Luenberger observer (3.172) *to the system* (3.96)*, converges asymptotically towards zero. Consequently, the observer parameters* L_l *are to be computed as follows*

$$L_l = \mathbb{P}^{-1}\mathcal{X}_l^T \tag{3.179}$$

$$L_l = \mathbb{P}^{-1}\mathcal{X}_l^T \quad \text{for all} \quad \mathrm{l} = 0, \ldots, \mathrm{s}. \tag{3.180}$$

Theorem 10. *If there exist symmetric positive definite matrices* $\mathbb{P} \in \mathbb{R}^{n\times n}$*,* $\mathbb{S}_{ij} \in \mathbb{R}^{n_i\times n_i}$*, matrices* $\mathcal{X}_l \in \mathbb{R}^{p\times n}$*,* $i = 1, \ldots, m$*,* $j = 1, \ldots, n_i$*,* $l = 0, \ldots, s$*, of appropriate dimensions so that the convex optimization problem* $\min(\mu)$ *subject to the constraint* (3.181) *is solvable,*

$$\begin{bmatrix} \mathbb{M}(\varrho) & \begin{bmatrix}\Sigma_1^T & \ldots & \Sigma_m^T\end{bmatrix} \\ & \\ (\star) & -\Lambda\mathbb{S} \end{bmatrix} < 0, \ \forall \varrho \in \mathbb{V}_\rho \tag{3.181}$$

with

$$\mathbb{M}(\varrho) = \begin{bmatrix} -\mathbb{P} + \mathbb{I}_n & 0 & \mathbb{M}_{13}(\varrho) \\ & & \\ 0 & -\mu\mathbb{I}_z & \mathbb{M}_{23}(\varrho) \\ & & \\ \mathbb{M}_{13}^\top(\varrho) & \mathbb{M}_{23}^\top(\varrho) & -\mathbb{P} \end{bmatrix} \tag{3.182}$$

$$\mathbb{M}_{13}(\varrho) = \left(A_0^T\mathbb{P} - C^T\mathcal{X}_0\right) + \sum_{l=1}^{s} \varrho^l\left(A_l^T\mathbb{P} - C^T\mathcal{X}_l\right) \tag{3.183}$$

$$\mathbb{M}_{23}(\varrho) = E^\top\mathbb{P} - D^\top\left(\mathcal{X}_0 + \sum_{l=1}^{s}\varrho^l\mathcal{X}_l\right) \tag{3.184}$$

$$\Sigma_i = \left[\Sigma_{i1}^T \ldots \Sigma_{in_i}^T\right]^T, \qquad \Sigma_{ij}^T = \begin{bmatrix} 0 \\ 0 \\ \mathbb{P}\mathcal{H}_{ij} \end{bmatrix} + \begin{bmatrix} H_i^T\mathbb{S}_{ij} \\ 0 \\ 0 \end{bmatrix} \tag{3.185}$$

$$\begin{aligned} \Lambda &= \textit{block-diag}\Big(\Lambda_1, ..., \Lambda_m\Big), \quad \Lambda_i &= \textit{block-diag}\left(\tfrac{2}{b_{i1}}\mathbb{I}_{n_i}, \ldots, \tfrac{2}{b_{in_i}}\mathbb{I}_{n_i}\right) \\ \mathbb{S} &= \textit{block-diag}\Big(\mathbb{S}_1, \ldots, \mathbb{S}_m\Big), \quad \mathbb{S}_i &= \textit{block-diag}\Big(\mathbb{S}_{i1}, \ldots, \mathbb{S}_{in_i}\Big) \end{aligned} \tag{3.186}$$

the, the estimation error obtained by applying the discrete Luenberger like observer (3.172) *to the system* (3.126) *satisfies the* $\mathcal{H}_\infty$ *criterion* (3.78) *with* $\nu = \lambda_{\max}(\mathbb{P})$*. Consequently, the estimation error is* $\mathcal{H}_\infty$ *asymptotically stable and the observer parameters* L_l *are to be computed by*

$$L_l = \mathbb{P}^{-1}\mathcal{X}_l^T \quad \text{for all} \quad \mathrm{l} = 0, \ldots, \mathrm{s}. \tag{3.187}$$

The proof of Theorems 7, 8, 9 and 10 have been omitted from the current section in order to avoid repetition. Nevertheless, they can be easily reproduced by following the same synthesis philosophy provided in Sections 3.4.2, 3.4.3, 3.4.4 and 3.4.5, respectively.

3.4.7.2 Extension to the Nonlinear Output Case

Often, in AD applications the most cheap and reliable measurements are nonlinear functions of the model state variables [48], [15], [47], especially the gas phase measurements which are always performed at industrial scale and are reliable. Therefore, with the aim to match and implement the theoretical results in real AD applications, we take advantage from these easily performed measurements at industry scale, which are nonlinear functions of the model state variables as in [64] to reconstruct the unmeasurable variables. Therefore, we extend the observer design methodology to the class of systems with nonlinear outputs modelled by the following equations

$$\begin{cases} \dot{x} = A(\rho)x + B\gamma(x) + g(u,t) \\ y = Cx + Th(x) \end{cases} \tag{3.188}$$

where the model parameters are the same as defined in (3.9), and in addition to that the matrix $T \in \mathbb{R}^{p\times q}$ is a constant matrix. The nonlinear function $h: \ \mathbb{R}^n \longrightarrow \ \mathbb{R}^q$ is the nonlinear part of the output signal, which can be verified to be globally Lipschitz due to the state boundedness proved in Section 2.5. It is obvious that we can write $h(x)$

under the detailed form

$$h(x) = \begin{bmatrix} h_1(F_1 x) \\ \vdots \\ h_i(\overbrace{F_i x}^{\theta_i}) \\ \vdots \\ h_q(F_q x) \end{bmatrix} \tag{3.189}$$

with $F_i \in \mathbb{R}^{p_i \times n}$.

In order to reconstruct the system states, we consider the following observer structure

$$\dot{\hat{x}} = A(\rho)\hat{x} + B \begin{bmatrix} \gamma_1(\hat{\vartheta}_1) \\ \vdots \\ \gamma_i(\hat{\vartheta}_i) \\ \vdots \\ \gamma_m(\hat{\vartheta}_m) \end{bmatrix} + L(\rho)\Big(y - \hat{y}\Big) \tag{3.190a}$$

with

$$L(\rho) = L_0 + \sum_{j=1}^{s} \rho_j L_j \quad \text{and,} \quad \hat{y} = C\hat{x} + T \begin{bmatrix} h_1(\hat{\theta}_1) \\ \vdots \\ h_i(\hat{\theta}_i) \\ \vdots \\ h_q(\hat{\theta}_q) \end{bmatrix} \tag{3.190b}$$

where

$$\hat{\vartheta}_i = H_i \hat{x} \quad \text{and} \quad \hat{\theta}_{\mathrm{i}} = \mathrm{F_i \hat{x}} \tag{3.190c}$$

The observer gains $L_i \in \mathbb{R}^{n \times p}$ are to be determined so that the estimation error $e = x - \hat{x}$ converges asymptotically towards zero.

Since $h(.)$ is globally Lipschitz, then from Lemma 1 there exist functions

$$\psi_{ij} \ : \ \mathbb{R}^{p_i} \times \mathbb{R}^{p_i} \longrightarrow \ \mathbb{R}$$

and constants $\overline{a}_{ij}, \overline{b}_{ij}$, such that

$$T(h(\theta) - h(\hat{\theta})) = \sum_{i,j=1}^{q,p_i} \psi_{ij}(z_i)\mathcal{F}_{ij}\Big(\theta_i - \hat{\theta}_i\Big) \tag{3.191}$$

with

$$\min(\psi_{ij}) \leq \psi_{ij}(z_i) \leq \max(\psi_{ij}) \tag{3.192}$$

where

$$\psi_{ij}(z_i) = \frac{\partial h_i}{\partial \theta_i}(z_i), \text{ and } \quad \mathcal{F}_{\mathrm{ij}} = \mathrm{T_i e_{p_i}^T(j)}. \tag{3.193}$$

with T_i is the i^{th} column of the matrix T and

$$\theta_i \leq z_i \leq \hat{\theta}_i \tag{3.194}$$

For shortness, we set $\psi_{ij} = \psi_{ij}(z_i)$.

Since $\theta_i - \hat{\theta}_i = F_i e$, then we have

$$h(\theta) - h(\hat{\theta}) = \sum_{i,j=1}^{q,p_i} \psi_{ij} \mathcal{F}_{ij} F_i e \tag{3.195}$$

Consequently, the dynamics equation of the estimation error is given by

$$\dot{e} = \left(\mathbb{A}_L(\rho) + \sum_{i,j=1}^{m,n_i} \phi_{ij} \mathcal{H}_{ij} H_i - L(\rho) \sum_{i,j=1}^{q,p_i} \psi_{ij} \mathcal{F}_{ij} F_i \right) e \tag{3.196}$$

where $\mathbb{A}_L(\rho) = A(\rho) - L(\rho)C$.

Since we know, a priori, that $\min(\psi_{ij}) \neq 0$ in equation (3.192), then we find more suitable to write

$$0 \leq \psi_{ij} - \min(\psi_{ij}) \leq \underbrace{\max(\psi_{ij}) - \min(\psi_{ij})}_{\bar{b}_{ij}} \tag{3.197}$$

and then, to add and subtract $\min(\psi_{ij})$ from ψ_{ij} in equation (3.196) as the following

$$\dot{e} = \left(\mathbb{A}_L(\rho) + \sum_{i,j=1}^{m,n_i} \phi_{ij} \mathcal{H}_{ij} H_i - L(\rho) \sum_{i,j=1}^{q,p_i} (\psi_{ij} + \min(\psi_{ij}) - \min(\psi_{ij})) \mathcal{F}_{ij} F_i \right) e \tag{3.198}$$

equivalently, we write

$$\dot{e} = \Bigg(\mathbb{A}_L(\rho) - L(\rho) \underbrace{\sum_{i,j=1}^{q,p_i} \min(\psi_{ij})\mathcal{F}_{ij}F_i}_{\overline{C}} + \sum_{i,j=1}^{m,n_i} \phi_{ij}\mathcal{H}_{ij}H_i - L(\rho) \sum_{i,j=1}^{q,p_i} (\underbrace{\psi_{ij} - \min(\psi_{ij})}_{\varphi_{ij}})\mathcal{F}_{ij}F_i \Bigg) e \tag{3.199}$$

with

$$0 \leq \varphi_{ij} \leq \bar{b}_{ij} \tag{3.200}$$

Now, that the dynamic equation of the estimation error has been obtained (3.199), we provide in Theorem 11 the LMI conditions to be solved in order to find the observer gains which make the estimation error asymptotic stable around zero.

Theorem 11. *If there exist symmetric positive definite matrices $\mathbb{P} \in \mathbb{R}^{n\times n}$, $\mathbb{S}_{ij} \in \mathbb{R}^{n_i\times n_i}$, $j = 1,\dots,n_i$, $\overline{\mathbb{S}}_{ij} \in \mathbb{R}^{p_i\times p_i}$, $j = 1,\dots,p_i$, $i = 1,\dots,m$, and matrices $\mathcal{X}_l \in \mathbb{R}^{p\times n}$, $l = 0,\dots,s$, of appropriate dimensions so that the following LMI conditions are feasible*

$$\begin{bmatrix} \Psi & \begin{bmatrix}\Pi_1^T & \dots & \Pi_m^T\end{bmatrix} & \begin{bmatrix}\overline{\Pi}_1^T & \dots & \overline{\Pi}_q^T\end{bmatrix} \\ (\star) & -\Lambda\mathbb{S} & 0 \\ (\star) & (\star) & -\overline{\Lambda}\,\overline{\mathbb{S}} \end{bmatrix} < 0 \tag{3.201}$$

where

$$\begin{aligned} \Psi = {} & A_0^T\mathbb{P} + \mathbb{P}A_0 - C^T\mathcal{X}_0 - \mathcal{X}_0^TC - \overline{C}^T\mathcal{X}_0 - \mathcal{X}_0^T\overline{C} + \\ & \sum_{i=1}^{s} \rho_i \left(A_i^T\mathbb{P} + \mathbb{P}^TA_i - C^T\mathcal{X}_i - \mathcal{X}_i^TC - \overline{C}^T\mathcal{X}_i - \mathcal{X}_i^T\overline{C} \right) \end{aligned} \tag{3.202}$$

$$\Pi_i = \left[\Pi_{i1}^T \dots \Pi_{in_i}^T\right]^T, \quad \Pi_{ij} = \mathcal{H}_{ij}^T\mathbb{P} + \mathbb{S}_{ij}\mathcal{H}_i \tag{3.203}$$

$$\overline{\Pi}_i = \left[\overline{\Pi}_{i1}^T \dots \overline{\Pi}_{ip_i}^T\right]^T, \quad \overline{\Pi}_{ij} = \mathcal{F}_{ij}^T\mathcal{X}_l + \overline{\mathbb{S}}_{ij}(-F_i) \tag{3.204}$$

and

$$\mathbb{S} = \textit{block-diag}(\mathbb{S}_1,\dots,\mathbb{S}_m), \quad \mathbb{S}_i = \textit{block-diag}(\mathbb{S}_{i1},\dots,\mathbb{S}_{in_i}) \tag{3.205}$$

$$\Lambda = block\text{-}diag(\Lambda_1, ..., \Lambda_m), \quad \Lambda_i = block\text{-}diag\left(\Lambda_{i1}, \ldots, \Lambda_{in_i}\right) \tag{3.206}$$

with

$$\Lambda_{ij} = \frac{2}{b_{ij}} \mathbb{I}_{n_i}, \tag{3.207}$$

and

$$\overline{\mathbb{S}} = block\text{-}diag(\overline{\mathbb{S}}_1, \ldots, \overline{\mathbb{S}}_q), \quad \overline{\mathbb{S}}_i = block\text{-}diag(\overline{\mathbb{S}}_{i1}, \ldots, \overline{\mathbb{S}}_{ip_i}) \tag{3.208}$$

$$\overline{\Lambda} = block\text{-}diag(\overline{\Lambda}_1, ..., \overline{\Lambda}_q), \quad \overline{\Lambda}_i = block\text{-}diag\left(\overline{\Lambda}_{i1}, \ldots, \overline{\Lambda}_{ip_i}\right) \tag{3.209}$$

with

$$\overline{\Lambda}_{ij} = \frac{2}{\overline{b}_{ij}} \mathbb{I}_{p_i} \tag{3.210}$$

Finally, the observer gains are to be computed by

$$L_l = \mathbb{P}^{-1} \mathcal{X}_l^T \quad \text{for all} \quad \mathrm{l} = 0, \ldots, \mathrm{s}. \tag{3.211}$$

Proof. As usual, to analyse the stability of the estimation error (3.199), we use a quadratic Lyapunov function

$$V = e^T P e, \quad P = P^T > 0$$

whose derivative $\dot{V}(e)$ along the trajectories (3.199) is given by

$$\begin{aligned}\dot{V} = e^T \Bigg[& \left(\mathbb{A}_L(\rho) - L(\rho)\overline{C} + \sum_{i,j=1}^{m,n_i} \phi_{ij} \mathcal{H}_{ij} H_i - L(\rho) \sum_{i,j=1}^{q,p_i} \varphi_{ij} \mathcal{F}_{ij} F_i \right)^T \mathbb{P} \\ & + \mathbb{P} \left(\mathbb{A}_L(\rho) - L(\rho)\overline{C} + \sum_{i,j=1}^{m,n_i} \phi_{ij} \mathcal{H}_{ij} H_i - L(\rho) \sum_{i,j=1}^{q,p_i} \varphi_{ij} \mathcal{F}_{ij} F_i \right) \Bigg] e \end{aligned} \tag{3.212}$$

We equivalently rewrite equation (3.212) as the following

$$\begin{aligned}\dot{V} \quad = \quad & e^T \Bigg(\underbrace{\mathbb{A}_L^T(\rho)\mathbb{P} - \overline{C}^T L^T(\rho)\mathbb{P} + \mathbb{P}\mathbb{A}_L(\rho) - \mathbb{P}L(\rho)\overline{C}}_{\Psi} \Bigg) e + e^T \sum_{i,j=1}^{m,n_i} \phi_{ij} \Bigg(\underbrace{\mathbb{P}\mathcal{H}_{ij}}_{\mathbb{X}_{ij}^T} \underbrace{H_i}_{\mathbb{Y}_i} + H_i^T \mathcal{H}_{ij}^T \mathbb{P} \Bigg) e \\ & + e^T \sum_{i,j=1}^{q,p_i} \varphi_{ij} \Bigg(\underbrace{\mathbb{P}L(\rho)\mathcal{F}_{ij}}_{\overline{\mathbb{X}}_{ij}^T} \underbrace{(-F_i)}_{\overline{\mathbb{Y}}_{ij}} + (-F_i)^T \mathcal{F}_{ij}^T L^T(\rho)\mathbb{P} \Bigg) e \end{aligned} \tag{3.213}$$

Now, by applying Lemma 2 we obtain

$$\mathbb{X}_{ij}^T\mathbb{Y}_i + \mathbb{Y}_i^T\mathbb{X}_{ij} \leq \frac{1}{2}\Big(\mathbb{X}_{ij} + \mathbb{S}_{ij}\mathbb{Y}_i\Big)^T\mathbb{S}_{ij}^{-1}\overbrace{\Big(\mathbb{X}_{ij} + \mathbb{S}_{ij}\mathbb{Y}_i\Big)}^{\Pi_{ij}} \tag{3.214}$$

and

$$\overline{\mathbb{X}}_{ij}^T\overline{\mathbb{Y}}_{ij} + \overline{\mathbb{Y}}_{ij}^T\overline{\mathbb{X}}_{ij} \leq \frac{1}{2}\Big(\overline{\mathbb{X}}_{ij} + \overline{\mathbb{S}}_{ij}\overline{\mathbb{Y}}_{ij}\Big)^T\overline{\mathbb{S}}_{ij}^{-1}\overbrace{\Big(\overline{\mathbb{X}}_{ij} + \overline{\mathbb{S}}_{ij}\overline{\mathbb{Y}}_{ij}\Big)}^{\overline{\Pi}_{ij}} \tag{3.215}$$

for any symmetric positive definite matrices $\mathbb{S}_{ij}$ and $\overline{\mathbb{S}}_{ij}$. Moreover, from (3.21) and (3.200) and the fact that $a_{ij} = 0$, then inequality $\dot{V} < 0$ holds if

$$\Psi - \sum_{i,j=1}^{m,n_i}\left(\Pi_{ij}^T\Big(-\frac{2}{b_{ij}}\mathbb{S}_{ij}\Big)^{-1}\Pi_{ij}\right) - \sum_{i,j=1}^{q,p_i}\left(\overline{\Pi}_{ij}^T\Big(-\frac{2}{\bar{b}_{ij}}\overline{\mathbb{S}}_{ij}\Big)^{-1}\overline{\Pi}_{ij}\right) < 0 \tag{3.216}$$

consequently, by Schur lemma, inequality (3.216) is equivalent to the LMI (3.201). This ends the proof. □

3.4.7.3 Application and Simulation Results

As already challenged previously, we aim to increase the applicability of the proposed nonlinear observer in real biogas plants, where usually the cheapest and simplest measurements to process are those related to the gas phase. Therefore, we propose in this section to apply the designed nonlinear observer (3.190) to the AD model (2.11) while taking the gases flow rate measurements as the nonlinear outputs. Thus, we will use both the co_2 and ch_4 gas flow rates (q_c and q_m, respectively) to design the observer. Since, we want to design a full order observer, or in other words to reconstruct the full state vector, then we add the measurements of x_1 and x_6 as the linear outputs. This is not regarded as an issue because the measurement of organic substrates and alkalinity are frequently encountered in applications and there exist nowadays very advanced sensors to perform them [160], [161], [162], [47], [163], [164]. Moreover, this grant us an exemple where we illustrate how to combine the linear and nonlinear outputs to design the proposed observer. Nevertheless, we would like to say that even if we had only the gases measurements $q_c(x)$ and $q_m(x)$, the system remains detectable and thus, it is always possible to design an observer. In the following, we will give the parameters that allow to write the AD model (2.11) in the form (3.188) when considering available the measurements of x_1, x_6, $q_c(x)$ and $q_m(x)$. Thus, to do so, the parameters ρ,

A_0 and A_1 remain as defined in (3.48), but this time $\gamma(x) = \mu_1(x_1)x_2$ only, because $q_m(x) = k_6\mu_2(x_3)x_4$ is measured and thus (for shortness, we set sometimes $q_c(x) = q_c$ and $q_m(x) = q_m$)

$$B = \begin{bmatrix} k_1, & 1, & k_2, & 0, & k_4, & 0 \end{bmatrix}^T, \quad \gamma(x) = \mu_1(x_1)x_2 \tag{3.217}$$

$$g(u,t) = \begin{bmatrix} u_1 S_{1in}, & 0, & u_1(S_{2in} + S_{2ad}) - \frac{k_3}{k_6} q_m, & \frac{1}{k_6} q_m, & u_1 C_{in} - \frac{k_5}{k_6} q_m - q_c, & u_1 Z_{in} + u_2 Z_{ad} \end{bmatrix}^T \tag{3.218}$$

$$C = \begin{bmatrix} 1 & 0 & 0 & 0 & 0 & 0 \\ 0 & 0 & 0 & 0 & 0 & 1 \\ 0 & 0 & 0 & 0 & 0 & 0 \\ 0 & 0 & 0 & 0 & 0 & 0 \end{bmatrix}, \quad T = \begin{bmatrix} 0 & 0 \\ 0 & 0 \\ 1 & 0 \\ 0 & 1 \end{bmatrix}, \quad h(x) = \begin{bmatrix} q_m(x) \\ q_c(x) \end{bmatrix} \tag{3.219}$$

Moreover, for the nonlinear observer (3.190) design, we have

$$m = 1, \quad s = 1, \quad n_1 = 2, \quad \gamma_1(x) = \mu_1(x_1)x_2, \quad q = 2, \tag{3.220}$$

$$h_1(x) = q_m(x), \quad p_1 = 2, \quad h_2(x) = q_c(x), \quad p_2 = 4, \quad B_1 = B \tag{3.221}$$

and

$$\begin{aligned} H_1 &= \begin{bmatrix} 1 & 0 & 0 & 0 & 0 & 0 \\ 0 & 1 & 0 & 0 & 0 & 0 \end{bmatrix}, \quad F_1 = \begin{bmatrix} 0 & 0 & 1 & 0 & 0 & 0 \\ 0 & 0 & 0 & 1 & 0 & 0 \end{bmatrix} \\ F_2 &= \begin{bmatrix} 0 & 0 & 1 & 0 & 0 & 0 \\ 0 & 0 & 0 & 1 & 0 & 0 \\ 0 & 0 & 0 & 0 & 1 & 0 \\ 0 & 0 & 0 & 0 & 0 & 1 \end{bmatrix}, \quad T_1 = \begin{bmatrix} 0 \\ 0 \\ 1 \\ 0 \end{bmatrix}, \quad T_2 = \begin{bmatrix} 0 \\ 0 \\ 0 \\ 1 \end{bmatrix} \end{aligned} \tag{3.222}$$

In order to run an illustrative simulation, we have taken $\rho_{min} = 0.1$ day^{-1}, $\rho_{max} = 0.9$ day^{-1}, $S_{1in} = 16\ g/l$, $S_{2in} = 170$ mmol/l, $C_{in} = 76.15$ mmol/l, $Z_{in} = 200$ mmol/l, $Z_{ad} = 700$ mmol/l, $S_{2ad} = 0$ mmol/l, and the parameter values given in Table 2.2. Moreover, after solving the LMIs (3.201) by using LMI MATLAB Toolbox, we have obtained the following observer gains

$$L_0 = \begin{bmatrix} 72.8803 & -19.9816 & -0.1810 & -0.0295 \\ -2.0351 & 0.5502 & 0.0050 & 0.0008 \\ -201.6596 & 55.2874 & 0.5013 & 0.0817 \\ 0.0021 & -0.0006 & 0.0002 & 0.0000 \\ -87.5869 & 24.0129 & 0.2177 & 0.0355 \\ 0.2292 & 4.2017 & -0.0000 & 0.0000 \end{bmatrix} \tag{3.223}$$

$$L_1 = 10^3 \times \begin{bmatrix} 1.8086 & -0.5672 & 0.0000 & 0.0000 \\ -0.0498 & 0.0156 & -0.0000 & -0.0000 \\ -5.0098 & 1.5693 & -0.0000 & -0.0000 \\ -0.0001 & -0.0000 & 0.0000 & 0.0000 \\ -2.1759 & 0.6816 & -0.0000 & -0.0000 \\ 0.0066 & -0.0010 & 0.0000 & 0.0000 \end{bmatrix} \tag{3.224}$$

The control input u_1 has been varied during the simulation as represented in Figure

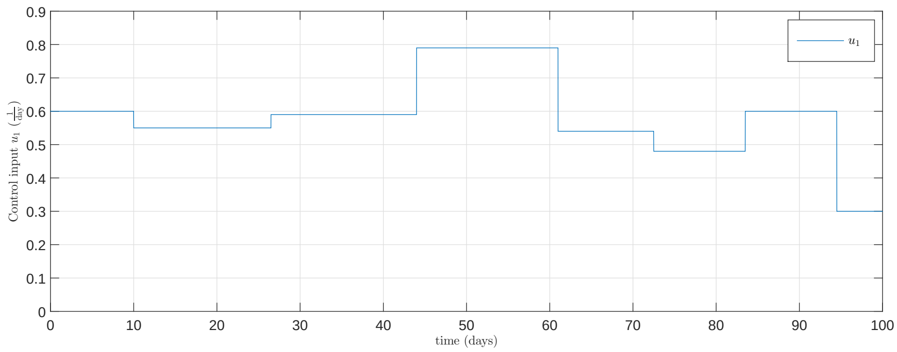

FIGURE 3.31: Control input u_1 $\left(\frac{1}{\text{day}}\right)$.

3.31 and we have set $u_2 = 0.02$ day^{-1}. Besides, we have initialized the system and the observer by $x_0 = [2, 0.5, 12, 0.7, 53, 49, 55]^T$ and $\hat{x}_0 = [2, 1, 15, 1.7, 58, 49, 55]^T$, respectively. After running the simulation for 100 days, we have obtained the results depicted in Figures 3.32-3.37. As it can be seen from the later figures, the results are promising. Indeed, over the wide initial estimation error the observer is converging asymptotically to the simulated system states in relatively short period of time. These results testify the potential of the design methodology. Of course the design methodology can be extended to the generalized Arcak's like observer designed in Section 3.4.2 and the $\mathcal{H}_\infty$ nonlinear observer presented in Section 3.4.3. Furthermore, the observer can be discretized as in Sections 3.4.4 and 3.4.5.

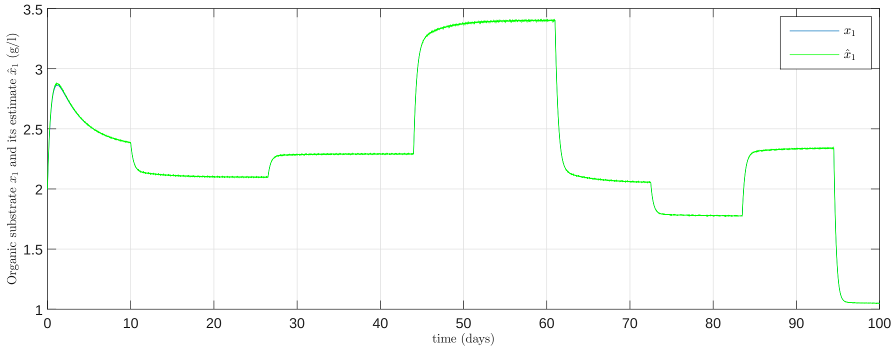

FIGURE 3.32: Substrate concentration x_1 and its estimate $\hat{x}_1$ (g/l).

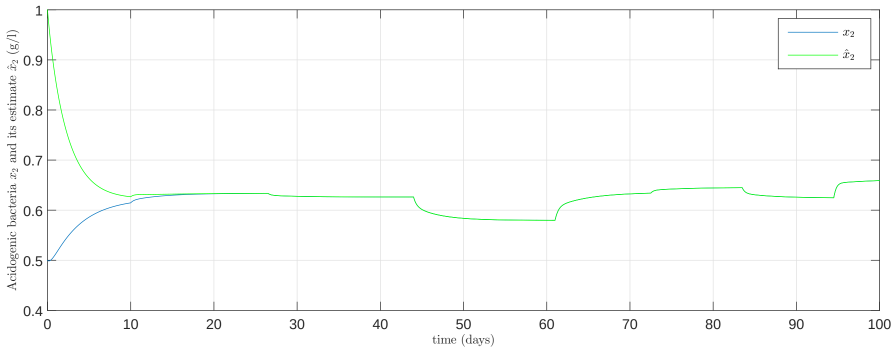

FIGURE 3.33: Acidogenic bacteria x_2 and its estimate $\hat{x}_2$ (g/l).

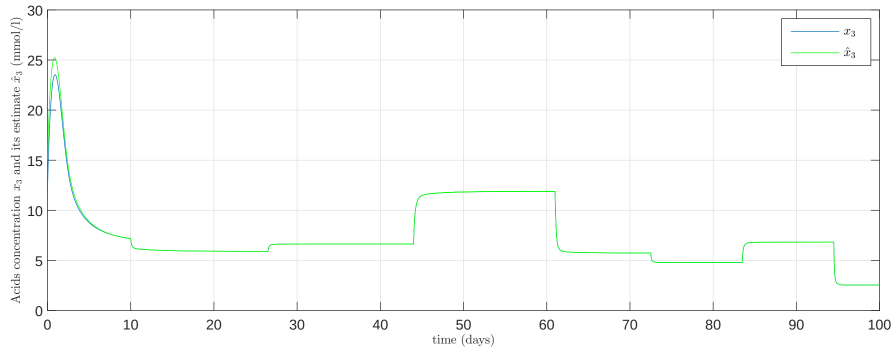

FIGURE 3.34: Acetate concentration x_3 and its estimate $\hat{x}_3$ (mmol/l).

3.5 Conclusion

In this chapter, we have developed a new method to design nonlinear observers for the AD process. It is based on the use of the DMVT which transforms the nonlinear

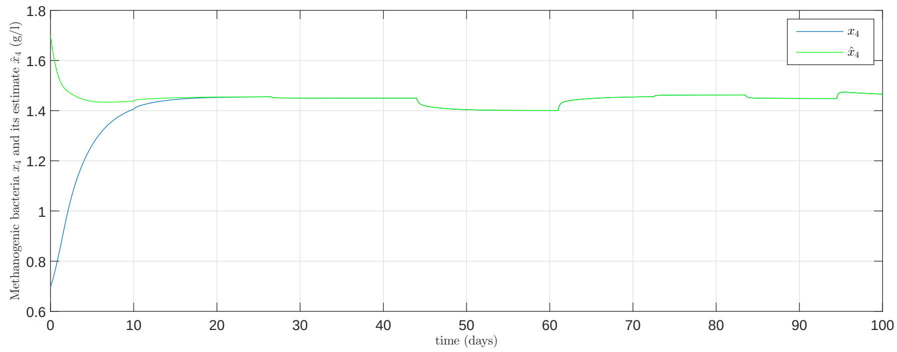

FIGURE 3.35: Mathenogenic bacteria x_4 and its estimate $\hat{x}_4$ (g/l).

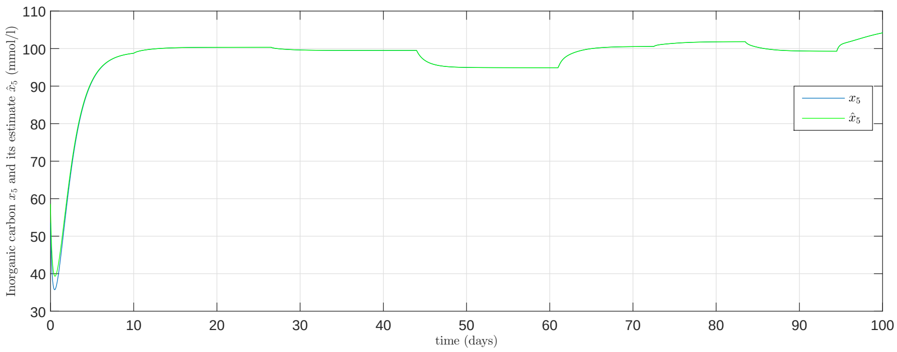

FIGURE 3.36: Inorganic carbon x_5 and its estimate $\hat{x}_5$ (mmol/l).

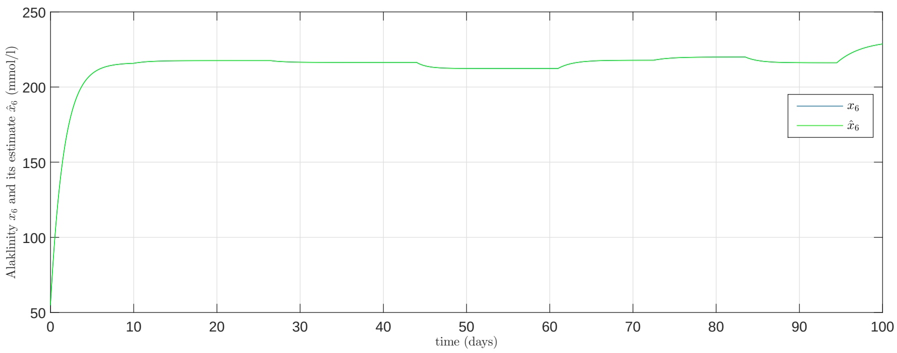

FIGURE 3.37: Alkalinity concentration x_6 and its estimate $\hat{x}_6$ (mmol/l).

error to an LPV system. Then, using the LPV techniques and due to the boundedness of the state variables and the Lipschitz property of the included nonlinearities in the model, we have synthesized LMI conditions to ensure the asymptotic stability of the estimation error. The feasibility of obtained LMI conditions has been enhanced by the use of judicious reformulation of the Young's inequality.

Different LMI-based nonlinear observers have been proposed for the AD process. The LMI-based invariant like observer which has been applied with success to our application.

But, due to its local applicability, we have designed an LMI-based nonlinear observer of the form of the generalized Arcak's observer [148]. It has shown satisfactory results when it was applied to the AD model in absence of disturbances. However, once the system got disturbed the observer performances decreased and it poorly rejected the perturbation. Thus, it has been extended by including the $\mathcal{H}_\infty$ criterion in its synthesis. Positively, it was applied successfully to the system and has been shown robust to dynamic and measurement disturbances. Besides, we have shown how to descritize the nonlinear observers and we have proposed new LMI conditions to ensure their convergence to the system state variables. The discrete observers were also applier with success to the AD model. We would like to say that the results were presented in a general way in order to make them usable for other applications. Moreover, in all the performed simulations we have selected as much as possible the most encountered measurements in AD processes at industrial scale.

Furthermore, with the aim to increase application of the proposed design methodology in real applications (biogas plants especially), we have extended it to the case of nonlinear outputs. Indeed, the nonlinear outputs in biogas plants, at industrial scale, are the cheapest and the easiest to perform. Hence, we have applied the findings to the AD system by numerical simulation and firmly the results have been found promising. Obviously, the design methodology for the systems with nonlinear outputs can be extended to the generalized Arcak's like observer as in Section 3.4.2, enhanced by including the $\mathcal{H}_\infty$ criterion in the observer synthesis as in Section 3.4.3 and finally discritized as in Sections 3.4.4 and 3.4.5.

Chapter 4

Control of Biogas Plants

4.1 Introduction

In the last decade, a significant interest has been attributed to AD control. As stated in the main introduction 1, depending on the model complexity and the available measurements, different control strategies have been designed to satisfy some specific criteria. Among the designed controls for the AM2 model [4] with the aim to control the concentration of bicarbonate alkalinity by mean of an added control input to the model, we find the linearizing control [22] and the input to output linearizing control [120], [123]. In [22], the objective was to enhance the biogas quality while in [120] and [123] the objective was to stabilize the digester. Whether in the first or the second control strategies, the magnitude of the added input was assumed to be very small so that it could be excluded from the dynamics of the model state variables other than the alkalinity concentration. This assumption makes the control design easier. Especially, the input to output linearizing control, where this assumption relax the complexity of the nonlinear transformation of the system. However, even if the control becomes easier when neglecting the effect of the added dilution rate in the dynamic of the first fifth state variables of the model, this is not very consistent.

Another control strategy using the MPC has been proposed in [132] to control the biogas production for a demand-driven electricity production. The idea is to optimize the plant feeding according to a fluctuating timetable of energy demand. The control was applied to a full scale research plant and has shown satisfactory results. However, although the satisfactory results, the analytical proof of the closed loop system is yet difficult to prove.

Combining the ideas from [120], [123], [22] and [132], where the alkalinity addition is used to stabilize the reactor and enhance the biogas quality, and the plant feeding is optimized so that it follows a production timetable, we propose in our turn to control the system so that it tracks an admissible reference trajectory planned by the designer. In other words, the user plans the evolution of the system according to some desired criteria, then we control the system to satisfy that planned evolution. To do so, we will propose a simple state feedback control. In contrast to [120], [123], [22], we will keep the model mass balance as it is, we do not simplify the effect of the alkalinity flow in the dynamics of the model state variables.

The rest of the chapter is organised as follows. In Section 4.2, we will design a control strategy to track an admissible reference trajectory. This will be based on full knowledge of the state vector. Then, in Section 4.3, we will extend the design methodology to account for the non availability of the full state vector. Thus, we will include one of the observers designed in Chapter 3 in the control scheme. In order to prove the stability of the closed loop system, we will provide two synthesis methods to find the controller and the observer parameters. In Section 4.3.2, we will present the first method where the observer and the controller gains will be computed separately, using two quasi independent LMI conditions. While in Section 4.3.3, both of the controller and the observer gains will be computed simultaneously using unified LMI conditions. In Section 4.4, we will present the simulation results when applying the control scheme to the AD model used in the previous chapters. Finally, in Section 4.5, we will conclude the chapter.

4.2 State-Feedback Trajectory Tracking via LMIs

First, let us recall the AD model presented in Section 2.3 under the following form

$$\dot{x} = f(x) + g(x)u \tag{4.1}$$

where $x = [x_1,\ x_2,\ x_3,\ x_4,\ x_5,\ x_6]^T$, $u = [u_1,\ u_2]^T$ and

$$f(x) = \begin{bmatrix} -k_1\mu_1(x_1)x_2 \\ \mu_1(x_1)x_2 \\ k_2\mu_1(x_1)x_2 - k_3\mu_2(x_3)x_4 \\ \mu_2(x_3)x_4 \\ k_4\mu_1(x_1)x_2 + k_5\mu_2(x_3)x_4 - q_c(x) \\ 0 \end{bmatrix}, \quad g(x) = \begin{bmatrix} S_{1in} - x_1 & -x_1 \\ -\alpha x_2 & -\alpha x_2 \\ S_{2in} - x_3 & -x_3 \\ -\alpha x_4 & -\alpha x_4 \\ C_{in} - x_5 & -x_5 \\ Z_{in} - x_6 & Z_{ad} - x_6 \end{bmatrix} \tag{4.2}$$

and the fed concentrations S_{1in}, S_{2in}, C_{in}, Z_{in} and Z_{ad} are assumed to be constant or piecewise constant. The model output is taken as the following

$$y_1 = [x_1, x_3, x_6]^T \tag{4.3}$$

$$y_2 = q_c(x) \tag{4.4}$$

In order to design a reference tracking control for the AD model (4.1), and with the aim to present the results in a general way, we rewrite the model (4.1) as

$$\dot{x} = N[x \quad x]\ u + G\gamma(x) + Bu \tag{4.5}$$

with

$$N = -\text{block-diag}\,(1, \alpha, 1, \alpha, 1, 1) \tag{4.6}$$

$$G = \begin{bmatrix} -k_1 & 1 & k_2 & 0 & k_4 & 0 \\ 0 & 0 & -k_3 & 1 & k_5 & 0 \\ 0 & 0 & 0 & 0 & -1 & 0 \end{bmatrix}^T \tag{4.7}$$

$\gamma_1(x) = \mu_1(x_1)x_2$, $\gamma_2(x) = \mu_2(x_3)x_4$, $\gamma_3(x) = q_c(x)$, and

$$B = \begin{bmatrix} S_{1in} & 0 & S_{2in} & 0 & C_{in} & Z_{in} \\ 0 & 0 & 0 & 0 & 0 & Z_{ad} \end{bmatrix}^T \tag{4.8}$$

To simplify the presentation and to get a convenient structure of the dynamics (4.5), we proceed as in the observer design presented in Chapter 3 by rewriting the term $N[x \ \ x]\ u$ as follows:

$$N[x \ \ x]\ u \triangleq A(\rho^u)x(t) \triangleq \rho^u N x(t) \tag{4.9}$$

where $\rho^u = u_1 + u_2$.

For practical considerations and from the boundedness of the state variables, the input control variables are assumed to be bounded. That is, we have

$$\rho_{\min} \leq \rho^u \leq \rho_{\max}. \tag{4.10}$$

Hence, the dynamics (4.5) can be simplified and rewritten as

$$\dot{x} = A(\rho^u)x + G\gamma(x) + Bu. \tag{4.11}$$

Remark 5. The LPV reformulation (4.11) is introduced in the goal to simplify the tracking problem and avoid the presence of bilinear coupling between the control input and the state of the system. Hence the reference tracking will be done using only the B matrix. Indeed, the bilinear part depends on $\rho^u = u_1 + u_2$, which is viewed as a bounded scalar for practical considerations (generally the input is saturated to avoid washout of bacteria and emptying the digester). However, the input u related to the B matrix will be used for tracking.

The control objective consists in tracking a given desired trajectory $x_d(t)$ corresponding to a desired input $u_d(t)$, where (x_d, u_d) is assumed to be an admissible solution to the system (4.11). That is the pair (x_d, u_d) satisfies the dynamics:

$$\dot{x}_d = A(\rho^{u_d})x_d + G\gamma(x_d) + Bu_d. \tag{4.12}$$

Hence, the tracking control can be

$$u = -K(\rho^{u_d})\tilde{x} + u_d \tag{4.13}$$

where

$$\tilde{x} = x - x_d \tag{4.14}$$

represents the tracking error vector, and the control gain is given by

$$K(\rho^{u_d}) = K_0 + \sum_{j=1}^{s} \rho_j^{u_d} K_j \tag{4.15}$$

Therefore, the dynamics of the reference tracking error (4.14) can be written as:

$$\dot{\tilde{x}} = \left(A(\rho^{u_d}) - BK(\rho^{u_d}) + \sum_{i,j=1}^{m,n_i} \varphi_{ij}(t)\mathcal{H}_{ij}H_i \right) \tilde{x} + \underbrace{\Big(A(\rho^{u}) - A(\rho^{u_d})\Big)x_d}_{\omega(t)} \tag{4.16}$$

where

$$\sum_{i,j=1}^{m,n_i} \varphi_{ij}(t)\mathcal{H}_{ij}H_i\tilde{x} = G(\gamma(x) - \gamma(x_d)), \quad \mathcal{H}_{ij} = Ge_m^T(i)e_{n_i}(j) \tag{4.17}$$

from the DMVT 2 and Lemma 1, and $\varphi_{ij}(t) = \frac{\partial \gamma_i}{\partial x_j}(\nu_i)$, with $\nu_i \in Co(x, x_d)$, and satisfy

$$\underline{\varphi}_{ij} \leq \varphi_{ij} \leq \overline{\varphi}_{ij}. \tag{4.18}$$

The aim consists in finding the controller gain matrices $K_i, i = 0, \ldots, s$, so that the tracking error $\tilde{x}$ satisfies the following $\mathcal{H}_\infty$ criterion:

$$\|\tilde{x}\|_{\mathcal{L}_2^n} \leq \sqrt{\mu\|\omega\|^2_{\mathcal{L}_2^n} + \nu\|\tilde{x}_0\|^2} \tag{4.19}$$

where $\mu > 0$ is the gain from ω to $\tilde{x}$, and $\nu > 0$ is to be determined.

Usually, we use Lyapunov functions to get checkable conditions guaranteeing (4.19). In the LMI framework, we take a quadratic Lyapunov function $V(\tilde{x})$, such that

$$\vartheta(t) \triangleq \frac{\mathrm{d}V}{\mathrm{d}t}(\tilde{x}) + \|\tilde{x}\|^2 - \mu\|\omega\|^2 \leq 0. \tag{4.20}$$

By analogy to the results of Chapter 3, we obtain the following proposition which provides sufficient LMI conditions under which the inequality (4.20) holds.

Theorem 12. *If there exist symmetric positive definite matrices $\mathbb{P}, \mathcal{Z}_{ij}, i, j = 1, \ldots, n$, and matrices $\mathbb{Y}_j, j = 0, \ldots, s$, of appropriate dimension, such that the following convex* *optimization problem holds:*

$$\min(\mu) \quad \textit{subject to} \quad (4.22) \tag{4.21}$$

$$\begin{bmatrix} \Theta & \overbrace{\begin{bmatrix} \Sigma_1 & \dots & \Sigma_m \end{bmatrix}}^{\Sigma} \\ & \\ & \\ (\star) & -\Lambda\mathbb{Z} \end{bmatrix} \leq 0, \ \forall \varrho \in \{\rho_{\min}, \rho_{\max}\} \tag{4.22}$$

with

$$\Theta = \begin{bmatrix} \Theta_{11} & \begin{bmatrix} \mathbb{P} \\ 0 \end{bmatrix} \\ (\star) & -\mathbb{I}_n \end{bmatrix}, \quad \Theta_{11} = \begin{bmatrix} \mathbb{A}\Big(\mathbb{P}, \mathbb{Y}, \varrho\Big) & \mathbb{I}_n \\ (\star) & -\mu\mathbb{I}_n \end{bmatrix} \tag{4.23}$$

$$\mathbb{A}\Big(\mathbb{P}, \mathbb{Y}, \varrho\Big) \quad = \quad \mathbb{P}A_0^T + A_0\mathbb{P} - \mathbb{Y}_0 B^\top - B\mathbb{Y}_0^\top + \sum_{j=1}^{s} \varrho_j \Big(\mathbb{P}A_j^T + A_0\mathbb{P} - \mathbb{Y}_j B^\top - B\mathbb{Y}_j^\top\Big) \tag{4.24}$$

$$\Sigma_i = \Big[\mathcal{N}_i^1\Big(\mathbb{P}, \mathbb{Y}, \mathcal{Z}_{i1}\Big) \dots \mathcal{N}_i^{n_i}\Big(\mathbb{P}, \mathbb{Y}_i, \mathcal{Z}_{in_i}\Big)\Big] \tag{4.25}$$

$$\mathcal{N}_i^j\Big(\mathbb{P}, \mathbb{Y}, \mathcal{Z}_{ij}\Big) = \begin{bmatrix} \mathbb{P}H_i^T \\ 0 \\ 0 \end{bmatrix} + \begin{bmatrix} \mathcal{H}_{ij} \\ 0 \\ 0 \end{bmatrix} \mathbb{Z}_{ij} \tag{4.26}$$

$$\Lambda = \textit{block-diag}\Big(\Lambda_1, ..., \Lambda_m\Big) \tag{4.27}$$

$$\Lambda_i = \textit{block-diag}\left(\frac{2}{\bar{\varphi}_{i1}}\mathbb{I}_{n_i}, \dots, \frac{2}{\bar{\varphi}_{in_i}}\mathbb{I}_{n_i}\right), \tag{4.28}$$

$$\mathbb{Z} = \textit{block-diag}\Big(\mathbb{Z}_1, \dots, \mathbb{Z}_m\Big) \tag{4.29}$$

$$\mathbb{Z}_i = \textit{block-diag}\Big(\mathcal{Z}_{i1}, \dots, \mathcal{Z}_{in_i}\Big). \tag{4.30}$$

Then the $\mathcal{H}_\infty$ criterion (4.19) is satisfied with the tracking controller gains

$$K_j = \mathbb{Y}_j^\top \mathbb{P}^{-1}, \ j = 1, \dots, s.$$

The disturbance attenuation level μ *is the minimum value returned by* (4.21)*, and* $\nu = \lambda_{\max}(\mathbb{P})$.

Proof. The proof is not complicated. We should follow the same steps as in Chapter 3 for the observer design conjointly with an additional use of a convenient congruence principe. To avoid repetition, it is not necessary to show here all the steps. The Lyapunov function candidate is given by

$$V(\tilde{x}) = \tilde{x}^{\top}\mathbb{P}^{-1}\tilde{x}.$$

now, from Chapter 3, we can deduce easily that a sufficient condition ensuring inequality (4.20) is

$$\begin{bmatrix} \mathbb{A}_K(\rho^{u_d}) + \mathbb{I}_n & \mathbb{P}^{-1} \\ (\star) & -\mu\mathbb{I}_n \end{bmatrix} + \sum_{i,j=1}^{m,n_i} \varphi_{ij}(t) \left(\overbrace{\begin{bmatrix} \mathbb{P}^{-1}\mathcal{H}_{ij} \\ 0 \end{bmatrix}}^{\mathbb{X}_{ij}^T} \overbrace{\begin{bmatrix} H_i & 0 \end{bmatrix}}^{\mathbb{Y}_i} + \mathbb{Y}_i^T\mathbb{X}_{ij} \right) \leq 0 \tag{4.31}$$

where

$$\mathbb{A}_K(\rho^{u_d}) \triangleq \left(A(\rho^{u_d}) - BK(\rho^{u_d})\right)^T \mathbb{P}^{-1} + \mathbb{P}^{-1}\left(A(\rho^{u_d}) - BK(\rho^{u_d})\right) \tag{4.32}$$

By pre and post multiplying the right hand side of (4.67) by $\begin{bmatrix} \mathbb{P} & 0 \\ 0 & \mathbb{I}_n \end{bmatrix}$, applying the Schur Lemma, and using the Young's inequality in the following manner:

$$\mathbb{X}_{ij}^T\mathbb{Y}_i + \mathbb{Y}_i^T\mathbb{X}_{ij} \leq \frac{1}{2}\left[\mathbb{Y}_i + \mathbb{Z}_{ij}\mathbb{X}_{ij}\right]^T \mathbb{Z}_{ij}^{-1}\left[\mathbb{Y}_i + \mathbb{Z}_{ij}\mathbb{X}_{ij}\right],$$

we obtain the Theorem 12. This ends the proof. □

Remark 6. It is worth to notice that when $\underline{\varphi}_{ij} < 0$, we have to use $\bar{\underline{\varphi}}_{ij} = \bar{\varphi}_{ij} - \underline{\varphi}_{ij}$ instead of $\bar{\varphi}_{ij}$ and rearrange the matrix Θ to obtain the exact corresponding terms.

4.3 Observer-Based Reference Trajectory Tracking

4.3.1 Formulation of the problem

In reference trajectory tracking problem (this is the case with most control design problems), the state of the system, $x(t)$, is generally not available for feedback. That is why often a state observer is necessary. This section is devoted to this issue. We will provide two different LMI-based tracking design techniques. The first one gives some separation results, where the design of the observer and the controller gains are computed separately by solving two quasi-independent LMI conditions. The second method consists in designing the observer-based controller gains simultaneously by solving a single LMI condition.

As a state observer, we consider the same one as given in Chapter 3. Therefore, the structure of the observer-based trajectory tracking model is defined as the following:

$$\dot{\hat{x}} = A(\rho^u)\hat{x} + \sum_{i=1}^{m} G_i\gamma_i(\hat{\vartheta}_i) + Bu + L(\rho^u)\Big(y - C\hat{x}\Big) \tag{4.33a}$$

$$u = -K(\rho^{u_d})\,(\hat{x} - x_d) + u_d \tag{4.33b}$$

$$\hat{\vartheta}_i = H_i\hat{x} + \mathcal{K}_i(\rho)(y - C\hat{x}), \tag{4.33c}$$

where

$$K(\rho^{u_d}) = K_0 + \sum_{j=1}^{s} \rho_j^{u_d} K_j \tag{4.33d}$$

and

$$L(\rho^u) = L_0 + \sum_{j=1}^{s} \rho_j^u L_j,\;\; \mathcal{K}_i(\rho^u) = \mathcal{K}_{i0} + \sum_{j=1}^{s} \rho_j^u \mathcal{K}_{ij}. \tag{4.33e}$$

The estimation error is given by

$$\dot{e}(t) = \left(\mathbb{A}_L(\rho^u) + \sum_{i,j=1}^{m,n_i} \phi_{ij}(t)\mathcal{H}_{ij}\Big(H_i - \mathcal{K}_i(\rho^u)C\Big)\right) e(t) \tag{4.34}$$

where $\mathbb{A}_L(\rho^u) = A(\rho^u) - L(\rho^u)C$. Notice that the notations of Chapter 3 are some times used here without recalling them in order to avoid repetition.

The dynamics of the reference tracking error (4.16) becomes

$$\dot{\tilde{x}} = \left(A(\rho^{u_d}) - BK(\rho^{u_d}) + \sum_{i,j=1}^{m,n_i} \varphi_{ij}(t)\mathcal{H}_{ij}H_i \right) \tilde{x} + BK(\rho^{u_d})e + \underbrace{\Big(A(\rho^{u}) - A(\rho^{u_d})\Big)x_d}_{\omega(t)} \tag{4.35}$$

In the next two sections, we will provide two different LMI techniques to handle the problem of trajectory tracking based on state observer.

4.3.2 First LMI technique: Parallel design

This section is devoted to an LMI technique, which ensures the exponential convergence of the state estimation error to zero and guaranties the $\mathcal{H}_\infty$ asymptotic stability of the tracking error. We will present a kind of separation principle for nonlinear systems. Note that in linear case, the separation principle means that we can investigate separately the convergence of the estimation error and the stability of the tracking error by using the concept of eigenvalues. However, in the nonlinear case, the separation results that we will provide are based on the Lyapunov analysis and on the use of the well-known Barbalat's lemma.

Since the dynamics (4.34) do not depend on the reference tracking error $\tilde{x}(t)$ and the functions $\phi_{ij}(t)$ are bounded, then we can study the convergence of the estimation error $e(t)$ separately and will use it in the dynamics of the tracking error as a bounded disturbance exponentially converging towards zero. On the other hand, it is useless to reproduce the convergence analysis of $e(t)$ because it was done in Chapter 3. We will only recall the sufficient LMI conditions modified in order to have exponential convergence, instead of asymptotic one.

The following theorem provides the synthesis conditions expressed in term of LMIs.

Theorem 13. *The closed-loop system* (4.35) *is $\mathcal{H}_\infty$ asymptotically stabilizable by the observer-based feedback* (4.33)*, if there exist symmetric positive definite matrices $\mathbb{P}$, $\mathbb{Q}$, $\mathcal{Z}_{ij}$, $\mathcal{S}_{ij}$, $i, j = 1, \ldots, n$, and matrices $\mathbb{Y}_i, \mathbb{X}_i, \mathcal{X}_{ij}$ of appropriate dimensions such that for given two positive scalar β, the LMI conditions* (4.36) *are fulfilled and the convex optimization problem* (4.41) *is solvable.*

1. *LMIs for the observer gains:*

$$\begin{bmatrix} \mathbb{A}\Big(\mathbb{Q},\mathbb{X},\varrho\Big)+\beta\mathbb{Q} & \overbrace{\begin{bmatrix}\Pi_1 & \dots & \Pi_m\end{bmatrix}}^{\Pi} \\ (\star) & -\Lambda\mathbb{S} \end{bmatrix} \leq 0, \ \forall\varrho\in\{\rho_{\min},\rho_{\max}\} \tag{4.36}$$

with

$$\mathbb{A}\Big(\mathbb{Q},\mathbb{X},\varrho\Big) = A_0^T\mathbb{Q}+\mathbb{Q}A_0 - C^T\mathbb{X}_0 - \mathbb{X}_0^TC + \sum_{j=1}^{s}\varrho_j\Big(A_j^T\mathbb{Q}+\mathbb{Q}A_j - C^T\mathbb{X}_j - \mathbb{X}_j^TC\Big) \tag{4.37}$$

and

$$\Pi_i = \Big[\mathcal{M}_i^1\Big(\mathbb{Q},\mathcal{S}_{i1}\Big)\dots\ \mathcal{M}_i^{n_i}\Big(\mathbb{Q},\mathcal{S}_{in_i}\Big)\Big], \quad \mathcal{M}_i^j\Big(\mathbb{Q},\mathcal{S}_{ij}\Big) = \mathbb{Q}\mathcal{H}_{ij}+H_i^T\mathcal{S}_{ij} - C^\top\mathcal{X}_{ij} \tag{4.38}$$

$$\mathbb{S} = \textit{block-diag}\Big(\mathbb{S}_1,\dots,\mathbb{S}_m\Big) \tag{4.39}$$

$$\mathbb{S}_i = \textit{block-diag}\Big(\mathcal{S}_{i1},\dots,\mathcal{S}_{in_i}\Big). \tag{4.40}$$

The observer gains L_j and $\mathcal{K}_{ij}$ are computed as

$$L_j = \mathbb{Q}^{-1}\mathbb{X}_j^T, \quad \mathcal{K}_{ij} = \mathcal{S}_{ij}^{-1}\mathcal{X}_{ij}^T.$$

2. *Optimization problem for the controller gains:*

$$\min(\mu) \quad \textit{subject to} \quad (4.42) \tag{4.41}$$

$$\begin{bmatrix} \Theta & \overbrace{\begin{bmatrix}\Sigma_1 & \dots & \Sigma_m\end{bmatrix}}^{\Sigma} \\ (\star) & -\Lambda\mathbb{Z} \end{bmatrix} \leq 0, \ \forall\varrho\in\{\rho_{\min},\rho_{\max}\} \tag{4.42}$$

with

$$\Theta = \begin{bmatrix} \Theta_{11} & \begin{bmatrix} \mathbb{P} \\ 0 \end{bmatrix} \\ (\star) & -\mathbb{I}_n \end{bmatrix}, \quad \Theta_{11} = \begin{bmatrix} \mathbb{A}\Big(\mathbb{P}, \mathbb{Y}, \varrho\Big) & \mathbb{I}_n \\ (\star) & -\mu\mathbb{I}_n \end{bmatrix} \tag{4.43}$$

$$\mathbb{A}\Big(\mathbb{P}, \mathbb{Y}, \varrho\Big) = \mathbb{P}A_0^T + A_0\mathbb{P} - \mathbb{Y}_0 B^\top - B\mathbb{Y}_0^\top + \sum_{j=1}^{s} \varrho_j \Big(\mathbb{P}A_j^T + A_0\mathbb{P} - \mathbb{Y}_j B^\top - B\mathbb{Y}_j^\top\Big) \tag{4.44}$$

The matrix blocks Σ_i *and* $\mathbb{Z}$ *are defined in Theorem 12. Thus, the* $\mathcal{H}_\infty$ *criterion* (4.19) *is satisfied with the tracking controller gains*

$$K_j = \mathbb{Y}_j^\top \mathbb{P}^{-1}, \ j = 1, \ldots, s.$$

The disturbance attenuation level μ *is the minimum value returned by* (4.41)*, and* $\nu = \lambda_{\max}(\mathbb{P})$.

Proof. The proof is easy and standard. It is based on the use of the Barbalat's lemma since the dynamics of the augmented system with the state $\begin{bmatrix} \tilde{x} \\ e \end{bmatrix}$ has a triangular structure. For more details, we refer the reader to [133]. For the observer convergence we use the Lyapunov function $V_1(e)$ and for the tracking error we use $V_2(\tilde{x})$ and the $\mathcal{H}_\infty$ criterion (4.19), where

$$V_1(e) = e^\top \mathbb{Q} e, \ V_2(\tilde{x}) = \tilde{x}^\top \mathbb{P}^{-1} \tilde{x} \tag{4.45}$$

□

4.3.3 Second approach: Simultaneous design

This section is dedicated to a second observer-based trajectory tracking method. Contrarily to the first method, the second one provides a unified LMI synthesis condition ensuring the convergence of the global augmented system containing the tracking error vector and the estimation error. For simplicity we assume without loss of generality that the observer does not contain output feedback in the nonlinear terms, i.e. $\mathcal{K}_i(\rho_t) \equiv 0$.

Using the augmented vector $\zeta \triangleq \begin{bmatrix} \tilde{x} \\ e \end{bmatrix}$, the dynamics of the tracking error and the estimation error given by (4.35) and (4.34), respectively, can be rewritten under the following unified form:

$$\dot{\zeta} = \left(\begin{bmatrix} \overbrace{A(\rho^{u_d}) - BK(\rho^{u_d})}^{\mathbb{A}_K(\rho^{u_d})} & BK(\rho^{u_d}) \\ 0 & \mathbb{A}_L(\rho^u) \end{bmatrix} + \sum_{i,j=1}^{m,n_i} \begin{bmatrix} \varphi_{ij}(t)\mathcal{H}_{ij}H_i & 0 \\ 0 & \phi_{ij}(t)\mathcal{H}_{ij}H_i \end{bmatrix} \right) \zeta + \begin{bmatrix} \mathbb{I}_n \\ 0 \end{bmatrix} \underbrace{\Big(A(\rho^u) - A(\rho^{u_d})\Big) x_d}_{\omega(t)} \quad (4.46)$$

The aim consists in finding the gain matrices L_j and K_j so that the augmented error ζ satisfies the following $\mathcal{H}_\infty$ criterion:

$$\|\zeta\|_{\mathcal{L}_2^{2n}} \leq \sqrt{\mu \|\omega\|^2_{\mathcal{L}_2^n} + \nu \|\zeta_0\|^2} \quad (4.47)$$

where $\mu > 0$ is the gain from x_d to ζ, and $\nu > 0$ is to be determined.

In order to satisfy (4.47), we use a quadratic Lyapunov function $V(\zeta)$, such that

$$\vartheta(t) \triangleq \frac{\mathrm{d}V}{\mathrm{d}t}(\zeta) + \|\zeta\|^2 - \mu\|\omega\|^2 \leq 0. \quad (4.48)$$

By analogy to the previous results, we obtain the following proposition which provides sufficient LMI conditions under which the inequality (4.48) is satisfied.

Theorem 14. *Assume that there exist symmetric positive definite matrices $\mathbb{P}$, $\mathbb{Q}$, $\mathbb{S}_{ij}$, $\bar{\mathbb{S}}_{ij}$, $i, j = 1, \ldots, n$, and matrices $\mathbb{X}_i, \mathbb{Y}_i, i = 0, \ldots, s$, of appropriate dimensions, such that for a given positive scalar ϵ, the following convex optimization problem holds:*

$$\min(\mu) \quad \textit{subject to} \quad (4.50) \quad (4.49)$$

$$\begin{bmatrix} \Theta & \overbrace{\begin{bmatrix} \Sigma_1 & \dots & \Sigma_m \end{bmatrix}}^{\Sigma} \\ \\ \\ (\star) & -\Lambda\mathbb{M} \end{bmatrix} \leq 0, \ \forall(\varrho, \bar{\varrho}) \in \mathbb{V}_\rho \times \mathbb{V}_{\bar{\varrho}} \tag{4.50}$$

where

$$\Theta = \begin{bmatrix} \Theta_{11} & \begin{bmatrix} \mathbb{P} \\ 0 \\ 0 \end{bmatrix} & \begin{bmatrix} \epsilon B \mathbb{Y}^\top(\bar{\varrho}) \\ \mathbb{I}_n \\ 0 \end{bmatrix} \\ (\star) & -\mathbb{I}_n & 0 \\ (\star) & (\star) & -2\epsilon\mathbb{P} \end{bmatrix} \tag{4.51}$$

$$\Theta_{11} = \begin{bmatrix} \mathbb{B}\Big(\mathbb{P}, \mathbb{Y}, \bar{\varrho}\Big) & 0 & \mathbb{I}_n \\ (\star) & \mathbb{A}\Big(\mathbb{Q}, \mathbb{X}, \varrho\Big) & 0 \\ \mathbb{I}_n & 0 & -\mu\mathbb{I}_n \end{bmatrix} \tag{4.52}$$

$$\mathbb{A}\Big(\mathbb{Q}, \mathbb{X}, \varrho\Big) = A_0^T\mathbb{Q} + \mathbb{Q}A_0 - C^T\mathbb{X}_0 - \mathbb{X}_0^T C + \sum_{j=1}^{s} \varrho_j \Big(A_j^T\mathbb{Q} + \mathbb{Q}A_j - C^T\mathbb{X}_j - \mathbb{X}_j^T C\Big) \tag{4.53}$$

$$\mathbb{B}\Big(\mathbb{P}, \mathbb{Y}, \bar{\varrho}\Big) = \mathbb{P}A_0^T + A_0\mathbb{P} - \mathbb{Y}_0 B^\top - B\mathbb{Y}_0^\top + \sum_{j=1}^{s} \bar{\varrho}_j \Big(\mathbb{P}A_j^T + A_0\mathbb{P} - \mathbb{Y}_j B^\top - B\mathbb{Y}_j^\top\Big) \tag{4.54}$$

$$\mathbb{Y}^\top(\bar{\varrho}) = \mathbb{Y}_0 + \sum_{j=1}^{s} \bar{\varrho}_j \mathbb{Y}_j, \tag{4.55}$$

$$\Sigma_i = \Big[\mathcal{N}_i^1\Big(\mathbb{S}_{i1}, \bar{\mathbb{S}}_{i1}\Big) \dots \mathcal{N}_i^{n_i}\Big(\mathbb{S}_{in_i}, \bar{\mathbb{S}}_{in_i}\Big)\Big] \tag{4.56}$$

$$\mathcal{N}_i^j\left(\mathbb{S}_{ij},\bar{\mathbb{S}}_{ij}\right)=\begin{bmatrix}\begin{bmatrix}\mathbb{P}H_i^T\\0\\0\\0\\0\end{bmatrix}+\begin{bmatrix}\mathcal{H}_{ij}\\0\\0\\0\\0\end{bmatrix}\mathbb{S}_{ij} & \begin{bmatrix}0\\\mathbb{Q}\mathcal{H}_{ij}\\0\\0\\0\end{bmatrix}+\begin{bmatrix}0\\H_i^T\\0\\0\\0\end{bmatrix}\bar{\mathbb{S}}_{ij}\end{bmatrix} \tag{4.57}$$

$$\Lambda = \textit{block-diag}\Big(\Lambda_1, ..., \Lambda_m\Big) \tag{4.58}$$

$$\Lambda_i = \textit{block-diag}\left(\Lambda_i^1, \ldots, \Lambda_i^{n_i}\right) \tag{4.59}$$

$$\Lambda_i^j = \textit{block-diag}\left(\frac{2}{b_{ij}}\mathbb{I}_{2n_i}\right) \tag{4.60}$$

$$\mathbb{M} = \textit{block-diag}\Big(\mathbb{M}_1, \ldots, \mathbb{M}_m\Big) \tag{4.61}$$

$$\mathbb{M}_i = \textit{block-diag}\Big(\mathbb{M}_i^1, \ldots, \mathbb{M}_i^{n_i}\Big) \tag{4.62}$$

$$\mathbb{M}_i^j = \textit{block-diag}\Bigg(\mathbb{S}_{ij}, \bar{\mathbb{S}}_{ij}\Bigg). \tag{4.63}$$

Then the $\mathcal{H}_\infty$ criterion (4.47) is satisfied with the observer-based tracking controller gains

$$L_j = \mathbb{Q}^{-1}\mathbb{X}_j^T, \quad K_j = \mathbb{Y}_j^\top \mathbb{P}^{-1}, \ j = 1, \ldots, s.$$

The disturbance attenuation level μ is the minimum value returned by (4.49), and $\nu = \max\left(\lambda_{\max}\mathbb{P}^{-1}, \lambda_{\max}\mathbb{Q}\right)$.

Proof. In order to satisfy the criterion (4.47), we use the following quadratic Lyapunov function

$$V(\zeta) = \zeta^T \begin{bmatrix}\mathbb{P}^{-1} & 0\\ 0 & \mathbb{Q}\end{bmatrix}\zeta,$$

where

$$\mathbb{Q} = \mathbb{Q}^T > 0 \text{ and } \mathbb{P} = \mathbb{P}^T > 0.$$

By calculating the derivative of $V(\zeta)$ along the trajectories of (4.46), we obtain:

$$\begin{aligned}\dot{V}(\zeta) \quad &= \tilde{x}^T \left[\mathbb{P}^{-1} \left(\mathbb{A}_K(\rho^{u_d}) + \sum_{i,j=1}^{m,n_i} \varphi_{ij} \mathcal{H}_{ij} H_i \right) + \left(\mathbb{A}_K(\rho^{u_d}) + \sum_{i,j=1}^{m,n_i} \varphi_{ij} \mathcal{H}_{ij} H_i \right)^T \mathbb{P}^{-1} \right] \tilde{x} \\ &+ e^T \left[\mathbb{Q} \left(\mathbb{A}_L(\rho^{u}) + \sum_{i,j=1}^{m,n_i} \phi_{ij} \mathcal{H}_{ij} H_i \right) + \left(\mathbb{A}_L(\rho^{u}) + \sum_{i,j=1}^{m,n_i} \phi_{ij} \mathcal{H}_{ij} H_i \right)^T \mathbb{Q} \right] e \\ &+ 2\tilde{x}^T \mathbb{P}^{-1} B K(\rho^{u_d}) e + 2\tilde{x}^T \mathbb{P}^{-1} \omega(t). \end{aligned} \tag{4.64}$$

Hence, $\vartheta(t) \leq 0$ (equation (4.48)) if the following inequality is fulfilled:

$$\begin{aligned} &\begin{bmatrix} \mathbb{D}\Big(\mathbb{A}_K(\rho^{u_d}), \mathbb{A}_L(\rho^{u})\Big) + \mathbb{I}_{2n} & \begin{bmatrix} \mathbb{P}^{-1} & 0 \\ 0 & \mathbb{Q} \end{bmatrix} \begin{bmatrix} \mathbb{I}_n \\ 0 \end{bmatrix} \\ (\star) & -\mu \mathbb{I}_n \end{bmatrix} \\ &+ \sum_{i,j=1}^{m,n_i} \varphi_{ij}(t) \left(\overbrace{\begin{bmatrix} \mathbb{P}^{-1}\mathcal{H}_{ij} \\ 0 \\ 0 \end{bmatrix}}^{\mathbb{X}_{ij}^T} \overbrace{\begin{bmatrix} H_i & 0 & 0 \end{bmatrix}}^{\mathbb{Y}_i} + \mathbb{Y}_i^T \mathbb{X}_{ij} \right) \\ &+ \sum_{i,j=1}^{m,n_i} \phi_{ij}(t) \left(\overbrace{\begin{bmatrix} 0 \\ \mathbb{Q}\mathcal{H}_{ij} \\ 0 \end{bmatrix}}^{\bar{\mathbb{X}}_{ij}^T} \overbrace{\begin{bmatrix} 0 & H_i & 0 \end{bmatrix}}^{\bar{\mathbb{Y}}_i} + \bar{\mathbb{Y}}_i^T \bar{\mathbb{X}}_{ij} \right) \\ &+ \begin{bmatrix} \mathbb{P}^{-1} B K \\ 0 \\ 0 \end{bmatrix} \begin{bmatrix} 0 & \mathbb{I}_n & 0 \end{bmatrix} + \begin{bmatrix} 0 \\ \mathbb{I}_n \\ 0 \end{bmatrix} \begin{bmatrix} (BK)^T \mathbb{P}^{-1} & 0 & 0 \end{bmatrix} \leq 0 \end{aligned} \tag{4.65}$$

where

$$\begin{aligned} \mathbb{D}\Big(\mathbb{A}_K(\rho^{u_d}), \mathbb{A}_L(\rho^{u})\Big) \triangleq &\begin{bmatrix} \mathbb{A}_K(\rho^{u_d}) & 0 \\ 0 & \mathbb{A}_L(\rho^{u}) \end{bmatrix}^T \begin{bmatrix} \mathbb{P}^{-1} & 0 \\ 0 & \mathbb{Q} \end{bmatrix} \\ &+ \begin{bmatrix} \mathbb{P}^{-1} & 0 \\ 0 & \mathbb{Q} \end{bmatrix} \begin{bmatrix} \mathbb{A}_K(\rho^{u_d}) & 0 \\ 0 & \mathbb{A}_L(\rho^{u}) \end{bmatrix} \end{aligned} \tag{4.66}$$

By pre and post multiplying the right hand side of (4.65) by

$$\begin{bmatrix} \mathbb{P} & 0 & 0 \\ 0 & \mathbb{I}_n & 0 \\ 0 & 0 & \mathbb{I}_n \end{bmatrix},$$

we get the following equivalent inequality:

$$\begin{aligned}
&\begin{bmatrix} \mathbb{T}_{(\mathbf{1.1})} + \mathbb{P}\mathbb{P} & 0 & \mathbb{I}_n \\ 0 & \mathbb{T}_{(\mathbf{2.2})} + \mathbb{I}_n & 0 \\ \mathbb{I}_n & 0 & -\mu\mathbb{I}_n \end{bmatrix} \\
&+ \sum_{i,j=1}^{m,n_i} \varphi_{ij}(t) \left(\overbrace{\begin{bmatrix} \mathcal{H}_{ij} \\ 0 \\ 0 \end{bmatrix}}^{\mathbb{X}_{ij}^T} \overbrace{\begin{bmatrix} H_i\mathbb{P} & 0 & 0 \end{bmatrix}}^{\mathbb{Y}_i} + \mathbb{Y}_i^T \mathbb{X}_{ij} \right) \\
&+ \sum_{i,j=1}^{m,n_i} \phi_{ij}(t) \left(\overbrace{\begin{bmatrix} 0 \\ \mathbb{Q}\mathcal{H}_{ij} \\ 0 \end{bmatrix}}^{\bar{\mathbb{X}}_{ij}^T} \overbrace{\begin{bmatrix} 0 & H_i & 0 \end{bmatrix}}^{\bar{\mathbb{Y}}_i} + \bar{\mathbb{Y}}_i^T \bar{\mathbb{X}}_{ij} \right) \\
&+ \overbrace{\begin{bmatrix} BK \\ 0 \\ 0 \end{bmatrix}}^{\mathbb{V}^T} \overbrace{\begin{bmatrix} 0 & \mathbb{I}_n & 0 \end{bmatrix}}^{\mathbb{U}} + \begin{bmatrix} 0 \\ \mathbb{I}_n \\ 0 \end{bmatrix} \begin{bmatrix} (BK)^T & 0 & 0 \end{bmatrix} \leq 0
\end{aligned} \tag{4.67}$$

where

$$\mathbb{T}_{(\mathbf{1.1})} = \mathbb{P}\mathbb{A}_K^\top(\rho^{u_d}) + \mathbb{A}_K(\rho^{u_d})\mathbb{P},$$

$$\mathbb{T}_{(\mathbf{2.2})} = \mathbb{A}_L^\top(\rho^{u})\mathbb{Q} + \mathbb{Q}\mathbb{A}_L(\rho^{u}).$$

Finally, the use of Schur Lemma and the Young's inequality in the following manner:

$$\mathbb{X}_{ij}^T\mathbb{Y}_i + \mathbb{Y}_i^T\mathbb{X}_{ij} \leq \frac{1}{2}\Big[\mathbb{Y}_i + \mathbb{S}_{ij}\mathbb{X}_{ij}\Big]^T \mathbb{S}_{ij}^{-1}\Big[\mathbb{Y}_i + \mathbb{S}_{ij}\mathbb{X}_{ij}\Big],$$

$$\bar{\mathbb{X}}_{ij}^T\bar{\mathbb{Y}}_i + \bar{\mathbb{Y}}_i^T\bar{\mathbb{X}}_{ij} \leq \frac{1}{2}\Big[\bar{\mathbb{X}}_{ij} + \bar{\mathbb{S}}_{ij}\bar{\mathbb{Y}}_i\Big]^T \bar{\mathbb{S}}_{ij}^{-1}\Big[\bar{\mathbb{X}}_{ij} + \bar{\mathbb{S}}_{ij}\bar{\mathbb{Y}}_i\Big],$$

$$\mathbb{V}^T\mathbb{U} + \mathbb{U}^T\mathbb{V} \leq \frac{1}{2}\Big[\mathbb{U} + \epsilon\mathbb{Z}\mathbb{V}\Big]^T \Big(\epsilon\mathbb{Z}\Big)^{-1}\Big[\mathbb{U} + \epsilon\mathbb{Z}\mathbb{V}\Big],$$

leads to the Theorem 14. $\square$

4.4 Simulation Results

In this section, we illustrate by numeric simulation the proposed control strategy to track a constant reference trajectory planned by the plant operator. We will investigate both cases, when the full state vector is available for measurement and when only its partial measurement is available which is the most realistic case.

4.4.1 State-feedback Trajectory traking

In order to simulate the control strategy proposed in Section 4.2, we use the model parameters given in Table 2.2 and the state bounds provided in Section 2.5. Besides, for simulation we take $S_{1in} = 16\ g/l$, $S_{2in} = 170$ mmol/l, $C_{in} = 76.15$ mmol/l, $Z_{in} = 200$ mmol/l, $Z_{ad} = 700$ mmol/l, $\rho_{min} = 0.1$ day^{-1}, $\rho_{max} = 0.8$ day^{-1},

After solving the optimization problem (4.21) given by Theorem 12, by using the LMI Toolbox of Matlab, we have obtained the following controller gain

$$K_0 = \begin{bmatrix} 0.0007 & 0.0020 & 0.0002 & 0.0722 & -0.0000 & -0.0001 \\ -0.0008 & -0.0021 & -0.0008 & -0.0209 & 0.0000 & 0.0000 \end{bmatrix}$$

$K_1 = 0$ and $\mu = 0.5$.

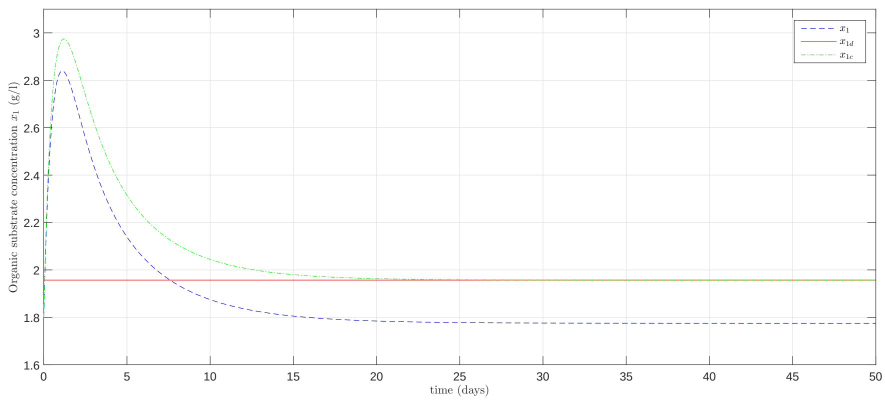

FIGURE 4.1: Organic substrate concentration x_1 (g/l).

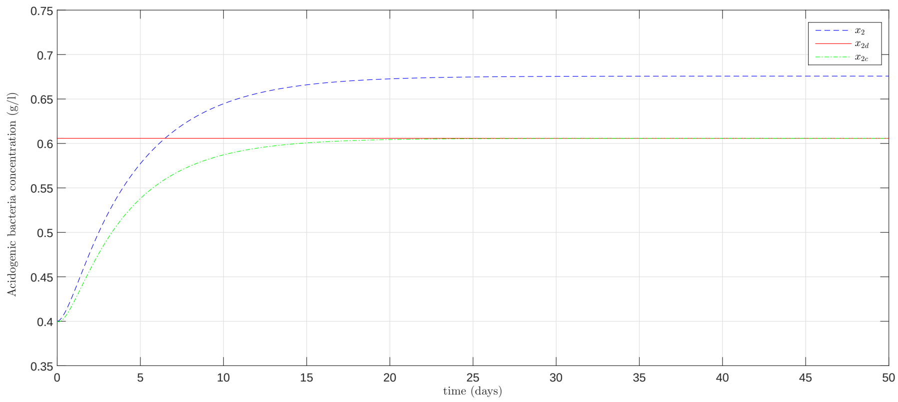

FIGURE 4.2: Acidogenic bacteria concentration (g/l).

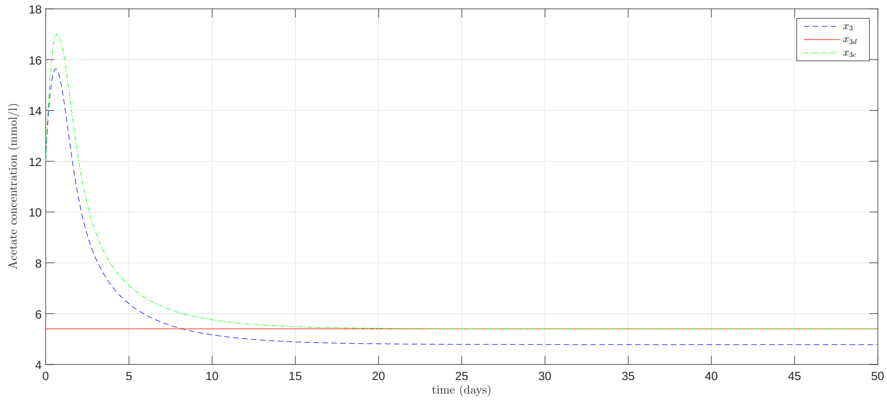

FIGURE 4.3: Acetate concentration (mmol/l).

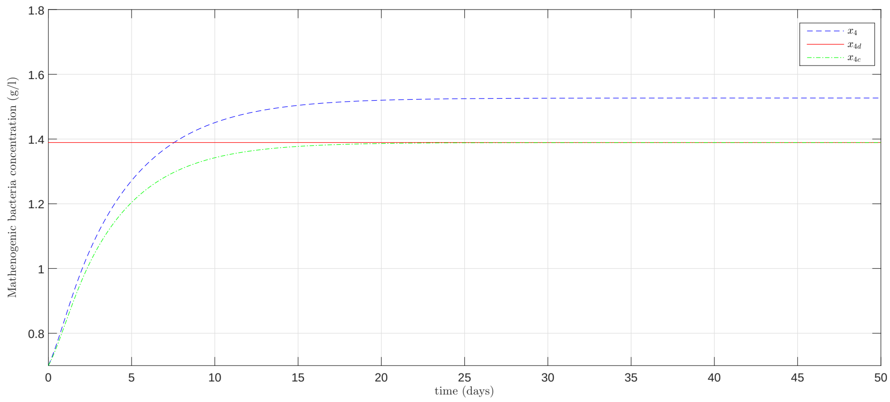

FIGURE 4.4: Mathenogenic bacteria concentration (g/l).

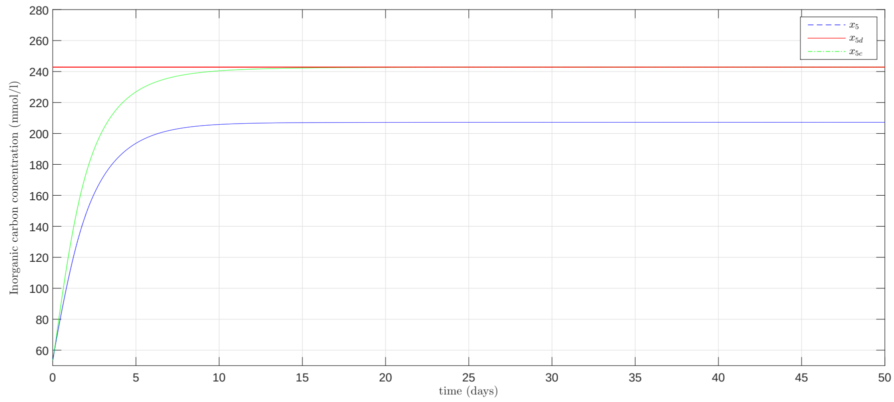

FIGURE 4.5: Inorganic carbon concentration (mmol/l).

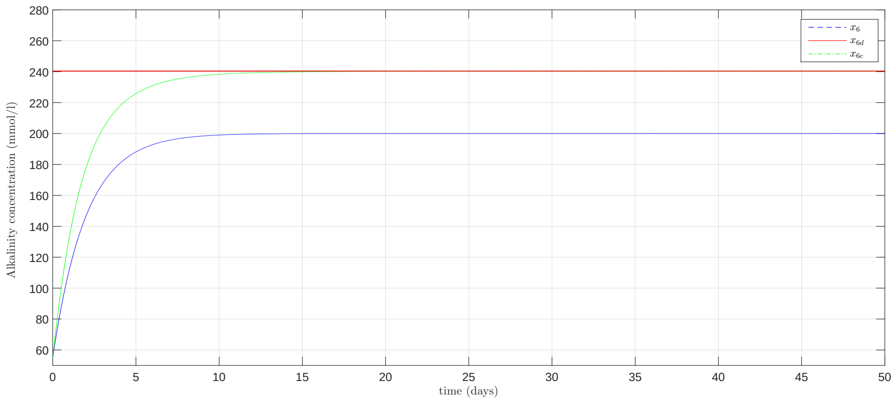

FIGURE 4.6: Alkalinity concentration (mmol/l).

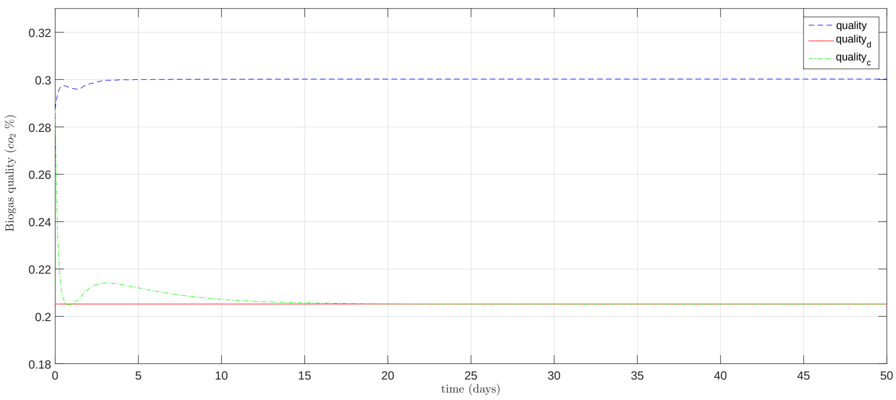

FIGURE 4.7: Biogas quality (co_2%).

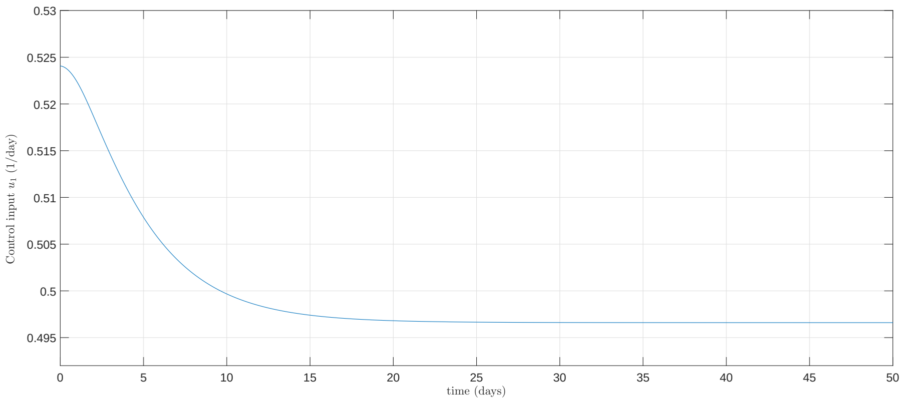

FIGURE 4.8: Control input u_1 (1/day).

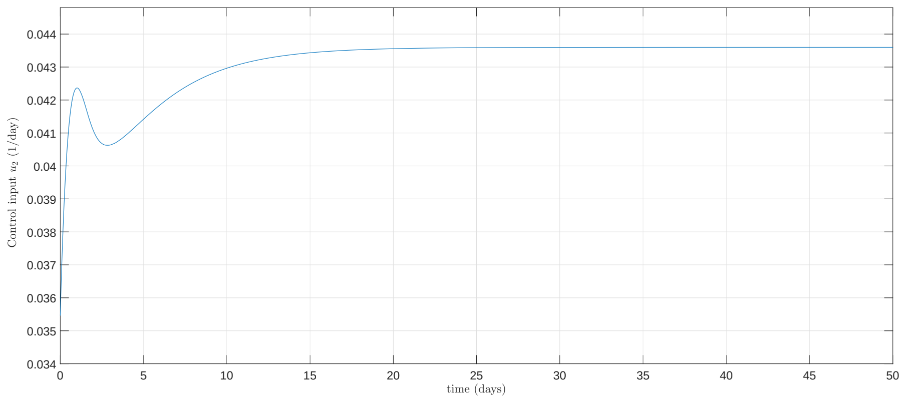

FIGURE 4.9: Control input u_2 (1/day).

In this example, the system is initialized at $x(0) = [1.8, 0.4, 12, 0.7, 109.15, 55]^T$ and we want to track the desired reference given by $x_d = [1.9572, 0.6058, 5.4, 1.3893, 242.8, 240.3413]^T$ and $u_d = [0.4966, 0.0436]^T$, which corresponds to an enhanced quality of biogas at steady state, containing only 20.5% of co_2 gas. The simulation results are reported in Figures 4.1-4.9. In the first seven former figures, we compare the state trajectories and the biogas quality when applying the control strategy (green dash dotted line, the under-script 'c' means controlled) and when not applying the control (blue dashed line). As it can be noticed from those figures, despite the initial gap between the initialization and the desired reference, the controlled system is tracking the desired reference and the biogas quality is enhanced from 30% to 20.5% of countenance of co_2 gas. Moreover, the required control inputs u_1 and u_2 which are depicted in Figures 4.8-4.9, respectively, show satisfactory behaviour. Indeed, the dilution rate of the system changes smoothly and remains in its acceptable domain of variation.

4.4.2 Observer-Based Reference Trajectory Tracking

Often, in real applications, not all the state variables of the system are measurable, thus only the partial measurement of the state vector is available. Moreover, in the AD process, it is known that measurement of the different bacteria concentrations is difficult, time consuming and costly to process. Therefore, in this section, we will suppose that only measurements of some substrate concentrations and the co_2 gas flow rate are available as given in equations (4.3), (4.4). Thus, we will investigate the second control strategy, observer-based reference trajectory tracking 4.3.

In order to show the efficiency of the proposed two design methodologies, parallel and simultaneous design, for the observer-based control to track the desired reference, we will run the same numeric simulation as previously (using the same model parameters, operating and initial conditions as in Section 4.4.1). Then, we will compare the obtained results.

4.4.2.1 Parallel Design

After solving the LMI conditions (4.36) which have been found to be feasible for $\beta = 0.06$, by using the LMI Toolbox of Matlab, and the optimization problem (4.41) given by Theorem 13, we have found the following controller gain

$$K_0 = \begin{bmatrix} 0.0007 & 0.0020 & 0.0002 & 0.0722 & -0.0000 & -0.0001 \\ -0.0008 & -0.0021 & -0.0008 & -0.0209 & 0.0000 & 0.0000 \end{bmatrix}$$

$K_1 = 0$, $\mu = 0.43$, and the following observer parameters

$$L_0 = \begin{bmatrix} 77.0743 & -29.9151 & 0.0000 \\ -1.9248 & 0.7410 & -0.0000 \\ -36.2480 & 429.9256 & 0.0000 \\ -0.7587 & -1.4631 & -0.0000 \\ -318.3944 & -408.7394 & -0.0000 \\ -0.0000 & -0.0000 & 0.9954 \end{bmatrix}, \quad L_1 = \begin{bmatrix} 120.7145 & 26.3467 & 0.0000 \\ -3.0766 & -0.6662 & -0.0000 \\ 133.0371 & 90.6119 & -0.0000 \\ -2.0359 & -0.7101 & -0.0000 \\ -751.4685 & -243.3368 & 0.0000 \\ -0.0000 & -0.0000 & -0.8690 \end{bmatrix}$$

$$\mathcal{K}_{10} = \begin{bmatrix} 0.8492 & 0.1310 & 0.0000 \\ -0.7609 & 0.6798 & -0.0000 \end{bmatrix}, \quad \mathcal{K}_{11} = \begin{bmatrix} -0.0090 & 0.0129 & -0.0000 \\ 0.0140 & -0.0240 & -0.0000 \end{bmatrix}$$

$$\mathcal{K}_{20} = \begin{bmatrix} -0.0283 & 0.7706 & 0.0000 \\ -0.1384 & -1.1604 & -0.0000 \end{bmatrix}, \quad \mathcal{K}_{21} = \begin{bmatrix} -0.0008 & -0.0060 & -0.0000 \\ 0.0008 & 0.0091 & -0.0000 \end{bmatrix}$$

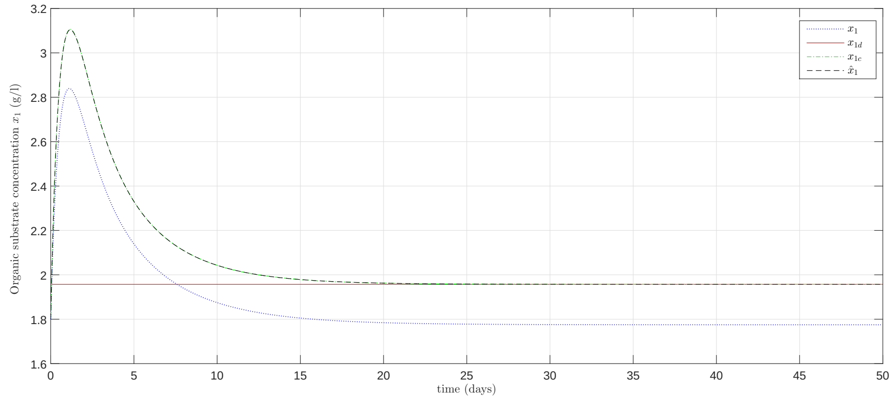

FIGURE 4.10: Organic substrate concentration x_1 (g/l).

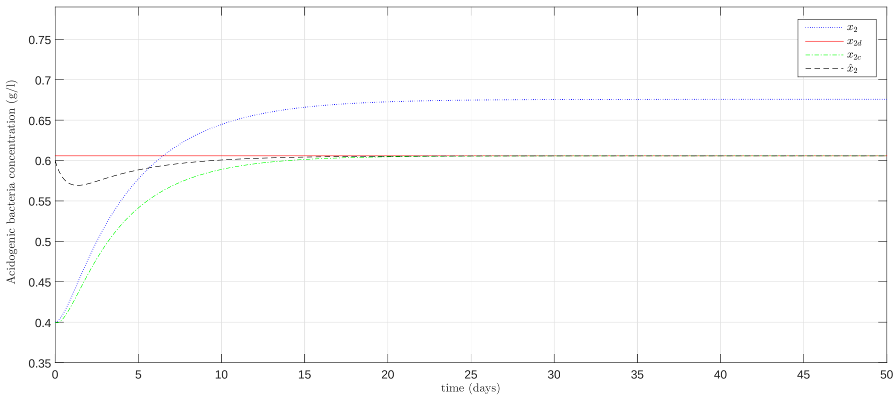

FIGURE 4.11: Acidogenic bacteria concentration (g/l).

Moreover, to run the simulation we have initialised the system as in the previous section and the observer by $\hat{x}_0 = [1.8, 0.6, 12, 0.3, 45, 55]^T$. We depict the simulation results in Figures 4.10-4.18. As it can be seen from these figures, although the large initial estimation error the observer is converging to the simulated state of the system and the closed loop system tracks the desired reference trajectory. Moreover, the behaviour of the controller remains smooth and very acceptable.

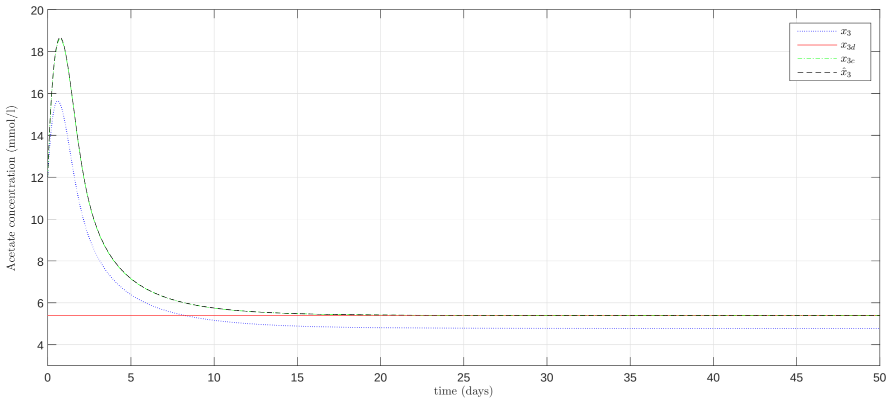

FIGURE 4.12: Acetate concentration (mmol/l).

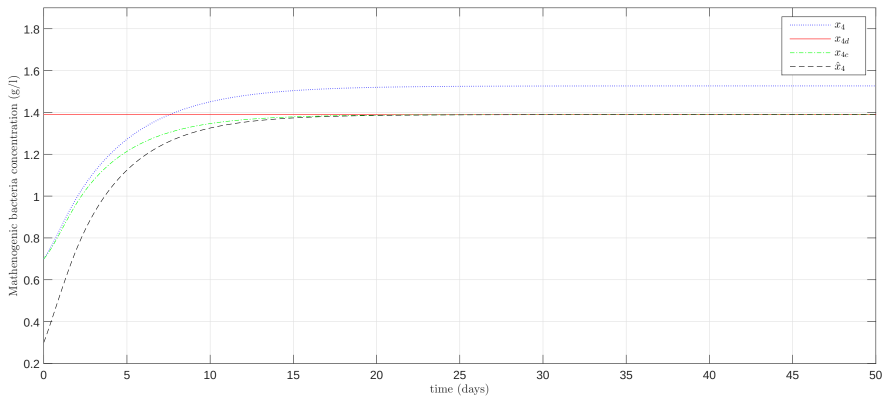

FIGURE 4.13: Mathenogenic bacteria concentration (g/l).

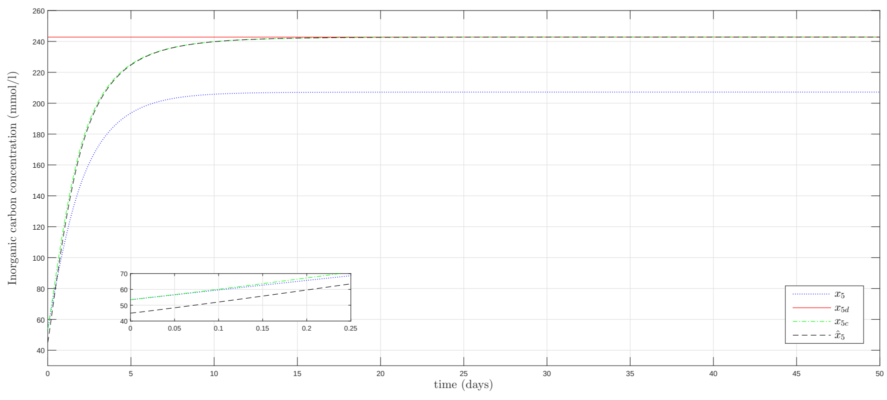

FIGURE 4.14: Inorganic carbon concentration (mmol/l).

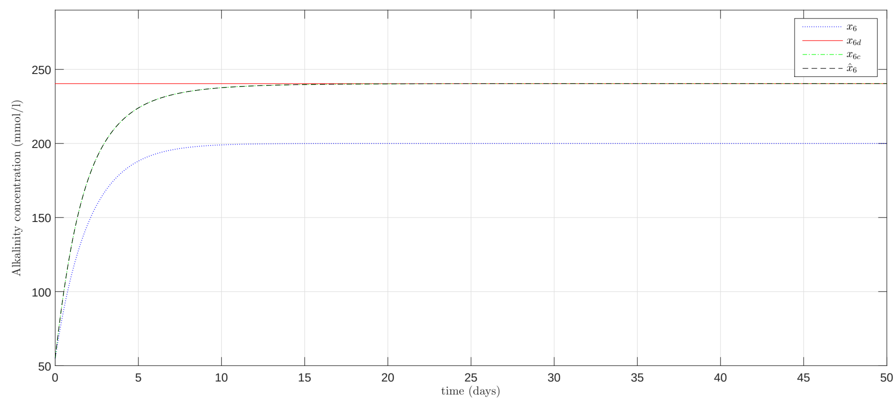

FIGURE 4.15: Alkalinity concentration (mmol/l).

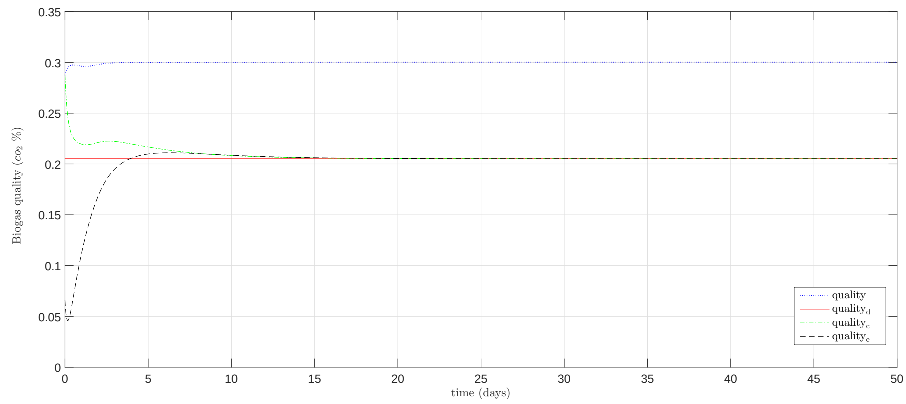

FIGURE 4.16: Biogas quality (co_2%).

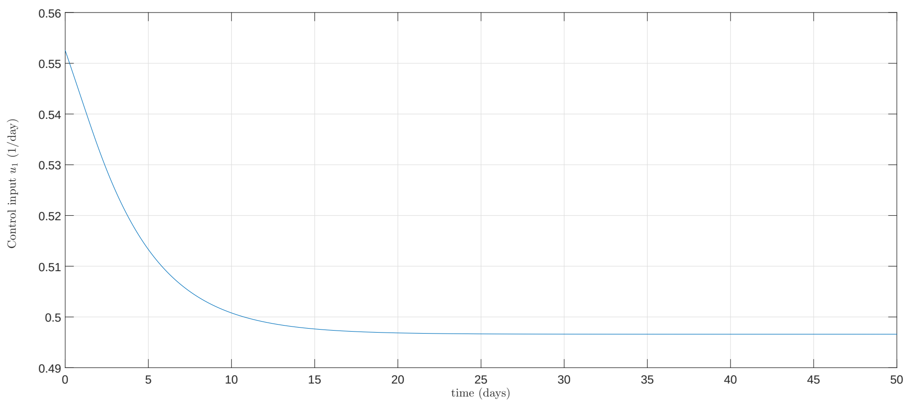

FIGURE 4.17: Control input u_1 (1/day).

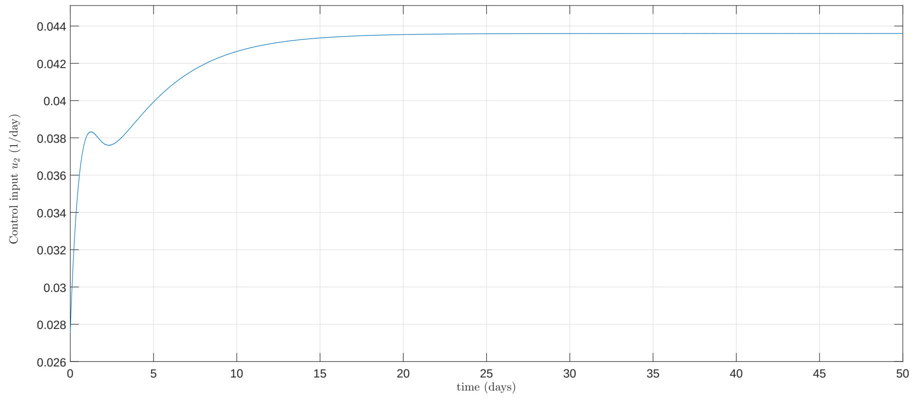

FIGURE 4.18: Control input u_2 (1/day).

4.4.2.2 Simultaneous Design

In this section, we simulate the simultaneous design approach where we compute the controller and observer parameters by solving unified LMI conditions. Hence, we solve the optimization problem (4.49) given by Theorem 14.

Using the LMI Toolbox of Matlab, the same parameter values and operating conditions as previously (Sections 4.4.1 and 4.4.2.1), we have found the LMI conditions (4.50) feasible for $\epsilon = 10$. Hence, we have obtained the following observer and control parameters

$$L_0 = \begin{bmatrix} 1941 & -7101.3 & 16.193 \\ -46.037 & 169.51 & -0.42981 \\ -7212.1 & 77611 & -194.51 \\ 6.8699 & -216.27 & 0.5592 \\ 29.072 & -65770 & 172.44 \\ 0.015661 & -0.076595 & 1.1282 \end{bmatrix}, \quad L_1 = \begin{bmatrix} -4522.5 & -1174.2 & -10.376 \\ 108.25 & 27.94 & 0.2354 \\ 81081 & 12913 & 64.577 \\ -255.86 & -36.065 & -0.13418 \\ -82473 & -10981 & -33.41 \\ -0.17246 & -0.045071 & -1.0134 \end{bmatrix}$$

$$K_0 = \begin{bmatrix} 0.0019 & 0.0061 & 0.0007 & 0.1989 & 0.0000 & -0.0004 \\ -0.0005 & -0.0017 & -0.0002 & -0.0571 & -0.0000 & 0.0004 \end{bmatrix}$$

$K_1 = 0$ and $\mu = 0.48$. After processing the simulation, we have obtained the results depicted in Figures 4.19-4.27, where we can see clearly that, although the large initial estimation error and the gap between the initial state of the simulated system and the desired reference, the controlled system is responding to the designed control and tracking the desired reference. Indeed, the observer is converging to the states of the simulated system and the later is tracking the reference. Moreover, the control is smooth and ranging in an acceptable interval of variation. Nevertheless, if we compare the results obtained by the parallel and simultaneous design approaches, we will notice that for the same initialisation and desired reference, more control efforts are required by the simultaneous design, whatever for u_1 or u_2 as it can be seen in Figure 4.28. This fact may me due to the larger values of both observer and controller gains ensuring the feasibility of the LMI conditions (4.50).

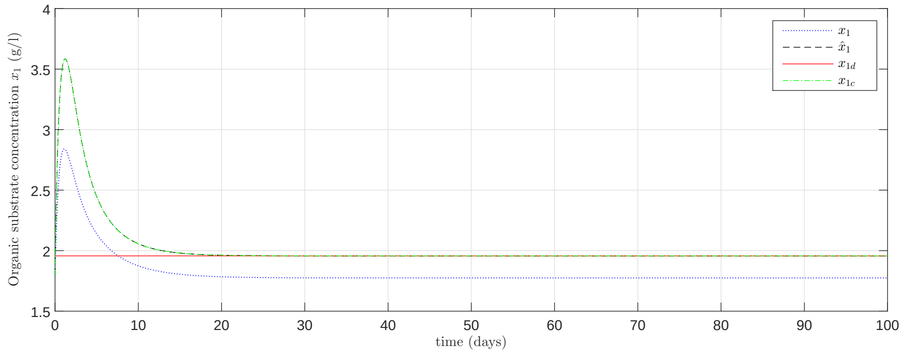

FIGURE 4.19: Organic substrate concentration x_1 (g/l).

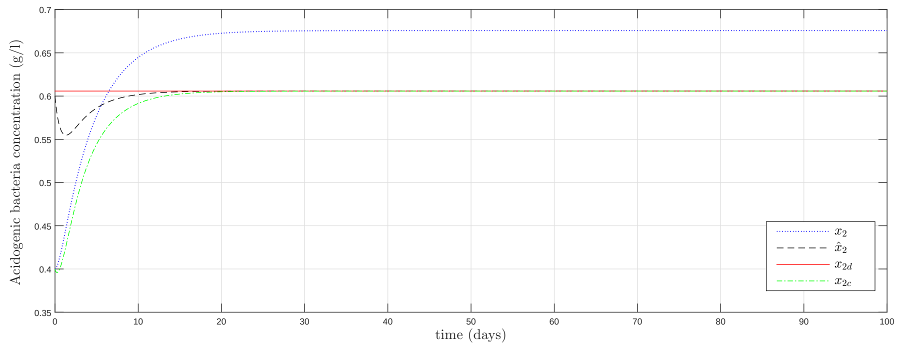

FIGURE 4.20: Acidogenic bacteria concentration (g/l).

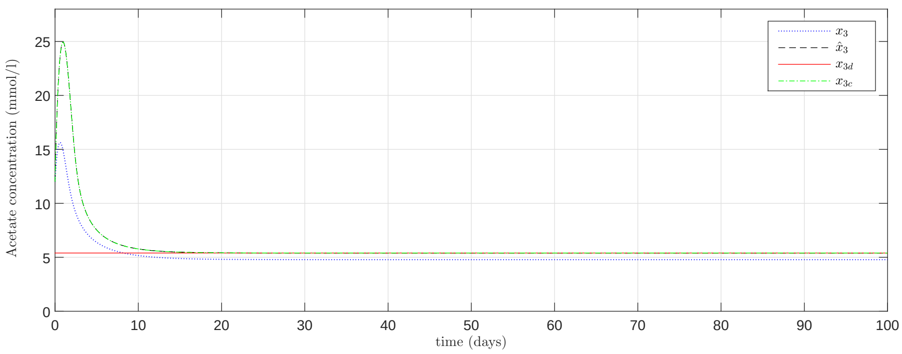

FIGURE 4.21: Acetate concentration (mmol/l).

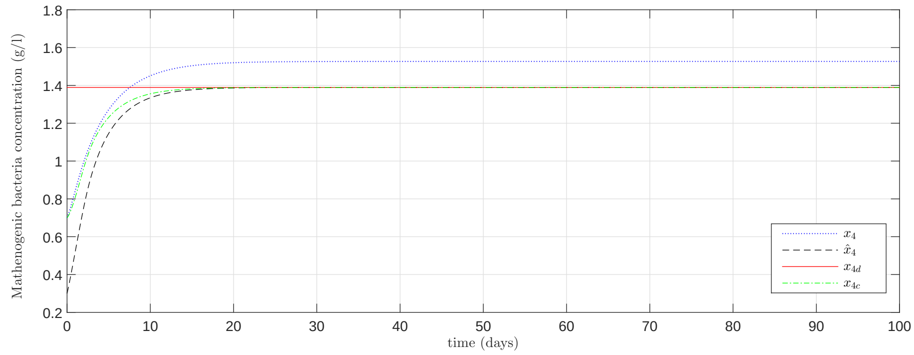

FIGURE 4.22: Mathenogenic bacteria concentration (g/l).

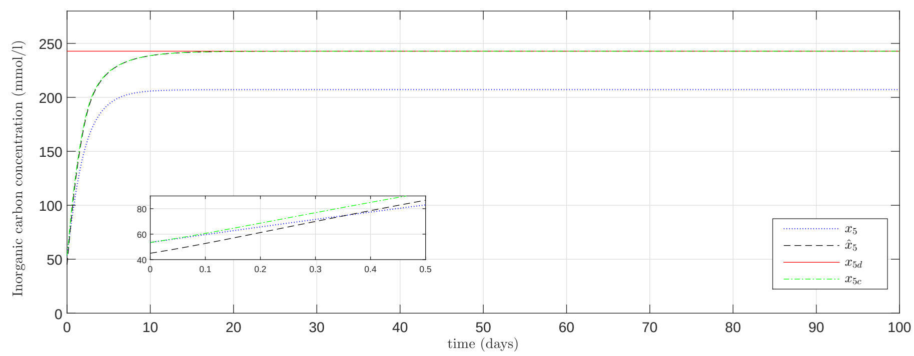

FIGURE 4.23: Inorganic carbon concentration (mmol/l).

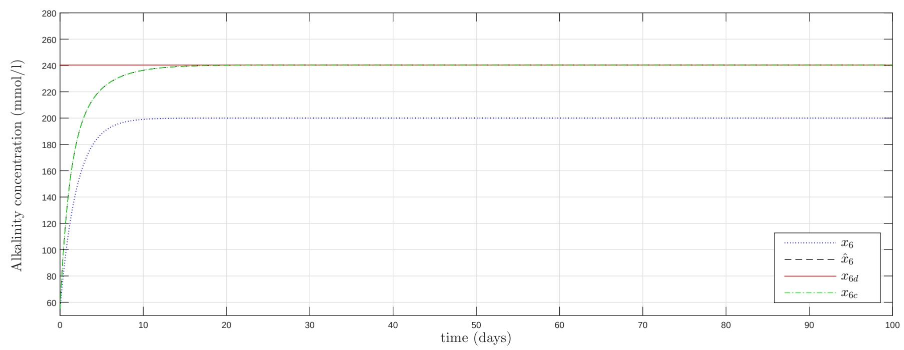

FIGURE 4.24: Alkalinity concentration (mmol/l).

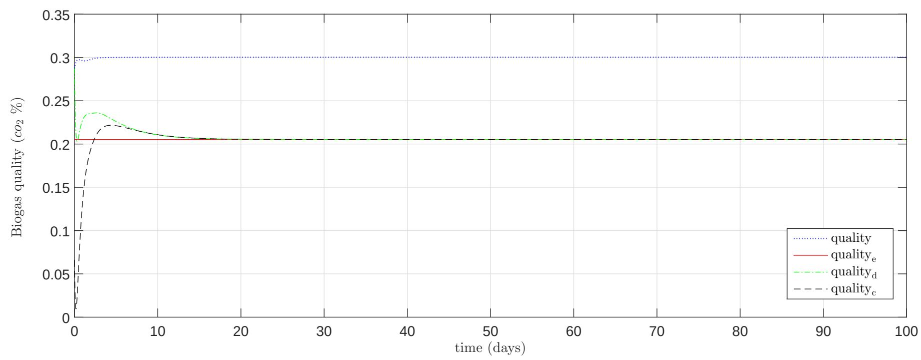

FIGURE 4.25: Biogas quality (co_2%).

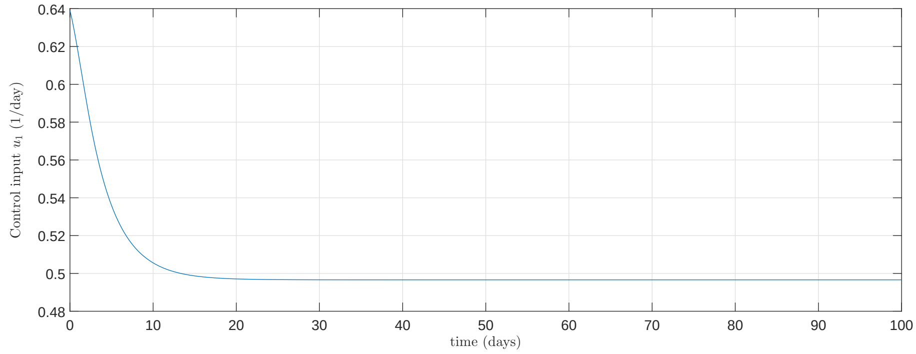

FIGURE 4.26: Control input u_1 (1/day).

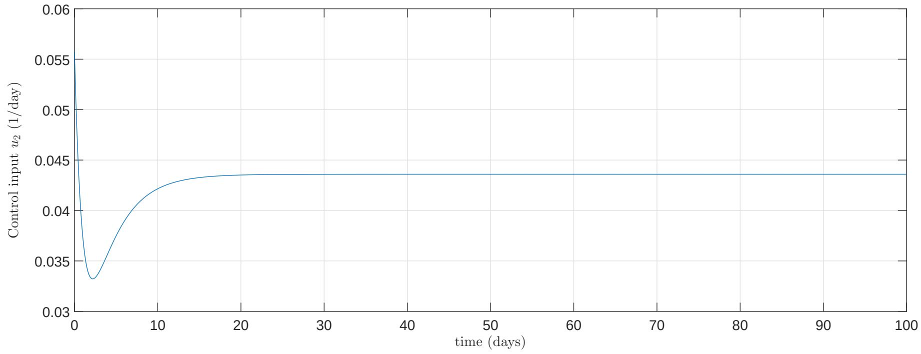

FIGURE 4.27: Control input u_2 (1/day).

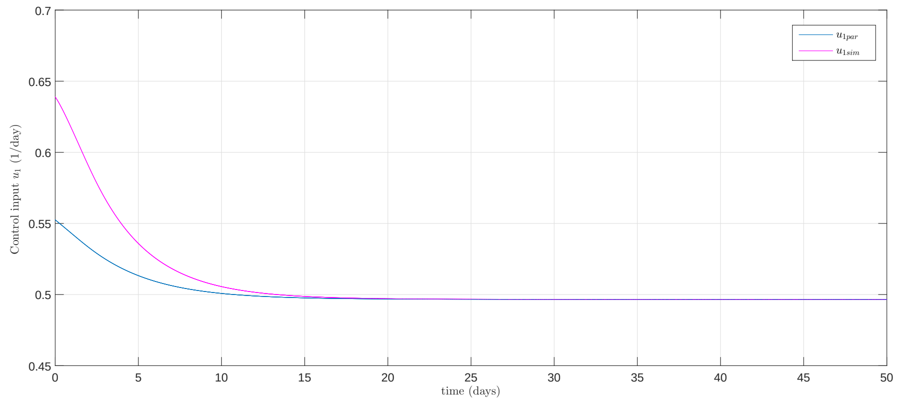

FIGURE 4.28: Control input u_1 (1/day) (*par*: parallel, *sim*: simultaneous).

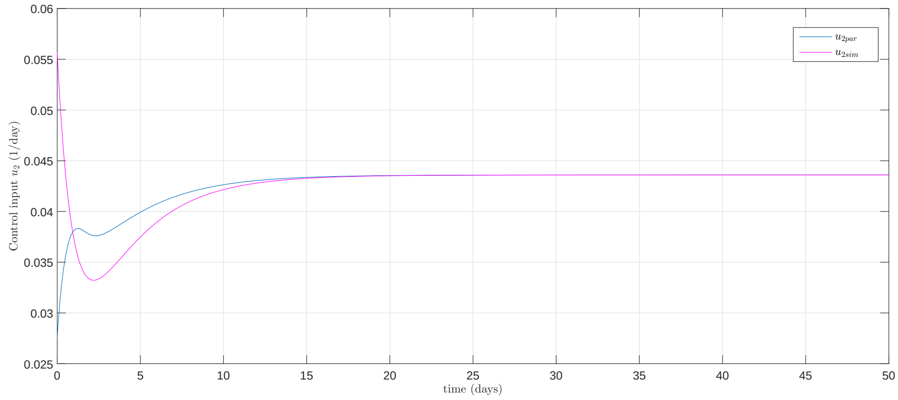

FIGURE 4.29: Control input u_2 (1/day) (*par*: parallel, *sim*: simultaneous).

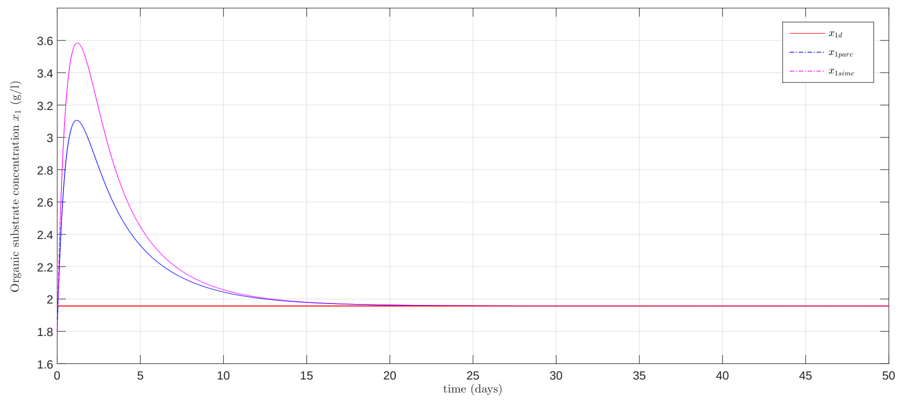

FIGURE 4.30: Organic substrate concentration x_1 (g/l) (*parc*: parallel control, *simc*: simultaneous control).

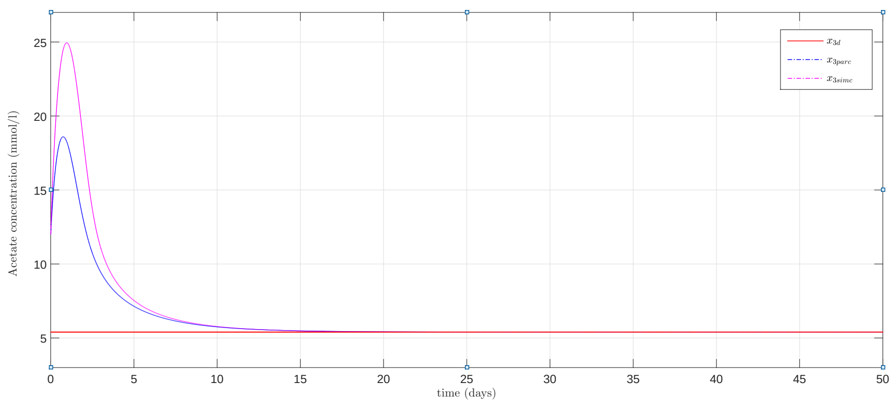

FIGURE 4.31: Acetate concentration (mmol/l) (*parc*: parallel control, *simc*: simultaneous control).

Moreover, the impact of the higher control amplitude obtained by the simultaneous design approach at the transient time is reflected of the transient response of the state variables. For example, we compare the time response of the states x_1 and x_3 obtained by the two approaches (x_{iparc} and x_{isimc} correspond to the controlled state x_i obtained by parallel and simultaneous design approach, respectively) in Figures 4.30 and 4.31, respectively. As it can be seen, the transient response of the two state variables is more aggressive when using the simultaneous design.

Finally, we conclude that both design methodologies for the observer-based feedback control allow to find appropriate observer and controller parameters which enable the system to track the desired reference. According to the simulation results, the control amplitude remains in a suitable interval of variation. However, more investigations are required to deal with the saturation of the control inputs and stability of the closed system under such saturation.

4.5 Conclusion

In this chapter, we have proposed a state feedback control to track a reference trajectory. In order to prove the stability of the closed loop system, we have provided non restrictive LMI conditions easily tractable by convex optimization algorithm. Moreover, due to the lack of monitoring that experience the AD applications, we have considered the state estimation through the inclusion of an exponential observer in the control design. In the sequel, we have provided two methodologies to find the observer and controller parameters which ensure the stability of the closed loop system (system composed from the system, controller and the observer).

We point out that the design has been done for a full state feedback control. However, it can be easily applied for partial feedback control or linear combination of the state variables by taking, for example, the tracking error $\tilde{x} = T(x - x_d)$, where T is a linear matrix of appropriate dimension. All the findings remain applicable provided to adapt the equation dimensions. Moreover, it is not difficult to investigate the case of disturbed dynamics and measurements of the system. However, further research is required to account for saturation constraints in the control inputs.

Chapter 5

General Conclusion

5.1 Summary

In this thesis, we have proposed a formal modelling framework for the AD process, which promotes the integration of biogas plants in the power grid. Actually, we have added to the AM2 model [4] two control inputs reflecting the addition of stimulating substrates. These additional control inputs add more degrees of freedom in the control of biogas production [165]. Then, we have proved the positiveness and boundedness of the model state variables. Due to this proof, we could design different types of nonlinear state observers. The design of the state observers has been presented in a general way, in order to make them usable for other applications. First, we have designed an invariant like nonlinear state observer, which was applied successfully to the proposed AD model [166]. However, due to its local properties we have proposed a more global nonlinear state observer of the same form as the Arcak's observer [157]. Moreover, to account for the disturbances affecting the model dynamics and the measurements, we have included the $\mathcal{H}_\infty$ criterion in the observer design. Because the software sensors, in real applications, are usually driven by sampled data, we have also extended the observer design to the discrete time case. Additionally, we have generalized the designed nonlinear state observers to the most encountered case in real plants: the case of nonlinear outputs.

The used technique to design of the different observers is based on the use of the DMVT which allows to transform the nonlinear dynamics of the estimation error to an LPV system. Then using the LPV techniques we have formulated the stability conditions in the form of tractable LMI conditions. In order to relax the feasibility of the synthesised LMI conditions, we have included additional decision variables in their design through the use of a suitable reformulation of the Young's inequality.

Furthermore, we have proposed a framework where in alliance with the power grid demand, the biogas plant operator can plan in timely manners for a desired evolution of the biogas production. This desired evolution is regarded as a reference trajectory for the system. Thus, we have proposed a control scheme to track that reference trajectory. To account for the non availability of the full state vector to perform the tracking control, we have combined its design with an exponential nonlinear observer. Thus, to ensure the closed loop stability we have proposed two design methodologies. In the first, the observer and the controller gains are computed separately. This method relies on the use of the Barbalat's lemma [133], [134]. While in the second method, both the observer and the controller parameters are computed simultaneously using unified LMI conditions.

5.2 Outlook

In future, it would be interesting to identify the modelling framework parameters using appropriate data collected from a real process.

Moreover, throughout Chapter 3 and Chapter 4, the input concentrations of the fed waste S_{1in}, S_{2in}, C_{in} and Z_{in} were assumed to be known and constant. It is worthwhile to extend the results for unknown or uncertain input concentrations [167], [168].

Besides, further research is required to include the saturation constraints of the manipulated variables in the control design and stability analysis. Likewise, more investigations are needed to determine the reference trajectories which allow to satisfy the power grid request. Finally, before applying the theoretical results to a real plant, it would be very interesting to analyse the finite time stability of the controlled system [169].

Appendix A

Equations of the ADM1 Model

When the system is modelled by Differential Algebraic Equations (DAE system), the resulted state space model contains 26 state variables (concentrations). It involves 19 biochemical rate processes, three gas-liquid transfer processes and additional six acid-base kinetic processes. In order to characterise the acid-base dissociation in aquatic systems, each of Volatile Fatty Acids (VFAs), inorganic carbon (IC) and inorganic nitrogen (IN) states are split into two components. Dynamics of the biodegradable organic matter included in the ADM1 are summarized in the subsequent sections. The complete Petersen matrix describing the liquid phase reactions is depicted in Figures A.1 and A.2, and for more details we refer the reader to [2], [3] and [37].

A.1 Liquid Phase Equations

A.1.1 Soluble Matter

$$\frac{dS_v}{dt} = \frac{q_{in}}{V}(S_{su,in} - S_{su}) + \rho_2 + (1 - f_{fa,li}\rho_4) - \rho_5 \tag{A.1}$$

$$\frac{dS_a}{dt} = \frac{q_{in}}{V}(S_{aa,in} - S_{aa}) + \rho_3 - \rho_6 \tag{A.2}$$

$$\frac{dS_{fa}}{dt} = \frac{q_{in}}{V}(S_{fa,in} - S_{fa}) + f_{fa,li}\rho_4 - \rho_7 \tag{A.3}$$

$$\frac{dS_{va}}{dt} = \frac{q_{in}}{V}(S_{va,in} - S_{va}) + (1 - Y_{aa})f_{va,aa}\rho_6 - \rho_8 \tag{A.4}$$

$$\frac{dS_{bu}}{dt} = \frac{q_{in}}{V}(S_{bu,in} - S_{bu}) + (1 - Y_{aa})f_{bu,su}\rho_5 + (1 - Y_{aa})f_{va,aa}\rho_6 - \rho_9 \tag{A.5}$$

$$\begin{aligned}\frac{dS_{pro}}{dt} &= \frac{q_{in}}{V}(S_{pro,in} - S_{pro}) + (1 - Y_{su})f_{pro,su}\rho_5 + (1 - Y_{aa})f_{pro}\rho_6 \\ &\quad +(1 - Y_{c_4})0.54\rho_8 - \rho_{10}\end{aligned} \tag{A.6}$$

$$\begin{aligned}\frac{dS_{ac}}{dt} &= \frac{q_{in}}{V}(S_{ac,in} - S_{ac}) + (1 - Y_{su})f_{ac,su}\rho_5 + (1 - Y_{aa})f_{ac,aa}\rho_6 \\ &\quad +(1 - Y_{fa})0.7\rho_7 + (1 - Y_{c_4})0.31\rho_8\rho_9 + (1 - Y_{aa})0.57\rho_{10} - \rho_{11}\end{aligned} \tag{A.7}$$

$$\begin{aligned}\frac{dS_{h_2}}{dt} &= \frac{q_{in}}{V}(S_{h_2,in} - S_{h_2}) + (1 - Y_{su})f_{h_2,su}\rho_5 + (1 - Y_{aa})f_{h_2,aa}\rho_6 - \rho_{T,h_2} \\ &\quad +(1 - Y_{fa})0.3\rho_7 + (1 - Y_{c_4})0.2\rho_9 + (1 - Y_{pro})0.43\rho_{10} - \rho_{12}\end{aligned} \tag{A.8}$$

$$\frac{dS_{ch_4}}{dt} = \frac{q_{in}}{V}(S_{ch_4,in} - S_{ch_4}) + (1 - Y_{ac})\rho_{11} + (1 - Y_{h_2})\rho_{12} - \rho_{T,ch_4} \tag{A.9}$$

$$\frac{dS_{IC}}{dt} = \frac{q_{in}}{V}(S_{IC,in} - S_{IC}) + \sum_{j=1}^{19}\left(\sum_{i=1-9,11-14} C_i\nu_{i,j}\rho_j\right) - \rho_{T,co_2} \tag{A.10}$$

$$\begin{aligned}\frac{dS_{IN}}{dt} &= \frac{q_{in}}{V}(S_{IN,in} - S_{IN}) - Y_{su}N_{bac}\rho_5 + (N_{aa} - Y_{aa}N_{bac})\rho_6 - Y_{fa}N_{bac}\rho_7 \\ &\quad -Y_{c_4}N_{bac}\rho_8 - Y_{c_4}N_{bac}\rho_9 - Y_{pro}N_{bac}\rho_{10} - Y_{ac}N_{bac}\rho_{11} - Y_{h_2}N_{bac}\rho_{12} \\ &\quad +(N_{bac} - N_{xc})\sum_{i=13}^{19}\rho_i + (N_{xc} - f_{xi,xc}NI - f_{si,xc}NI - f_{pr,xc}N_{aa})\rho_1\end{aligned} \tag{A.11}$$

$$\frac{dS_I}{dt} = \frac{q_{in}}{V}(S_{I,in} - S_I) + f_{SI,xc}\rho_1 \tag{A.12}$$

where

$$\sum_{j=1}^{19}\left(\sum_{i=1-9,11-14} C_i\nu_{i,j}\rho_j\right) = \sum_{k=1}^{12} s_k\rho_k + s_{13}\left(\rho_{13} + \rho_{14} + \rho_{15} + \rho_{16} + \rho_{17} + \rho_{18} + \rho_{19}\right) \tag{A.13}$$

with

$$s_1 = -C_{xc} + f_{si,xc}C_{si} + f_{ch,xc}C_{ch} + f_{pr,xc}C_{pr} + f_{li,xc}C_{li} + f_{xi,xc}C_{xi} \tag{A.14}$$

$$s_2 = -C_{ch} + C_{su} \tag{A.15}$$

$$s_3 = -C_{pr} + C_{aa} \tag{A.16}$$

$$s_4 = -C_{li} + 1 - f_{fa,li}C_{su} + f_{fa,li}C_{fa} \tag{A.17}$$

$$s_5 = -C_{su} + (1 - Y_{su})\,(f_{bu,su}C_{bu} + f_{pro,su}C_{pro} + f_{ac,su}C_{ac}) + Y_{su}C_{bac} \tag{A.18}$$

$$s_6 = -C_{aa} + (1 - Y_{aa})\,(f_{va,aa}C_{va} + f_{bu,aa}C_{bu} + f_{pro,aa}C_{pro} + f_{ac,aa}C_{ac}) + Y_{aa}C_{bac} \tag{A.19}$$

$$s_7 = -C_{fa} + (1 - Y_{fa})\,0.7C_{ac} + Y_{fa}C_{bac} \tag{A.20}$$

$$s_8 = -C_{va} + (1 - Y_{c4})\,0.54C_{pro} + (1 - Y_{c4})\,0.31C_{ac} + Y_{c4}C_{bac} \tag{A.21}$$

$$s_9 = -C_{bu}\,(1 - Y_{c4})\,0.8C_{ac} + Y_{c4}C_{bac} \tag{A.22}$$

$$S_{10} = -C_{pro} + (1 - Y_{pro})\,0.57C_{ac} + Y_{pro}C_{bac} \tag{A.23}$$

$$s_{11} = -C_{ac} + (1 - Y_{ac})\,C_{ch4} + Y_{ac}C_{bac} \tag{A.24}$$

$$s_{12} = (1 - Y_{h2})\,C_{ch4} + Y_{ac}C_{bac} \tag{A.25}$$

$$s_{13} = -C_{bac} + C_{xc} \tag{A.26}$$

A.1.2 Particulate Matter

$$\frac{dX_c}{dt} = \frac{q_{in}}{V}(X_{c,in} - X_c) - \rho_1 + \sum_{i=13}^{19} \rho_i \quad \text{(A.27)}$$

$$\frac{dX_{ch}}{dt} = \frac{q_{in}}{V}(X_{ch,in} - X_{ch}) + fch, xc\rho_1 - \rho_2 \quad \text{(A.28)}$$

$$\frac{dX_{pr}}{dt} = \frac{q_{in}}{V}(X_{pr,in} - X_{pr}) + fpr, xc\rho_1 - \rho_3 \quad \text{(A.29)}$$

$$\frac{dX_{li}}{dt} = \frac{q_{in}}{V}(X_{li,in} - X_{li}) + fli, xc\rho_1 - \rho_4 \quad \text{(A.30)}$$

$$\frac{dX_{su}}{dt} = \frac{q_{in}}{V}(X_{su,in} - X_{su}) + Y_{su}\rho_5 - \rho_{13} \quad \text{(A.31)}$$

$$\frac{dX_{aa}}{dt} = \frac{q_{in}}{V}(X_{aa,in} - X_{aa}) + Y_{aa}\rho_6 - \rho_{14} \quad \text{(A.32)}$$

$$\frac{dX_{fa}}{dt} = \frac{q_{in}}{V}(X_{fa,in} - X_{fa}) + Y_{fa}\rho_7 - \rho_{15} \quad \text{(A.33)}$$

$$\frac{dX_{pro}}{dt} = \frac{q_{in}}{V}(X_{pro,in} - X_{pro}) + Y_{pro}\rho_{10} + Y_{ch}\rho_8 + Y_{c_4}\rho_8 - \rho_{16} \quad \text{(A.34)}$$

$$\frac{dX_a}{dt} = \frac{q_{in}}{V}(X_{a,in} - X_a) + Y_{ac}\rho_{11} - \rho_{18} \quad \text{(A.35)}$$

$$\frac{dX_{h_2}}{dt} = \frac{q_{in}}{V}(X_{h_2,in} - X_{h_2}) + Y_{ac}\rho_{11} - \rho_{19} \quad \text{(A.36)}$$

$$\frac{dX_I}{dt} = \frac{q_{in}}{V}(X_{I,in} - X_I) + f_{xI,xc}\rho_1 \quad \text{(A.37)}$$

A.2 Process Rates

A.2.1 Hydrolysis Rates

$$\rho_1 = k_{dis}.X_c \quad \text{(A.38)}$$

$$\rho_2 = k_{hyd,ch}.X_{ch} \quad \text{(A.39)}$$

$$\rho_3 = k_{hyd,pr}.X_{pr} \quad \text{(A.40)}$$

$$\rho_4 = k_{hyd,li}.X_{li} \quad \text{(A.41)}$$

A.2.2 Uptake Rates

$$\rho_5 = k_{m,su} \cdot \frac{S_{su}}{K_{S,su} + S_{su}} . X_{su} . I_5 \tag{A.42}$$

$$\rho_6 = k_{m,aa} \cdot \frac{S_{aa}}{K_{S,aa} + S_{aa}} . X_{aa} . I_6 \tag{A.43}$$

$$\rho_7 = k_{m,fa} \cdot \frac{S_{fa}}{K_{S,fa} + S_{fa}} . X_{fa} . I_7 \tag{A.44}$$

$$\rho_8 = k_{m,c_4} \cdot \frac{S_{va}}{K_{S,c_4} + S_{va}} . X_{c_4} \cdot \frac{1}{1 + \frac{S_{bu}}{S_{va}}} . I_8 \tag{A.45}$$

$$\rho_9 = k_{m,c_4} \cdot \frac{S_{bu}}{K_{S,c_4} + S_{bu}} . X_{c_4} \cdot \frac{1}{1 + \frac{S_{va}}{S_{bu}}} . I_9 \tag{A.46}$$

$$\rho_{10} = k_{m,pr} \cdot \frac{S_{pro}}{K_{S,pro} + S_{pro}} . X_{pro} . I_{10} \tag{A.47}$$

$$\rho_{11} = k_{m,ac} \cdot \frac{S_{ac}}{K_{S,ac} + S_{ac}} . X_{ac} . I_{11} \tag{A.48}$$

$$\rho_{12} = k_{m,h_2} \cdot \frac{S_{h_2}}{K_{S,h_2} + S_{h_2}} . X_{h_2} . I_{12} \tag{A.49}$$

A.2.3 Decay Rates

$$\rho_{13} = k_{dec,X_{su}} . X_{su} \tag{A.50}$$

$$\rho_{14} = k_{dec,X_{aa}} . X_{aa} \tag{A.51}$$

$$\rho_{15} = k_{dec,X_{fa}} . X_{fa} \tag{A.52}$$

$$\rho_{16} = k_{dec,X_{c_4}} . X_{c_4} \tag{A.53}$$

$$\rho_{17} = k_{dec,X_{pr}} . X_{pr} \tag{A.54}$$

$$\rho_{18} = k_{dec,X_{ac}} . X_{ac} \tag{A.55}$$

$$\rho_{19} = k_{dec,X_{h_2}} . X_{h_2} \tag{A.56}$$

A.2.4 Process Inhibitions

$$I_{5,6} = I_{pH,aa}.I_{IN,lim} \tag{A.57}$$

$$I_{7} = I_{pH,fa}.I_{IN,lim}.I_{h_2,fa} \tag{A.58}$$

$$I_{8,9} = I_{pH,aa}.I_{IN,lim}.I_{h_2,c_4} \tag{A.59}$$

$$I_{10} = I_{pH,aa}.I_{IN,lim}.I_{h_2,pro} \tag{A.60}$$

$$I_{11} = I_{pH,ac}.I_{IN,lim}.I_{NH_3} \tag{A.61}$$

$$I_{12} = I_{pH,h_2}.I_{IN,lim} \tag{A.62}$$

$$I_{pH,aa} = \begin{cases} \exp\left(-3\left(\frac{pH-pH_{UL,aa}}{pH_{UL,aa}-pH_{LL,aa}}\right)^2\right) & pH < pH_{UL,aa} \\ 1 & pH > pH_{UL,aa} \end{cases} \tag{A.63}$$

$$I_{pH,ac} = \begin{cases} \exp\left(-3\left(\frac{pH-pH_{UL,ac}}{pH_{UL,ac}-pH_{LL,ac}}\right)^2\right) & pH < pH_{UL,ac} \\ 1 & pH > pH_{UL,ac} \end{cases} \tag{A.64}$$

$$I_{pH,h_2} = \begin{cases} \exp\left(-3\left(\frac{pH-pH_{UL,h_2}}{pH_{UL,h_2}-pH_{LL,h_2}}\right)^2\right) & pH < pH_{UL,h_2} \\ 1 & pH > pH_{UL,h_2} \end{cases} \tag{A.65}$$

$$I_{IN,lim} = \frac{1}{1+\frac{K_{s,IN}}{S_{IN}}} \tag{A.66}$$

$$I_{h_2,fa} = \frac{1}{1+\frac{S_{h_2}}{K_{I,h_2,fa}}} \tag{A.67}$$

$$I_{h_2,c_8} = \frac{1}{1+\frac{S_{h_2}}{K_{I,h_2,c_4}}} \tag{A.68}$$

$$I_{h_2,pro} = \frac{1}{1+\frac{S_{h_2}}{K_{I,h_2,pro}}} \tag{A.69}$$

$$I_{NH_3} = \frac{1}{1+\frac{S_{NH_3}}{K_{I,NH_3}}} \tag{A.70}$$

A.3 Acid-base Dissociation

In order to characterize the acid-base dissociation in aquatic systems, the VFAs, inorganic carbon (IC) and inorganic nitrogen (IN) are split into two components, free and ionic forms:

$$S_{Cat^+} + S_{NH_4^+} + S_{H^+} - S_{HCO_3^-} - \frac{S_{ac^-}}{64} - \frac{S_{pro^-}}{112} - \frac{S_{bu^-}}{160} - \frac{S_{va^-}}{208} - S_{OH^-} - S_{An^-} = 0 \tag{A.71}$$

with

$$S_{OH^-} - \frac{K_w}{S_{H^+}} = 0 \tag{A.72}$$

$$S_{va^-} - \frac{K_{a,va}.S_{va,total}}{K_{a,va} + S_{H^+}} = 0 \tag{A.73}$$

$$S_{bu^-} - \frac{K_{a,bu}.S_{va,total}}{K_{a,bu} + S_{H^+}} = 0 \tag{A.74}$$

$$S_{pro^-} - \frac{K_{a,bu}.S_{pro,total}}{K_{a,bu} + S_{H^+}} = 0 \tag{A.75}$$

$$S_{HCO_3^-} - \frac{K_{a,co_2}.S_{IC}}{K_{a,co_2} + S_{H^+}} = 0 \tag{A.76}$$

$$S_{IN} - S_{NH_3} - S_{NH_4^+} = 0 \tag{A.77}$$

$$S_{IC} - S_{co_2} - S_{HCO_3^-} = 0 \tag{A.78}$$

A.4 Liquid/ gas Transfer

$$\rho_{T,h_2} = k_{La}(S_{liq,h_2} - 16K_{h,h_2}P_{gas,h_2}) \tag{A.79}$$

$$\rho_{T,ch_4} = k_{La}(S_{liq,ch_4} - 64K_{h,ch_4}P_{gas,ch_4}) \tag{A.80}$$

$$\rho_{T,IC} = k_{La}(S_{liq,co_2} - K_{h,co_2}P_{gas,co_2}) \tag{A.81}$$

To pass from concentrations to pressures, the ideal gas low is used $P = SRT$ where S is the concentration in $KgCODm^{-3}$.

Gas phase equations are similar to the liquid phase equations except that there is no additive influent flow

$$\frac{dS_{gas,i}}{dt} = \frac{-S_{gas,i}q_{gas}}{V_{gas}} + \rho_{T,i}\frac{V_{liq}}{V_{gas}} \tag{A.82}$$

$$P_{gas,h_2} = S_{gas,h_2}\frac{RT}{16} \tag{A.83}$$

$$P_{gas,ch_4} = S_{gas,ch_4}\frac{RT}{64} \tag{A.84}$$

$$P_{gas,co_2} = S_{gas,co_2}RT \tag{A.85}$$

The reactor head space is assumed to be water vapour saturated, the P_{gas,H_2O} is given by the following equation:

$$P_{gas,H_2O} = 0,013exp\left(5290\left(\frac{1}{298} - \frac{1}{T}\right)\right) \tag{A.86}$$

and if the total pressure is constant $P_{gas} = 1,013\ bar$, so

$$q_{gas} = \frac{RT}{P_{gas} - P_{gas,H_2O}}V_{liq}\left(\frac{\rho_{T,h_2}}{16} + \frac{\rho_{T,ch_4}}{64} + \rho_{T,co_2}\right) \tag{A.87}$$

else

$$P_{gas} = P_{gas,h_2} + P_{gas,ch_4} + P_{gas,co_2} + P_{gas,H_2O} \tag{A.88}$$

and

$$q_{gas} = K_p(P_{gas} - P_{atm}) \tag{A.89}$$

where K_p is the pipe resistance (m^3d^{-1}bar) and P_{atm} is the external atmospheric pressure.

A.5 Gas Phase Equations

$$\frac{dS_{gas,h_2}}{dt} = \frac{-S_{gas,h_2}q_{gas}}{V_{gas}} + \rho_{T,h_2}\frac{V_{liq}}{V_{gas}} \tag{A.90}$$

$$\frac{dS_{gas,ch_4}}{dt} = \frac{-S_{gas,ch_4}q_{gas}}{V_{gas}} + \rho_{T,ch_4}\frac{V_{liq}}{V_{gas}} \tag{A.91}$$

$$\frac{dS_{gas,co_2}}{dt} = \frac{-S_{gas,co_2}q_{gas}}{V_{gas}} + \rho_{T,co_2}\frac{V_{liq}}{V_{gas}} \tag{A.92}$$

j	Component → i / Process ↓	1 S_{su}	2 S_{aa}	3 S_{fa}	4 S_{va}	5 S_{bu}	6 S_{pro}	7 S_{ac}	8 S_{h2}	9 S_{ch4}	10 S_{IC}	11 S_{IN}	12 S_I	Rate (ρ_j, kg COD.m^{-3}.d^{-1})
1	Disintegration												$f_{sI,xc}$	$k_{dis}X_c$
2	Hydrolysis carbohydrates	1												$k_{hyd,ch}X_{ch}$
3	Hydrolysis of proteins		1											$k_{hyd,pr}X_{pr}$
4	Hydrolysis of lipids	$1\text{-}f_{fa,li}$		$1\text{-}f_{fa,li}$										$k_{hyd,li}X_{li}$
5	Uptake of sugars	−1				$(1\text{-}Y_{su})f_{bu,su}$	$(1\text{-}Y_{su})f_{pro,su}$	$(1\text{-}Y_{su})f_{ac,su}$	$(1\text{-}Y_{su})f_{h2,su}$		$-\sum_{i=9,11-24} C_i v_{i,5}$	$-(Y_{su})N_{bac}$		$k_{m,su}\frac{S_{su}}{K_S+S}X_{su}I_1$
6	Uptake of amino acids		−1		$(1\text{-}Y_{aa})f_{va,aa}$	$(1\text{-}Y_{aa})f_{bu,aa}$	$(1\text{-}Y_{aa})f_{pro,aa}$	$(1\text{-}Y_{aa})f_{ac,aa}$	$(1\text{-}Y_{aa})f_{h2,aa}$		$-\sum_{i=1-9,11-24} C_i v_{i,6}$	$N_{aa}-(Y_{aa})N_{bac}$		$k_{m,aa}\frac{S_{aa}}{K_S+S_{aa}}X_{aa}I_1$
7	Uptake of LCFA			−1				$(1\text{-}Y_{fa})\ 0.7$	$(1\text{-}Y_{fa})\ 0.3$			$-(Y_{fa})N_{bac}$		$k_{m,fa}\frac{S_{fa}}{K_S+S_{fa}}X_{fa}I_2$
8	Uptake of valerate				−1		$(1\text{-}Y_{c4})\ 0.54$	$(1\text{-}Y_{c4})\ 0.31$	$(1\text{-}Y_{c4})\ 0.15$			$-(Y_{c4})N_{bac}$		$k_{m,c4}\frac{S_{va}}{K_S+S_{va}}X_{c4}\frac{1}{1+S_{bu}/S_{va}}I$
9	Uptake of butyrate					−1		$(1\text{-}Y_{c4})\ 0.8$	$(1\text{-}Y_{c4})\ 0.2$			$-(Y_{c4})N_{bac}$		$k_{m,c4}\frac{S_{bu}}{K_S+S_{bu}}X_{c4}\frac{1}{1+S_{va}/S_{bu}}I$
10	Uptake of propionate						−1	$(1\text{-}Y_{pro})\ 0.57$	$(1\text{-}Y_{pro})\ 0.43$		$-\sum_{i=1-9,11-24} C_i v_{i,10}$	$-(Y_{pro})N_{bac}$		$k_{m,pr}\frac{S_{pro}}{K_S+S_{pro}}X_{pro}I_2$
11	Uptake of acetate							−1		$(1\text{-}Y_{ac})$	$-\sum_{i=1-9,11-24} C_i v_{i,11}$	$-(Y_{ac})N_{bac}$		$k_{m,ac}\frac{S_{ac}}{K_S+S_{ac}}X_{ac}I_3$
12	Uptake of hydrogen								−1	$(1\text{-}Y_{h2})$	$-\sum_{i=1-9,11-24} C_i v_{i,12}$	$-(Y_{h2})N_{bac}$		$k_{m,h2}\frac{S_{h2}}{K_S+S_{h2}}X_{h2}I_1$
13	Decay of X_{su}													$k_{dec,Xsu}X_{su}$
14	Decay of X_{aa}													$k_{dec,Xaa}X_{aa}$
15	Decay of X_{fa}													$k_{dec,Xfa}X_{fa}$
16	Decay of X_{c4}													$k_{dec,Xc4}X_{c4}$
17	Decay of X_{pro}													$k_{dec,Xpro}X_{pro}$
18	Decay of X_{ac}													$k_{dec,Xac}X_{ac}$
19	Decay of X_{h2}													$k_{dec,Xh2}X_{h2}$
		Monosaccharides (kgCOD·m^{-3})	Amino acids (kgCOD·m^{-3})	Long chain fatty acids (kgCOD·m^{-3})	Total valerate (kgCOD·m^{-3})	Total butyrate (kgCOD·m^{-3})	Total propionate (kgCOD·m^{-3})	Total acetate (kgCOD·m^{-3})	Hydrogen gas (kgCOD·m^{-3})	Methane gas (kgCOD·m^{-3})	Inorganic carbon (kmoleC·m^{-3})	Inorganic nitrogen (kmoleN·m^{-3})	Soluble inerts (kgCOD·m^{-3})	Inhibition factors: $I_1 = I_{pH} I_{IN,lim}$; $I_2 = I_{pH} I_{IN,lim} I_{h2}$; $I_3 = I_{pH} I_{IN,lim} I_{NH3,Xac}$

FIGURE A.1: Biochemical rate coefficients ($\nu_{i,j}$) and kinetic rate equations (ρ_j) for soluble components ($i = 1$–12, $j = 1$–19) [3].

	Component → i	13	14	15	16	17	18	19	20	21	22	23	24	Rate (ρ_j, kg COD.m^{-3}.d^{-1})
j	Process ↓	X_c	X_{ch}	X_{pr}	X_{li}	X_{su}	X_{aa}	X_{fa}	X_{c4}	X_{pro}	X_{ac}	X_{h2}	X_I	
1	Disintegration	-1	$f_{ch,xc}$	$f_{pr,xc}$	$f_{li,xc}$								$f_{xI,xc}$	$k_{dis}X_c$
2	Hydrolysis carbohydrates		-1											$k_{hyd,ch}X_{ch}$
3	Hydrolysis of proteins			-1										$k_{hyd,pr}X_{pr}$
4	Hydrolysis of lipids				-1									$k_{hyd,li}X_{li}$
5	Uptake of sugars					Y_{su}								$k_{m,su}\frac{S_{su}}{K_S+S}X_{su}I_1$
6	Uptake of amino acids						Y_{aa}							$k_{m,aa}\frac{S_{aa}}{K_S+S_{aa}}X_{aa}I_1$
7	Uptake of LCFA							Y_{fa}						$k_{m,fa}\frac{S_{fa}}{K_S+S_{fa}}X_{fa}I_2$
8	Uptake of valerate								Y_{c4}					$k_{m,c4}\frac{S_{va}}{K_S+S_{va}}X_{c4}\frac{1}{1+S_{bu}/S_{va}}I$
9	Uptake of butyrate								Y_{c4}					$k_{m,c4}\frac{S_{bu}}{K_S+S_{bu}}X_{c4}\frac{1}{1+S_{va}/S_{bu}}I$
10	Uptake of propionate									Y_{pro}				$k_{m,pr}\frac{S_{pro}}{K_S+S_{pro}}X_{pro}I_2$
11	Uptake of acetate										Y_{ac}			$k_{m,ac}\frac{S_{ac}}{K_S+S_{ac}}X_{ac}I_3$
12	Uptake of hydrogen											Y_{h2}		$k_{m,h2}\frac{S_{h2}}{K_S+S_{h2}}X_{h2}I_1$
13	Decay of X_{su}	1				-1								$k_{dec,Xsu}X_{su}$
14	Decay of X_{aa}	1					-1							$k_{dec,Xaa}X_{aa}$
15	Decay of X_{fa}	1						-1						$k_{dec,Xfa}X_{fa}$
16	Decay of X_{c4}	1							-1					$k_{dec,Xc4}X_{c4}$
17	Decay of X_{pro}	1								-1				$k_{dec,Xpro}X_{pro}$
18	Decay of X_{ac}	1									-1			$k_{dec,Xac}X_{ac}$
19	Decay of X_{h2}	1										-1		$k_{dec,Xh2}X_{h2}$
		Composites (kgCOD·m^{-3})	Carbohydrates (kgCOD·m^{-3})	Proteins (kgCOD·m^{-3})	Lipids (kgCOD·m^{-3})	Sugar degraders (kgCOD·m^{-3})	Amino acid degraders (kgCOD·m^{-3})	LCFA degraders (kgCOD·m^{-3})	Valerate and butyrate degraders (kgCOD·m^{-3})	Propionate degraders (kgCOD·m^{-3})	Acetate degraders (kgCOD·m^{-3})	Hydrogen degraders (kgCOD·m^{-3})	Particulate inerts (kgCOD·m^{-3})	Inhibition factors: $I_1 = I_{pH} I_{IN,lim}$; $I_2 = I_{pH} I_{IN,lim} \cdot I_{h2}$; $I_3 = I_{pH} I_{IN,lim} \cdot I_{NH3,Xac}$

FIGURE A.2: Biochemical rate coefficients ($\nu_{i,j}$) and kinetic rate equations (ρ_j) for soluble components ($i = 13$–24, $j = 1$–19) [3].

Appendix B

Interface between the ADM1 and the Reduced Model

Interface between the ADM1 variables and the reduced model AM2 as given in [145]:

$$
\begin{aligned}
&x_1 = S_{su} + S_{aa} + S_{fa} + X_c + X_{ch} + X_{pr} + X_{li} \\
&x_2 = (X_{su} + X_{aa} + X_{fa})/1.55 \\
&x_3 = \left(\tfrac{S_{va}}{208} + \tfrac{S_{bu}}{160} + \tfrac{S_{pro}}{112} + \tfrac{S_{ac}}{64}\right).1000 \\
&x_4 = (X_{ac} + X_{h2} + X_{c4} + X_{pro})/1.55 \\
&x_5 = S_{ic}.1000 \\
&x_6 = \left(\tfrac{S_{va}}{208} + \tfrac{S_{bu}}{160} + \tfrac{S_{pro}}{112} + \tfrac{S_{ac}}{64} + s_{hco3}\right).1000 \\
&co_2 = S_{co2}.1000 \\
&bic = S_{hco3}.1000 \\
&q_c = \rho_{T,10}.1000 \\
&q_m = \rho_{T,9}.1000 \\
&P_C = \tfrac{P_{gaz,co_2}}{P_{gaz,co_2} + P_{gaz,ch_4}}
\end{aligned}
\tag{B.1}
$$

with the corresponding units, x_1 $(kgDCO/m^3)$, x_2 $(kgSV/m^3)$, x_3 (mM), x_4 $(kgSV/m^3)$, x_5 (mM), x_6 (mM), co_2 (mM), bic (mM), q_c (mM/day), q_m (mM/day) and P_C (atm).

Appendix C

Mathematical Complement

Definition 5. In linear algebra, a symmetric real matrix $S \in \mathbb{R}^{n \times n}$ is said to be

1. positive-definite $\quad S > 0 \quad$ iff $x^T S x > 0, \ \forall\, x \in \mathbb{R}^n, \ x \neq 0.$
2. positive semi-definite $\quad S \geq 0 \quad$ iff $x^T S x \geq 0, \ \forall\, x \in \mathbb{R}^n, \ x \neq 0.$
3. negative-definite $\quad S < 0 \quad$ iff $x^T S x < 0, \ \forall\, x \in \mathbb{R}^n, \ x \neq 0.$
4. negative semi-definite $\quad S \geq 0 \quad$ iff $x^T S x \leq 0, \ \forall\, x \in \mathbb{R}^n, \ x \neq 0.$

Definition 6. *(Schur complement [158])* The Schur complement of an invertible matrix A, of the matrix M

$$M := \begin{pmatrix} A & B \\ C & D \end{pmatrix}$$

is the matrix $D - CA^{-1}B$.

Definition 7. *(Schur lemma [158])* Suppose A and C are symmetric matrices ($A = A^T$ and $C = C^T$), then

$$\begin{pmatrix} A & B \\ B^T & C \end{pmatrix} > 0$$

if and only if

$$C - B^T A^{-1} B > 0 \ \text{ if } \ A > 0$$

or equivalently, if and only if

$$A - BC^{-1}B^T > 0 \ \text{ if } \ C > 0.$$

Definition 8. ***(Convex set)*** A set E is said to be convex if

$$\lambda x_1 + (1-\lambda)x_2 \in E$$

$\forall\ (x_1, x_2) \in E$, $\forall\ \lambda \in [0,1]$.

Geometrically this means that, a convex set is a region such that, for every pair of points within the region, every point on the straight line segment that joins the pair of points is also within the region.

Definition 9. ***(Convex function)*** A function $\varphi\ :\ \mathbb{R}^n \to \mathbb{R}$ is said to be convex if

$$\varphi\Big(\lambda x_1 + (1-\lambda)x_2\Big) \leq \lambda\varphi(x_1) + (1-\lambda)\varphi(x_2)$$

$\forall\ (x_1, x_2) \in \mathbb{R}^{n^2}$, $\forall\ \lambda \in [0,1]$.

A function φ is strictly convex if

$$\varphi\Big(\lambda x_1 + (1-\lambda)x_2\Big) < \lambda\varphi(x_1) + (1-\lambda)\varphi(x_2)$$

$\forall\ x_1 \neq x_2$, $\forall\ \lambda \in]0,1[$.

Appendix D

Stability of dynamical systems : Lyapunov Stability

Stability theory of a dynamical system studies the trajectory of that system around an equilibrium point. That is, analysing how the state trajectory will progress when the initial state (the system state at initial conditions) is located in the neighbourhood of one of the system equilibrium points.

Stability in the sense of Lyapunov is a general theory dedicated to the study of dynamical systems described by a differential equation. A system is stable according to the Lyapunov stability theory if the solution of the differential equation describing the system under consideration, with an initial state located around one of its equilibrium point, will remain in a closed ball around the equilibrium point.

D.1 Continous-time systems stability

Consider the class of nonlinear systems described by the following differential equation:

$$\dot{x}(t) = f(x(t), t), \quad x(t_0) = x_0 \tag{D.1}$$

where $x(t) \in \mathbb{R}^n$ is the state vector, $f(x(t), t) : \mathbb{R}^n \times \mathbb{R}^+ \to \mathbb{R}^n$ is continue vector function, and x_e is the equilibrium point of (D.1) such that $f(x_e, t) = 0$. $\forall\ t \geq t_0$, $x(t_0)$ and t_0 are the initial state and initial time, respectively. We denote by $x(t, t_0, x_0)$ the solution of system (D.1) at $t \geq t_0$.

Throughout this thesis, only the stability of the estimation error is studied. For this reason, we assume that the nonlinear system (D.1) possesses a unique equilibrium point $x_e = 0$. This assumption leads to represent some definitions of the stability of system the (D.1) at the origin.

Definition 10. ***(Stability)*** The equilibrium point $x_e = 0$ (origin) of the system (D.1) is said to be stable, in the sense of Lyapunov, if for each $\varepsilon > 0$, there is a positive scalar $\delta(\varepsilon, t_0)$ such that

$$\|x(t_0)\| < \delta(\varepsilon, t_0) \quad \Rightarrow \quad \|x(t, t_0, x_0)\| < \varepsilon, \ \forall \ t \geq t_0 \geq 0$$

The system (D.1) is said to be unstable if it is not stable.

Definition 11. ***(uniform stability)*** The equilibrium point $x_e = 0$ of system (D.1) is said to be uniformly stable, in the sense of Lyapunov, if for each $\varepsilon > 0$, there is a positive scalar $\delta(\varepsilon)$ such that:

$$\|x(t_0)\| < \delta(\varepsilon) \quad \Rightarrow \quad \|x(t, t_0, x_0)\| < \varepsilon, \ \forall \ t \geq t_0 \geq 0$$

Definition 12. ***(asymptotic stability)*** The equilibrium point $x_e = 0$ of system (D.1) is said to be asymptotically stable, if it is stable and there exists a positive scalar $\delta(t_0)$ such that

$$\|x(t_0)\| < \delta(t_0) \quad \Rightarrow \quad \lim_{t \to \infty} \|x(t, t_0, x_0)\| = 0, \ \forall \ t \geq t_0 \geq 0$$

Definition 13. ***(Attractivity)*** The equilibrium point $x_e = 0$ of system (D.1) is an attractive point of (D.1), if for each $\varepsilon > 0$, there is a positive scalar $\delta(t_0)$ such that :

$$\|x_0\| < \delta(t_0) \quad \Rightarrow \quad \lim_{t \to \infty} (x(t, t_0, x_0)) = 0, \ \forall \ t \geq t_0.$$

if $\delta(t_0) = +\infty$, the origin is said to be globally attractive.

Definition 14. ***(exponential stability)*** The equilibrium point $x_e = 0$ of system (D.1) is said to be exponentially stable, if there exist positive scalars α and β such that :

$$\|x(t, t_0, x_0)\| \leq \alpha \exp(-\beta(t - t_0)), \ \forall \ t \geq t_0, \ \forall \ x_0 \in \mathcal{B}_r.$$

If $\mathcal{B}_r = \mathbb{R}^n$, the system is said to be globally exponentially stable.

D.2 Discrete-time systems stability

Consider the discrete-time system described by the following difference equation

$$x(k+1) = f(x(k), k), \quad x(k_0) = x_0 \tag{D.2}$$

where $x(k) \in \mathbb{R}^n$ is the state vector, $f(x(k), k) : \mathbb{R}^n \times \mathbb{R}^+ \rightarrow \mathbb{R}^n$ is a continuous vector function, $x(k_0)$ and k_0 are the initial state vector and the initial time, respectively. We denote by $x(k, k_0, x_0)$ the solution of the difference equation (D.2) at $k \geq k_0$.
The stability definitions for continuous-time systems (D.1) remain valid for discrete-time systems (D.2), except the exponential stability which changes.

Definition 15. ***(Exponential Stability)*** The equilibrium point $x_e = 0$ of system (D.1) is said to be globally exponentially stable, if there exists two positive scalars α and $0 < \rho < 1$ such that :

$$\|x(k, k_0, x_0)\| \leq \alpha \|x_0\| \rho^{(k-k_0)}, \ \forall\ k \geq k_0 \geq 0, \ \forall\ x_0 \in \mathcal{B}_r.$$

If $\mathcal{B}_r = \mathbb{R}^n$, the system is said to be globally exponential stable.

The use of the previous definitions to check the stability of a system of the form (D.1) (resp. D.2) requires an explicit solution. In most cases, it is not easy to compute the explicit solution of a nonlinear system or even impossible, which makes these definitions difficult to apply. The Lyapunov direct method is an efficient alternative to overcome this difficulty, such that the existence of the so-called Lyapunov function and the negativity of its derivative with respect to time, ensure the local or the the global stability of the system under consideration.

D.3 Lyapunov direct method

Lyapunov direct method allows to determine the stability of a dynamical system without resorting to calculate the solution of (D.1) (resp. D.2). The method is a generalization of the fact that a physical system whose energy is not increasing is somewhat stable. In other words, the Lyapunov direct method studies the rate of energy change of a system, which provides a clear idea on its stability.

Definition 16. Let $V(x,t)\ :\ \mathbb{R}^n \times \mathbb{R}^+ \to \mathbb{R}^+$ to be scalar continuous function. $V(x,t)$ is said to be proper positive definite if

1. $\forall\, t \in \mathbb{R}^+, \forall\, x \in \mathbb{R}^n,\ x \neq 0 \quad V(x,t) > 0;$
2. $\forall\, t \in \mathbb{R}^+,\ \ V(x,t) = 0 \ \ \Rightarrow \ \ x = 0;$
3. $\forall\, t \in \mathbb{R}^+,\ \lim_{\|x\| \to \infty} V(x,t) = \infty.$

Definition 17. ***(Lyapunov function)*** A function $V(x,t)$ of class $\mathcal{C}^1$ is a local Lyapunov function (resp. global) for system (D.1), if it is proper positive definite and if there exists a subset $\mathcal{V}_0 \subset \mathbb{R}^n$ containing the origin, such that $\forall\, x \in \mathcal{V}_0$ (resp. $x \in \mathbb{R}^n$) :

$$\dot{V}(x,t) = \frac{\partial V(x,t)}{\partial t} + \frac{\partial V(x,t)}{\partial x} f(x(t),t) \leq 0.$$

If $\dot{V}(x,t) < 0$, then $V(x,t)$ is called a strict Lyapunov function for system (D.1).

Definition 18. ***(Lyapunov direct method)*** If system (D.1) admits a Lyapunov function (resp. strict Lyapunov function), then the origin is a locally stable equilibrium point (resp. asymptotically stable).
This result can be generalized for global Lyapunov function. $\forall\, x \in \mathbb{R}^n$.

Definition 19. ***(Exponential Stability)*** The origin of system (D.1) is locally exponentially stable, if there exists scalars $\alpha, \beta, \gamma > 0,\ p \geq 0$ and a Lyapunov function $V(x,t)\ :\ \mathcal{V}_0 \times \mathbb{R}^+ \to \mathbb{R}^+$ of class $\mathcal{C}^1$, such that $\forall\, x \in \mathcal{V}_0$:

1. $\alpha \|x\|^p \leq V(x,t) \leq \beta \|x\|^p;$
2. $\dot{V}(x,t) < -\gamma V(x,t).$

If $\mathcal{V}_0 = \mathbb{R}^n$, then the origin of (D.1) is globally exponentially stable.

Remark 7. By choosing a quadratic Lyapunov function $V(x(t),t) = x^T(t)Px(t)$, $P = P^T > 0$, then the origin of the linear system $\dot{x}(t) = Ax(t)$ is globally exponentially stable if P is a solution for the matrix equation $A^T P + PA = -Q$, for any positive definite matrix Q.

The Lyapunov's direct method can be applied for both continuous-time and discrete-time systems. The exponential stability of a discrete-time system is expressed as follows:

Definition 20. ***(Exponential Stability)*** The origin of system (D.2) is locally exponentially stable, if there exists a proper definite positive Lyapunov function $V(x_k, k) : \mathcal{B}_r \times \mathbb{R}^+ \to \mathbb{R}^+,\ V(0, k) = 0$, an scalars α, β et $0 < \gamma < 1$ such that, $\forall\, x_0 \in \mathcal{B}_r$ et $\forall\, k \geq k_0 \geq 0$:

1. $\alpha \|x_k\|^2 \leq V(x, t) \leq \beta \|x_k\|^2$;
2. The Lyapunov sequence $\{V(x_k, k)\}_{k=k_0,\ldots}$ is strictly decreasing, i.e :

$$\Delta V(x_k, k) = V(x_{k+1}, k+1) - V(x_k, k) \leq -\gamma V(x_k, k)$$

   where

$$x_{k+1} = x(k+1, k_0, x_0) = f(x(k+1), k+1).$$

Remark 8. By choosing the Lyapunov quadratic function $V(x_k, k) = x_k^T P x_k,\ P = P^T > 0$, The origin of the discrete-time linear system $x_{k+1} = Ax_k$ is globally asymptotically stable, if and only if P is a solution for the matrix equation $A^T P A - P = -Q$, for any positive definite matrix Q.

Bibliography

[1] L. Appels, J. Lauwers, J. Degrève, L. Helsen, B. Lievens, K. Willems, J. Van Impe, and R. Dewil. Anaerobic digestion in global bio-energy production: Potential and research challenges. *Renewable and Sustainable Energy Reviews*, 15(9):4295 – 4301, 2011.

[2] D.J Batstone, J. Keller, I. Angelidaki, S.V. Kalyuzhny, S.G. Pavlostathis, A. Rozzi, W.T.M. Sanders, H. Siegrist, and V.A. Vavilin. *Anaerobic Digestion Model No. 1 (ADM1).* IWA Publishing, 2002. ISBN 1-900222-78-7.

[3] D.J. Batstone, J. Keller, I. Angelidaki, S.V. Kalyuzhnyi, S.G Pavlostathis, A. Rozzi, W.T.M Sanders, H. Siegrist, and V.A. Vavilin. The iwa anaerobic digestion model no 1 (adm1). *Water Science and Technology*, 45(10):65–73, 2002.

[4] O. Bernard, Z. Hadj-Sadok, D. Dochain, A. Genovesi, and J.Ph. Steyer. Dynamical model development and parameter identification for an anaerobic wastewater treatment process. *Biotechnology and bioengineering*, 75(4):424–438, 2001.

[5] J. Hansen, M. Sato, R. Ruedy, K. Lo, D.W. Lea, and M. Medina-Elizade. Global temperature change. *Proceedings of the National Academy of Sciences*, 103(39): 14288–14293, 2006.

[6] L.V. Alexander, X. Zhang, T.C Peterson, J. Caesar, B. Gleason, A. Klein Tank, M. Haylock, D. Collins, B. Trewin, F. Rahimzadeh, et al. Global observed changes in daily climate extremes of temperature and precipitation. *Journal of Geophysical Research: Atmospheres*, 111(D5), 2006.

[7] R.K. Pachauri, M.R. Allen, V.C. Barros, J. Broome, et al. *Climate change 2014: synthesis report. Contribution of Working Groups I, II and III to the fifth assessment report of the Intergovernmental Panel on Climate Change.* IPCC, 2014.

[8] S. Rahmstorf, A. Cazenave, J.A. Church, J.E Hansen, R.F. Keeling, D.E. Parker, and R.C.J Somerville. Recent climate observations compared to projections. *Science*, 316(5825):709–709, 2007.

[9] C. Mora, A.G Frazier, R.J Longman, R.S Dacks, M.M. Walton, E.J. Tong, J.J. Sanchez, L.R. Kaiser, Y.O. Stender, J.M. Anderson, et al. The projected timing of climate departure from recent variability. *Nature*, 502(7470):183–187, 2013.

[10] S. Gosh. Anaerobic Digestion for Renewable Energy and Environmental Restoration. *Proceedings of the 8th IWA International Conference on Anaerobic Digestion*, 1:9–15, 1997.

[11] I. Angelidaki, L. Ellegaard, and B.K. Ahring. Applications of the anaerobic digestion process. In *Biomethanation II*, pages 1–33. Springer, 2003.

[12] P. Weiland. Biogas production: current state and perspectives. *Applied microbiology and biotechnology*, 85(4):849–860, 2010.

[13] L. Yu, P.C Wensel, J. Ma, and S. Chen. Mathematical modeling in anaerobic digestion (AD). *Journal of Bioremediation & Biodegradation*, 2014, 2013.

[14] S. Rasi, A. Veijanen, and J. Rintala. Trace compounds of biogas from different biogas production plants. *Energy*, 32:1375–1380, 2007.

[15] Ph.J Hobbs A.J Ward, P.J Holliman, and D.L Jones. Optimisation of the Anaerobic Digestion of Agricultural Resources. *Bioresource technology*, 99(17):7928–7940, 2008.

[16] J. Huang and R.J. Crookes. Assessment of Simulated Biogas as a Fuel for the Spark Ignition Engine. *Fuel*, 77(15):1793–1801, 1998.

[17] LC Smith, DJ. Elliot, and A. James. Mixing in upflow anaerobic filters and its influence on performance and sscale-up. *Water Research*, 30(12):3061–3073, 1996.

[18] K.V. Rajeshwari, M. Balakrishnan, A. Kansal, K. Lata, and V.V.N. Kishore. State-of-the-art of anaerobic digestion technology for industrial wastewater treatment. *Renewable and Sustainable Energy Reviews*, 4(2):135 – 156, 2000.

[19] H. Bouallagui, Y. Touhami, R. Ben Cheikh, and M. Hamdi. Bioreactor performance in anaerobic digestion of fruit and vegetable wastes. *Process Biochemistry*, 40(3–4):989 – 995, 2005.

[20] Ch. Rojas, Sh. Fang, F. Uhlenhut, A. Borchert, I. Stein, and M. Schlaak. Stirring and biomass starter influences the anaerobic digestion of different substrates for biogas production. *Engineering in Life Sciences*, 10(4):339–347, 2010.

[21] W.P. Barber and D.C. Stuckey. The use of the anaerobic baffled reactor (abr) for wastewater treatment: a review. *Water Research*, 33(7):1559 – 1578.

[22] J. Hess. *Modélisation de la Qualité du Biogas Produit par un Fermenteur Méthanogène et sa Stratégie de Régulation en Vue de sa Valorisation.* PhD thesis, Université de Nice - Sophia Antipolis, 2008.

[23] B. Benyahia. *Modélisation et Observation des Bioprocédés à Membranes: Application à la Digestion Anaérobie.* PhD thesis, Université de Tlemcen, Algérie et Univesité de Montpelier 2, France, 2012.

[24] F. Haugen, R. Bakke, and B. Lie. Adapting dynamic mathematical models to a pilot anaerobic digestion reactor. 2013.

[25] J.F. Andrews. A mathematical model for the continuous culture of microorganisms utilizing inhibitory substrates. *Biotechnology and Bioengineering*, 10(4):707–723, 1968.

[26] D.T Hill and C.L Barth. A dynamic model for simulation of animal waste digestion. *Water Pollution Control Federation*, pages 2129–2143, 1977.

[27] D.R Boone and M.P Bryant. Propionate-degrading bacterium, syntrophobacter wolinii sp. nov. gen. nov., from methanogenic ecosystems. *Applied and Environmental Microbiology*, 40 (3):626–632, 1980.

[28] J.A Eastman and J.F Ferguson. Solubilization of particulate organic carbon during the acid phase of anaerobic digestion. *Water Pollution Control Federation*, pages 352–366, 1981.

[29] T.C Stadtman and H.A Barker. Studies on the methane fermenttaion ix.: The origin of methane in the acetate and methanol fermentations by methanosarcina1. *Journal of Bacteriology*, 61(1):81–86, 1951.

[30] I. Angelidaki and B.K Ahring. Thermophilic anaerobic digestion of livestock waste: The effect of ammonia. *Applied Microbiology and Biotechnology*, 38(4):560–564, 1993.

[31] G. Lyberatos and I.V Skiadas. Modelling of anaerobic digestion- a review. *Global Nest Int J*, 1(2):63–76, 1999.

[32] G. Bastin and D. Dochain. *On-line Estimation and Adaptive Control of Bioreactors*. Process Measurement and Control. Elsevier, 1990. ISBN 9780444884305.

[33] V.A. Vavilin, S.V. Rytov, and L.Y Lokshina. A description of hydrolysis kinetics in anaerobic degradation of particulate organic matter. *Bioresource technology*, 56 (2):229–237, 1996.

[34] I. Angelidaki, L. Ellegaard, and B.K Ahring. A comprehensive model of anaerobic bioconversion of complex substrates to biogas. *Biotechnology and Bioengineering*, 63(3):363–372, 1999.

[35] H. Siegrist, D. Renggli, and W. Gujer. Mathematical modelling of anaerobic mesophilic sewage sludge treatment. *Water Science and Technology*, 27(2):25–36, 1993.

[36] D.J. Batstone, J. Keller, R.B. Newell, and M. Newland. Modelling anaerobic degradation of complex wastewater. i: Model development. *Bioresource Technology*, 75 (1):67–74, 2000.

[37] C. Rosén and U. Jeppsson. Aspects on adm1 implementation within the bsm2 framework. *TEIE*, 2005.

[38] M.Y. Lee, C.W. Suh, Y.T. Ahn, and H.S. Shin. Variation of adm1 by using temperature-phased anaerobic digestion (tpad) operation. *Bioresource technology*, 100(11):2816–2822, 2009.

[39] I. Ramirez, E.IP Volcke, R. Rajinikanth, and J.Ph. Steyer. Modeling microbial diversity in anaerobic digestion through an extended adm1 model. *Water research*, 43(11):2787–2800, 2009.

[40] I. Ramirez, A. Mottet, H. Carrère, S. Déléris, F. Vedrenne, and J.Ph. Steyer. Modified adm1 disintegration/hydrolysis structures for modeling batch thermophilic anaerobic digestion of thermally pretreated waste activated sludge. *Water research*, 43(14):3479–3492, 2009.

[41] A. Spagni, M. Ferraris, and S. Casu. Modelling wastewater treatment in a submerged anaerobic membrane bioreactor. *Journal of Environmental Science and Health, Part A*, 50(3):325–331, 2015.

[42] S. Marsili-Libelli and S. Beni. Shock load modelling in the anaerobic digestion process. *Ecological modelling*, 84(1):215 – 232, 1996.

[43] I. Simeonov, V. Lubenova, and I. Queinnec. Parameter and state estimation of an anaerobic digestion of organic wastes model with addition of stimulating substances. *Bioautomation*, 12:88–105, 2009.

[44] J. Harmand, F. Miens, and J.Ph. Steyer. High gain observer for diagnosing an anaerobic fixed bed reactor. In *Control Conference (ECC), 2001 European*, pages 2829–2834. IEEE, 2001.

[45] C. Kravaris, V. Sotiropoulos, C. Georgiou, N. Kazantzis, M.Q Xiao, and A.J. Krener. Nonlinear observer design for state and disturbance estimation. *Systems & Control Letters*, 56(11):730–735, 2007.

[46] P.F Pind, I. Angelidaki, B.K Ahring, K. Stamatelatou, and G.Lyberatos. Monitoring and control of anaerobic reactors. In *Biomethanation II*, pages 135–182. Springer, 2003.

[47] M. Madsen, J.B. Holm-Nielsen, and K.H. Esbensen. Monitoring of anaerobic digestion processes: A review perspective. *Renewable and Sustainable Energy Reviews*, 15(6):3141 – 3155, 2011.

[48] P. Vanrolleghem and D Lee. On-line monitoring equipment for wastewater treatment processes: state of the art. *Water Science and Technology*, 47(2):1–34, 2003.

[49] X. Jin, X. Li, N. Zhao, I. Angelidaki, and Y. Zhang. Bio-electrolytic sensor for rapid monitoring of volatile fatty acids in anaerobic digestion process. *Water Research*, 111:74 – 80, 2017.

[50] R. Moletta. Technologies de traitement des effluents industriels par la méthanisation. *La méthanisation (2e ed.)*, page 133, 2011.

[51] D. G. Luenberger. *Optimization by vector space methods*. John Wiley & Sons, 1969.

[52] David G. Luenberger. An introduction to observers. *IEEE Transactions on Automatic Control*, ac-16(6):596–602, 1971.

[53] H. W. Sorenson. *Kalman Filtering Theory and Application*. IEEE Press, 1990.

[54] R.E. Kalman. A new approach to linear filtering and prediction problems. *Journal of basic Engineering*, 82(1):35–45, 1960.

[55] R.E. Kalman and R.S. Bucy. New results in linear filtering and prediction theory. *Journal of basic engineering*, 83(1):95–108, 1961.

[56] G. Besançon. *Nonlinear observers and applications*, volume 363. Springer, 2007.

[57] G.B. Wang, S.S. Peng, and H.P. Huang. A sliding observer for nonlinear process control. *Chemical Engineering Science*, 52(5):787–805, 1997.

[58] Masoud Soroush. Nonlinear state-observer design with application to reactors. *Chemical Engineering Science*, 52(3):387 – 404, 1997.

[59] M. Lombardi, K. Fiaty, and P. Laurent. Implementation of observer for on-line estimation of concentration in continuous-stirred membrane bioreactor: Application to the fermentation of lactose. *Chemical Engineering Science*, 54(13):2689 – 2696, 1999. ISSN 0009-2509. doi: http://dx.doi.org/10.1016/S0009-2509(98)00417-5.

[60] D. Theilliol, J.C. Ponsart, J. Harmand, C. Join, and P. Gras. On-line estimation of unmeasured inputs for anaerobic wastewater treatment processes. *Control Engineering Practice*, 11(9):1007–1019, 2003.

[61] R. Belmonte-Izquierdo, S. Carlos-Hernandez, and E.N. Sánchez. A new neural observer for an anaerobic bioreactor. *International journal of neural systems*, 20 (01):75–86, 2010.

[62] M.Z. Hadj-Sadok and J.L. Gouzé. Estimation of uncertain models of activated sludge processes with interval observers. *Journal of Process Control*, 11(3):299–310, 2001.

[63] O. Bernard, B. Chachuat, and J.Ph. Steyer. *State estimation for wastewater treatment processes*. Wiley, Oxford, UK, 2007.

[64] O. Bernard and J.L Gouzé. Closed loop observers bundle for uncertain biotechnological models. *Journal of Process Control*, 14(7):765–774, 2004.

[65] M. Perrier, S. Feyo de Azevedo, E.C. Ferreira, and D. Dochain. Tuning of observer-based estimators: theory and application to the on-line estimation of kinetic parameters. *Control Engineering Practice*, 8(4):377–388, 2000.

[66] V. Lubenova, I. Simeonov, and I. Queinnec. Two-step Parameter and State Estimation of the Anaerobic Digestion. In *Proc. 15th IFAC Word Congress, Barcelona, July*, pages 21 – 26, 2002.

[67] G. Stephanopoulos and K.Y. San. Studies on on-line bioreactor identification. i. theory. *Biotechnology and Bioengineering*, 26(10):1176–1188, 1984.

[68] L.J.S. Lukasse, K.J. Keesman, and G. van Straten. A recursively identified model for short-term predictions of nh4/no3 – concentrations in alternating activated sludge processes. *Journal of Process Control*, 9(1):87 – 100, 1999.

[69] D. Dochain. State and parameter estimation in chemical and biochemical processes: a tutorial. *Journal of Process Control*, 13(8):801 – 818, 2003.

[70] F. Haugen, R. Bakke, and B. Lie. State estimation and model-based control of a pilot anaerobic digestion reactor. *Journal of Control Science and Engineering*, 2014:3, 2014.

[71] E. Rocha-Cozatl, M. Sbarciog, L. Dewasme, J.A. Moreno, JA, and A. Vande Wouwer. State and input estimation of an anaerobic digestion reactor using a continuous-discrete unknown input observer. *IFAC-PapersOnLine*, 48(8):129–134, 2015.

[72] J. Mohd Ali, N.H. Hoang, M.A. Hussain, and D. Dochain. Review and classification of recent observers applied in chemical process systems. *Computers & Chemical Engineering*, 76:27 – 41, 2015.

[73] R.D. Gudi, S.L. Shah, and M.R. Gray. Adaptive multirate state and parameter estimation strategies with application to a bioreactor. *AIChE Journal*, 41(11): 2451–2464, 1995.

[74] M. Soroush. State and parameter estimations and their applications in process control. *Computers & Chemical Engineering*, 23(2):229–245, 1998.

[75] K.J. Åström. *Introduction to stochastic control theory.* Courier Corporation, 2012.

[76] J. P. Gauthier, H. Hammouri, and S. Othman. A simple observer for nonlinear systems, applications to bioreactors. IEEE *Transactions on Automatic Control*, 37(6):875–880, 1992.

[77] M.L. Fall, M. Farza, M. M'Saad, E. Pigeon, and O. Gehan. Cascade observer for a class of nonlinear systems with output delays. In *Proceedings of the ECC*, 2013.

[78] M. Farza, M. M'Saad, T. Ménard, M. L. Fall, O. Gehan, and E. Pigeon. Simple cascade observer for a class of nonlinear systems with long output delays. *IEEE Transactions on Automatic Control*, 60(12):3338–3343, 2015.

[79] G. Lara-Cisneros, R. Aguilar-López, D. Dochain, and R. Femat. On-line estimation of vfa concentration in anaerobic digestion via methane outflow rate measurements. *Computers & Chemical Engineering*, 94:250–256, 2016.

[80] P.J. Olver. *Equivalence, Invariants and Symmetry.* London Mathematical Society Lecture Note. Cambridge University Press, 1995. ISBN 9780521478113.

[81] N. Aghannan and P. Rouchon. On Invariant Asymptotic Observers. In *In Proceedings of the 41st IEEE Conference on Decision and Control*, volume 2, pages 1479–1484, 2002.

[82] S. Bonnabel, P. Martin, and P. Rouchon. Symmetry-preserving observers. *ArXiv Mathematics e-prints*, 2006. Provided by the SAO/NASA Astrophysics Data System.

[83] I. Didi, H. Dib, and B. Cherki. An invariant observer for a chemostat model. *Automatica*, 50(9):2321–2326, 2014.

[84] I. Didi. *Sur l'Observation des Systèmes Non Linéaires Invariants: Application aux Bioprocédés.* PhD thesis, Université AbouBekr Belkaid, 2009.

[85] S. Karellas, I. Boukis, and G. Kontopoulos. Development of an investment decision tool for biogas production from agricultural waste. *Renewable and Sustainable Energy Reviews*, 14(4):1273 – 1282, 2010.

[86] C. Kaminker and F. Stewart. The role of institutional investors in financing clean energy. *OECD Working Papers on Finance, Insurance and Private Pensions*, (23):1, 2012.

[87] J.Ph. Steyer, P. Buffière, D. Rolland, and volume=33 number=9 pages=2059–2068 year=1999 publisher=Elsevier R. Moletta, journal=Water Research. Advanced control of anaerobic digestion processes through disturbances monitoring.

[88] H.O. Méndez-Acosta, R. Femat, V. González-Alvarez, and J.Ph. Steyer. Substrate regulation in an anaerobic digester based on geometric control. *Proceedings of the IFAC-CLCA,2002*, 2002.

[89] H.O Méndez-Acosta, B. Palacios-Ruiz, J.Ph. Steyer, V. Alcaraz-González, E. Latrille, and V. González-Álvarez. Nonlinear approach for the vfa regulation in an anaerobic digester. *IFAC Proceedings Volumes*, 40(4):79–84, 2007.

[90] K. Chaib-Draa, H. Voos, M. Alma, and M. Darouach. Adaptive control of the methane flow rate in biogas plants. In *2015 3rd International Conference on Control, Engineering Information Technology (CEIT)*, pages 1–6, 2015.

[91] D. Gaida et al. *Dynamic real-time substrate feed optimization of anaerobic co-digestion plants*. Leiden Institute of Advanced Computer Science (LIACS), Faculty of Science, Leiden University, 2014.

[92] SP. Graef and JF. Andrews. Stability and control of anaerobic digestion. *Water Pollution Control Federation*, pages 666–683, 1974.

[93] A. Rozzi. Modelling and control of anaerobic digestion processes. *Transactions of the Institute of Measurement and Control*, 6(3):153–159, 1984.

[94] M. Romli, P.F. Greenfield, and P.L. Lee. Effect of recycle on a two-phase high-rate anaerobic wastewater treatment system. *Water Research*, 28(2):475 – 482, 1994.

[95] G.B. Ryhiner, E. Heinzle, and I.J. Dunn. Modeling and simulation of anaerobic wastewater treatment and its application to control design: case whey. *Biotechnology Progress*, 9(3):332–343, 1993.

[96] R. Cord-Ruwisch, T.I. Mercz, C.Y. Hoh, and G.E. Strong. Dissolved hydrogen concentration as an on-line control parameter for the automated operation and optimization of anaerobic digesters. *Biotechnology and bioengineering*, 56(6):626–634, 1997.

[97] S. Carlos-Hernandez. A new adaptive pi for bicarbonate regulation in an anaerobic digestion process. *Asian Journal of Control*, 13(6):785–796, 2011.

[98] H. Zhou, H. Li, and F. Wang. Anaerobic digestion of different organic wastes for biogas production and its operational control performed by the modified adm1. *Journal of Environmental Science and Health, Part A*, 47(1):84–92, 2012.

[99] J. Alvarez-Ramirez, M. Meraz, O. Monroy, and A. Velasco. Feedback control design for an anaerobic digestion process. *Journal of Chemical Technology and Biotechnology*, 77(6):725–734, 2002.

[100] C. García-Diéguez, F. Molina, and E. Roca. Multi-objective cascade controller for an anaerobic digester. *Process Biochemistry*, 46(4):900–909, 2011.

[101] J. Liu, G. Olsson, and B. Mattiasson. Extremum-seeking with variable gain control for intensifying biogas production in anaerobic fermentation. *Water Science and Technology*, 53(4-5):35–44, 2006.

[102] J. von Sachs, U. Meyer, P. Rys, and H. Feitkenhauer. New approach to control the methanogenic reactor of a two-phase anaerobic digestion system. *Water research*, 37(5):973–982, 2003.

[103] I.M. Alatiqi, A.A. Dadkhah, and N.M. Jabr. Dynamics and multivariable control analysis for anaerobic digestion. *The Chemical Engineering Journal*, 43(3):B81–B91, 1990.

[104] J. Lauwers, L. Appels, I.P. Thompson, J. Degrève, J.F. Van Impe, and R. Dewil. Mathematical modelling of anaerobic digestion of biomass and waste: Power and limitations. *Progress in Energy and Combustion Science*, 39(4):383–402, 2013.

[105] I. Simeonov and I. Queinnec. Linearizing control of the anaerobic digestion with addition of acetate (control of the anaerobic digestion). *Control Engineering Practice*, 14(7):799 – 810, 2006.

[106] L. Mailleret, O. Bernard, and J.Ph. Steyer. Nonlinear adaptive control for bioreactors with unknown kinetics. *Automatica*, 40(8):1379–1385, 2004.

[107] L. Mailleret, O. Bernard, and J.Ph. Steyer. Robust regulation of anaerobic digestion processes. *Water Science and Technology*, 48(6):87–94, 2003.

[108] P. Renard, V. Van Breusegem, M.T Nguyen, and E.J Nyns. Implementation of an adaptive controller for the startup and steady-state running of a biomethanation

process operated in the CSTR mode. *Biotechnology and Bioengineering*, 38:805 – 812, 1991.

[109] D. Dochain and M. Perrier. Control design for nonlinear wastewater treatment processes. *Water Science and Technology*, 28(11-12):283–293, 1993.

[110] O. Bernard, M. Polit, Z. Hadj-Sadok, M. Pengov, D. Dochain, M. Estaben, and P. Labat. Advanced monitoring and control of anaerobic wastewater treatment plants: software sensors and controllers for an anaerobic digester. *Water Science and Technology*, 43(7):175–182, 2001.

[111] E. Petre, D. Selişteanu, and D. Şendrescu. On adaptive control of an anaerobic digestion bioprocess. *reactions*, 1:4, 2007.

[112] V. Alcaraz-González, J. Harmand, A. Rapaport, J.Ph. Steyer, V. González-Alvarez, and C. Pelayo-Ortiz. Robust interval-based siso regulation under maximum uncertainty conditions in an anaerobic digester. In *Intelligent Control, 2001.(ISIC'01). Proceedings of the 2001 IEEE International Symposium on*, pages 240–245. IEEE, 2001.

[113] A. Rapaport and J. Harmand. Robust regulation of a class of partially observed nonlinear continuous bioreactors. *Journal of Process Control*, 12(2):291–302, 2002.

[114] E. Petre, D. Selişteanu, and D. Şendrescu. Adaptive and robust-adaptive control strategies for anaerobic wastewater treatment bioprocesses. *Chemical engineering journal*, 217:363–378, 2013.

[115] R. Antonelli and A. Astolfi. Nonlinear controllers design for robust stabilization of continuous biological reactors. In *Control Applications, 2000. Proceedings of the 2000 IEEE International Conference on*, pages 760–765. IEEE, 2000.

[116] R. Antonelli, J. Harmand, J.Ph. Steyer, and A. Astolfi. Output feedback regulation of an anaerobic digestion process. In *American Control Conference, 2002. Proceedings of the 2002*, volume 5, pages 4062–4067. IEEE, 2002.

[117] F. Viel, F. Jadot, and G. Bastin. Robust feedback stabilization of chemical reactors. *IEEE Transactions on Automatic Control*, 42(4):473–481, 1997.

[118] A. Isidori. *Nonlinear control systems*. Springer Science & Business Media, 2013.

[119] H.O Méndez-Acosta, R. Femat, and D.U Campos-Delgado. Improving the performance on the chemical oxygen demand regulation in anaerobic digestion. *Industrial & Engineering Chemistry Research*, 43(1):95–104, 2004.

[120] B. Palacios-Ruiz, H.O. Méndez-Acosta, V. Alcaraz-Gonzalez, V. Gonzalez-Alvarez, and C. Pelayo-Ortiz. Regulation of volatile fatty acids and total alkalinity in anaerobic digesters. *IFAC Proceedings Volumes*, 41(2):13611–13616, 2008.

[121] H.O Méndez-Acosta, D.U Campos-Delgado, R. Femat, and V. González-Alvarez. A robust feedforward/feedback control for an anaerobic digester. *Computers & chemical engineering*, 29(7):1613–1623, 2005.

[122] H.O. Méndez-Acosta, B. Palacios-Ruiz, V. Alcaraz-González, J.Ph. Steyer, V. González-Álvarez, and E. Latrille. Robust control of volatile fatty acids in anaerobic digestion processes. *Industrial & Engineering Chemistry Research*, 47 (20):7715–7720, 2008.

[123] HO Méndez-Acosta, B Palacios-Ruiz, V Alcaraz-González, V González-Álvarez, and JP García-Sandoval. A robust control scheme to improve the stability of anaerobic digestion processes. *Journal of Process Control*, 20(4):375–383, 2010.

[124] Andrew Teel and Laurent Praly. Tools for semiglobal stabilization by partial state and output feedback. *SIAM Journal on Control and Optimization*, 33(5):1443–1488, 1995.

[125] R. Flores-Estrella, G. Quiroz, H. Mendez-Acosta, and R. Femat. $\mathcal{H}_\infty$ control of anaerobic digester for winery industry wastewater treatment. *Industrial & Engineering Chemistry Research*, 52(7):2625–2632, 2013.

[126] J. Liu, G. Olsson, and B. Mattiasson. Monitoring and control of an anaerobic upflow fixed-bed reactor for high-loading-rate operation and rejection of disturbances. *Biotechnology and bioengineering*, 87(1):43–53, 2004.

[127] J. Liu, G. Olsson, and B. Mattiasson. Control of an anaerobic reactor towards maximum biogas production. *Water Science and Technology*, 50(11):189–198, 2004.

[128] K. Boe, J.Ph. Steyer, and I. Angelidaki. Monitoring and control of the biogas process based on propionate concentration using online vfa measurement. *Water Science and Technology*, 57(5):661–666, 2008.

[129] A.J. Guwy, F.R. Hawkes, S.J. Wilcox, and D.L. Hawkes. Neural network and on-off control of bicarbonate alkalinity in a fluidised-bed anaerobic digester. *Water Research*, 31(8):2019 – 2025, 1997.

[130] P. Holubar, L. Zani, M. Hager, W. Fröschl, Z. Radak, and R. Braun. Advanced controlling of anaerobic digestion by means of hierarchical neural networks. *Water Research*, 36(10):2582–2588, 2002.

[131] J. Jimenez, E. Latrille, J. Harmand, A. Robles, J. Ferrer, D. Gaida, C. Wolf, F. Mairet, O. Bernard, V. Alcaraz-Gonzalez, et al. Instrumentation and control of anaerobic digestion processes: a review and some research challenges. *Reviews in Environmental Science and Bio/Technology*, 14(4):615–648, 2015.

[132] E. Mauky, S. Weinrich, H.J. Nägele, H.F. Jacobi, J. Liebetrau, and M. Nelles. Model predictive control for demand-driven biogas production in full scale. *Chemical Engineering & Technology*, 2016.

[133] J.J.E. Slotine, W. Li, et al. *Applied nonlinear control*, volume 199. prentice-Hall Englewood Cliffs, NJ, 1991.

[134] K.S. Narendra and A.M. Annaswamy. *Stable adaptive systems.* Courier Corporation, 2012.

[135] K. Chaib-Draa, H. Voos, M. Darouach, and M.Alma. A formal modeling framework for anaerobic digestion systems. In *Proceedings of the* 2015 17^{th} *UKSIM-AMSS International Conference on Modelling and Simulation*, pages 426 – 431. IEEE Computer Society, 2015.

[136] K. Chaib-Draa, H. Voos, M. Alma, A. Zemouche, and M. Darouach. LMI-based $\mathcal{H}_\infty$ nonlinear state observer design for anaerobic digestion model. In *2017 25th Mediterranean Conference on Control and Automation (MED)*, pages 678–683, 2017.

[137] K. Chaib-Draa, H. Voos, M. Alma, A. Zemouche, and M. Darouach. An LMI-based $\mathcal{H}_\infty$ discrete-time non linear state observer design for an anaerobic digestion model. In *20th IFAC World Congress, IFAC 2017*, 2017.

[138] K. Chaib-Draa, M. Alma, H. Voos, A. Zemouche, and M. Darouach. LMI-based invariant like nonlinear state observer for anaerobic digestion model. In *2017 25th*

Mediterranean Conference on Control and Automation (MED), pages 684–689, 2017.

[139] K. Chaib-Draa, H. Voos, M. Alma, A. Zemouche, and M. Darouach. LMI-based discrete-time nonlinear state observer for an anaerobic digestion model. In *2017 6th International Conference on Systems and Control (ICSC)*, pages 273–278, 2017.

[140] J. Alvarez-Ramirez, M. Meraz, O. Monroy, and A. Velasco. Feedback control design for an anaerobic digestion process. *Journal of Chemical Technology and Biotechnology*, 77(6):725–734, 2002.

[141] A.J. Guwy, F.R. Hawkes, S.J. Wilcox, and D.L. Hawkes. Neural network and on-off control of bicarbonate alkalinity in a fluidised-bed anaerobic digester. *Water Research*, 31(8):2019 – 2025, 1997.

[142] A. Holmberg and J.Ranta. Procedures for parameter and state estimation of microbial growth process models. *Automatica*, 18(2):181–193, 1982.

[143] T.G Müller, N. Noykova, M. Gyllenberg, and J. Timmer. Parameter identification in dynamical models of anaerobic waste water treatment. *Mathematical Biosciences*, 177:147–160, 2002.

[144] N. Noykova, T.G MuÈller, M. Gyllenberg, and J. Timmer. Quantitative analyses of anaerobic wastewater treatment processes: Identifiability and parameter estimation. *Biotechnology and Bioengineering*, 78:89–103, 2002.

[145] S. Hassam. *Modélisation de la Qualité du Biogas Produit par un Fermenteur Méthanogène et sa Stratégie de Régulation en Vue de sa Valorisation.* PhD thesis, Université de Tlemcen, 2016.

[146] L. Farina and S. Rinaldi. *Positive linear systems: theory and applications*, volume 50. John Wiley & Sons, 2011.

[147] C. Kravaris, J. Hahn, and Y. Chu. Advances and selected recent ddevelopments in state and parameter estimation. *Computers and Chemical Engineering*, 51:111 – 123, 2013.

[148] M. Arcak and P. Kokotovic. Nonlinear observers: A circle criterion design. In *Decision and Control, 1999. Proceedings of the 38th IEEE Conference on*, volume 5, pages 4872–4876. IEEE, 1999.

[149] R.E. Kalman. Mathematical description of linear dynamical systems. *Journal of the Society for Industrial and Applied Mathematics, Series A: Control*, 1(2): 152–192, 1963.

[150] R. Hermann and A. Krener. Nonlinear controllability and observability. *IEEE Transactions on Automatic Control*, 22(5):728–740, 1977.

[151] D. Williamson. Observation of bilinear systems with application to biological control. *Automatica*, 13(3):243–254, 1977.

[152] H.K. Khalil. *Nonlinear Systems.* Prentice Hall, Upper Saddle River, NJ, 2002.

[153] A. Zemouche, M. Boutayeb, and G. I. Bara. Observers for a class of Lipschitz systems with extension to $\mathcal{H}_\infty$ performance analysis. *Systems & Control Letters*, 57(1):18–27, 2008.

[154] A. Zemouche, R. Rajamani, B. Boulkroune, H. Rafaralahy, and M. Zasadzinski. $\mathcal{H}_\infty$ circle criterion observer design for Lipschitz nonlinear systems with enhanced LMI conditions. In *IEEE American Control Conference*, Boston, MA, USA., July 2016.

[155] H. Shim, Y.I. Son, and J.H. Seo. Semi-global observer for multi-output nonlinear systems. *Systems and Control Letters*, 43(4):233–244, 2001.

[156] S. Ibrir. Circle-criterion approach to discrete-time nonlinear observer design. *Automatica*, 43(8):1432–1441, 2007.

[157] M. Arcak and P. Kokotovic. Observer-based control of systems with slope-restricted nonlinearities. *IEEE Transactions on Automatic Control*, 46(7):1146–1150, 2001.

[158] S. Boyd, L. El Ghaoui, E. Feron, and V. Balakrishnan. Linear matrix inequalities in system and control theory. In *SIAM Studies in Applied Mathematics*, Philadelphia, USA, 1994.

[159] K. Zhou and J.C. Doyle. *Essentials of robust control*, volume 104. Prentice hall Upper Saddle River, NJ, 1998.

[160] N. Yao, J. Wang, and Y. Zhou. Rapid determination of the chemical oxygen demand of water using a thermal biosensor. *Sensors*, 14(6):9949–9960, 2014.

[161] F.R. Hawkes, A.J. Guwy, D.L. Hawkes, and A.G. Rozzi. On-line monitoring of anaerobic digestion: application of a device for continuous measurement of bicarbonate alkalinity. *Water science and technology*, 30(12):1–10, 1994.

[162] L. Cheng, W. Charles, and R. Cord-Ruwisch. Automatic online buffer capacity (alkalinity) measurement of wastewater using an electrochemical cell. *Environmental technology*, 37(19):2467–2472, 2016.

[163] J.Ph. Steyer, J.C. Bouvier, T. Conte, P. Gras, J. Harmand, and J.P. Delgenes. On-line measurements of cod, toc, vfa, total and partial alkalinity in anaerobic digestion processes using infra-red spectrometry. *Water Science and Technology*, 45(10):133–138, 2002.

[164] W. Yang, J. Nan, and D. Sun. An online water quality monitoring and management system developed for the liming river basin in daqing, china. *Journal of environmental management*, 88(2):318–325, 2008.

[165] K. Chaib-Draa, H. Voos, M. Alma, and M. Darouach. Linearizing control of biogas flow rate and quality. In *2015 IEEE 20th Conference on Emerging Technologies Factory Automation (ETFA)*, pages 1–4, Sept 2015.

[166] K. Chaib-Draa, H. Voos, M. Alma, and M. Darouach. Invariant observer applied to anaerobic digestion model. In *2016 IEEE 21st International Conference on Emerging Technologies and Factory Automation (ETFA)*, pages 1–4, Sept 2016.

[167] M. Darouach, M. Zasadzinski, and S.J. Xu. Full-order observers for linear systems with unknown inputs. *IEEE transactions on automatic control*, 39(3):606–609, 1994.

[168] A. Zemouche and M. Boutayeb. Sobolev norms-based state estimation and input recovery for a class of nonlinear systems. design and experimental results. *IEEE Transactions on Signal Processing*, 57(3):1021–1029, 2009.

[169] F. Amato. *Robust control of linear systems subject to uncertain time-varying parameters*, volume 325. Springer, 2006.

Abstract

In this thesis, we propose a formal modelling framework for the anaerobic digestion process, where we add more degrees of freedom in the control of biogas production. Indeed, we add two additional control inputs to the standardized AM2 (Acidogenesis Methanogenesis, 2 steps) model, reflecting addition of stimulating substrates which enhance the biogas quality and quantity. Then, we describe how the parameters of the resulted nonlinear model can be identified, and we analyse the positiveness and boundedness of its state variables. Based on the derived mathematical model and the analysis results, we design different software sensors to overcome the lack of reliable and cheap sensors. Indeed, we present a general class of systems to which the considered process model belongs. Then, we design an LMI-based invariant like observer as well as an LMI-based nonlinear observer of the same form as the generalized Arcak's observer. Furthermore, with the aim to render the observer design more robust to disturbances, we include the $\mathcal{H}_\infty$ criterion in its synthesis. Also, to promote the use of the proposed observers in real applications, we extend the methodology to the discrete time case and to the case of nonlinear systems with nonlinear outputs. For the different observers design, we use the differential mean value theorem which allows the transformation of the nonlinear estimation error to a linear parameter varying system. Then, we use the Lipschitz conditions and the Lyapunov standard function to synthesize the stability conditions in the form of linear matrix inequalities. Finally, we enhance the feasibility of the later conditions by using a judicious reformulation of the Young's inequality.

In the thesis, we also deal with the process control where we propose a control strategy to track an admissible reference trajectory planned by the plant operator. Moreover, to account for the partial availability of the state vector measurements, we include an exponential nonlinear observer in the control synthesis. Thus, we design an observer based tracking control scheme. To perform the stability analysis of the closed loop system, composed of the system, the observer and the controller, we use the Barbalat's lemma conjointly with the techniques already mentioned for the observers design. Finally, we propose two different methods to compute the controller and the observer parameters. In the first one, we propose to compute them separately. While, in the second one we compute the parameters simultaneously.

Keywords: Nonlinear systems, anaerobic digestion, nonlinear observer, $\mathcal{H}_\infty$ criterion, nonlinear control.

Résumé

La digestion anaérobie est un procédé permettant de transformer les déchets organiques en énergie utile, telle que le biogaz. Ce procédé fait intervenir des organismes vivants dont le comportement spécifique est fortement non linéaire. Par ailleurs, il est connu pour être sensible aux perturbations et naturellement instable. Ainsi, le développement de méthodologies efficaces pour sa commande et sa supervision est essentiel afin d'obtenir des résultats satisfaisants. Par conséquent, l'objet de cette thèse porte sur la modélisation de ce système complexe, la synthèse d'observateurs et de lois de commande afin d'améliorer le fonctionnement du procédé dans les stations de biogaz.

Une modélisation formelle du procédé est alors proposée où des degrés de liberté additionnels ont été introduits dans la commande de production de biogaz. En effet, deux entrées de commande supplémentaires viennent compléter le modèle standard AM2 (Acidogenèse Methanogenesis, 2 étapes), reflétant l'ajout de substrats stimulants (acides et alcalinité) qui améliorent la qualité et la quantité du biogaz. Par la suite, l'identification des paramètres du modèle non linéaire résultant est traitée, ainsi que l'analyse de la positivité et la bornitude des variables d'état. Sur la base du modèle mathématique dérivé et des résultats de l'analyse, différents observateurs sont alors étudiés afin de surmonter le manque de capteurs fiables, autonomes et bons marché. En effet, deux observateurs sont alors développés, le premier dit invariant et le second non linéaire de la même forme que l'observateur généralisé d'Arcak. En outre, dans le but de rendre la conception d'observateurs plus robuste aux perturbations, le critère $\mathcal{H}_\infty$ est introduit dans la synthèse. Une extension de la méthodologie est proposée pour les systèmes discrets ainsi qu'aux systèmes non linéaires avec sorties non linéaires.

Pour la synthèse des différents observateurs, le théorème des accroissements finis est appliqué, ce qui permet de transformer la dynamique non linéaire de l'erreur d'estimation en un système linéaire à paramètres variants. La condition de Lipschitz est alors conjointement utilisée avec la fonction classique de Lyapunov pour la synthèse des conditions de stabilité sous forme d'Inégalités Matricielles Linéaires (LMIs). Enfin, afin d'améliorer la faisabilité de ces dernières conditions, une reformulation judicieuse de l'inégalité de Young est alors introduite.

Concernant la commande du procédé, une commande par retour d'état pour le suivi d'une trajectoire de référence est choisie. Prenant en compte la disponibilité partielle des mesures du vecteur d'état, un observateur exponentiel non linéaire est introduit dans la synthèse de la loi de commande. Ainsi, une commande par retour d'état basée observateur est obtenue. Pour effectuer l'analyse de stabilité du système en boucle fermée composée du procédé, de l'observateur et du contrôleur, le lemme de Barbalat est alors utilisé conjointement avec les techniques déjà mentionnées pour la synthèse d'observateurs. Enfin, deux différentes méthodes pour le calcul des paramètres du contrôleur et de l'observateur sont proposées. Séparément, dans un premier temps. Puis simultanément dans un second temps.

Mots-clés: Systèmes non linéaires, digestion anaérobie, observateur non linéaire, critère $\mathcal{H}_\infty$, commande non linéaire.